OPTIMIZATION OF HELICAL TURBINE

IN LOW HEAD APPLICATIONS

by

Cole Ryan Wright

and

Michael Christian Hansen

A dual thesis submitted to the faculty of
The University of Utah
in partial fulfillment of the requirements for the degree of

Master of Science

Department of Mechanical Engineering

The University of Utah

August 2011

The University of Utah Graduate School

STATEMENT OF THESIS APPROVAL

The thesis of **Cole Ryan Wright and Michael Christian Hansen**

has been approved by the following supervisory committee members:

Daniel O. Adams	, Chair	**6/6/2011** Date Approved
Meredith M. Metzger	, Member	**6/6/2011** Date Approved
Kent S. Udell	, Member	**6/6/2011** Date Approved

and by **Timothy A. Ameel** , Chair of

the Department of **Mechanical Engineering**

and by Charles A. Wight, Dean of The Graduate School.

ABSTRACT

With current and ever increasing demands for energy, coupled with the limit on fossil fuels and their negative environmental impacts, there is a drive to harvest clean, renewable energy. One solution for harvesting clean energy includes hydraulic sources. Unfortunately, many methods for harvesting hydraulic energy result in environmental impacts of their own. One popular method consists of damming a water source. Although this method is efficient, it has its detrimental impacts. Some downfalls include restricting marine wildlife from venturing upstream for spawning, as well as flooding upstream land. Therefore, there is an additional push to develop a technology that can cleanly and efficiently harvest hydraulic energy with little to no impact on the environment. This project looks at the development of a helical turbine which harvests respectable amounts of energy in low-head hydro sources while creating virtually no impact on the environment.

The scope of this project is two-fold. Modeling multiple turbine designs and quantifying their results would be beneficial in the design optimization process. While commercial software packages have the capabilities of solving such problems, they require extensive time and expertise to setup, solve, and analyze. However, by making a few assumptions, a computational model was developed that allowed for an accurate analysis of a turbine design as well as the quantitative comparison of multiple

configurations. While sources of error from the assumptions did not allow for complete agreement between experimental and computational results, the computational analysis provided a valuable tool for understanding the dynamics behind the operation of these turbines and how different parameters affect the performance of the system.

The study also includes experimentally optimizing the turbine for maximum power output. Multiple variables were tested including airfoil profile, the number of blades per turbine and the turbines' solidity. Due to not having a water channel which could meet the volume and velocity demands needed, a wind tunnel was used. Geometric and dynamic effects were scaled appropriately. Results from these tests were compared to the computational results for validity. The most efficient turbine design for this method of application was a 3 bladed, NACA-0022 with 55% solidity.

TABLE OF CONTENTS

LIST OF TABLES

ACKNOWLEDGEMENTS

A project of this proportion is rarely the work of one individual; in fact the writing of this thesis alone was comprised of two authors. Thus, at this time we would like to express our appreciation to those who have helped this thesis become a reality.

We would like to say thank you to our families for their support, guidance and most importantly patience throughout our coursework and research. We know it has been a long road, but we also know that it will be well worth the wait. Without your encouragement and support, we would not have had the drive to be able to accomplish a task like this.

Next we would like to express our gratitude to Dr. Adams and Dr. Metzger. These two individuals have been by our side through thick and thin. Without their strong technical foundations, this project would not be where it is today. We appreciate all of the time they have taken out of their already busy schedules to accommodate helping us.

Although there are too many individuals to name here, we would like to thank the many friends and faculty we have gotten to know while attending school here at the University of Utah. Without everyone's help this dream would have never become a reality.

CHAPTER 1

INTRODUCTION

1.1 Background

With the continued expansion and modernization of society, comes an ever increasing global demand for usable energy. Along with this demand come significant problems that concern both where this energy is derived as well as what effects both energy production and consumption have on the environment. Fossil fuels, the current dominant source for the worlds energy supply, are at the root of these concerns due to the limited supply of these fuels as well as the negative environmental impacts of their combustion.

As a result of these pressing concerns, much research has been done in search for alternative energy sources. One great potential for an alternative energy source is the hydro power stored in our worlds many waterways.[1-5] While hydro energy is not a new concept, as it has long been supplying power through waterwheels and hydro power dams, it has been very limited in its useful power producing applications.[6]Power producing dams have a long history of being highly efficient mechanisms, yet they have been greatly handicapped in practical implementation due to the high costs and the many environmental concerns they introduce.

Hydro power dams create and utilize potential energy by restricting flow of a waterway which results in the creation of a reservoir of water on the upstream side of the dam. As a reservoir of water increases in depth, the amount of potential energy stored in the water also increases. A large portion of this potential energy is then harvested by allowing water at the base of the dam to flow through specialized turbines. These turbines operate by minimizing the amount of water that can pass through them, thus creating a large pressure differential which causes the turbines to rotate at high speeds.[1-4]The problem however, with creating this massive reservoir upstream of a dam is three-fold. First, the damming of a river has a severe impact on the local environment. Often the stored water takes away from precious living space and farmlands. Also, not all locations are suitable for the creation of a dam. Second, dams greatly disrupt the rivers local ecosystem. One example includes the hindering of the upstream movement of spawning uh7ifish. Finally, a respectable percentage of the water that would normally make it downstream is either absorbed by the land or evaporated by the mere surface area of the man-made water body, a major problem for drought stricken areas.[1-5] For these reasons there is a world-wide drive in the scientific community to find a way to harvest energy from free-flowing, low-head, water sources which by their very nature greatly reduce or eliminate the aforementioned environmental problems.

The solution to this problem comes by analyzing Bernoulli's equation, which is the driving equation behind water turbines. This equation sums up the forms of energy associated with a fluid. While hydro dams harvest the potential energy from a body of water, free stream, low-head, hydraulic turbines harvest the kinetic energy of a fluid flow.

$$z + \frac{p}{\rho} + \frac{V^2}{2g} = const \qquad (1.1)$$

The first term in Bernoulli's equation z, is the fluid elevation with respect to the reference axis. For open channel streams this value is zero. The second term is the potential energy term and the third term refers to the kinetic energy. For turbines used in dam applications the goal is to maximize the potential energy term whereas for turbines in open channel flow the goal is to maximize the kinetic energy term. Accordingly, when looking at current technology, kinetic turbines can be classified into two groups, drag-based turbines and lift-based turbines.

Drag-based turbines are designed so that the drag force dominates the lift force.[6] An example of this type of turbine is the Savonius turbine shown in Figure 1.1. Lift-based turbines, on the other hand, are designed so that the lift force drives the turbine.[7] Examples of these types of turbines are the Darrius and Gorlov turbines as shown in Figure 1.2. Drag-based turbines, by nature, create large pressure differences across their surface resulting in a localized decrease of the velocity incident on their blades. Conversely, lift-based turbines operate by allowing the water to flow around airfoil shaped blades. This minimizes the pressure gradient across the turbine and maximizes the flow-speed incident across the blades.

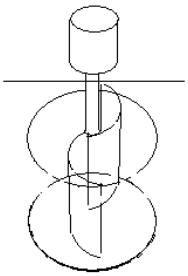

Figure 1.1. Pictorial representation of drag-based, Savonious turbine.

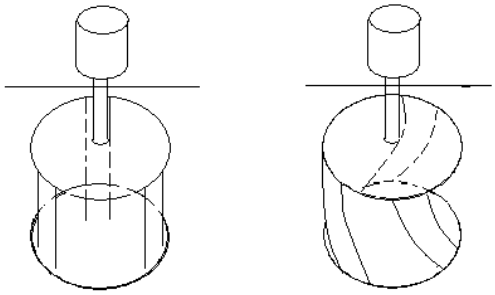

Figure 1.2. Pictorial representation of lift-based turbines. The image on the left represents the Darrius turbine while the image on the right represents the Gorlov turbine.

While there are many different types of lift-based turbines, the Darrius and Gorlov turbines are two of the most popular hydro-turbines being used today.[1-5] This is largely due to the significant advantages they have over other hydrokinetic turbines. The advantages of the Darrius turbine include its simple geometry and corresponding ease of manufacturing, the fact that it rotates unidirectional regardless of incoming flow, and its moderate efficiency of approximately 25% based on previous research.[1-4]

However, the Darrius turbine does have some costly and inherent disadvantages. The turbine is not self-starting and therefore some mechanism is normally required to start the turbine. Also, due to the design, this turbine exhibits oscillatory torque as it rotates. This produces an oscillation in the power output as well as significant amounts of vibration which can cause irreparable structural damage.[1-4]

The Gorlov turbine, due to the helical sweep of its blades, solves several of the problems of the Darrius turbine and additionally reaches a reported higher efficiency of 35% at maximum performance. The benefits of the Gorlov turbine include that it is self starting, it produces constant torque which also greatly reduces the effects of vibration

and there are no visible signs of energy loss due to cavitation.[1-4] Last but not least, the power output of a turbine is generally proportional to the diameter of the turbine since power is based on torque and torque is based on diameter. Consequently, the larger the turbine diameter, the more power will be produced for the same angular speed and turbine configuration. However, there is a limit to how much this diameter can increase before structural damage occurs to the turbine due to centrifugal forces. Thus, most turbines have a maximum diameter and thus a maximum power output. Yet, the final inherent benefit of the helical turbine is that the diameter can be decreased while simultaneously increasing the length with no power losses. Since centrifugal forces do not depend on turbine length, there is no theoretical limit to how tall these turbines are and thus no limit to the amount of power that can be harvested. The limit comes down to environmental conditions where the turbine will be installed.

1.2 Problem Statement

It is the goal of this research to investigate computationally and verify experimentally, the variables that are a part of the lift-based, helical-bladed turbine with an end result of producing the most efficient turbine design possible for low-head, low-speed, hydro applications. The computational approach will involve using computational fluid dynamics (CFD) software such as Fluent as well as the coding language Matlab to test multiple airfoils, solidities, number of blades, pitch angle and overall turbine dimensions. Optimal, scaled designs will then be constructed and experimentally tested in a wind tunnel. All dynamic and geometric properties will be appropriately scaled down from a full-scale size by matching the dimensionless parameters that result from a Buckingham Pi analysis. All of the same variables examined computationally will also be

tested experimentally, except pitch angle, wherein the experimental results will be used to validate the computational findings. Once all of the design configurations are verified, the optimal design will be chosen based on maximum efficiency and power output. Ultimately, results will be scaled up to full-scale and a prototype will be built and tested in an open water channel to ensure all computational and experimental findings can be reproduced in a real world application.

1.3 Project Background

In 2008 the Grand Canyon River Outfitters Associations (GCROA) approached the University of Utah with the goal of making their rafting trip as serene as possible for their customers. Currently, GCROA trips consist of 7 to 21 days and the rafts are powered by gasoline motors. The issue with this setup is that fuel is expensive and the current motors are noisy and tend to release unpleasant fumes all of which take away from the pure, quiet, and serene nature of the Grand Canyon. Consequently, GCROA desired an efficient system which was clean, quieter and allowed for the true nature of the Grand Canyon to be enjoyed.[5] Thus in 2008, a team of University of Utah students developed an electric motor and battery bank to achieve this goal. Six, twelve-volt batteries were arranged in series to supply power to the electric motor setup. Although this setup met GCROA's demand, there was an obvious issue with the motor performance as power was drained from the battery bank. Therefore, the University of Utah also aimed to find a way to recharge this battery bank while still maintaining the goal of clean, quiet and efficient systems. This recharging system would be used in conjunction with the electric setup to provide full power to the motor, allowing it to run at top performance and maximum efficiency each day. In addressing the recharging issue

the team decided to look into renewable energy sources available in the Grand Canyon. It was decided that from the available sources, solar and wind energy were unpredictable and limited and could not be relied upon to re-charge the power lost each day. However, the water level and water velocity in the Grand Canyon is nearly constant all year long making it the best prospect for harvesting energy. To meet the goals of GCROA the team decided to take advantage of the kinetic energy naturally found in the Grand Canyon waterway. It was decided that a helical turbine would be the best method of harvesting this energy. Due to time constraints and lack of knowledge the team decided to use previously published data to construct a six-bladed, 48% solidity turbine using a NACA 0009 airfoil profile. The NACA 0009 airfoil was initially selected due to the fact that is was initially designed to perform in low Reynolds number regimes which was the case for the fluid flow in consideration. The 48% solidity was chosen as it has been used in many previous studies and six blades were chosen, in comparison to the conventional three, in order scale down the turbine to fit within a design envelope suggested by GCROA. The turbine design was then constructed and tested with the allowable time left in the academic year. Unfortunately, the turbine was only able to be tested at a flow-speed of 0.69 m/s or 2.00 ft/s. Testing of this turbine led to Figure 1.3 which is the torque versus angular velocity curve and Figure 1.4 which is the power versus angular velocity curve.

As can be seen from these figures, this turbine produced extremely small amounts of power. To calculate the efficiency, Equation 1.2 is used which determines the total power available to be harvested from the water given the turbines size

$$P_A = \frac{1}{2} A V^3 \tag{1.2}$$

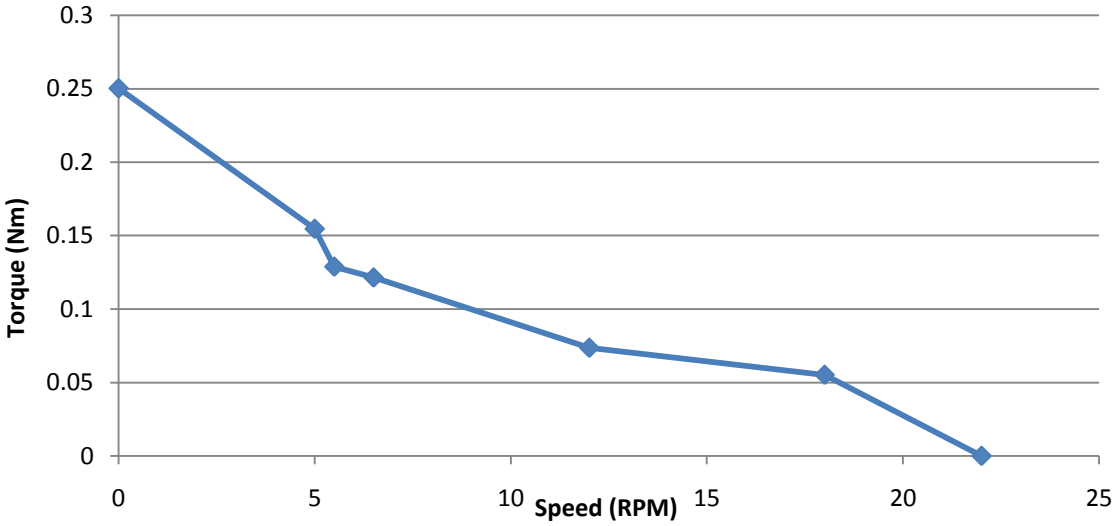

Figure 1.3. Torque/Speed curve generated by experimental data collected in Immigration Canyon at flows of 0.69 m/s or 2.00 ft/s.

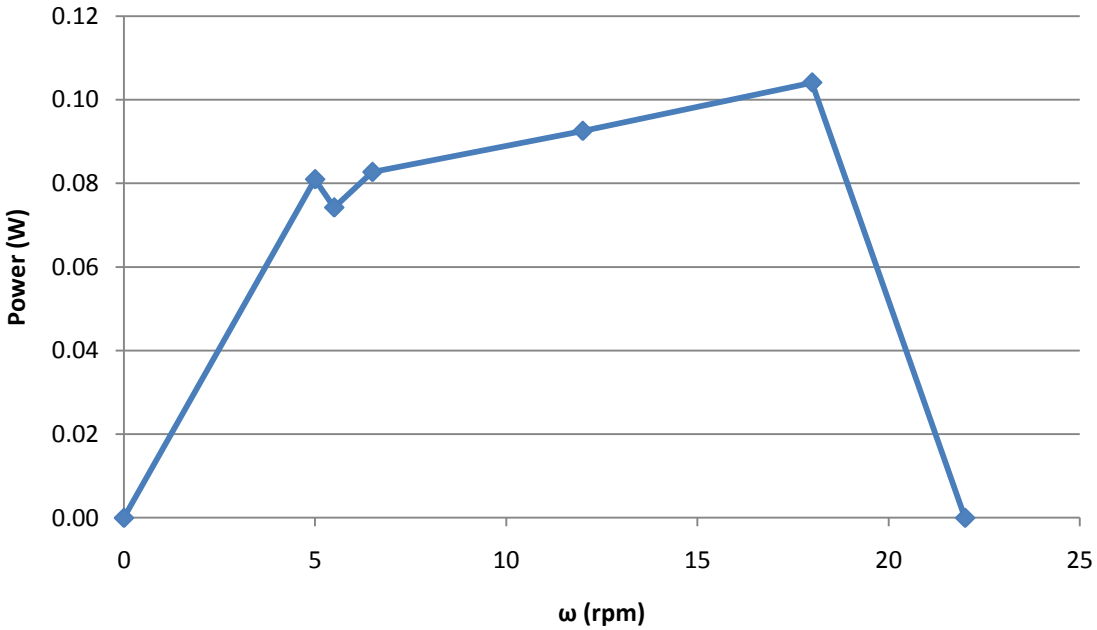

Figure 1.4. Power/Speed curve generated by experimental data collected in Immigration Canyon at flows of 0.69 m/s or 2.00 ft/s.

where $P_A$is the available power in the water, A is the frontal area of the turbine and V is the water velocity. However, only a percentage of the total power available can be harvested. That percentage is known as the turbines efficiency and is denoted by Equation 1.3

$$P_H = \eta P_A \tag{1.3}$$

where P_H represents the total power harvested and η represents the efficiency of the system.

From these equations it is expected that 42 Watts of power are available to be harvested, yet only 0.1 Watts were harvested, yielding an efficiency of 0.2%. Due to this poor result and lack of thorough testing, it was decided to take an additional year to understand exactly how this turbine works and how the variables of airfoil profile, number of blades and turbine solidity affect the overall turbine performance.

One additional note, all hydraulic turbines have a maximum efficiency limit which governs their performance. The goal in designing a turbine system is to operate as close to this theoretical maximum as possible. In order to do so it is important to understand what this theoretical limit is. In 1920, the Betz limit derivation predicted that the maximum efficiency for propeller-type turbines in free flow was 59.3 %. This derivation considered a one dimensional model for a plane turbine positioned in an incompressible fluid with rectilinear streams of constant velocity. This study by Betz used the same definition for efficiency as will be used in this thesis. The efficiency of the turbine is calculated by dividing the harvested turbine power by the total power available in fluid based on the turbine area. The problem with using the Betz study for this application is that the principal assumption behind his study is that the flow remains

rectilinear as it passes through the turbine and maintains a uniform distribution of the fluid pressure on the turbine. In an attempt to improve upon this model Gorlov, Gorban and Silantyev2 developed a new model known as the GGS which predicts a new maximum efficiency of 30.1 % based on a curvilinear flow assumption. This model uses the two-dimensional modified Kirchhoff flow which implies that the streamlines are redirected around the turbine blades in a curvilinear fashion versus rectilinear streamlines. This model states that maximum efficiency will be achieved when 61 % of the flow passes through the turbines cross sectional area. A number of tests by the authors show that the three-dimensional hydraulic helical turbine actually develops an efficiency of up to 35 % which is slightly larger than the theoretical prediction. The authors suggest that this could be explained by modeling a three-dimensional rotor as a combination of two plane turbines that reflect power contributions from the front and back parts of the original cross-flow turbine. Consequently, it will be assumed from this study that the helical turbine is capable of producing a maximum efficiency between 30 and 35 %.

CHAPTER 2

COMPUTATIONAL ANALYSIS

2.1 General Background

In light of the performance of the turbine generated for use in the Grand Canyon, and the difficulties in producing an efficient design, two major needs became apparent. First, a better understanding of the dynamic principles under which these lift-based turbines was required. Second, a method to quickly provide an optimized design for a given flow field to insure maximum efficiency and power generation was needed.

Due to the complex geometry of the turbine, in addition to the challenges of the ever changing flow field around the circumference of the turbine, it is challenging to fully understand, both physically and mathematically, which portions of the turbine are producing the most torque for a given flow condition. A thorough understanding is needed, however, if an optimal design is to be achieved. Furthermore, in order to tailor a turbine design to be able to deliver power with a maximum efficiency for a given flow field, the effects of the flow field on the system dynamics must be understood.

It was determined that a computational analysis of the system would provide the best means for both understanding the performance of the turbine as well as providing a means for design optimization. Using a computational program, multiple turbine designs and free-stream conditions could be analyzed and evaluated. Such evaluation would

provide a means to understand not only how the turbine operates, but would supply the needed information to perform a design optimization for a given flow condition.

2.2 Important Parameters

A number of important parameters which have a great impact on the performance of the turbine have been identified.[1-4] The parameters fall primarily into two categories, namely those governed by the geometry of the turbine, and those governed by the flow field in which the turbine is designed to be placed.

In general, the environmental parameters, or the parameters governed by the flow field in which the turbine is to be places, are fixed and the designer has little option to alter any of them in an attempt to increase efficiency. These parameters include important values such as the free stream velocity, and the density of the fluid.

Geometric parameters, however, are mostly free to be adjusted in order to improve turbine performance. While each of these parameters can be adjusted, many of them are dependant functions of each other. For instance, the cord length is one of the parameters that determine the solidity of the turbine. Therefore when the cord length is changed, the solidity is also altered.[2]

The important input parameters, as well as a brief description of each, are given below. These are the parameters that will be analyzed to gain a better understanding of the turbine operation, as well as improve design optimization.

- Free-Stream Velocity: The magnitude of the incoming flow velocity. For complex flow streams, this value can be assumed to be an average value of the flow speed through the turbine frontal area.

- Blade Profile: The two-dimensional cross sectional area of the hydrofoil which makes up the geometry of each blade section. The different blade profiles investigated in this study are shown in Figure 2.1.
- Cord Length: Length of the airfoil profile.
- Solidity: The percentage of the frontal area of the turbine that is taken up by the turbines blades.
- Number of Blades: Number of blades comprising the turbine. Generally numbering 2, 3 or 6.
- Blade Pitch: The angle between the cord and the line tangent to the circumference of the turbine at the point of the center of lift of the blade.
- Angle of sweep: The angle around the circumference that each blade sweeps.
- Rate of Twist: The rate at which the blade twists about the center axis of the turbine with respect to the height of the turbine.
- Fluid Density: The density of the fluid the flows around the blades.
- Turbine Height: The length of the center axis of the turbine.
- Turbine Diameter: Diameter of the circumference of the turbine, or the path that the center of lift of travels.

2.3 Computational Approach

There are many commercially available computational fluid dynamics (CFD) software packages available for modeling various flow fields. For this project the CFD package Fluent was used. This software package has the capability of handling both two dimensional and three dimensional flow field analyses.

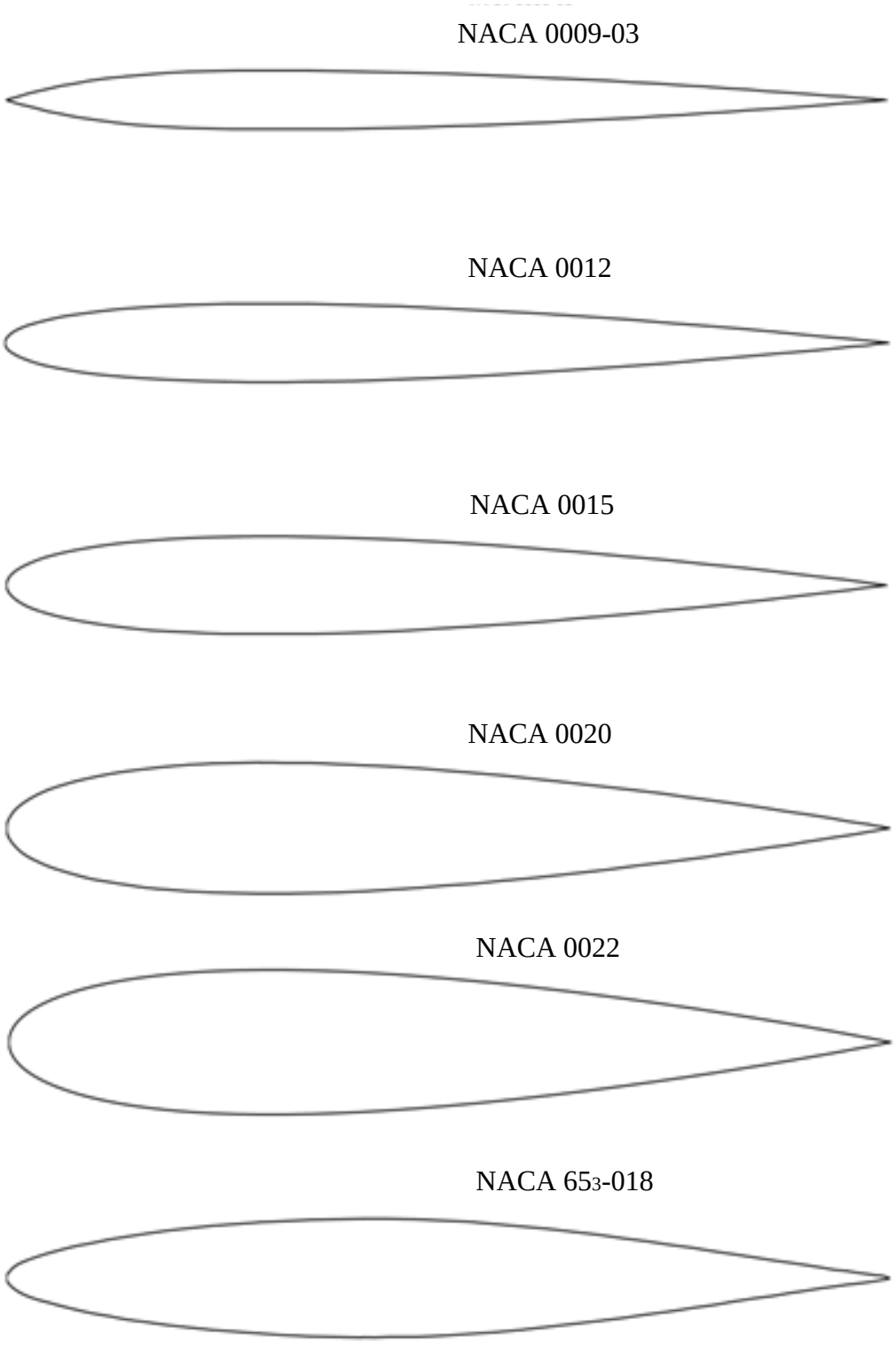

Figure 2.1. Comparison of the different symmetrical airfoils tested in this study.

Fluent is a finite element analysis program that breaks a flow field up into multiple small but finite elements then solves the governing equations of a fluid flow across each element. An iterative approach is used with convergence being reached when the residuals of key parameters fall below a specified threshold value. A Spalart-Allmaras model[36] is used to simulate the viscous effects of the flow.

Initial two-dimensional analyses of blade profile sections were used to evaluate the performance of many different profiles in various fluid flows. While these studies provided valuable comparisons of different profiles as shown in Figure 2.2, they didnot provide useful information as to the performance of the entire three-dimensional turbine system. It was apparent that a more sophisticated model would be needed.

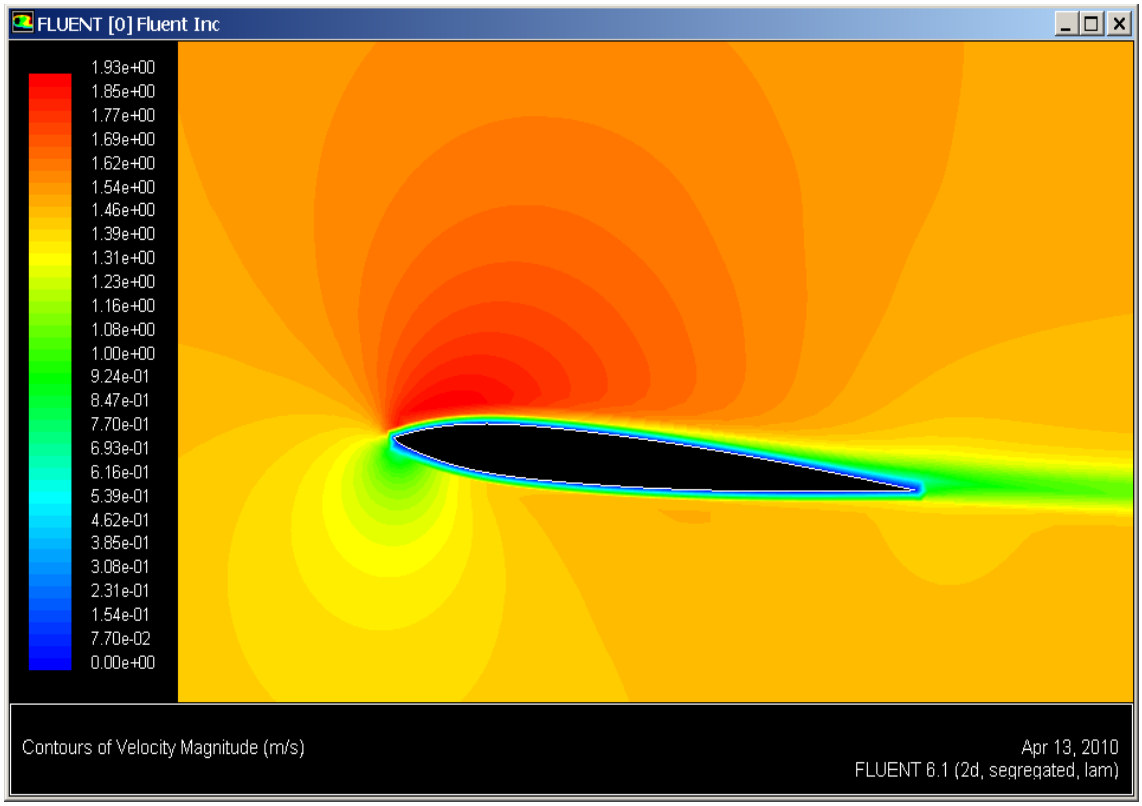

Figure 2.2. Contours of the free stream velocity magnitude about an airfoil at a small angle of attack.

Next a three-dimensional model of a single stationary turbine blade was tested. The test setup geometry is shown in Figure 2.3. It was deemed wise to start with just a single blade and then increase the complexity of the model as to ensure that the program could solve the problem. Unfortunately, the single blade model was very computationally expensive and took a significant amount of time, 6 to 10 hours depending on incoming flow direction, to converge. After a converged solution was reached, the value of the results was investigated. The forces acting on the blade was easily extracted as vectors in the standard orthogonal coordinate system. While the force vectors on the plane of the blade profile, both in the directions parallel to and perpendicular with the direction of the free stream flow, are useful, they do not provide enough information. While the integrated total force is reported, it is the values, and change of values, of the lift and drag forces, as a function of turbine height that is desired. This goes back to the earlier statement that one of the main goals of this analysis is to understand the dynamics involved in the operation of these turbines. One main part of this is goal is being able to understand how angles of attack and magnitudes of lift and drag change around the circumference of the turbine.

In addition to the inability to retrieve lift and drag data as a function of blade height and location, it also proved difficult to view the stream functions or pressure gradients across the blade. The memory needed for these graphical representations required more memory that what is available in a normal computer.

Furthermore, it should also be noted that these Fluent results are only for the case where the single turbine blade is fixed in place with absolutely no rotational effects. These rotational effects need to be included in order to accurately model the performance

of the turbine. Due to the large computational cost of the single stationary blade, and the difficulty of retrieving needed data, it was determined that it was not feasible to pursue using Fluent to analyze more complicated turbine geometry.

One easy to overlook, but important result should be mentioned. This result comes from the calculated force in the direction of the axis of the turbine. This reported force was negligibly small in comparison to the other two orthogonal forces. This indicates that there is very little turning of the water in that direction. In light of this it can be concluded that the effects in the direction along the axis of the turbine are negligible.

In light of the huge computational cost of running complex three dimensional scenarios in Fluent, and the fact that there isn't significant force generation in the axial direction, it was decided that it would be possible to develop a program that could greatly simplify the problem by making a few assumptions. This decision was based on the belief that if the flow effects in the axial direction can be neglected then the flow can be assumed to be two dimensional around each airfoil blade. This assumption is similar to that made by other vertical axis turbine studies such as that by Hyun Ju Jung et al.[8] Further simplifying the problem, each blade can be broken up into a large number of small finite sections that can be assumed to be two dimensional with no angle of twist. A model of these discrete sections is shown in Figure 2.4. By making these assumptions, once the behavior of the fluid flow around each section is determined, coefficients of lift and drag can be used to accurately calculate the resultant forces on each discrete section. Then, by summing up all of these forces, the overall performance of the turbine can be determined.

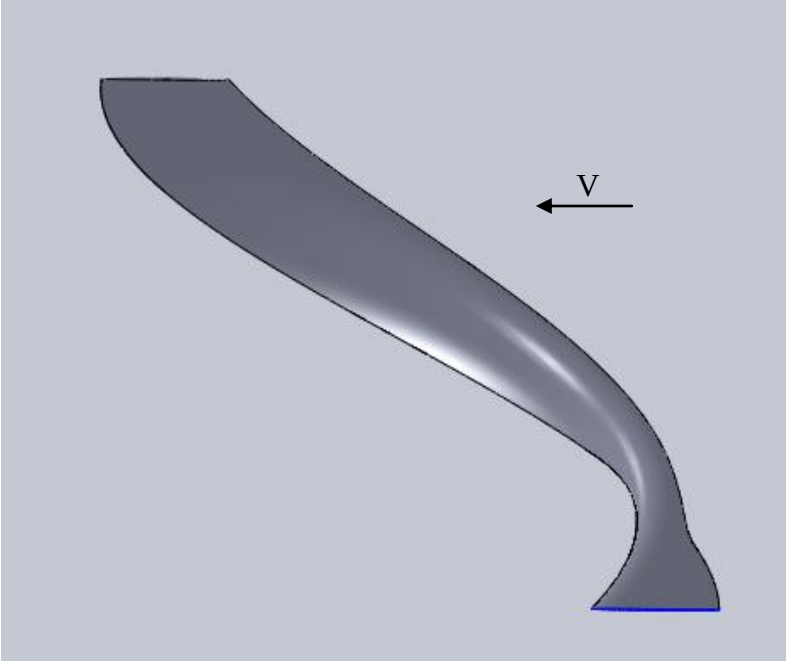

Figure 2.3. The setup for a three-dimensional analysis of a single stationary blade for an incoming velocity. This type of analysis is computationally expensive to perform.

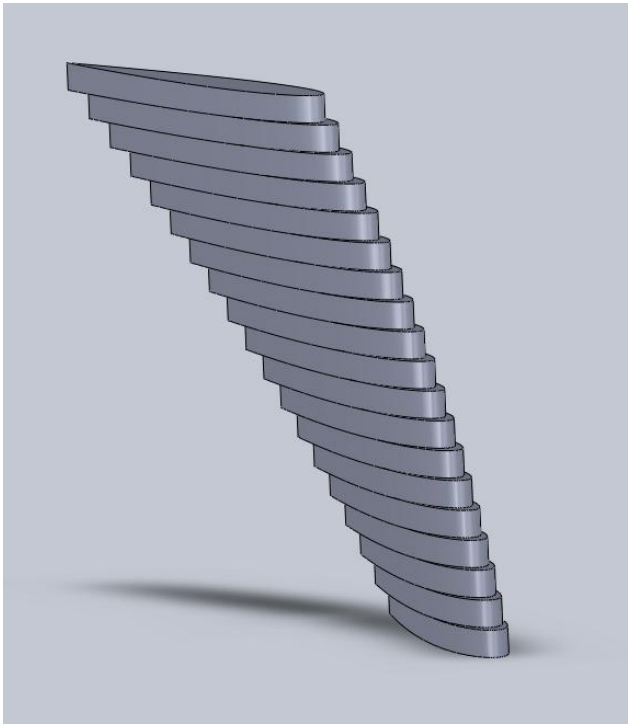

Figure 2.4. A single blade made up of multiple discrete sections.

2.4 Analytical Model Development

In order to develop a computational program to determine the performance of a hydraulic turbine, an analytical model is needed to supply the equations to be used in the computational analysis. For the turbine analysis, the free stream component of velocity V_{fs} on the discrete sections is equal in magnitude and direction to the velocity of the incoming fluid V. For the back half of the turbine, however, the magnitude is modified by the downstream momentum deficit a as shown in equation 2.1. The method of calculating the downstream momentum deficit will be discussed at the end of this section.

$$\vec{V}_{fs} = V(1 - a) \tag{2.1}$$

The magnitude of the induced velocity from rotation V_i is calculated by taking the rotational speed in rpm and converting it to rad/s, then multiplying it by the distance traveled per rotation. This is shown in equation 2.2. The vectoral representation of this velocity for each discrete section is placed tangent to the circumference of the turbine at the center of lift of each section.

$$V_i = \frac{2\pi r_m \omega(rpm)}{60} \tag{2.2}$$

Equation 2.3 shows the simple vectoral summation of the two velocity vectors to get the resultant velocity vector $\vec{V_r}$. This vector summation is shown in Figure 2.5.

$$\vec{V_r} = \vec{V_i} + \vec{V}_{fs} \tag{2.3}$$

The angle of attack is then found by taking the dot product between the resultant velocity vector $\vec{V_r}$ and the vector $\vec{C}$ which represents the vector of the cord of the profile. This is shown in equation 2.4 and Figure 2.6.

$$\alpha = \overrightarrow{V_r} \cdot \vec{C} \tag{2.4}$$

Given the angle of attack for each discrete section the coefficients of lift and drag, C_l and C_d, can look up off of tabulated data. Sources of coefficient data will be discussed in section 2.6. For a case where the angle of attack falls between two points on the table a cubic interpolation is used to retrieve the needed values. With these coefficients, the lift force *L* and drag force *D* can then be calculated using equations 2.5 and 2.6 where ρ is the density of the fluid and *A* is the planform area of the discrete section for a full rotation.

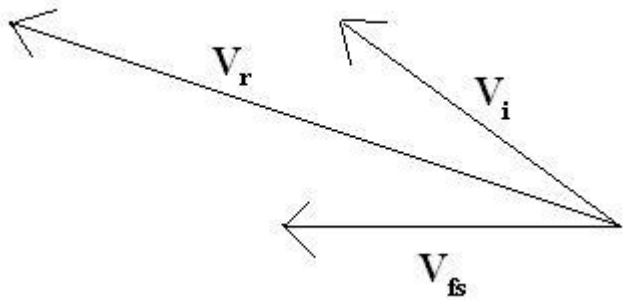

Figure 2.5. The vector summation from equation 2.3.

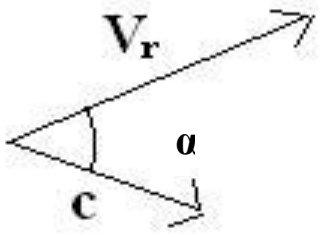

Figure 2.6. The angle of attack, α, between the cord and the resultant velocity.

$$L = \frac{1}{2}\rho V_r^2 A C_l \quad (2.5)$$

$$D = \frac{1}{2}\rho V_r^2 A C_d \quad (2.6)$$

With the values of the Lift and Drag forces known, the angle of attack can be used to break down these vectors into their normal and tangential components. Due to the use of symmetrical hydrofoils and the subsequent simplification of using angles of attack ranging from 0 to 180 degrees, the direction of the lift vector is not preserved in the dot product taken in equation 2.4 and must therefore be determined from the direction of the resultant velocity vector. This decomposition is showed in equations 2.7 through 2.10, and represented in Figure 2.7.

$$D_t = D\cos\alpha \quad (2.7)$$

$$D_n = D\sin\alpha \quad (2.8)$$

$$L_t = L\sin\alpha \quad (2.9)$$

$$L_n = L\cos\alpha \quad (2.10)$$

The summations of all the tangential force components for all discrete sections can then be summed up to find the total tangential force F_t on the system. This is shown in equation 2.11. The cross product of the tangential force and the radius r, as shown in equation 2.12, can then be taken to solve for the torque produced by the fluid flow over the discrete sections.

$$F_t = (\sum D_t + \sum L_t) \quad (2.11)$$

$$T = F_t \times r \quad (2.12)$$

The total torque extracted by the system can be solved for using a simplified version of the conservation of angular momentum equation[29] shown as equation 2.13.

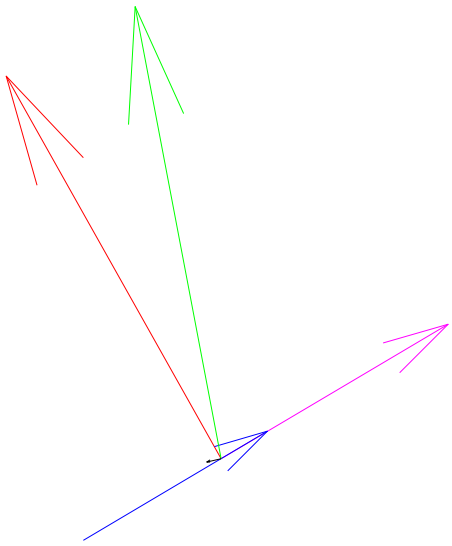

Figure 2.7. Converting the lift, green, and drag, black, vectors into normal, red, and tangential, magenta, vectors. The blue vector is the profile cord of the discrete section.

$$T_{shaft} = -2\rho r^3 V_{fs}\left(\frac{2\pi}{60}\right)(1-a) + T \tag{2.13}$$

Here again there is a term that uses the value of the downstream momentum deficit a. Currently the method for determining this value analytically hasn't been developed. Therefore, the current code uses experimental data from multiple case studies to determine this value. With the known free stream velocity, fluid density, and torque generation, equation 2.13 can be used to solve for a. The no-load speed is used to calculate this value.

2.5 Model Development

In the development of the computational model, a few conventions were set down to ensure consistency in the model setup for each discrete section. First, the axis of the turbine was centered the origin. Each discrete section was placed on the circumference of the turbine such that the center of lift was on the circumference and the profile cord was tangential to the circumference. Further convention was that the point at the top of the

circle, or the 12 o'clock position is considered to be at an angle of 0 degrees around the circle, and the angle increases clockwise around the circumference. Finally the incoming flow is assumed to be moving from the right to the left and the sections are oriented such that the discrete section at the 0 degree position is at an angle of attack of 0 degrees to the incoming flow. Figure 2.8 shows a representation of the model with just twelve of the discrete sections displayed. By limiting the number of discrete sections shown, the figure is uncluttered enough to provide useful data while still covering the whole range of angles of attack.

The first physical property considered is the incoming free stream velocity. This important, driving property is a function of the fluid flow in which the turbine will operate. The free stream velocity is represented in the code as a vectoral quantity. A free stream vector is created for each discrete section with the tail fixed to the leading edge of the discrete section profile, and extending in the downstream direction with a length equal in magnitude to that of the incoming flow as shown in Figure 2.9. This approach makes the assumption that the incoming flow equally affects each discrete section independent of location. From an observance of a similar turbine operating in a water flow, it quickly becomes apparent that this is a very poor assumption. By definition, when the incoming flow passes around the airfoil sections of the upstream portion of the turbine, the flow is turned aside, being changed in both its magnitude and direction. The amount that the upstream turbine sections affect the downstream turbine sections is largely a function of both the angular velocity of the turbine, as well as the solidity of the turbine. Thus the downstream sections of the turbine will be subject to free stream flow effects far different from the upstream sections. A simple approach to accounting for this

discrepancy is to apply a penalty to the magnitude of the downstream sections. This adjustment to the model is shown in Figure 2.10. For the current study, the penalty from equation 2.1 is used. Further study is needed to better understand and model this phenomenon. Finally, it has also been observed in shallow flow channels the existence of a vertical pressure gradient due to boundary layer. Though not taken into account in this model, such a gradient will affect the performance of the turbine by reducing the magnitude of the free stream velocity vector on some of the discrete sections.

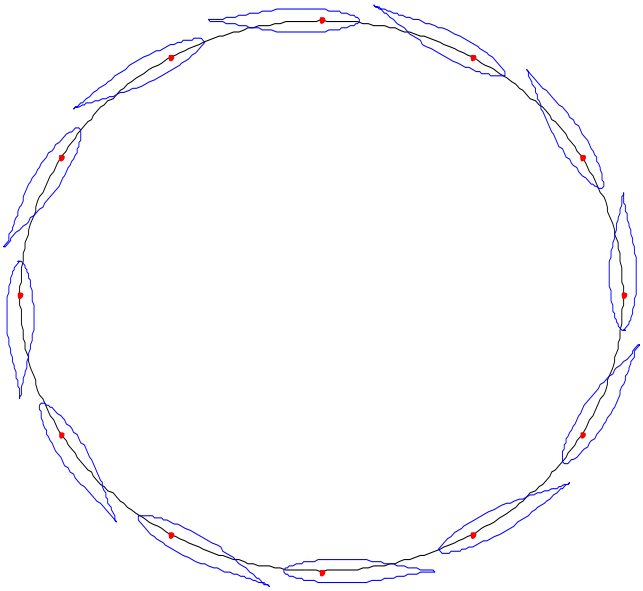

Figure 2.8. Twelve equally spaced discrete sections to demonstrate the model setup. Each section shown provides a visual for the hydrofoil performance of the discrete sections near the modeled section.

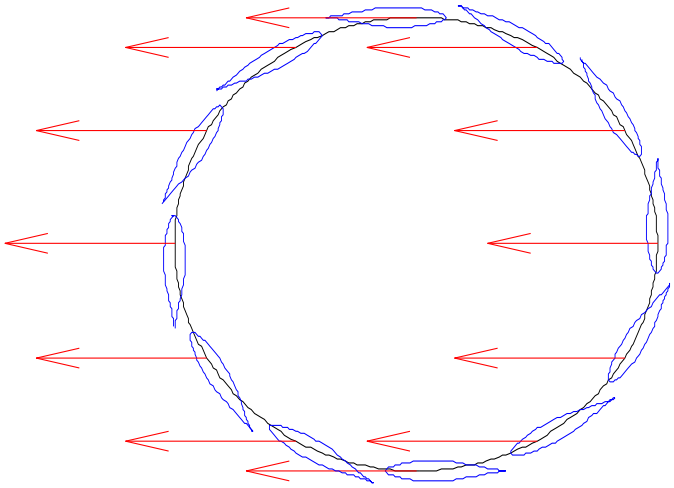

Figure 2.9. Free stream velocity vectors place on each discrete section.

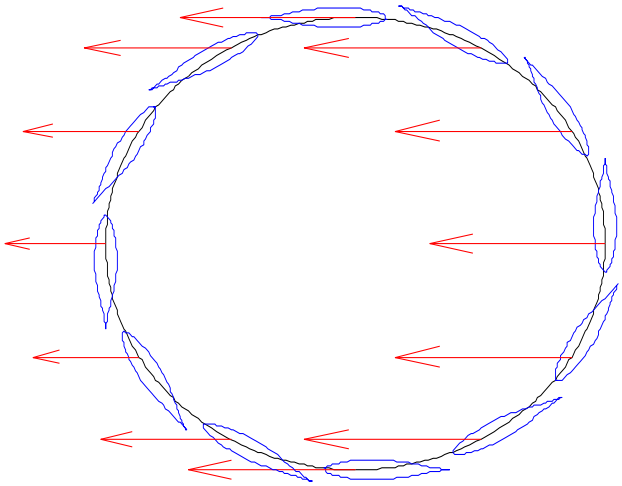

Figure 2.10. Free stream velocity vectors adjusted to compensate for downstream velocity reduction.

The flow around the discrete sections, induced by the rotation of the turbine through the fluid, is modeled next. This velocity is proportional to the rotational velocity of the blades, as well as the radius of the turbine. Unlike the free stream velocity, the induced velocity is equal in magnitude at all locations and for all discrete sections. Once again this velocity is represented as a vectoral quantity. Each vector is attached by its tail to the leading edge of each corresponding discrete section profile. The induced velocity vector then extends tangentially outward in the direction opposite that of the direction of the turbines rotation. These induced velocity vectors are displayed in Figure 2.11.

From these two velocities, a resultant velocity vector is derived. This is done through the vectoral summation of the free stream velocity vector and the induced velocity vector.[23-24] For every flow condition with a turbine rotational velocity greater than zero, the resultant velocity vector at each discrete section is unique in both magnitude and direction. The resultant velocity vectors for the special case where the induced velocity vectors have the same magnitude as the free stream velocity vectors are displayed in Figure 2.12. As is expected, there is no resultant velocity at the location 180 degrees around the circumference, or the location at the bottom of the figure where the two velocity components are equal in magnitude but opposite in direction so they directly cancel each other.

Observation of the velocity vectors in relation to the cord lines of the discrete section profiles indicate angles of attack ranging from 0 to 360 degrees. Due to the symmetry of the profile shapes considered, this range of angles of attack can be simplified to 0 to 180 degrees. The angle of attack is calculated by taking the dot product

of the cord length vector and the resultant velocity vector. The angle between these vectors can be seen visually in Figure 2.13.

At this point it is profitable to discuss some important observations that can be made about the turbine performance with respect to the resultant velocity vectors. From the case where the rotational speed of the turbine is 0, the only component to the resultant velocity is the free stream velocity. The angles of attack for this case are displayed in Figure 2.14. As is commonly understood from airfoil theory, the optimal performance for airfoils occurs as relatively small angles of attack up to stall. This presents two major problems for turbines with helically swept blades. First, the majority of the discrete sections in the case currently being considered have angles of attack that exceed the stall angle. Secondly, for small angles of attack, less than 10 degrees, while the lift to drag ratio is very favorable, the majority of the lift produced, being in the direction perpendicular to the profile cord, is in the direction normal to the blade, and thus does not contribute to generating the desired tangential torque. Fortunately, for the case considered, at the large angles of attack, close to ninety degrees, the majority of drag produced is in the positive tangential direction. In other words, the drag force on these sections contributes by increasing the total tangential force produced by the blades.

Another case worthy of consideration is the hypothetical one where there is an induced velocity from turbine rotation, but no incoming free stream velocity. We can see from Figure 2.11 that the resultant velocity vector for each discrete section is, by definition, at an angle of attack of zero with respect to the cord. Due to the symmetry of the airfoils, the coefficient of lift is 0 for no angle of attack.

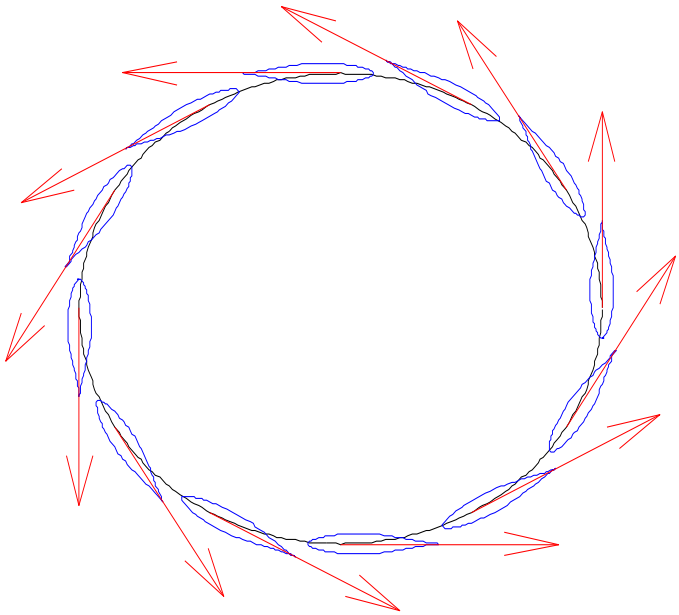

Figure 2.11. Induced velocity vectors are displayed on each discrete section.

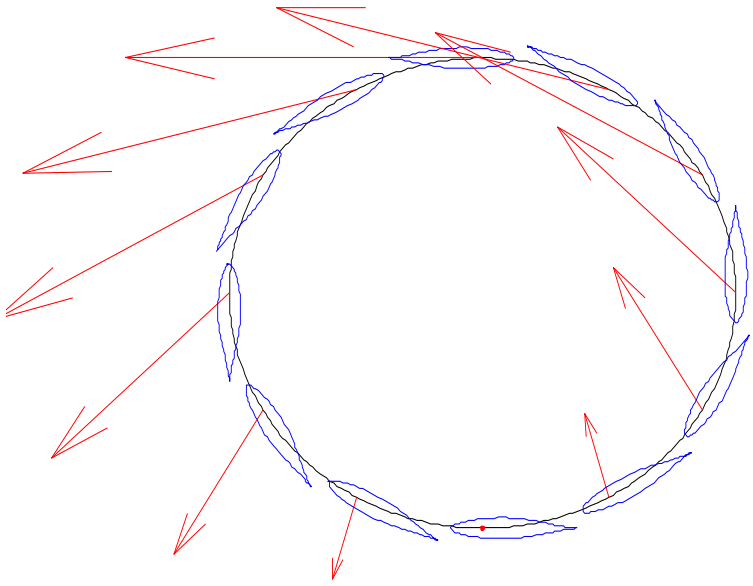

Figure 2.12. Resultant velocity vectors for each discrete section.

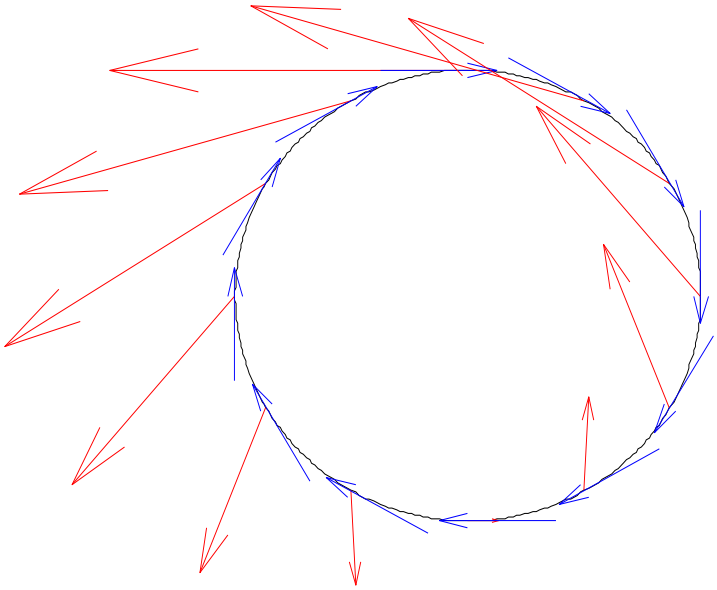

Figure 2.13. The angle of attack is the angle between the resultant velocity vectors and the vectors representing the profile cord.

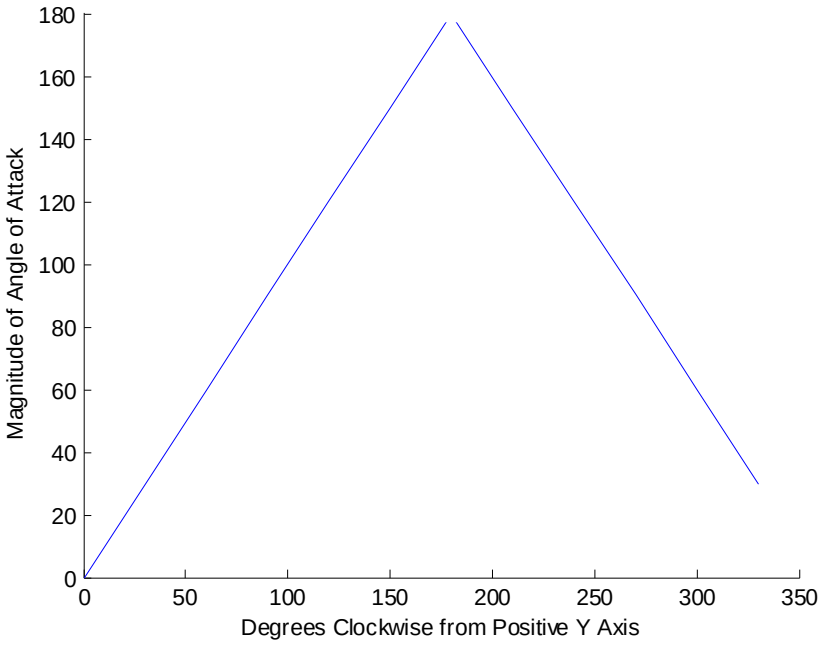

Figure 2.14. The range of angles of attack present for the case where there is no rotation.

The natural operating condition of the turbine, however, will include a combination of both free stream and induced velocity components. As can be seen from the two previously explored cases, as the induced velocity component begins to dominate the free stream velocity component at high rotational speeds, the resultant velocity vector is brought closer to the profile cord. But while all resultant velocity vectors are brought into more favorable angles of attack, the free stream velocity component ensures that the angle of attack will never be zero except at the two discrete sections where the free stream velocity is parallel with the profile cord. The optimal performance conditions, then, would be the condition where the majority of the discrete sections are at a favorable angle of attack, yet still at a large enough angle of attack that a large portion of the generated lift is in the positive tangential direction. This favorable range includes angles of attack generally between 15 and 45 degrees, thought this range changes slightly for different airfoil profiles. Figure 2.15 shows the angle of attack trends for a case when the free stream velocity vectors V_{fs} dominate the induced velocity vectors V_i or when the velocity component from the free stream velocity is larger in magnitude that the induced velocity vector. In Figure 2.16 the induced velocity vectors dominate.

Once the angle of attack has been calculated for each discrete section the coefficients of lift and drag can be determined.[29] As previously discussed, the assumption is being made that each discrete section can be considered as a two dimensional airfoil section with a finite length. Because of this assumption, previous, experimentally derived data for the appropriate airfoil at a specified angle of attack can be used. Discussion of the source of this coefficient data, as well as the confidence in and reliability of the data

will be discussed in section 2.6. Any instance where the desired angle of attack does not fall in the tabulated data, a cubic interpolation between adjacent points is used to obtain the needed values. Any error introduced through the interpolation is negligibly small compared to the inherent error in the coefficient values.

Using the lift and drag coefficients for each discrete section, the scalar values for the lift and drag forces can be calculated. To be analyzed in the code, however, these scalar force values need to be expressed in the proper vector format. For the drag force, the conversion to vector form is inherently simple. Since the drag force is in the same direction of the resultant incoming flow, the direction of each drag force vector is already known. All that needs to be done then is to scale the vector to the correct length. Determining the vector form of the lift force vector is not as simple. The lift force vector is, by definition, perpendicular to both the resultant incoming velocity vector and the drag force vector. There are two possible perpendicular directions that satisfy this. The correct direction is not expressed in the math. In order to determine the correct direction of the lift force vector an observation is made about the relationship of the incoming resultant flow vector and the cord length vector. By looking at whether the resultant velocity vector approaches the cord from inside the turbine circumference, as opposed to from outside the circumference, as well as the location of the resultant velocity vector with respect to the line perpendicular to the cord of the airfoil, the correct direction can be determined. This approach breaks down at the locations where the angle of attack is equal to 0, 90, and 180 degrees. The magnitude of the lift generated at these specific angles of attack is negligible small, and therefore the direction of the lift force vector is irrelevant.

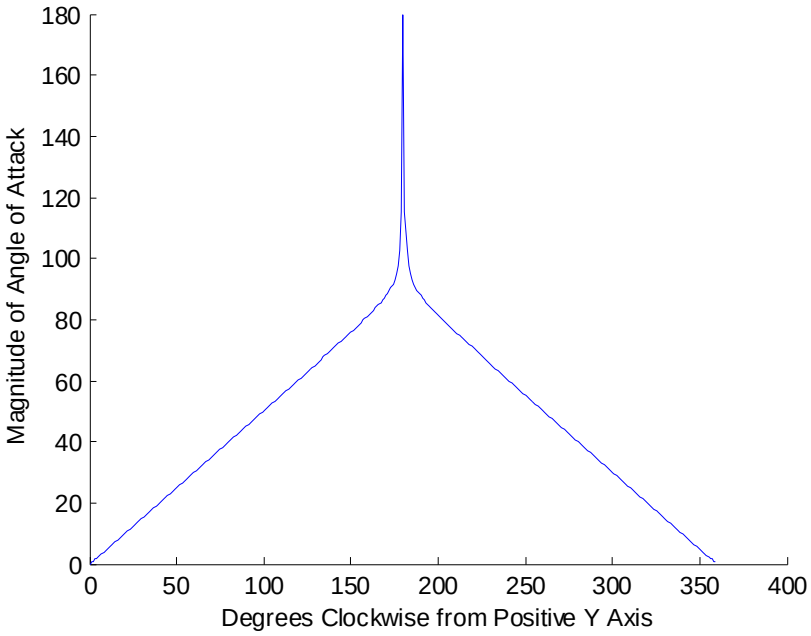

Figure 2.15. Angle of attack trends for the case where the free stream velocity vectors are just larger than the induced velocity vectors.

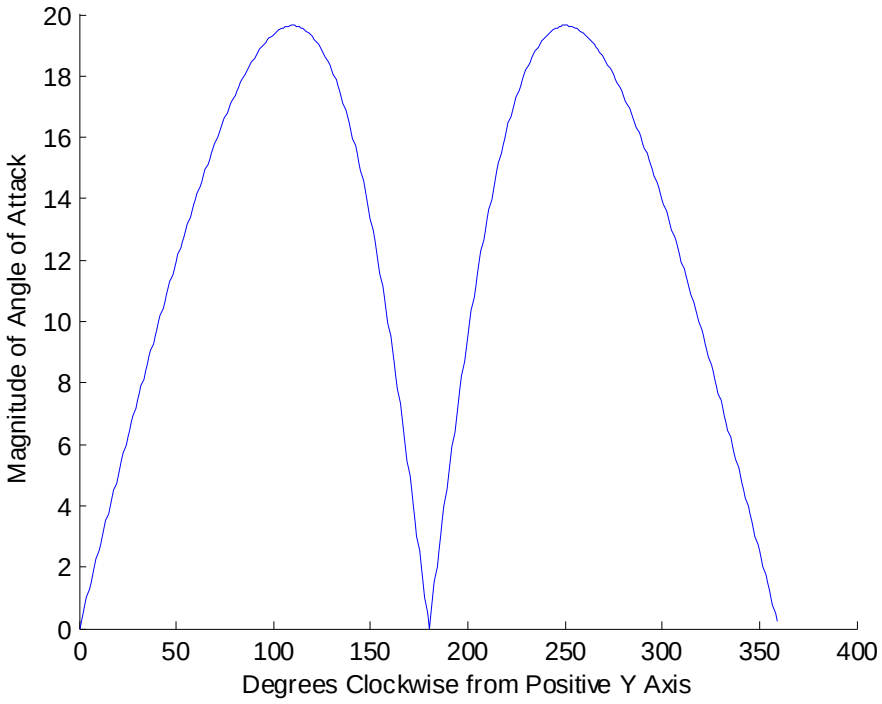

Figure 2.16. Angle of attack trends for a case where the induced velocity dominates the free stream velocity.

As can be seen from the lift and drag vectors around the turbine, as shown in Figure 2.17, both vectors contribute to the torque generation on the turbine. It is therefore necessary to break down these vectors into their normal and tangential components relative to the profile cord. The combination of both lift and drag tangential vectors provides the tangential force acting on each profile. The normal and tangential vectors are shown in Figure 2.18.

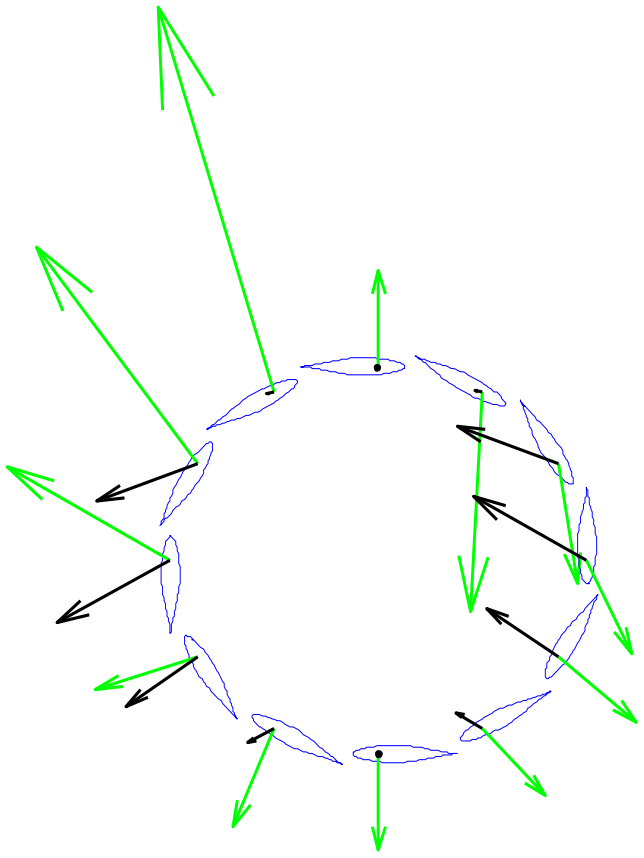

Figure 2.17. Lift and drag vectors on the discrete sections. The green vectors represent the lift, and the black vectors represent the drag.

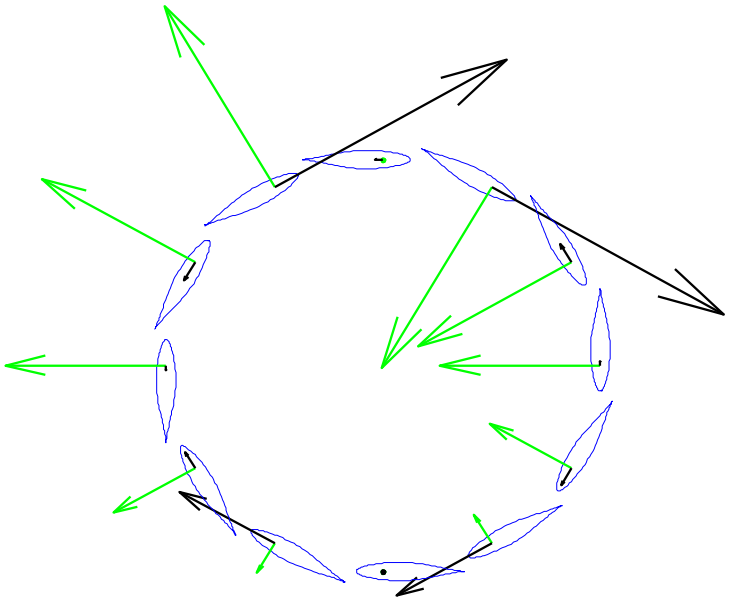

Figure 2.18. Normal and tangential vectors placed on the discrete sections. Green vectors are normal and tangential vectors are black.

These normal and tangential vectors provide a lot of important information about the performance of the turbine configuration being analyzed. The torque generation of the system is determined by taking the summation of each discrete section's tangential force and multiplying it by the moment arm which is the radius of the turbine. By analyzing the tangential force vector at each discrete section it can be seen which discrete sections are providing the greatest torque to the system. It is of note that at large angles of attack, the majority of the drag force is in the positive tangential direction. Thus, some high drag, low lift angles of attack are actually beneficial to the performance of the system. The vectoral summation of the normal vectors provides the drag on the system due to the motion of the airfoils. This drag, it is important to note, is only part of the total drag on the system. A significant portion of the total drag force is due to the pressure drop across

the turbine and is determined through a different method not discussed in this work, though a worst case prediction could be made by assuming the turbine to be a solid cylinder and determining the drag force on that cylinder caused by the flow field.

Even with the torque generation from the fluid flow over the discrete sections being determined, the full analysis in not complete. The torque generation by the system is not a function of solely the resultant tangential force, but rather the full conservation of angular momentum equation, equation 2.13, must be satisfied. This equation includes a term that represents the momentum deficit of the fluid at the rear of the turbine. Since an analytical method to determine the magnitude of this momentum deficit has yet to be developed, the experimental data were used to back-out what this value should be for multiple hydrofoils and flow conditions. It was hoped that there could be found a constant value for this deficit across all turbine geometries, but unfortunately this was not the case. These results are presented and discussed in section 2.7.

Now that the performance of the system has been determined, a set of iterative loops can be added in order to optimize the system design. This is done by varying the key input parameters and evaluating their effect on the performance of the turbine.

2.6 Coefficient Values

In order to create an analysis code that utilizes the two dimensional discrete sections method, it is vital that coefficients of lift and drag are available for all encountered angles of attack. In looking for sources of lift and drag coefficient data, it quickly became apparent that the needed data was not readily available. While thin airfoil theory and usage has long been studied, experimentation and analysis was limited to small angles of attack up to, and just past stall.[19-25] While this trend makes sense, most

airfoils were used for aircraft that do not operate at angles of attack greater than the stall angle; it presents a major problem for vertical axis turbine design. A common example of the available range of coefficients of lift is shown in Figure 2.19.

For any given operation conditions in which the free stream velocity dominates the induced rotational velocity contribution of the resultant velocity, angles of attack from 0 to 180 degrees will be present. Once again, due to symmetry, this represents all possible angles of attack. It is, therefore, essential for the current analysis that tabulated coefficient data be available for all possible angles of attack.

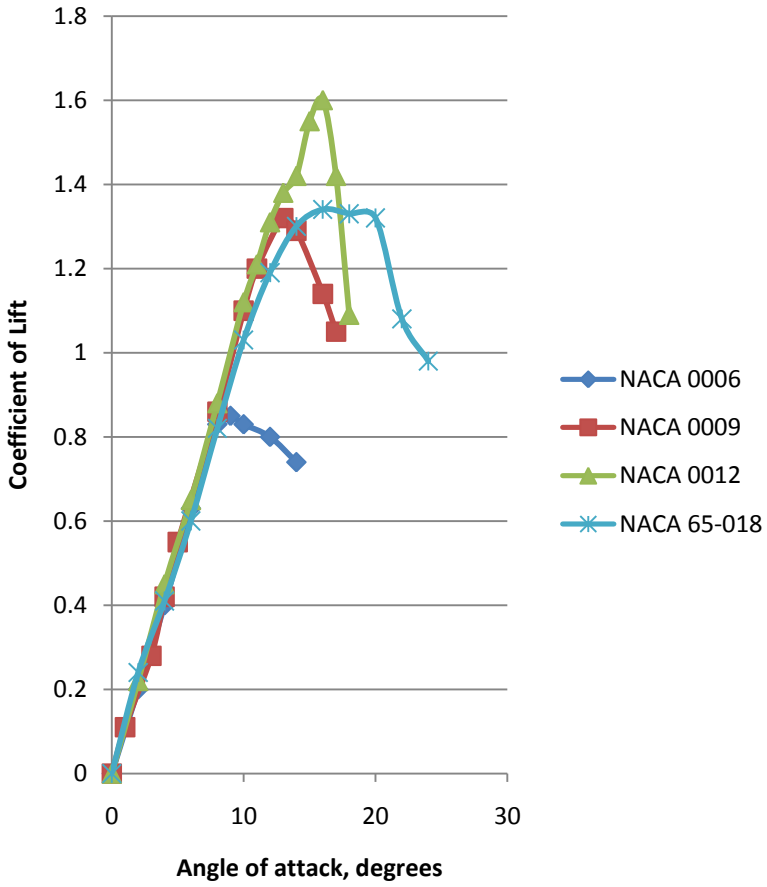

Figure 2.19. Coefficient of Lift values for different airfoil sections.[19]

Initial searches for tabulated data for the airfoils of interest at all possible angles of attack yielded no reliable results. Furthermore, each independent source of coefficients presented values for both lift and drag[19, 26-30]that differed from each other by up to 50 %. This introduced a level of uncertainty to the published experimental data. Thus computational fluid dynamic analysis software was used to calculate the needed coefficients. While computational packages such as Fluent do a good job analyzing simple two dimensional flow cases, a few issues arise with the current case.

ANSYS Fluent Version 12 was used to analyze the desired airfoils at angles of attack ranging from 0 to 180 degrees. The Spalart-Allmaras[36] analysis was used to model the viscous effects of the fluid, and sufficient downstream room was given to allow for convergence. While quick and accurate results were produced for small angles of attack, the computational analysis showed poor accuracy with regards to stall effects. When comparing the computational results with published experimental data near stall angles, it was apparent that the magnitude of the angle of attack was consistently under predicted just before stall and over predicted after stall. The relationship between the Fluent and Theory of Wing Sections[19] data is shown in Figure 2.20. Furthermore, angles of attack close to 90 degrees required a significantly increased downstream length for convergence to occur and needed a lengthy amount of time to converge.

Due to the stall inaccuracies and time requirements for large angles of attack, a more in-depth search was made to find published experimental data for 180 degree coefficients of similar airfoil profiles. A study was found in which Sandia National Laboratories[26] had partnered with Wichita State University to conduct a series of tests on

seven symmetric airfoils. These are shown as Figure 2.21. From these tests the coefficients of lift and drag for initial angles of attack, up to just past stall, follow a similar trend as data published in other sources. However, at about 30 degrees angle of attack to 150 degrees, the coefficients of lift and drag were the same values for all airfoils tested. This caused concern as to the accuracy and validity of the tests. From further thought, however, it was noted that at angles of attack close to 90 degrees, an airfoil would behave like a flat plate perpendicular to the flow. Furthermore, any airfoils with the same cord length should be expected to have almost similar behavior as such angles of attack. Yet, as the thickness of the airfoil increases, its shape more closely resembles an ellipse. Thus the behavior of an airfoil as the angle of attack approaches 90 degrees may more closely resemble the behavior of an ellipse than a flat plate. Finally it must also be noted that, by design, the leading edge of an airfoil is substantially thicker than the trailing edge of an airfoil. Considering together all of the aforementioned points, it is concluded that the behavior of an airfoil at angles of attack approaching 90 degrees will be bound by the behaviors of both a flat plate and an ellipse of lengths equal to that of the airfoil. Additionally, the behavior of the airfoil will not be symmetric about 90 degrees due to the fact that the leading edge will tend more to the behavior of the ellipse than the trailing edge. The flat plate and ellipse bounds for the coefficient of drag are shown in Figure 2.22. Also included is the coefficint of lift for a flat plate. This coefficient is used to provide a boundry for the coefficient of lift at angles of attack between 45 and 135 degrees.

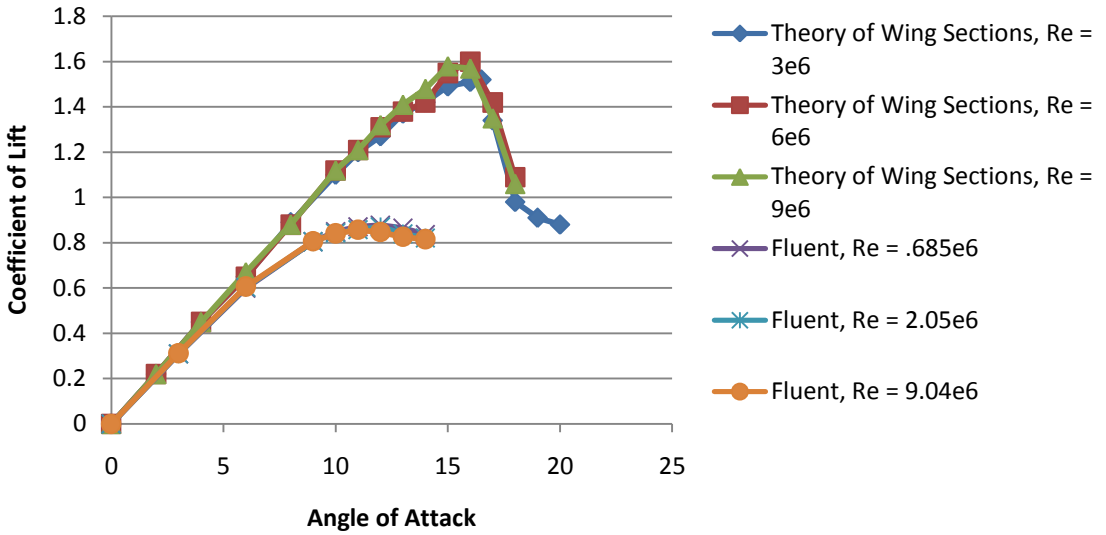

Figure 2.20. Comparison of coefficient of lift data between Theory of Wing Sections[19] and Fluent.

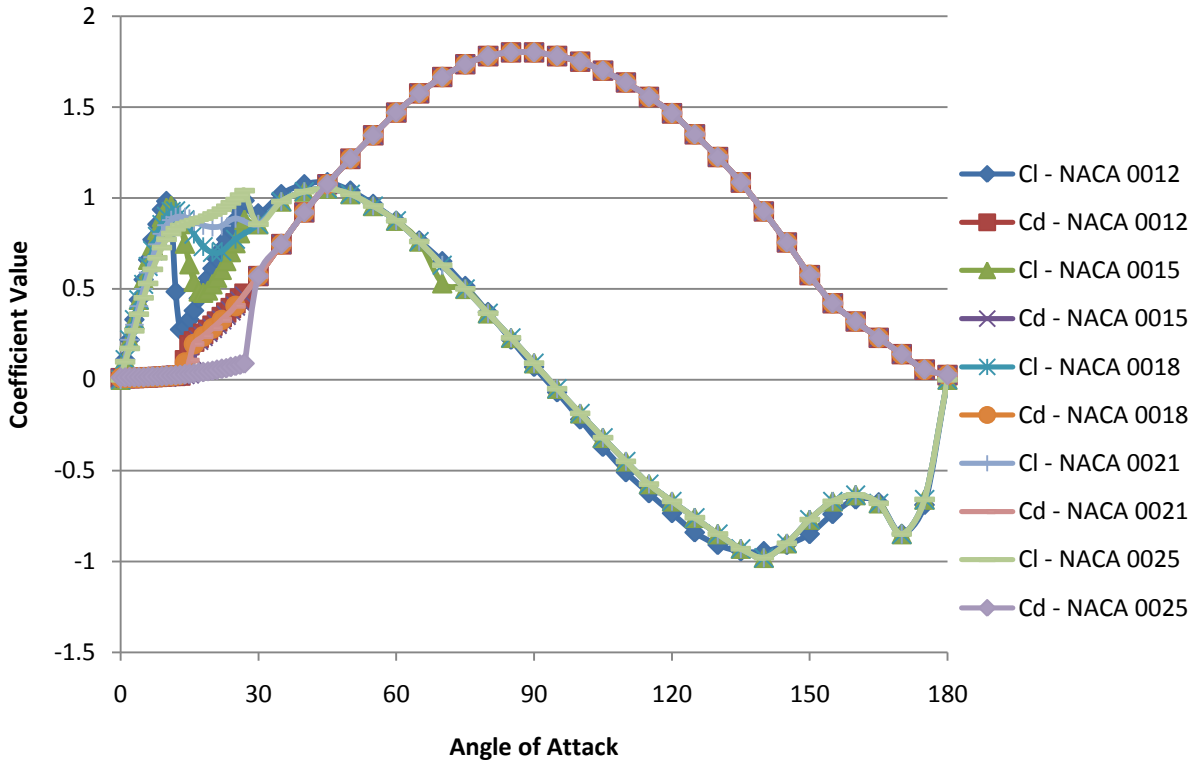

Figure 2.21. Coefficient data from Sandia research.[26]

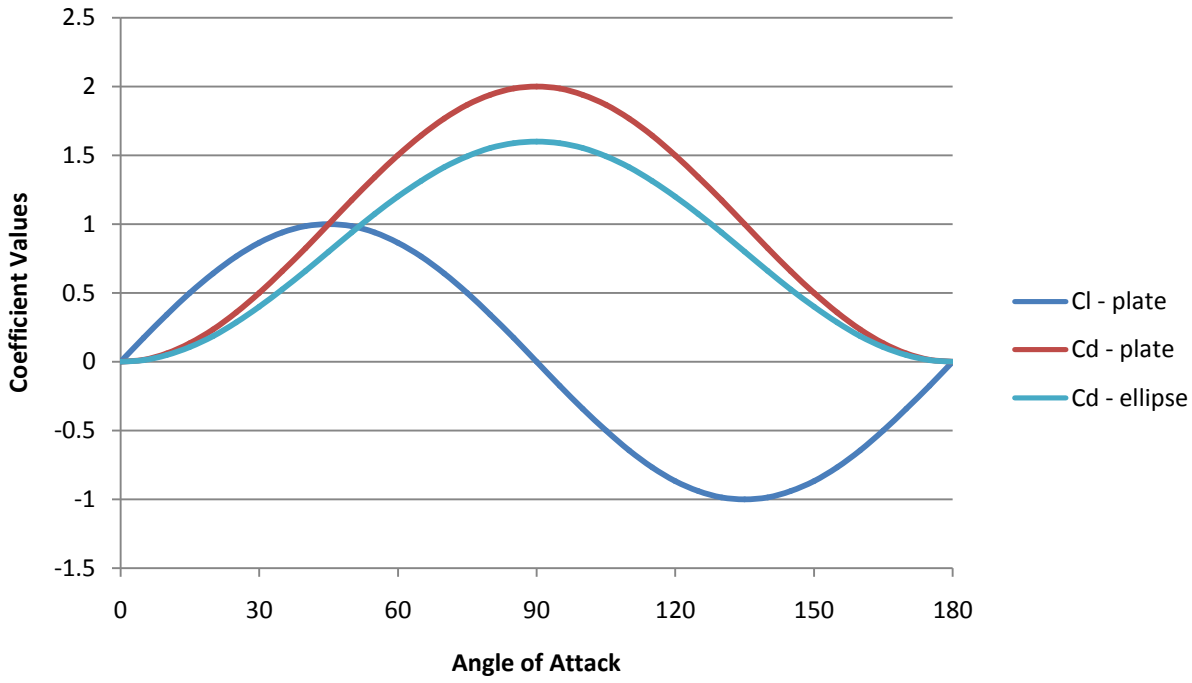

Figure 2.22. Coefficients for a flat plate and an ellipse[21-23]

One final point of interest, both the Fluent, and Sandia data indicate that at an angle of attack of 45 degrees the coefficient of lift equals the coefficient of drag, and that at 135 degrees, the coefficient of lift is equal to the negative of the coefficient of drag. Additionally, because the front of an airfoil more closely resembles an ellipse that the back end, the coefficient of lift is not equal to 0 at 90 degrees, but at an angle of attack just larger than 90 degrees. Unfortunately when comparing the experimentally and computationally published data, there exist large discrepancies for similar airfoils under similar flow conditions. The coefficients of lift from various sources[19-30] for the NACA 0012 airfoil at a Reynolds number ranging from 1e6 to 1e7 can be seen in Figure 2.23.

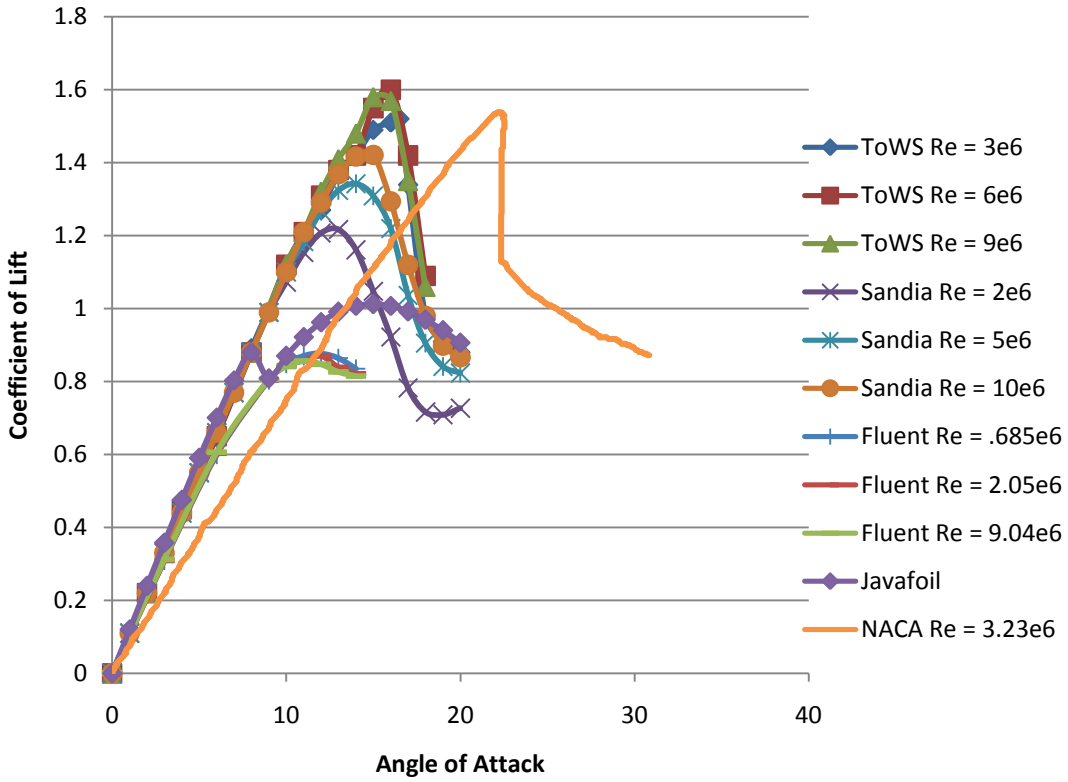

Figure 2.23. Inconsistencies in the different sources of coefficient of lift data.[19-30]

Utilizing all of the aforementioned data, trends and values, coefficient of lift and drag were determined for multiple symmetric airfoils. This was done by finding a best fit curve to all of the available data, giving more weight to sources in which a higher confidence can be placed. The values of the coefficients of lift and drag for the NACA 0009, NACA 0015, NACA 0020, NACA 0022, and NACA 65_3-018 that are used for the computational analysis are shown in Figures 2.24 and 2.25, respectively. For better accuracy of these values, a significant amount of testing, both experimentally and computationally, needs to be preformed. While current coefficient value estimations are based off of experimental results, the results of the current analysis propagate any errors in these values.

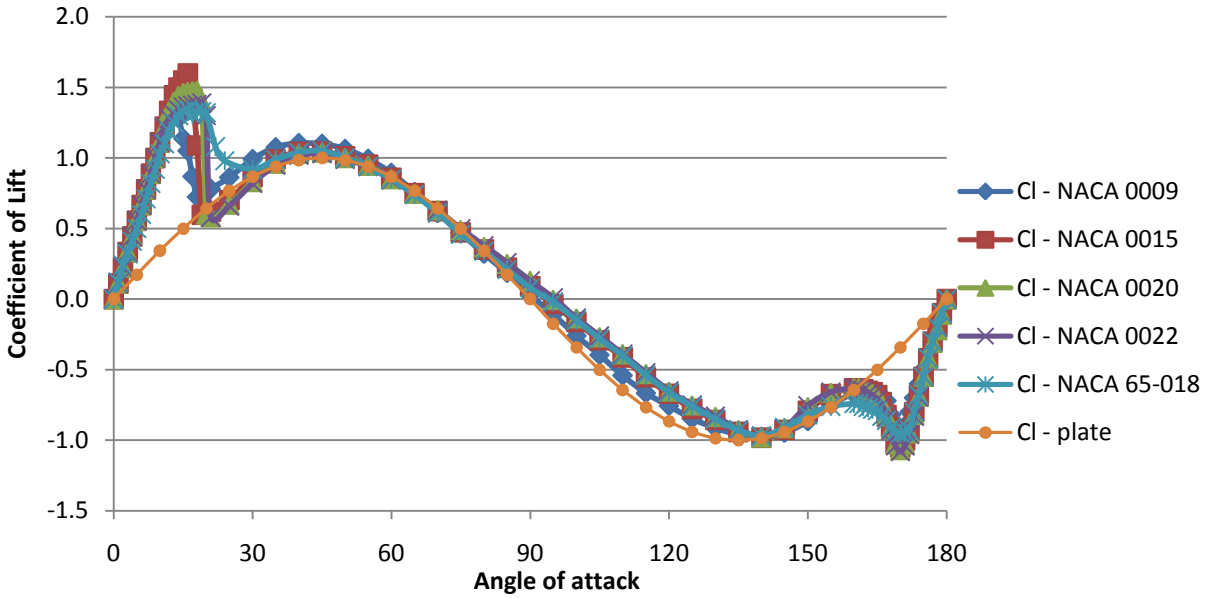

Figure 2.24. Coefficients of lift as used in the code.

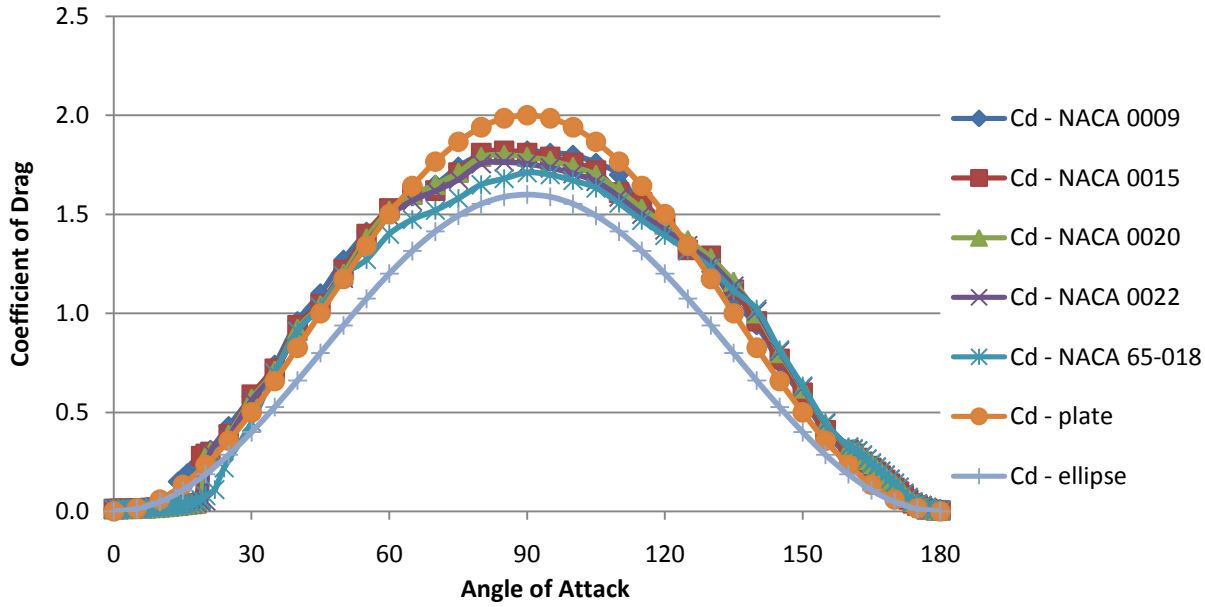

Figure 2.25. Coefficients of drag as used in the code.

Two further assumptions were made about the performance of these airfoils and their corresponding lift and drag coefficients. First, it was assumed that the values of the coefficients were independent of the Reynolds number of the fluid. This is not a great assumption, for it has been shown, both experimentally and computationally, that the performance of an airfoil is indeed dependant on the Reynolds number.[19-30]Looking at Figures 2.12 and 2.13, it can be seen that the extremes, both high and low, of the Reynolds number range occur at locations where the angle of attack is close to 0 degrees, and thus the lift and drag forces cases are near zero. The Reynolds number range for the locations that contribute the most to the tangential force are on the same order of magnitude, making this assumption acceptable.

The second assumption that was made is that the effects of hysteresis are negligible. Hysteresis, for this situation, is the phenomena where the performance of an airfoil in a fluid is a function of the direction of the airfoils change in angle of attack.[19] Simply put, the angle of attack at which flow separation and airfoil stall occurs while the angle of attack of the blade is being increased is different than the angle of attack at which stall and flow separation return to laminar, lift producing performance as the angle of attack of the blade is decreased. Thus, the performance of a discrete section a given angle of attack close to the separation and stall angle will perform differently depending on the trend in the change of their angle of attack.

2.7 Results

The original plan for this project was to be able to use the experimental data that was collected in conjunction with this project to validate and affirm the results produced by the computational model. However, due to errors in the coefficient data, as well as

from the assumptions that were made, there is a consistent under-estimation of the torque produced by the turbine model in comparison to the experimental data. Furthermore, the experimental data is needed to determine the magnitude of the downstream momentum loss. On a positive note, however, the code is producing the expected trends. These trends are shown in Figures 2.26 through 2.28. These figures show the comparison between experimental and computational torque speed curves for multiple turbine configurations.

A great amount of effort was put into the code to try and determine where the majority of the error was coming from and, additionally, if the magnitude of the error was consistent across multiple turbine blade profiles. It was determined that there was no obvious source of error in the code, and that the amount of error was different for each flow condition. The error, then, must be associated with one or more of the assumptions made in the development of the model. This error from these assumptions needs a significant amount of further study to fully understand the turbine behavior and improve its modeling.

Figures 2.29 through 2.31 show the required values of a needed to correctly model the no load speed for each configuration at multiple speeds. These values were calculated by solving equation 2.13 for a using the experimental values for rpm and torque. For the NACA 65_3-018 and the NACA 0022 the values are mostly constant. This trend, however, does not hold for the NACA 0020.

Finally, while the results do not completely match the experimental data, the model does provide a good method for learning about the governing dynamics of the system. Figures 2.32 and 2.33 show the normal and tangential vectors for two different flow situations. These figures show that depending of the speed of the incoming flow, the

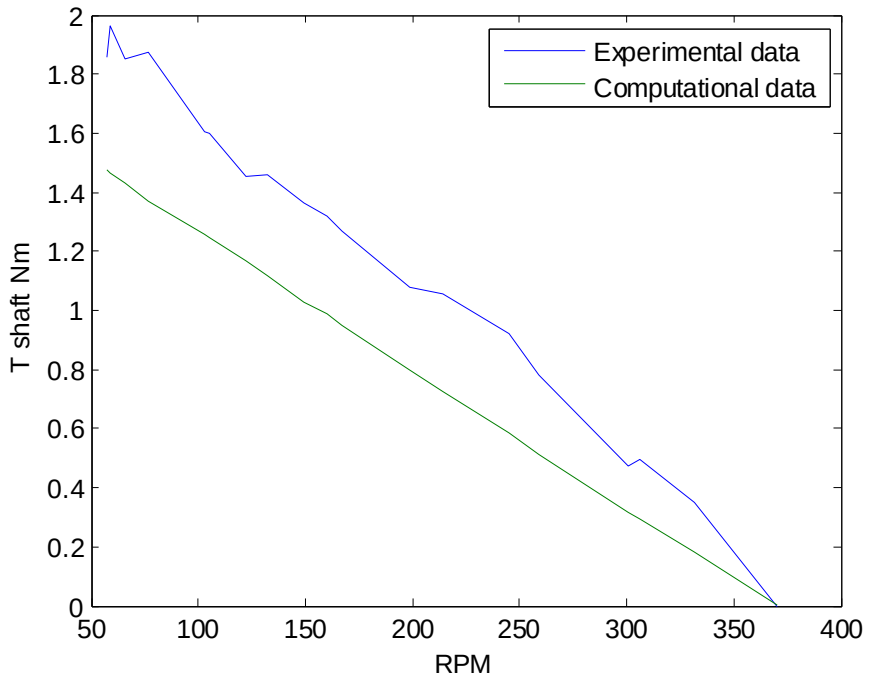

Figure 2.26. Comparison of computational and experimental torque speed data for NACA65-018

location of the discrete sections that produce the most torque change location around the circumference of the turbine. By studying where the greatest tangential force is generated, it can be understood how to modify the design to optimize power production. This is accomplished by designing the turbine to produce peak torque at the predicted operating conditions.

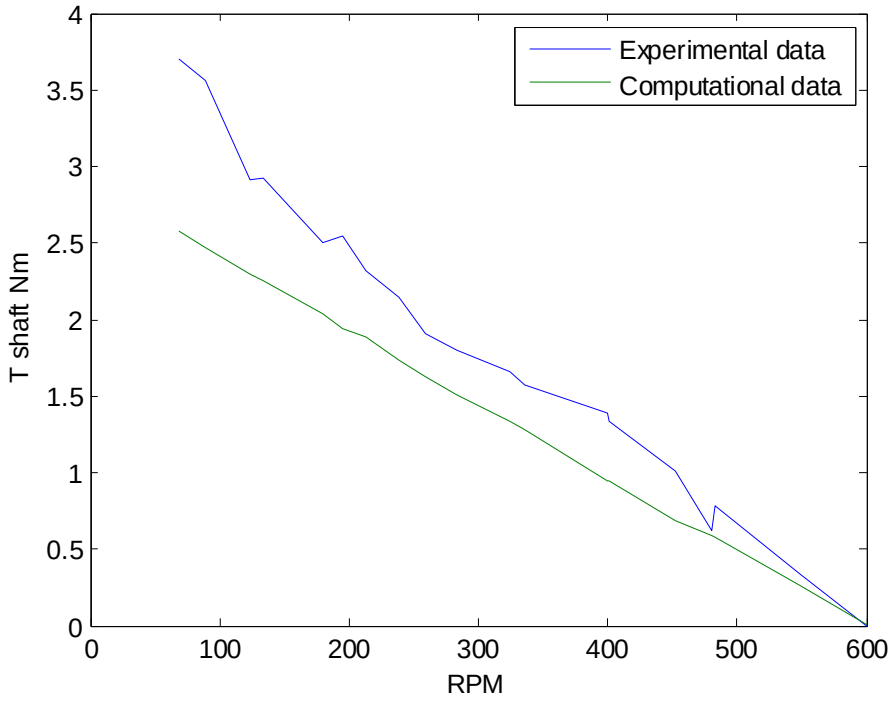

Figure 2.27. Comparison of computational and experimental torque speed data for NACA0020

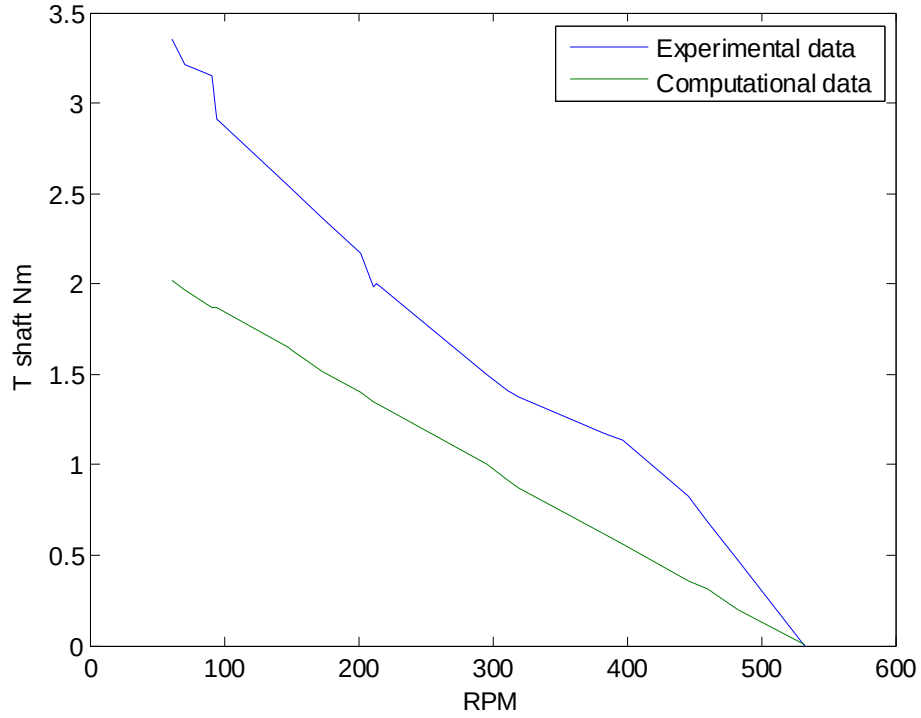

Figure 2.28. Comparison of computational and experimental torque speed data for NACA0022

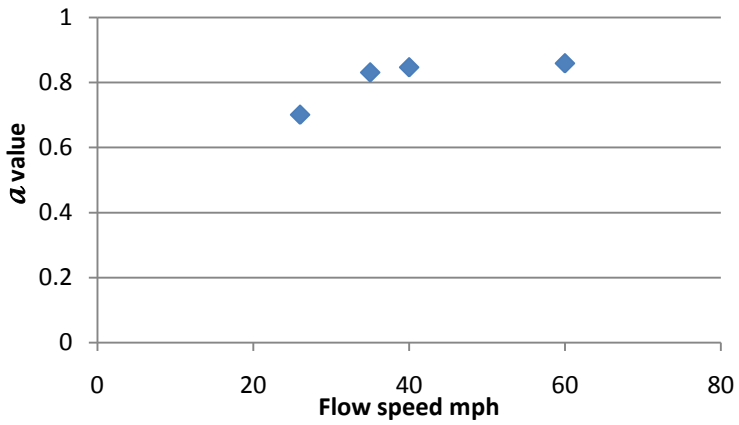

Figure 2.29. *a* values for the NACA0020

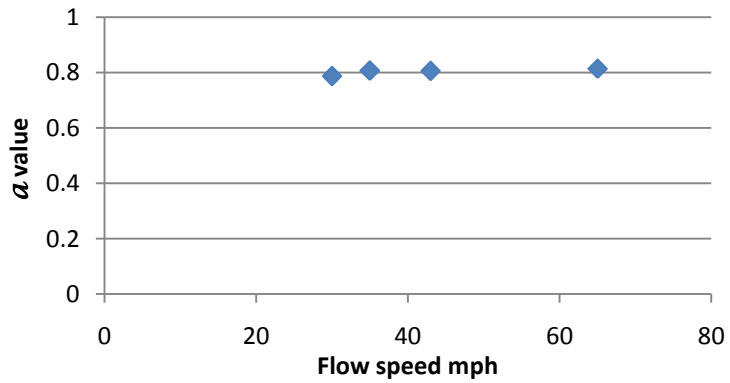

Figure 2.30. *a* values for the NACA0022

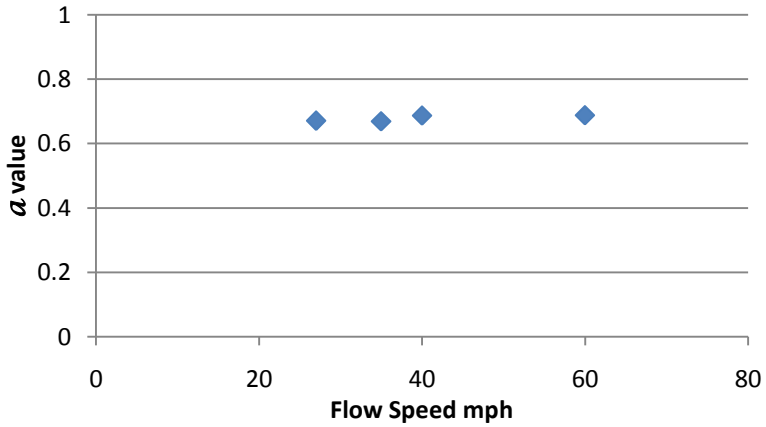

Figure 2.31. *a* values for the NACA65-018

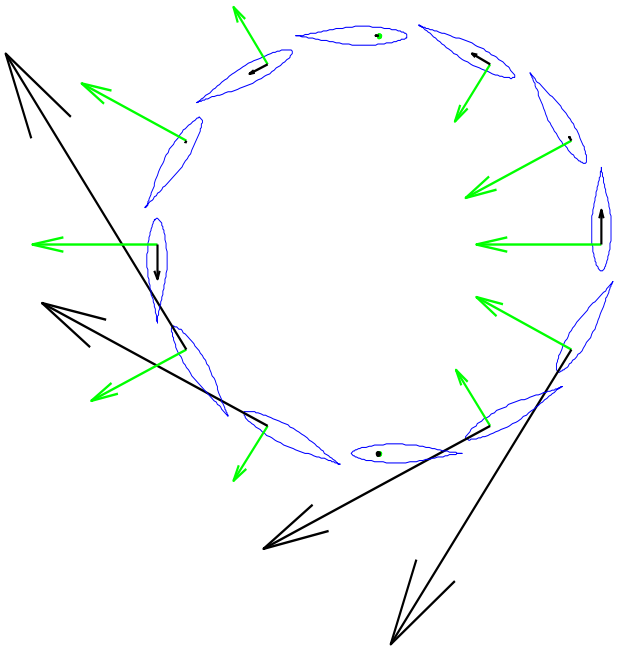

Figure 2.32. Normal and tangential vectors for the case were RPM = 0.

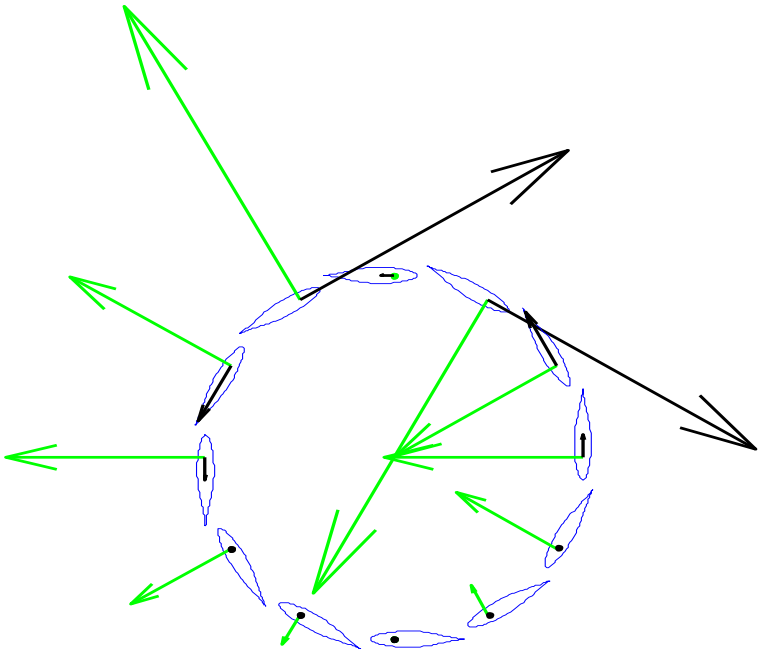

Figure 2.33. Normal and tangential vectors for the case were RPM > 0.

2.8 Sources of Error

From looking at the results, it is clear that there are sources of error still in the code. It is believed that most of this error can be attributed to the many assumptions made in the development of the code. The majority of these sources of error could be reduced by further study and understanding of the how these turbines work and how to refine the model to better represent the actual turbine performance.

The major assumption behind the development of the code is that the turbine can be modeled by dividing it into multiple thin, but finite, discrete sections. These sections can then be evaluated as an airfoil profile in a two-dimensional flow. This approach introduces some error by neglecting all three-dimensional effects. As discussed earlier, it is assumed that this simplification contributes only a small amount of error due to the fact that the flow and force generation is primarily in just the two dimensional plane.

A major source of error in the system is the error that was introduced from inherent discrepancies in the sources of the coefficients of lift and drag. Knowing the correct values for these coefficients is essential for correctly modeling the turbine performance. Any errors in these data will be greatly compounded through the analysis. One additional source of error in these coefficient values is due to the fact that it was assumed that the performance of these hydrofoils is independent of Reynolds number. While reliable sources[19] indicate that performance of the airfoils are largely independent of Reynolds number for a significant portion of the airfoils performance region, there are large changes in the velocity magnitude around the path of the turbine blades which result in some variance of airfoil performance.

An assumed, simplified model of the downstream momentum loss is used. This model applied an averaged, constant loss to the downstream velocity of the turbine. A more accurate model would reduce error by better modeling which discrete sections are affected by the momentum loss, and the magnitude of the loss at each section.

Stall angles and coefficient values are a function of the direction of rotation. This effect, called hysteresis, is ignored in the code. The major effect of hysteresis is that the angle of attack as which stall occurs as the angle of attack increases is different than the angle of attack at which the flow over the airfoil returns from stall performance to peak lift generation. This further contributes to the error in the coefficient data because there is only one set of coefficient data in the tabulated data used by the code.

The incoming flow vectors were assumed to be parallel to the direction of the incoming free stream velocity at each discrete section. Due to the pressure drop across the turbine, some of the flow will be forced around the turbine instead of through it. This effect will change both the magnitude and direction of these free stream velocity vectors. This is a function of both the solidity of the turbine as well as the rotational speed of the turbine. As either of these values increases, the more the turbine behaves like a solid cylinder.

A simple model using a constant momentum deficit at each downstream location was used to model the free stream velocity vectors on the sections at the back half of the turbine. This introduced some error into both the direction and magnitude of the resultant velocity vectors on the downstream discrete sections. A better model of this momentum and velocity deficiency could reduce these errors.

An average resultant velocity vector, located at the center of lift, was used. This is an average of all the resultant velocity vectors that would be incident along the length of the cord. Accuracy from this assumption decreases with cord length. It is not fully understood how this change of resultant velocity vectors along the length of the cord effects the performance of the airfoil.

Effects from the twist of the blades or from the offset of one discrete section from those next to it were ignored. This twisting phenomenon is closely related to the three-dimensional effects of the fluid flow that have been ignored in this analysis. Like the three dimensional effects, it is assumed that the effects from blade twist will be negligible.

2.9 Conclusion

In spite of the complicated nature of the system being analyzed, and the errors in the magnitudes of the computational results, there were still a large number of important conclusions that were achieved by the analysis.

The modeling and analysis of this type of turbine is both a unique and complicated problem. Multiple important input parameters greatly affect the performance of a turbine design. Furthermore each of these input parameters influence other key parameters. This greatly complicated the analysis process and compounded the number of test cases needed to fully understand the effects on performance of each input parameter.

The torque generated by the turbine is not solely a function of the tangential force acting on each of the blades. For a complete understanding of torque generation and energy transfer through the system, the conservation of momentum equation must be

satisfied. Understanding of the downstream momentum loss is crucial in evaluating the energy produced by a turbine.

In spite of the number of assumptions, and the associated error introduced to the model from each of them, the model still produces the correct trends for the turbine performance. The magnitude of the computational torque predictions, however, is consistently lower than those showed by the experimental results.

Peak performance of a discrete airfoil section for a given turbine configuration occurs when an airfoil profile exhibits a high coefficient of lift value at high angles of attack. This provides for a large lifting force at an angle of attack large enough to produce a significant force in the tangential direction. Trends from the current analysis indicate that a NACA0015 would improve performance.

For rotational speeds ω close to, and equal to zero, the discrete sections with angles of attack near 45 degrees produce a large drag force. Much of this force is in the tangential direction and contributes to torque generation. This phenomenon increases the ability of the turbine to be self starting.

The computational analysis indicates that greater performance can be achieved at higher rotational speeds. At these higher rpm speeds, the induced velocity dominates the free stream velocity and the angles of attack are shifted towards zero. This leads to more favorable angles of attack at all sections which results in greater torque generation potential. While current tests do not demonstrate these effects, they could provide great insight into methods aimed at improving the efficiency of the turbine design.

In light of the original project objectives, to provide an increased understanding of the governing principles of how these turbines operate and to provide a means to

optimize the design of a turbine system for a given flow condition, this project was successful in that it was able to provide a better and more thorough understanding of the dynamics of the design problem. Furthermore, the code was able to predict the correct trends for turbine performance. Discrepancies in the magnitudes of the results could be improved with more in depth study of key assumptions used in the code.

CHAPTER 3

EXPERIMENTAL ANALYSIS

3.1 Introduction

In addition to the aforementioned work an experimental analysis for the optimization of a helical turbine was also completed. The objectives of this chapter include validating the computational results found in Chapter 2 as well as experimentally testing multiple important parameters that affect turbine performance. The ultimate goal of this chapter is to find a much better performing turbine configuration compared to the initial water turbine design.

In order to complete these objectives, seven different turbine configurations were analyzed, manufactured, and experimentally tested. Three variable studies took place examining the effects on turbine performance due to airfoil selection, number of blades, and turbine solidity. The first study utilized a NACA 653-018, NACA 0020, and NACA 0022 airfoil to investigate how different profiles influence turbine efficiency. It should be noted that the NACA 0020 airfoil was chosen as a baseline profile, since the majority of helical turbine research to date has been done using this profile.[1-4] Next, keeping the airfoil constant (NACA 0022) the number of blades per turbine was varied. Two, three, and six blades per system were tested. The final variable included varying the solidity of the turbine while still keeping the airfoil (NACA 0022) and blade number (3) constant.

The solidities were varied in 7% increments from 41% to 55%. Solidity is defined as the fraction of the total projected frontal area of the turbine that the blades cover. All blades for the experimental test turbines were constructed with a rapid prototype machine. Due to the size constraints of the construction machinery, the two-bladed turbine was manufactured with a solidity of 41% and was compared to the three-bladed turbine of the same solidity for the number of blades per turbine study. The six-bladed turbine on the other hand, was able to be built at the standard solidity of 48%.

Multiple problems were encountered in testing the full-scale turbine in water, which were accounted for in testing the scaled models. First, a wind tunnel was used for testing these turbines. The wind tunnel allowed for maintaining constant incoming velocities with uniform flow, wherein the incoming flow-speed could be varied. Additionally, tests were designed to measure both torque and drag, wherein drag was not measured in testing the initial water turbine. Lastly, testing multiple configurations will yield great insight into the effects that each parameter has on turbine performance whereas only one configuration was able to be tested previously. The following sections of this chapter will discuss in detail how each of the experimental objectives was satisfied.

3.2 Analysis of Turbine Configurations

In order to understand the terminology in this section, Figure 3.1 was created to provide a visual cue concerning what a helical turbine looks like. This image was created as a drawing in SolidWorks. In this figure, the top image is the frontal view of the turbine wherein the axis and top hub have been removed for clarity. The bottom image is a top view of the turbine. This is a three bladed turbine, therefore it can be seen that each blade

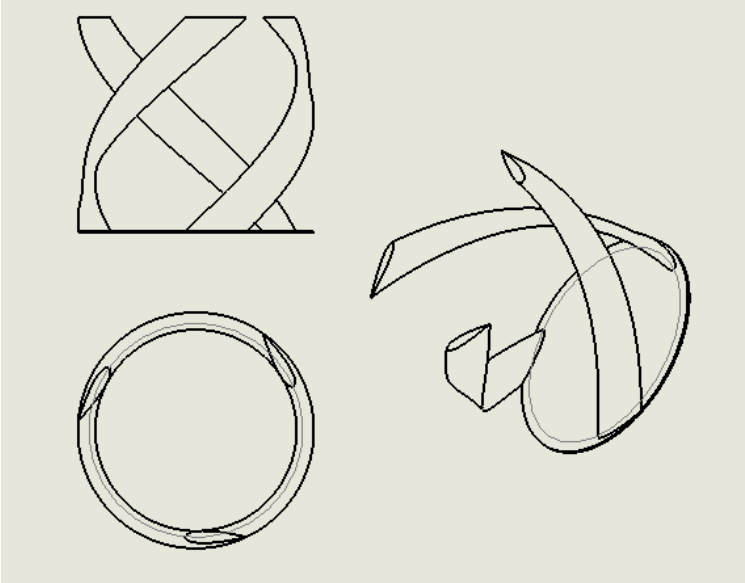

Figure 3.1. SolidWorks drawing of helical turbine example

sweeps 120 degrees thus covering the full 360 degree circumference. The final image on the right is a skewed view meant to give the reader more insight into the design of the turbine.

Knowing what a helical turbine looks like, the first study involved varying the blade profile. Of the many airfoil profiles to choose from, the study was restricted to airfoils that perform optimally in low Reynolds number regimes. This turbine must operate in flows of 0.69 to 1.83 m/s (2.00-6.00 ft/s). Using Equation 3.1, the range of Reynolds numbers was calculated.

$$Re = \frac{\rho V D}{\mu} \tag{3.1}$$

In this equation, ρ is the density of water, V is the incoming flow velocity, D is the turbine diameter and μ is the kinematic viscosity of water. The Reynolds numbers for this scenario ranged from 2.84E5 to 8.53E5. In comparison, the Reynolds number operating regime of most airfoils used for aircrafts ranges from 6.3E6 for a small Cesna to 2.0E9

for a Boeing 747.[31] Obviously, the Reynolds number regime for these turbines is quite low. Knowing this, the first choice for an airfoil profile was the NACA 0020, as this profile has been used and tested extensively by previous researchers.[1-4] This airfoil selection would allow for a baseline comparison while at the same time falling into the category of low Reynolds number airfoils. The Theory of Wing Sections manuscript was then consulted for additional profiles designed for optimal performance in low Reynolds number regimes.[19] With several airfoils to choose from, Figure 3.2 was generated. This figure compares the ratio between the coefficient of lift and the coefficient of drag as a function of the angle of attack.

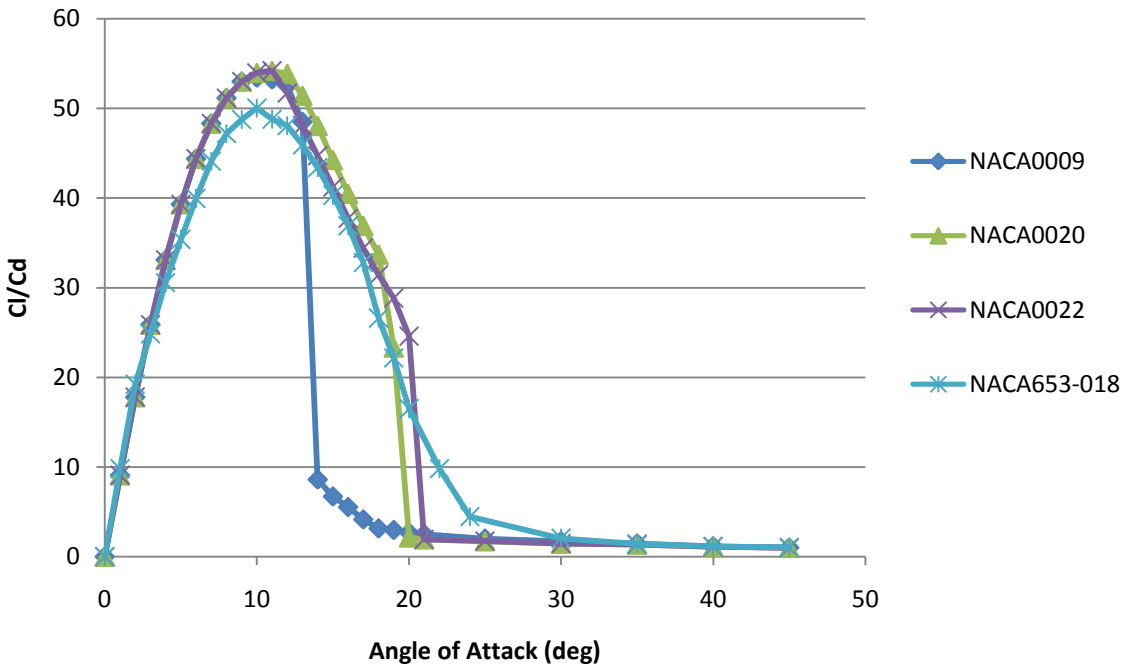

Figure 3.2. Plot of the ratio between the coefficient of lift and the coefficient of drag

The reason for using Figure 3.2 to select airfoils concerns the way in which these turbines operate and manipulate a uniform incoming flow, which is very different than a standard airfoil. Given an incoming flow-speed, these turbines are designed to utilize the lift force produced by the airfoil to begin rotating at some angular velocity. The constant incoming flow and resulting angular velocity combine to form an overall resultant velocity. This resultant velocity vector will change as the angular velocity increases until the turbine reaches a steady state. Once at steady state it is the resultant velocity vector which ultimately dictates the angle of attack that the blades see from the flow. Thus, Figure 3.2 shows at what angle of attack and at what magnitude the coefficient of lift is greater than the coefficient of drag. As can be seen in this figure the coefficient of lift is greater than the coefficient of drag for approximately 45 degrees, for all airfoils, however the magnitude of the differences of these coefficients is different for each airfoil. Since the amount of positive torque that will be created from an airfoil can ultimately be related to the area under each curve, Figure 3.2 provides an accurate method for selecting airfoils to be tested. From this process the NACA 0022 and NACA 653-018 profiles were additionally chosen for testing. For visual purposes, Figure 3.3 was created to show the profile difference between these three airfoils as well as the NACA 0009 which was used for the initial water turbine design.

The next study was to vary the number of blades per turbine, as it was suspected by the authors that flow interference between the blades would make a direct impact on the turbines efficiency.[8] This variable is much more difficult to model computationally as three dimensional, rotating models in CFD programs such as Fluent are extremely computationally expensive.

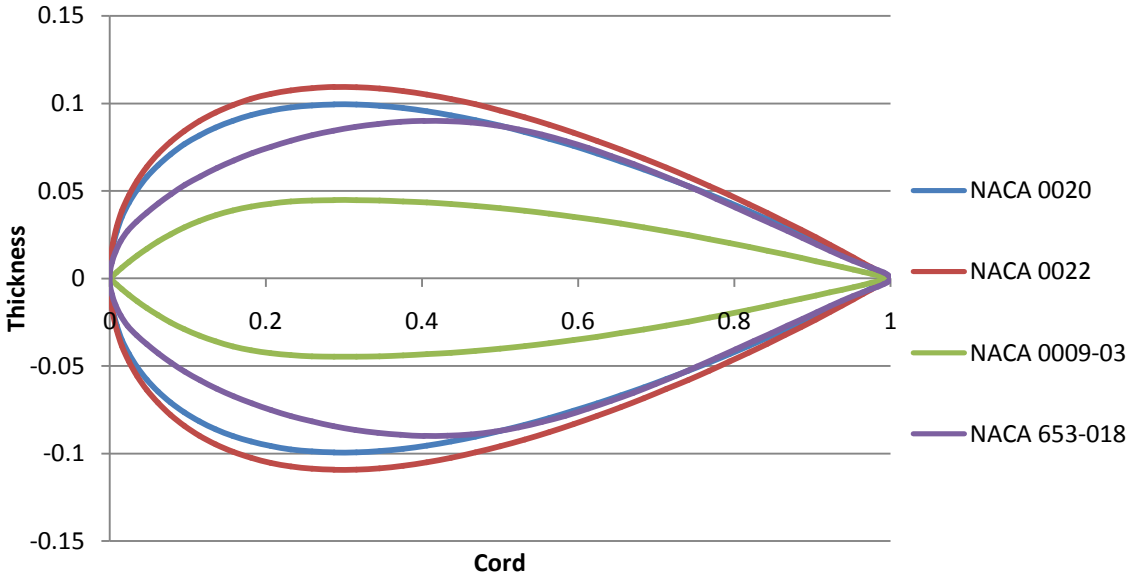

Figure 3.3. Airfoil profiles

Thus, it was decided that comparing the results of this variable experimentally would be the most appropriate. Three turbines were created using the NACA 0022 profile with two, three, and six blades per turbine. The number of blades per turbine was specifically chosen around the conventional three-bladed turbine so that one design would have less blades and one would have more. The three-bladed design was again chosen as a baseline, as the majority of previous research has been done with this design.[1-4] The six-bladed system was chosen as this would allow for a better understanding of the performance of the initial water turbine design (as it too was composed of six blades), while two blades were chosen to be the lowest sensible number of blades for manufacturing purposes.

The final test variable, solidity, is extremely important in the design of these turbines. Recall that solidity is defined as the projected frontal area of the turbine blades divided by the overall projected frontal area of the turbine. It can be imagined that if a helical turbine were allowed to rotate infinitely fast it would appear solid, replicating the shape of a cylinder. Once the angular velocity is achieved wherein the turbine replicates a solid cylinder, it obstructs all of the incoming flow rather than engulfing some portion of the incoming flow.[2] Thus, there is a vital connection between the solidity of the turbine and its angular velocity where the flow will discontinue flowing through the turbine (which is the necessary factor to harvest energy) and will begin flowing around the turbine. This implies that there is a point where too large of solidity or too high of a rotational speed would be detrimental to turbine performance. On the other end of the spectrum, because this is a lift-based turbine and lift is proportional to the planar area of the airfoil, there is a point where the value of solidity becomes too low and does not

provide enough lift to produce optimal, positive torque. Previous research indicates that the most common solidity tested is approximately 48%.[1-4] With this parameter being very sensitive to the turbines performance a 7% lower and higher solidity was chosen to be tested, as 41% and 55%, respectively. This value was chosen to create a large enough difference in performance for a trend to be noticed but not large enough to render a turbine useless. Once validated, the computational model can be used to complete a full study of solidity versus turbine efficiency in order to hone in on an optimal solidity for a given set of design constraints.

3.3 Turbine Scaling

Before manufacturing of the experimental turbines occurred, the original turbine design was properly scaled down to ensure both geometric and dynamic similarity between water and air. Knowing that torque and drag force would be tested, the Buckingham Pi procedure was used to determine the proper nondimensional parameters to match while scaling. To do this, torque and drag force are expressed as functions of the independent variables on which they depend as seen in Equation 3.2 and 3.3.

$$T = f(V, \rho, \mu, \omega, D, c, h) \tag{3.2}$$

$$F_D = f(V, \rho, \mu, \omega, D, c, h) \tag{3.3}$$

These equations can be rewritten in a form more conducive to the Buckingham Pi process. The Buckingham Pi Theorem[32] states: Given a relation among n parameters of the form

$$g(T, V, \rho, \mu, \omega, D, c, h) = 0 \tag{3.4}$$

$$g(F_D, V, \rho, \mu, \omega, D, c, h) = 0 \tag{3.5}$$

the n parameters may be grouped into n-m independent dimensionless ratios, or Π groups. Since both of these parameters are functions of the same variables the Buckingham Pi process will only be shown for torque as it is nearly identical for drag force. The next step is to select a set of fundamental, primary dimensions. For this case MLt was chosen as it encompasses all of the units for these systems, where *M* represents mass, *L* represents length and *t* represents time. All of the variables are then written in terms of their primary dimensions as seen in Table 3.1.

At this point the goal is to select a number of variables equal to the number of primary units chosen, such that no variable has repeating units. *D,* ρ, and ω were selected although this process could be solved equivalently by choosing a different set of variables that satisfy the previously mentioned requirement.

The next step is to set up dimensional equations by combining these parameters with each of the other parameters to form dimensionless groups. This process results in Equations 3.6, 3.8, 3.10, 3.12, and 3.14. Each of these equations is then solved as shown in the boxed equations. Substituting the results back into a single form yields Equations 3.7, 3.9, 3.11, 3.13 and 3.15 at which point each of these groups should be checked to ensure nondimensionality.

Table 3.1. Variables written in terms of their primary dimensions

T	V	ρ	μ	ω	D	c	h
$\frac{ML^2}{t^2}$	$\frac{L}{t}$	$\frac{M}{L^3}$	$\frac{M}{Lt}$	$\frac{1}{t}$	L	L	L

$$\pi_1 = D^a \rho^b \omega^c T = (L)^a \left(\frac{M}{L^2}\right)^b \left(\frac{1}{t}\right)^c \left(\frac{ML^2}{t^2}\right) = M^0 L^0 t^0 \quad (3.6)$$

M	b+1 = 0	a = -5
L	a – 3b+2=0	b = -1
t	-c-2 = 0	c = -2

$$\pi_1 = \frac{T}{\rho \omega^2 D^5} \quad (3.7)$$

$$\pi_2 = D^a \rho^b \omega^c V = (L)^a \left(\frac{M}{L^2}\right)^b \left(\frac{1}{t}\right)^c \left(\frac{L}{t}\right) = M^0 L^0 t^0 \quad (3.8)$$

M	b = 0	a = -1
L	a +1 = 0	b = 0
t	-c-1 = 0	c = -1

$$\pi_2 = \frac{V}{\omega D} \quad (3.9)$$

$$\pi_3 = D^a \rho^b \omega^c \mu = (L)^a \left(\frac{M}{L^2}\right)^b \left(\frac{1}{t}\right)^c \left(\frac{M}{Lt}\right) = M^0 L^0 t^0 \quad (3.10)$$

M	b+1 = 0	a = -2
L	a – 3b-1 = 0	b = -1
t	-c-1 = 0	c = -1

$$\pi_3 = \frac{\mu}{D^2 \rho \omega} \tag{3.11}$$

$$\pi_4 = D^a \rho^b \omega^c c = (L)^a \left(\frac{M}{L^2}\right)^b \left(\frac{1}{t}\right)^c (L) = M^0 L^0 t^0 \tag{3.12}$$

M	b = 0	a = -1
L	a – 3b+1 = 0	b = 0
t	-c = 0	c = 0

$$\pi_4 = \frac{c}{D} \tag{3.13}$$

$$\pi_4 = D^a \rho^b \omega^c h = (L)^a \left(\frac{M}{L^2}\right)^b \left(\frac{1}{t}\right)^c (L) = M^0 L^0 t^0 \tag{3.14}$$

M	b = 0	a = -1
L	a – 3b+1 = 0	b = 0
t	-c = 0	c = 0

$$\pi_5 = \frac{h}{D} \tag{3.15}$$

Thus, the parameters that must be matched to ensure similarity for torque are summarized in Equation 3.16. These are the same nondimensional groups that must be matched to ensure similarity in measuring drag force. Nevertheless, Equation 3.17 shows the final result of the Buckingham Pi process for drag force.

$$\frac{T}{\rho\omega^2 D^5} = f\left(\frac{V}{\omega D}, \frac{\mu}{D^2\rho\omega}, \frac{c}{D}, \frac{h}{D}\right) \tag{3.16}$$

$$\frac{F_D}{\rho\omega^2 D^4} = f\left(\frac{V}{\omega D}, \frac{\mu}{D^2\rho\omega}, \frac{c}{D}, \frac{h}{D}\right) \tag{3.17}$$

In order to match the prototype geometrically, the two parameters to be matched were

$$\frac{c}{D} \text{ and } \frac{h}{D}, \tag{3.18) \& (3.19}$$

where c is the chord length, h is the turbine height and D is the turbine diameter. To match the prototype dynamically, the two parameters to be matched were

$$\frac{V}{\omega D} \text{ and } \frac{\rho\omega D}{\mu} \tag{3.20) \& (3.21}$$

where V is the incoming velocity, ω is the angular velocity, D is the turbine diameter, ρ is the fluid density and μ is the kinematic viscosity of the fluid. Due to the wind tunnel size constraints (0.61 m by 0.91 m) and taking into account the effects of boundary layers and flow blockage (< 10% frontal area), a diameter of 0.25 m or 10 in. was selected. For clarity, any object tested in the wind tunnel should take up less than ten percent of the frontal area of the channel in order for boundary affects to be neglected. Using Equation 3.19, the geometric nondimensional model parameters were set equal to the prototype

parameters wherein a model turbine height of 0.25 m or 10 in. was determined. Cord lengths were determined identically, however, cord length isalso directly related to solidity. Keeping the diameter and height constant, as cord length is increased solidity increases and as cord length is decreased solidity decreases. Therefore, based on pre-determined solidity choices, the model cord lengths were solved for using Equation 3.22 which was developed by Gorlov after which Equation 3.18 was used to check and ensure geometric similarity.

$$\sigma = \frac{n}{\pi}\left(d + \sum_{k=1}^{n}\left(\sin\left(\frac{k\pi}{n} - d\right) - \sin\frac{k\pi}{n}\right)\right) \tag{3.22}$$

In Equation 3.22, σ denotes solidity, n is the number of blades and d represents half of the cord length. Equation 3.23 shows the relationship between the cord length and the variable d

$$d = \frac{1}{2}\sin^{-1}\frac{c}{r} \tag{3.23}$$

where c represents the cord length of the airfoil and r represents the radius of the turbine.[2]For visual purposes Figure 3.4 shows the relationship between the variable d and the cord length c.

To match the scaled models dynamically there were also two parameters (Equation 3.20 and 3.21) to be matched. The first parameter $\frac{V}{\omega D}$ of the prototype was set equal to that of the model and solved to obtain a range of wind tunnel velocities for testing. This process yields Equation 3.24.

$$V_m = V_p * \left[\frac{\rho_p}{\rho_m}\frac{\mu_m}{\mu_p}\frac{D_p}{D_m}\right] \tag{3.24}$$

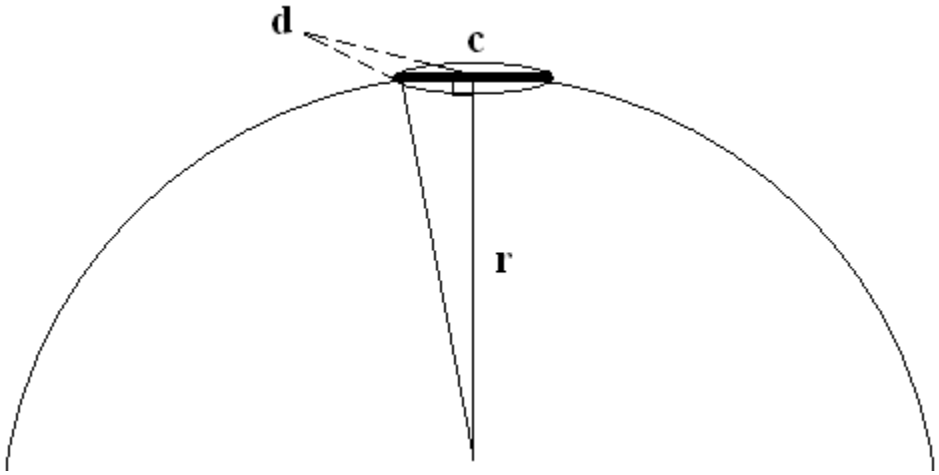

Figure 3.4. Relationship between *d* and *c*

where subscripts *m* and *p* stand for model and prototype respectively. Implementing Equation 3.24 and the known range of operating water speeds (0.69-1.83 m/s or 2.00-6.00 ft/s), the model (wind tunnel) velocities were calculated and are summarized in Table 3.2. These incoming flow speeds along with the model dimensions are all that needs to be known in order to conduct the experiment.

3.4 Turbine Manufacturing

In order to satisfy the demands of the test matrix a manufacturing practice needed to be employed that could produce a large quantity of blades (seven turbines with two to six blades per turbine) with good surface quality, in a timely manner, while utilizing a material that could structurally withstand winds in excess of 60 mph. The vacuum infused molding process used to make the initial carbon fiber blades for the prototype would take too long for this application. It was decided instead to use a rapid prototype machine (RPM)which made the finished product out of acrylonitrile butadiene styrene, otherwise known as ABS. This process was able to produce multiple blades during each print. The material was both structurally sound and provided an adequate surface finish which allowed skin friction to be neglected. Figure 3.5 shows an example of the RPM producing six blades in a single print while Table 3.3 summarizes the sizes of all the parts manufactured. It is important to note the steps involved in producing the blades from start

Table 3.2. Model velocities determined by matching Reynolds number

V_p (m/s)	Re	V_m (m/s)	V_m (mph)
0.61	2.84E+05	17.79	39.78
0.91	4.26E+05	26.68	59.68
1.22	5.68E+05	35.57	79.57
1.52	7.11E+05	44.46	99.46
1.83	8.53E+05	53.36	119.35

to finish. First, the blade cross sections were downloaded from the online applet Javafoil, with a unit-less cord length of one.[33]The two columns of data were copied into Excel wherein a third, z column was added, full of zeros. The three columns of data were copied from Excel and pasted into WordPad wherein the file was saved as a .txt document. Next, the file was read into Matlab using the built in textread function. The entire data sheet was then multiplied by the predetermined cord lengths shown in Table 3.3. The data were copied and pasted into a new WordPad document and saved again as a new .txt file. Lastly, the profile cross section was then imported into SolidWorks as an XYZ Curve. The profile was extruded to a height of 0.25 m or 10 in., swept around a0.25 m or 10in. circumference using the sweep tool and the value for the angle of twist and then patterned for the desired number of blades.

3.5 Test Procedure

From the test matrix, seven turbine configurations were constructed for wind tunnel tests. Figure 3.6 to Figure 3.12 show the pictorial representations of each of these configurations. The first three pictures relate to the first study which concerned the airfoil profile. It is not easy to see the differences between these turbines therefore Figure 3.3 should also be consulted to fully understand these pictures. The second test studied the effect on turbine performance due to the number of blades. For this study Figure 3.8 should be compared to Figure 3.9 while Figure 3.10 should be compared to Figure 3.12 as this comparison keeps blade profile and solidity constant. The final study concerned the effects of solidity on turbine performance. Figure 3.8, 3.10 and 3.11 should be consulted to visualize this study.

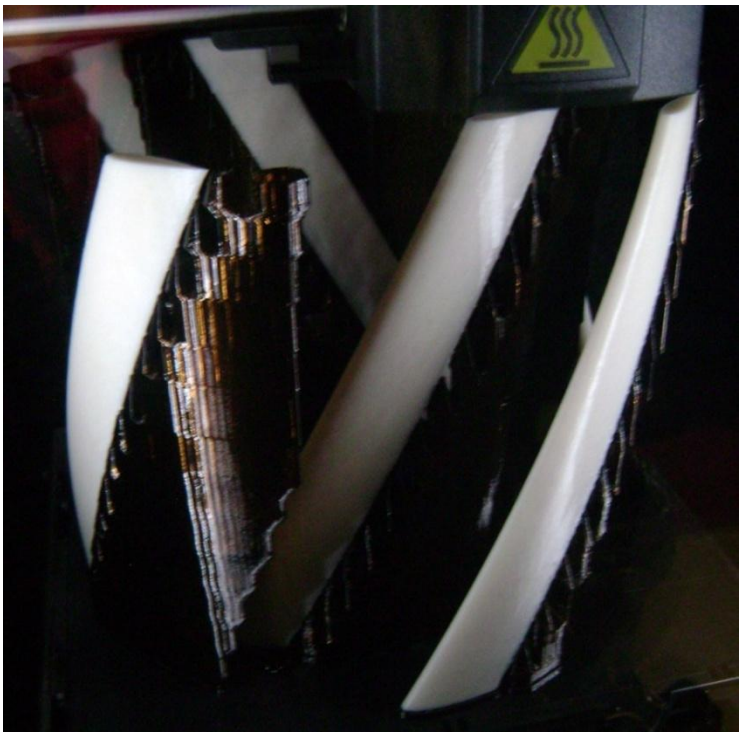

Figure 3.5. Rapid Prototype Machine printing NACA 0022 blades, six-bladed turbine

Table 3.3. Summary of the manufactured blade dimensions

Airfoil Profile	Cord Length (in)	Angle of Twist	Quantity of Blades
NACA 65$_3$-018, 48% Solidity	2.88	120	3
NACA 0020, 48% Solidity	2.88	120	3
NACA 0022, 48% Solidity	2.88	120	3
NACA 0022, 48% Solidity	1.44	60	6
NACA 0022, 41% Solidity	2.40	120	3
NACA 0022, 55% Solidity	3.39	120	3
NACA 0022, 41% Solidity	4.25	180	2

Additionally, Figure 3.13 shows the different cord lengths associated with each turbines corresponding solidity. All of the turbines in this figure utilize the NACA 0022 profile as well as three blades.

Once the blades were installed the next step involved setting up the wind tunnel. Figure 3.14 shows the wind tunnel in its entirety while Figure 3.15 shows the control

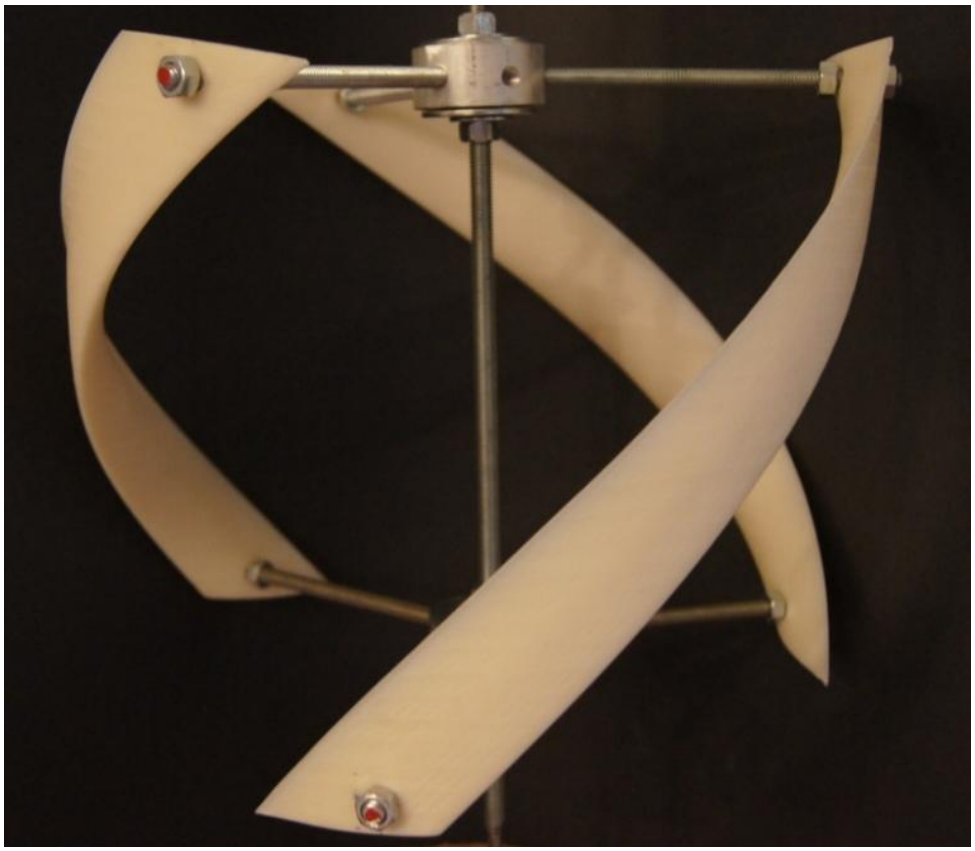

Figure 3.6. Model 3 bladed, NACA 653-018 profile, 48% solidity turbine

panel interface where the frequency of the wind tunnel was programmed. Page 6-3 of the Hitachi Inverter J300 Series Instruction Manual was followed to input the frequency for each wind tunnel test.[34]This is the only interface between the wind tunnel and the corresponding wind speed. The latter part of this section explains the process followed to understand the relationship between the wind tunnel input frequency and the output velocity of the air.

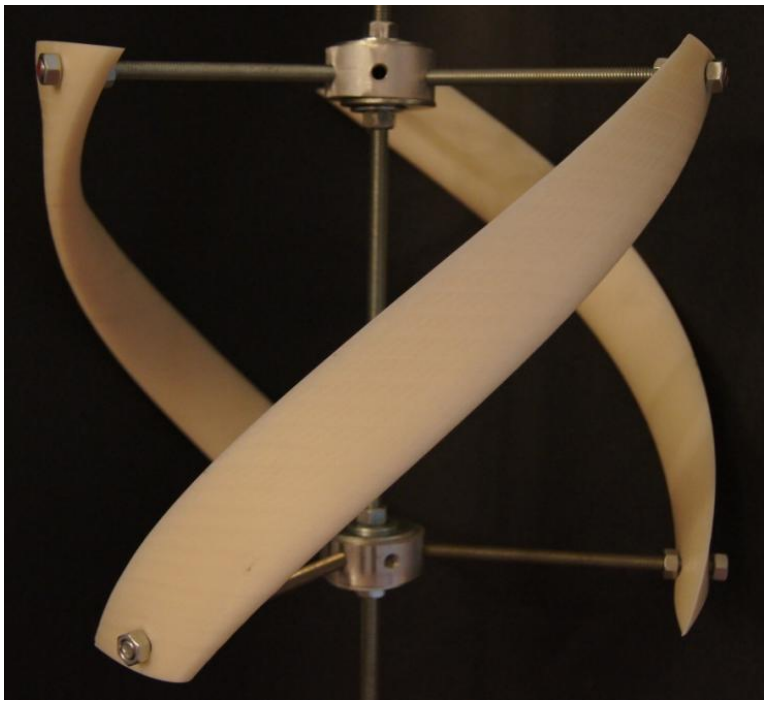

Figure 3.7. Model 3 bladed, NACA 0020 profile, 48% solidity turbine

Figure 3.8. Model 3 bladed, NACA 0022 profile, 48% solidity turbine

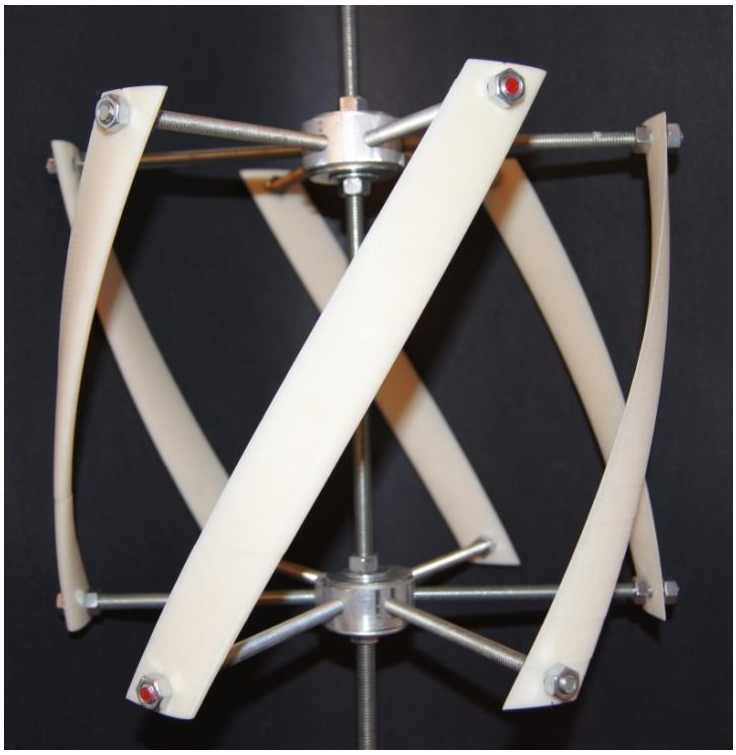

Figure 3.9. Model 6 bladed, NACA 0022 profile, 48% solidity turbine

Figure 3.10. Model 3 bladed, NACA 0022 profile, 41% solidity turbine

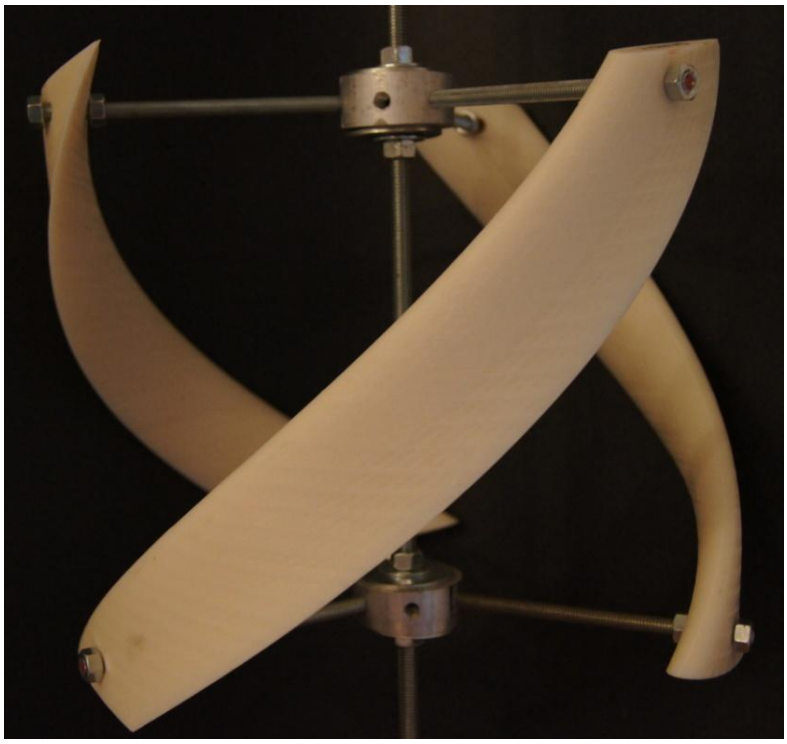

Figure 3.11. Model 3 bladed, NACA 0022 profile, 55% solidity turbine

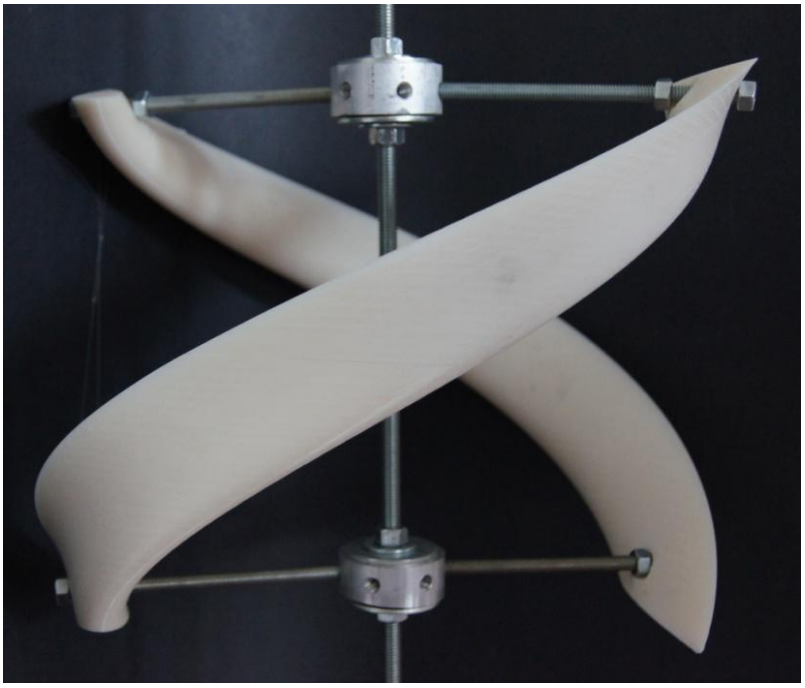

Figure 3.12. Model 2 bladed, NACA 0022 profile, 41% solidity turbine

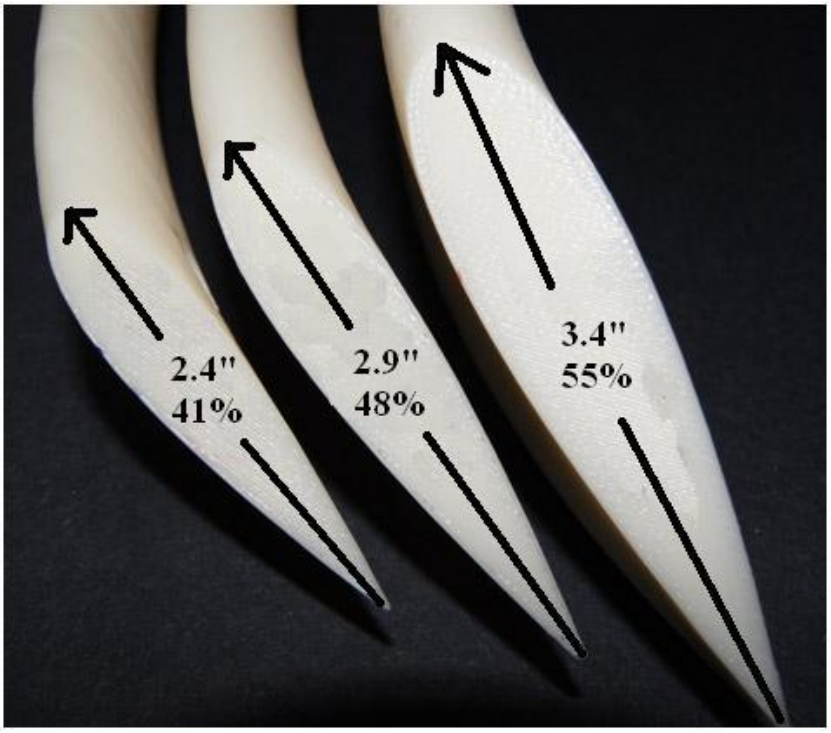

Figure 3.13. Cord lengths associated with corresponding solidities

Figure 3.14. Wind tunnel

Figure 3.15. Wind tunnel interface panel

Next, the housing was installed into the top and bottom panels of the wind tunnel. The housing in its entirety can be seen in Figure 3.16. A 5/16 in. diameter by 30 in. long piece of all-thread was used for the turbine shaft. This shaft was milled down to a smooth ¼ in. diameter on both ends for the purpose of securing the bearings and other testing equipment. The top was milled down 1 in. as its only purpose was to secure a bearing to the wind tunnel whereas the bottom was milled down 5 in. in order to stick out of the bottom of the wind tunnel far enough that additional testing equipment could be attached. This can be seen in Figures 3.17 and 3.18, respectively. For the torque tests, a ¼ in. flange mount bearing was installed flush with the top and bottom panel of the wind tunnel while for drag force tests ¼ in. base mount bearings were used. The sketches for these bearings come from McMaster Carr and can be seen in Figure 3.19 and 3.20, respectively. Figure 3.21 shows the 1 in. aluminum discs created as turbine hubs. As can be seen in this figure,¼ in. diameter holes were drilled and tapped every 60 degrees for the ease of assembling and disassembling blade spokes. Figure 3.22 shows the hub with

Figure 3.16. Turbine housing

the spokes attached. Here it can be seen that to switch between configurations spokes need simply be screwed or unscrewed into their appropriate locations. The blades are then sandwiched between the nuts on the end of each spoke. Figure 3.23 shows an individual spoke. The spokes are composed of ¼ in. diameter all-thread cut to lengths of 6 in. Lastly, Figure 3.24 shows the holes drilled through each end of the blade for this purpose of securing them to the spokes.

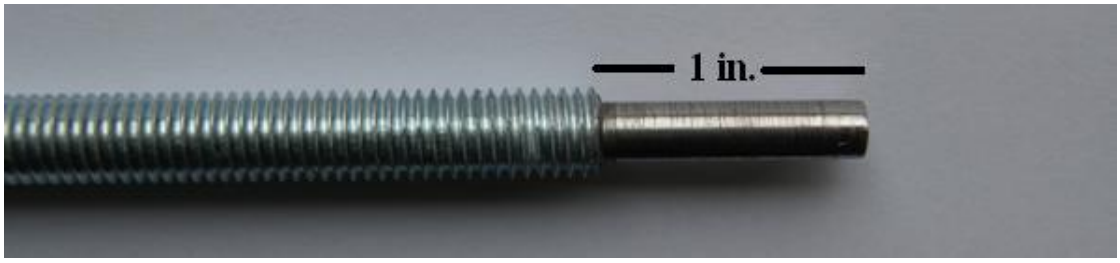

Figure 3.17. Top of turbine shaft

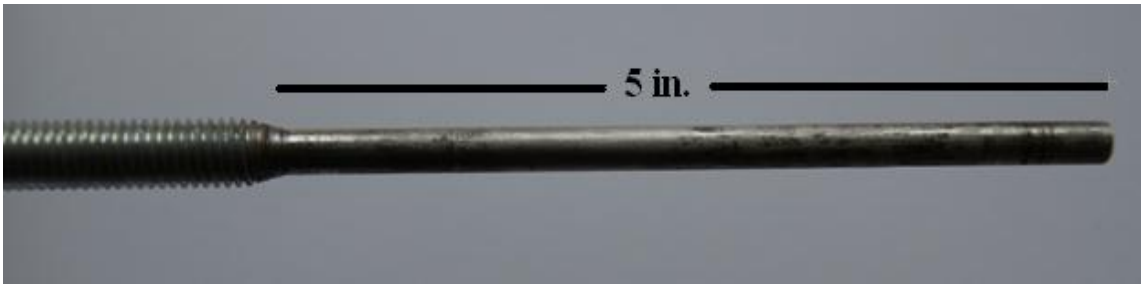

Figure 3.18. Bottom of turbine shaft

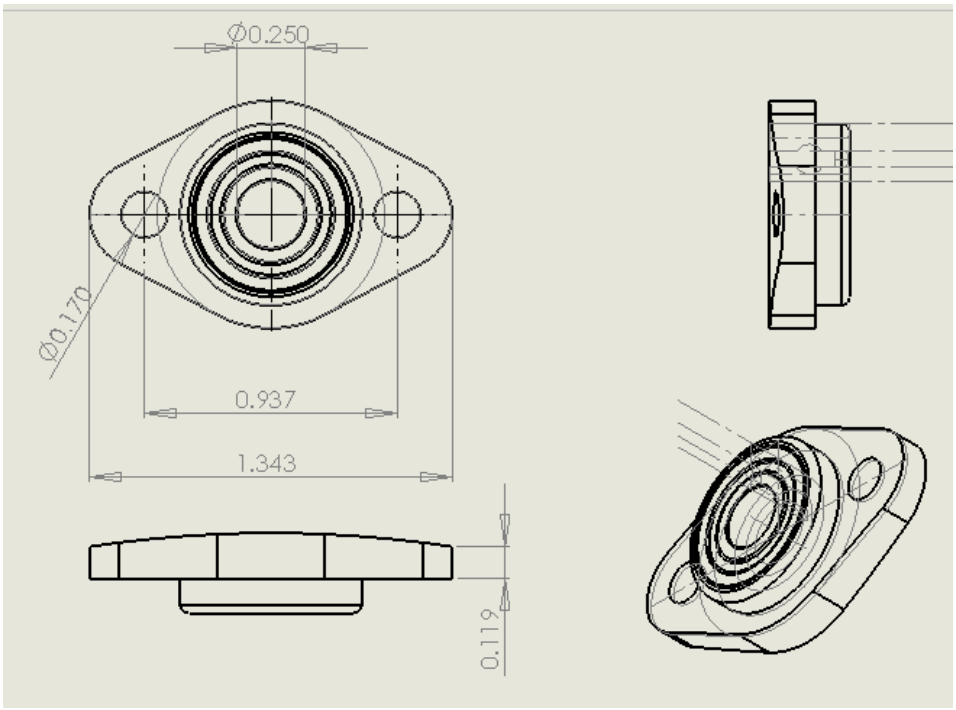

Figure 3.19. Flange mount bearing

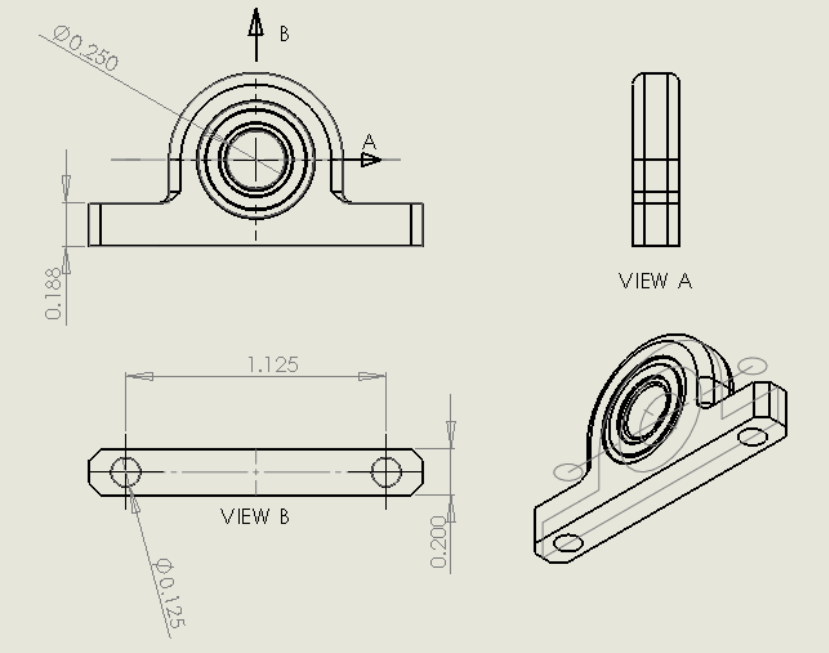

Figure 3.20. Base mount bearing

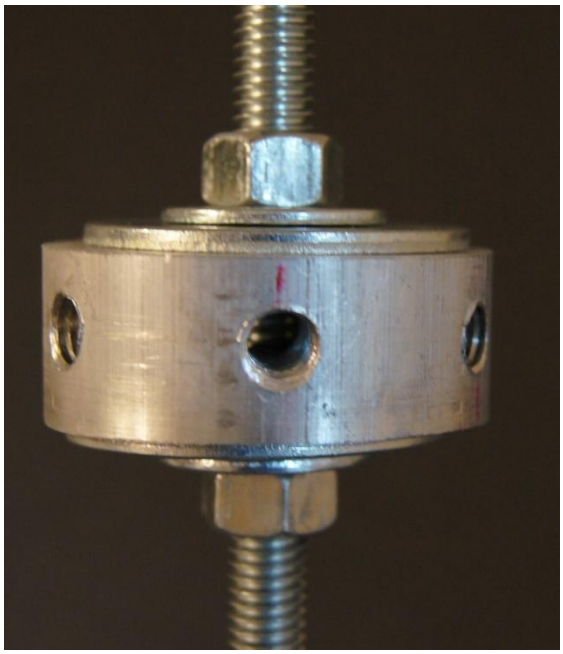

Figure 3.21. Turbine hub without spokes, holes spaced evenly 60 degrees apart

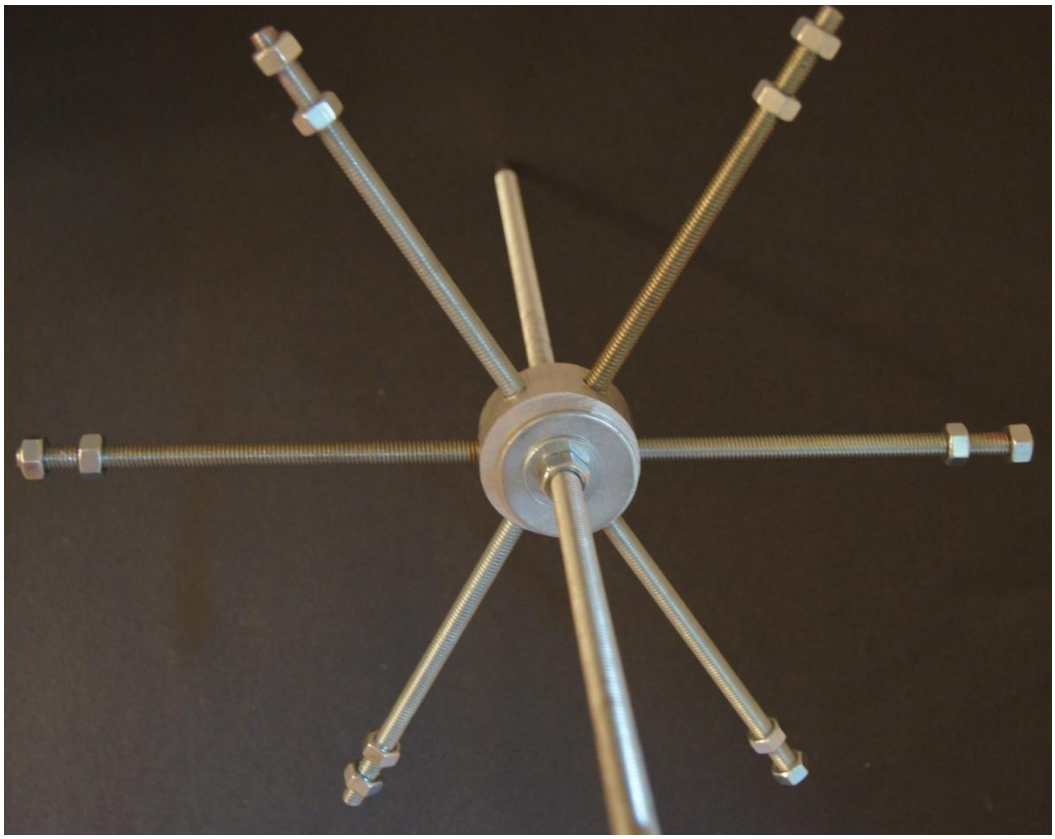

Figure 3.22. Turbine hub with spokes

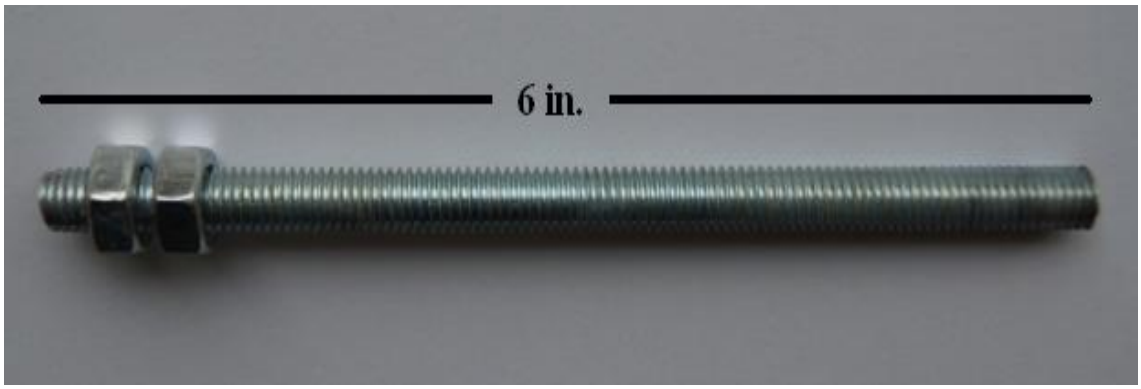

Figure 3.22. Spoke

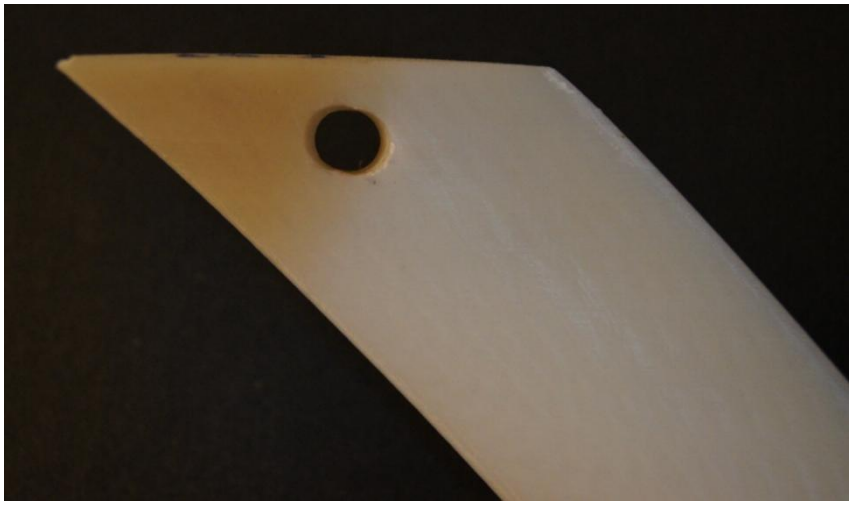

Figure 3.23. Blade with hole drilled for spokes

The first test setup consisted of a way to measure torque. This test utilized the conventional idea of a Prony Dynanomometer, wherein a braking system is used to absorb a portion of the torque generated by the turbine and transfer it to a measurement device.[35] In this case that measurement device is a cantilever beam with a strain gage attached to the fixed end which was ultimately connected to a strain gage box. A picture of the braking system as well as the cantilever beam can be seen in Figures 3.24 and 3.25, respectively. In Figure 3.24 it can be seen that tightening the screw squeezes the rubber stopper onto the shaft, in result increasing the load felt by the turbine shaft. The right most portion of the steel casing was used as the arm which transfers the load from the braking system to the cantilever beam. The cantilever beam was mounted to the bottom of the wind tunnel so that its end overlapped the braking system arm by approximately 1/2 in. This overlap allowed for contact to be maintained even when the beam was deflected the maximum amount. An ES 333 tachometer, Figure 3.26, was then secured to the bottom most portion of the turbine shaft. This tachometer was used to obtain the angular velocity measurements. Finally, a small beam was installed just below the

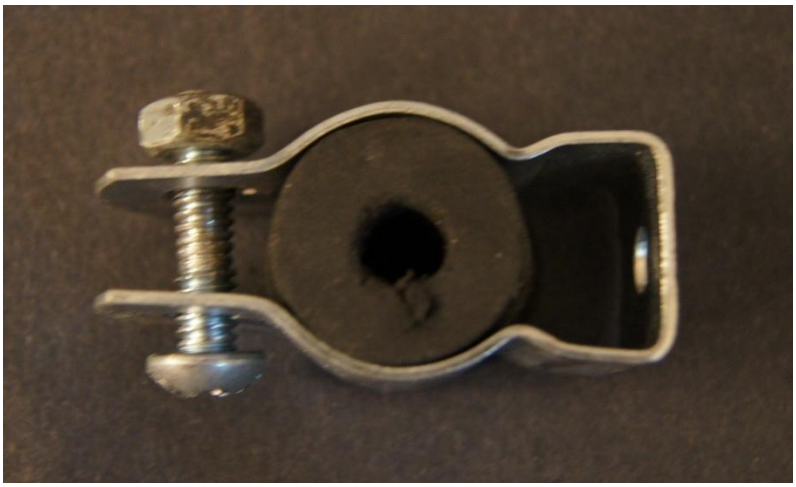

Figure 3.24. Rubber stopper braking system used to transfer torque

braking system to ensure the braking system would stay level especially during the light loading situations as it had the tendency to vibrate loose and fall down the shaft. The complete setup for the torque tests can be seen in Figure 3.27. Once the torque system was set up the wind tunnel was turned on and allowed to reach steady state while the strain gage box was zeroed. At this point, the braking system was removed from the shaft and the tachometer was used to obtain a no-load speed measurement. Next, the braking system was replaced and set to its most relaxed setting. Multiple strain measurements were then taken in conjunction with the corresponding tachometer measurement from this relaxed state of the braking system up to its tightest point just before stall occurred. Between each measurement the braking system was held away from the cantilever beam while the strain gage was zeroed. This process was repeated at each incoming flow speed ranging from approximately 6.71 to 26.8 m/s or 15 to 45 Hertz. After a full set of test measurements was obtained (15-45 Hertz) the process was repeated for two more sets, thus totaling three sets of data per turbine configuration. This was done to ensure repeatability and reproducibility.

Figure 3.25. Cantilever beam with strain gage

Figure 3.26. Tachometer

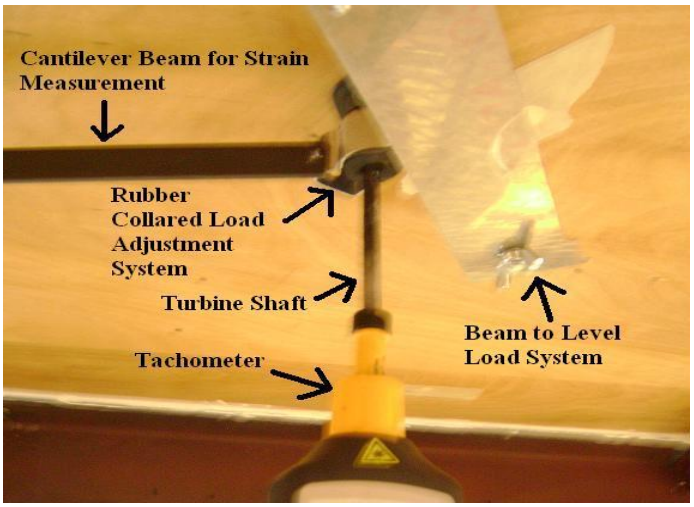

Figure 3.27. Experimental torque setup

The second test was developed to measure the drag force caused by the blades. This test consisted of two U-shaped aluminum housings with a beam mounted between the legs of the U as seen in the close-up, Figure 3.28. This beam had four strain gages applied. The two nearest the bearing measured the compressive strains while the two nearest the legs measured the tensile strains during loading. The four gages were wired into a Wheatstone as can be seen in Figure 3.29 as well as the schematic, Figure 3.30. The P+, P-, S+ and S- denote terminals found on the strain gage box for a Wheatstone Bridge circuit. Consequently, the P+, P-, S+ and S- wires from the top were intertwined with the corresponding P+, P-, S+ and S- wires from the bottom and then hooked to the strain gage box to provide one overall strain measurement from the two systems combined. Slots were then cut into the top and bottom frame of the wind tunnel, as seen in Figure 3.31, and the turbine was held in place by base mount bearings attached to middle of the beam on the U-shaped housing as seen in Figure 3.32. This setup allowed for the turbine shaft to deflect while in the wind tunnel, putting all of the drag force on the top and bottom bearings. The entire drag setup can be seen in Figure 3.33.

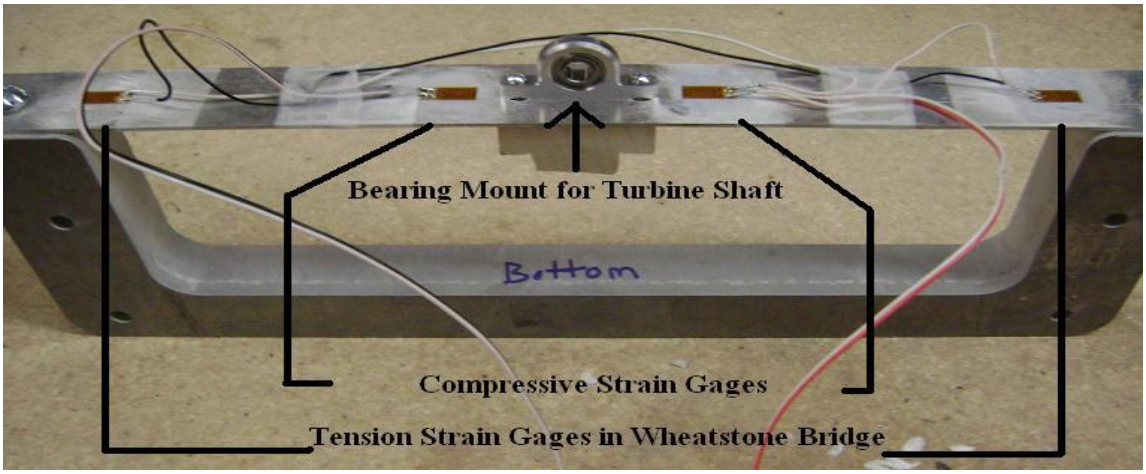

Figure 3.28. Close-up of Wheatstone Bridge, drag measurement system

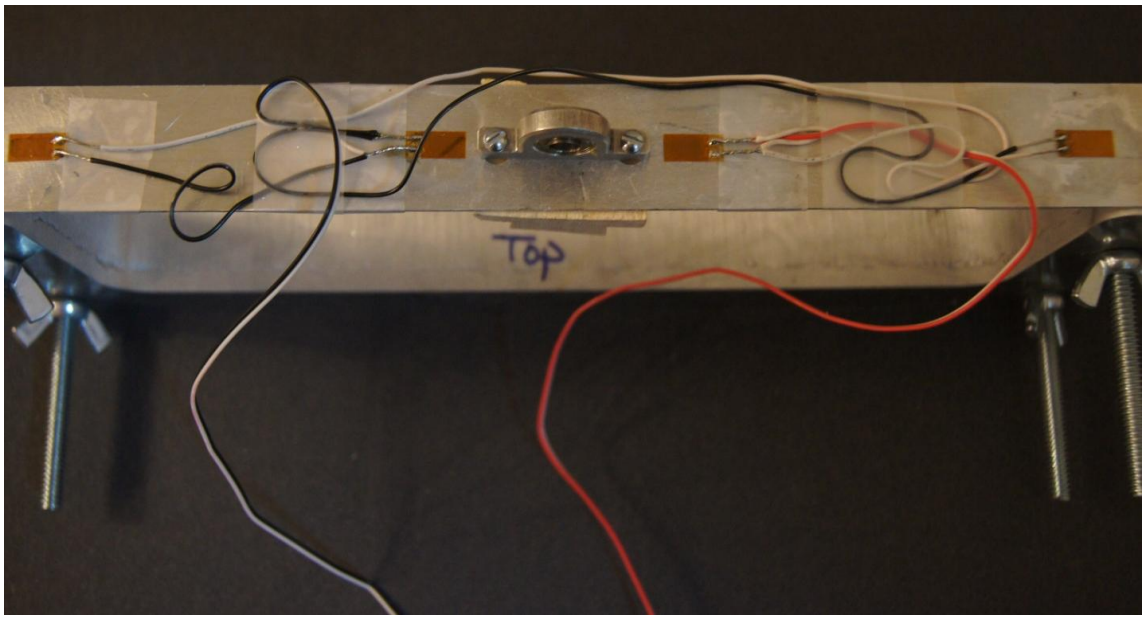

Figure 3.29. Actual Wheatstone bridge used for drag force measurement

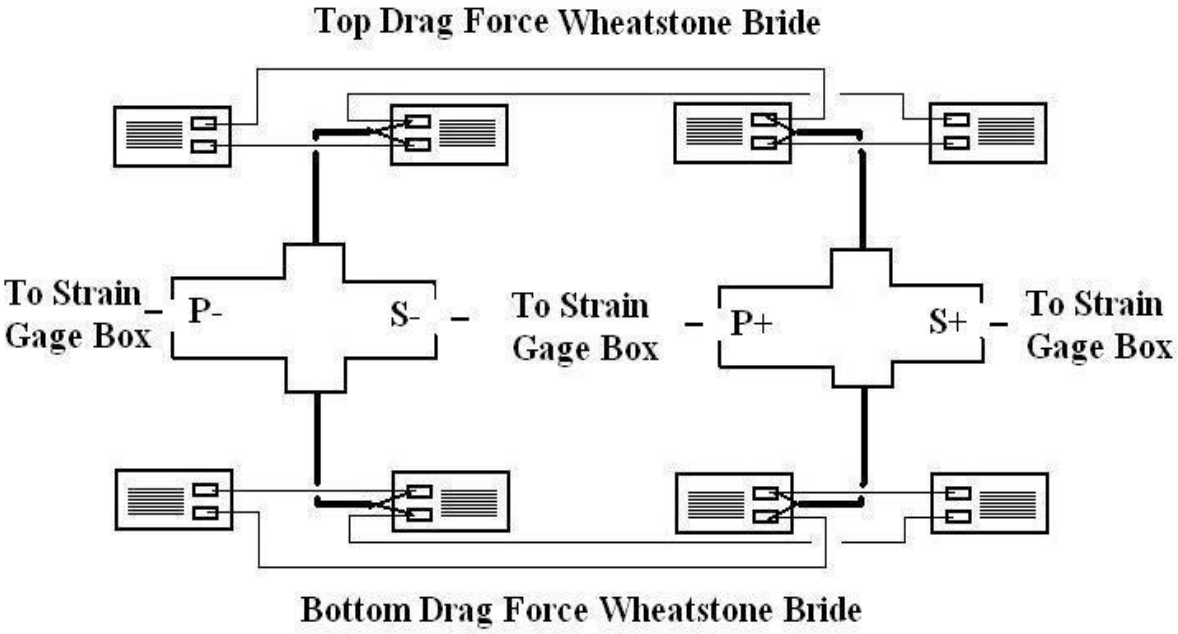

Figure 3.30. Wheatstone Bridge schematic

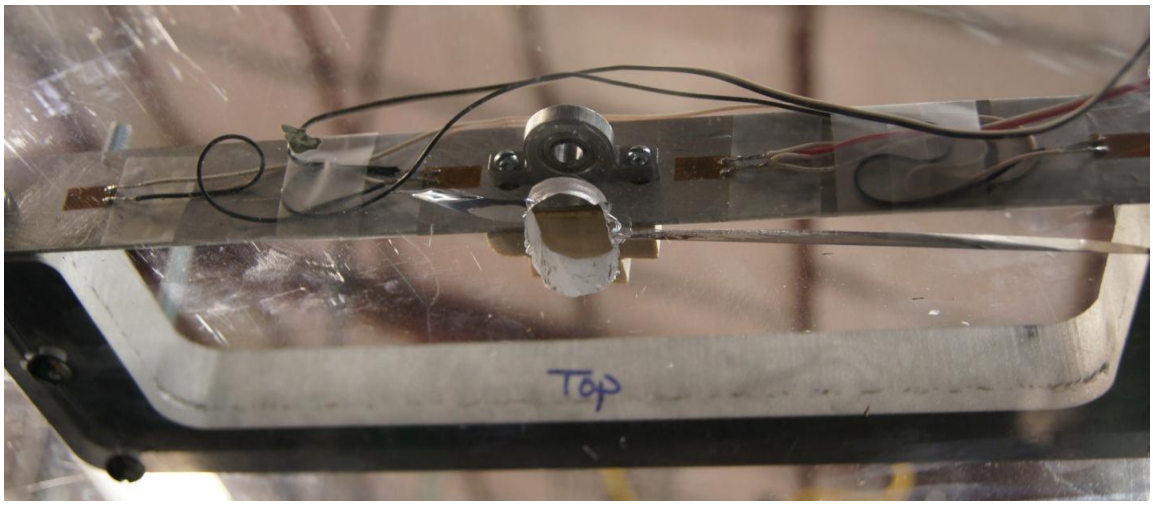

Figure 3.31. Slot cut in wind tunnel to allow for deflection in measuring drag for

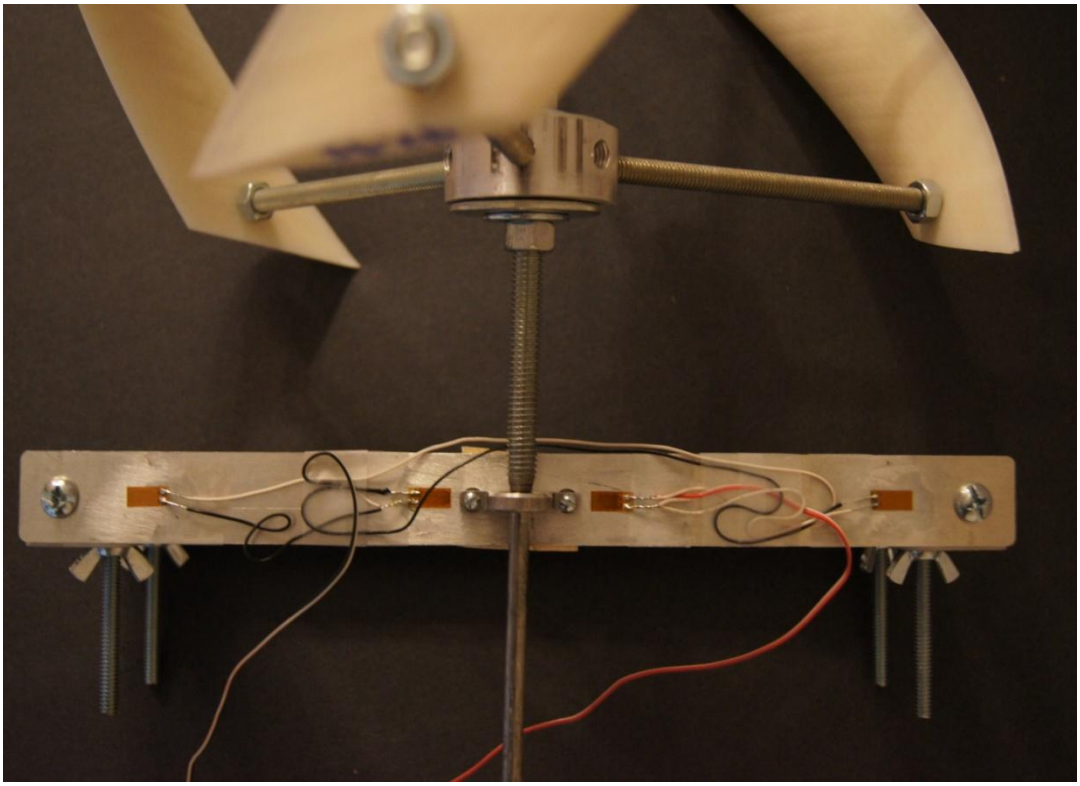

Figure 3.32. Flange mounted bearing holds turbine at the top and bottom

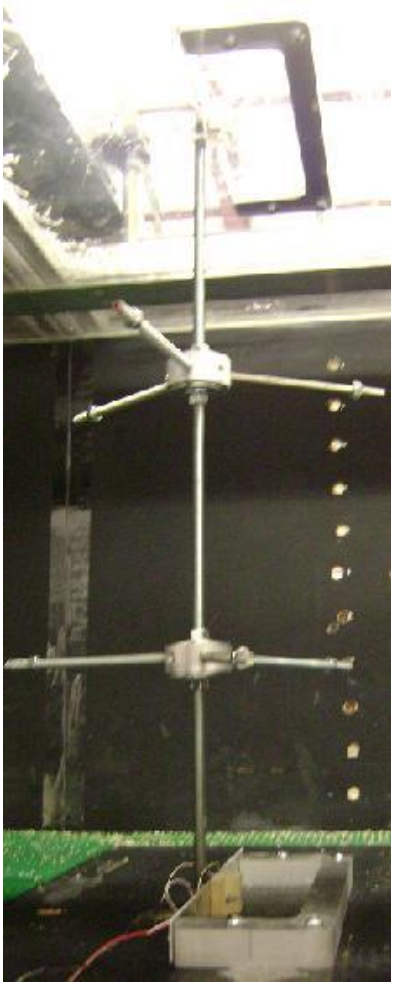

Figure 3.33. Experimental drag setup

Before running either test, both systems were calibrated. To calibrate the system, weights of known values were applied to the system at their point of loading and strain measurements were taken. For the cantilever beam (or torque test) this consisted of hanging a weight from the end of the beam while in a horizontal position with the fixed end held fixed. For the drag test this consisted of placing the weights in the center of the beam, where the bearing was installed. Because the drag test consisted of two measurements each beam was calibrated alone as well as both of the beams were calibrated together. Also, for the torque measurement two beams ended up being used,

one with a higher modulus than the initial design due to the fact that the initial beam selected for this test deflected too much at high loads wherein the braking arm could not maintain contact with the beam. Figure 3.34 shows the calibration curve for the lower modulus beam while Figure 3.35 shows the calibration curve for the higher modulus beam. Lastly, Figure 3.36 shows all of the calibration curves for the drag system. The equations on each of the figures were then used, given a strain measurement (y), to back out a load value (x).

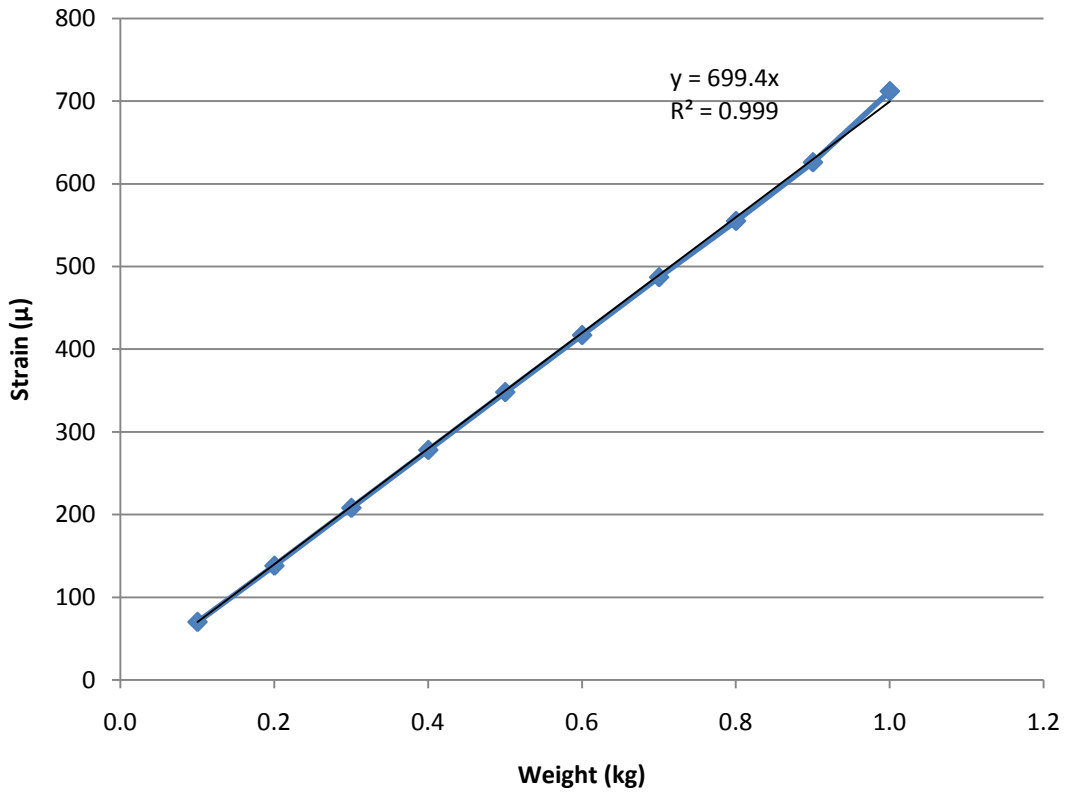

Figure 3.34. Cantilever beam calibration for lower modulus material

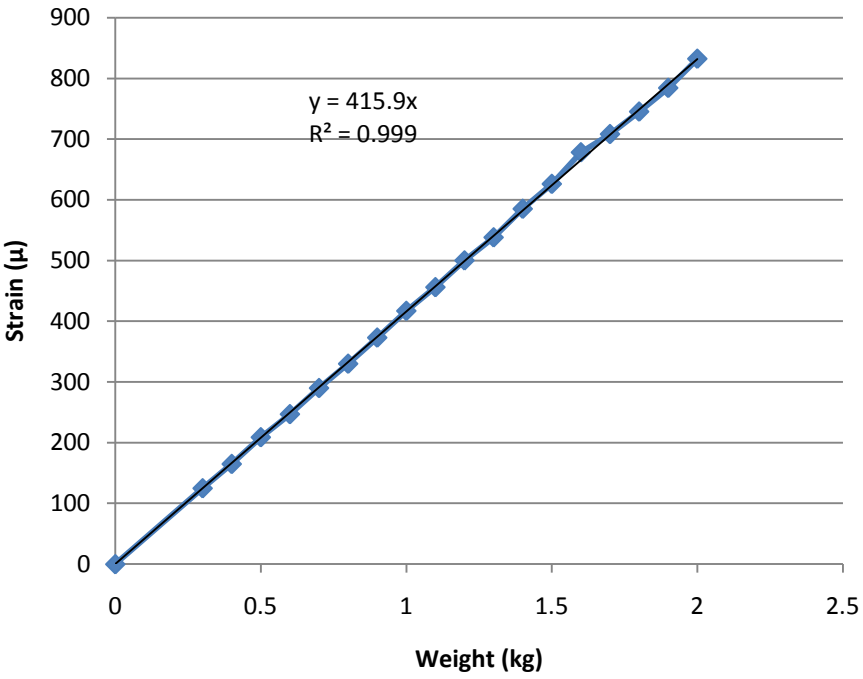

Figure 3.35. Cantilever beam calibration for higher modulus material

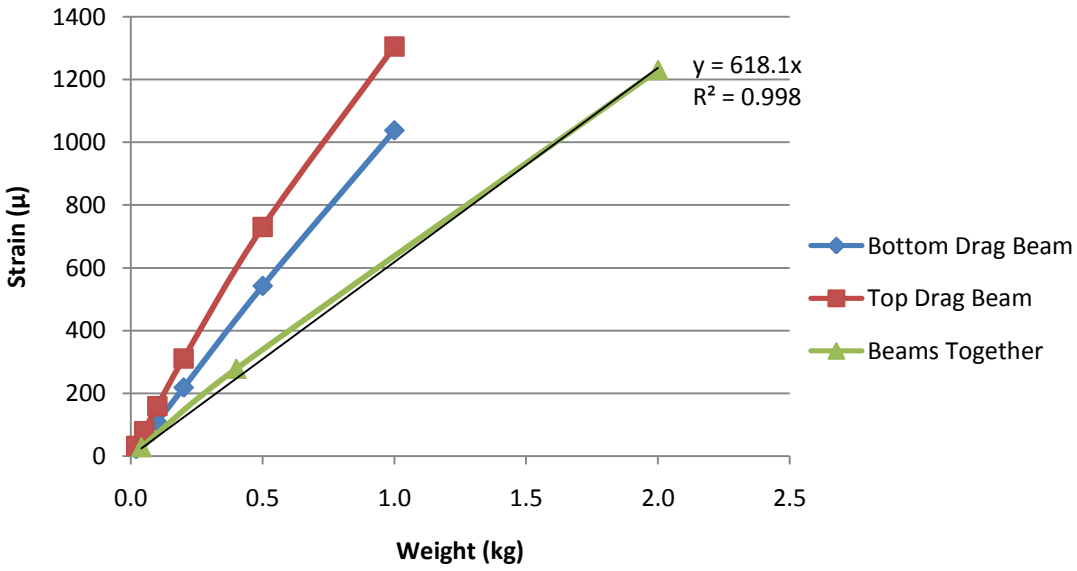

Figure 3.36. Strain calibration for drag instrumentation

A final relationship needed to be understood before testing could occur. As previously mentioned the test range for the wind tunnel velocities was determined, however, the only interface between the user and the wind tunnel is an input frequency as seen in Figure 3.15. Figure 3.37 shows a basic diagram of the setup that was used to identify this frequency versus wind tunnel output velocity relationship.

The following derivation was used as the calibration technique which was employed every day before testing, since the wind tunnel output velocity is based not only on the input frequency and blade pitch, but also on the daily temperature and atmospheric pressure. Equation 3.25 denotes the pressure equation for a pitot-static tube

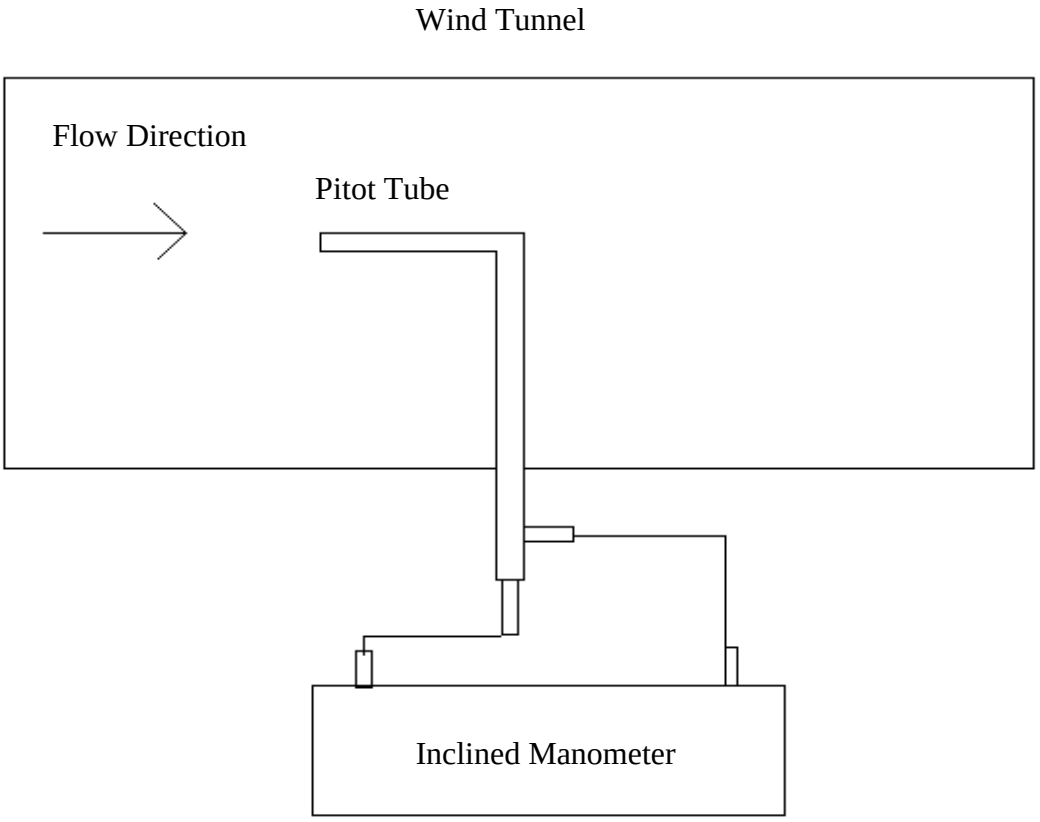

Figure 3.37. Schematic of wind tunnel calibration

$$P_t = P_s + \left(\frac{\rho V^2}{2}\right) \tag{3.25}$$

where P_t, the stagnation or total pressure is set equal to the sum of the static pressure P_s and the dynamic pressure $\left(\frac{\rho V^2}{2}\right)$. Solving this equation for the unknown wind tunnel velocity yields Equation 3.26

$$V = \sqrt{\frac{2(P_t - P_s)}{\rho}} \tag{3.26}$$

where ρ is the density of air. Utilizing the ideal gas law, density can be re-written as

$$\rho = \frac{P}{RT} \tag{3.27}$$

where R = 286.9 $\frac{J}{kgK}$ which is the ideal gas constant for air. The other two variables P stands for atmospheric pressure measured in mmHg and T stands for air temperature measured in Kelvin. Substituting Equation 3.27 into 3.26 yields Equation 3.28 with two pressure variables; therefore it is important to make a distinction between the two.

$$V = \sqrt{\frac{2(P_t - P_s)}{\frac{P}{RT}}} \tag{3.28}$$

The numerator is the pressure difference of water read from the manometer whereas the denominator is the atmospheric pressure read from the barometer using mercury as the fluid. These pressures can be re-written for both numerator and denominator as

$$P = \rho g h \tag{3.29}$$

where ρ is the density of the fluid (either water or mercury for the manometer or barometer respectively), g is the gravitational constant, and h is the manometer/barometer reading. Substituting Equation 3.29 for both fluids into 3.26 and simplifying, yields the final equation used to solve for the wind tunnel velocities.

$$V = \left[\frac{\rho_W h_W}{\frac{\rho_{Hg} h_{Hg}}{RT}}\right]^{1/2} \tag{3.30}$$

Each day that testing occurred Equation 3.30 was utilized. The wind tunnel was operated through the range of 10 to 25 Hertz and manometer readings were gathered. Only these low frequencies were used to calibrate the wind tunnel velocities as any frequency above 25 Hertz exceeded the manometer scale. A line was fit to the data gathered and extrapolated to develop the entire range of wind tunnel velocities from 15 to 45 Hertz. Lastly, before any testing occurred, the newly determined velocities were substituted into Equation 3.21 to ensure that the Reynolds number was appropriately matched between the full-scale and model testing.

3.6 Experimental Derivations

At this point all measurement systems had been constructed, calibrated and installed and testing was ready to commence. The first test consisted of measuring the turbine's angular velocity and the strain in the cantilever beam caused by torque. The goal of these measurements was to ultimately plot the torque/speed curves and power/speed curves for each turbine configuration, at each pre-determined speed. Once the turbine was at steady state the tachometer was used to obtain angular velocities, ω, in

rpm. These values were substituted into Equation 3.31 to convert the results to units of rad/s as that is the necessary unit for latter power calculations.

$$\omega\left(\frac{rad}{s}\right) = \frac{\omega(\frac{rev}{min})*2*\pi}{60} \tag{3.31}$$

Next, strain readings were obtained through which torque was determined utilizing the following method. Beginning with Hooke's Law

$$E = \frac{\sigma}{\varepsilon} \tag{3.32}$$

where E is the modulus of elasticity, σ represents the total stress and ε represents the total strain on the cantilevered beam. The stress can be re-written in terms of moment loading.

$$\sigma = \frac{My}{I} = \frac{PL\frac{t}{2}}{\frac{bt^3}{12}} \tag{3.33}$$

In Equation 3.33, M is the bending moment which is re-written in terms of the unknown load P and the length of the beam L. The variable y represents the distance from the neutral axis to the point of loading which is simply the thickness of the beam divided by 2. The symbol I represents the mass moment of inertia for a rectangle. Figure 3.38 depicts the beam, where P is the point of loading which would actually be into the page and L represents the length from the point of loading to the middle of the strain gage.

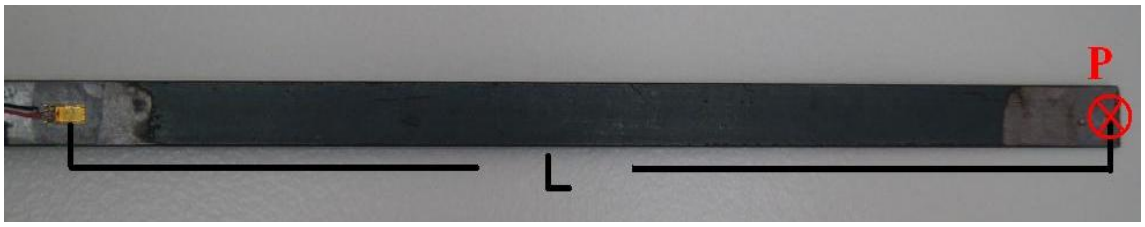

Figure 3.38. Depiction of cantilever beam

Substituting the stress term back into Hooke's Law (Equation 3.32), allows for the strain to be solved for and then re-written in terms of the unknown load *P*.

$$\varepsilon = \frac{6PL}{Ebt^2} \tag{3.34}$$

$$P = \frac{\varepsilon Ebt^2}{6L} \tag{3.35}$$

The load *P* is experimentally determined using the measured strain value at the cantilever end along with the initial beam calibration data. This process was previously mentioned in Section 3.5 where the strain value is substituted into the calibration equation as the y-variable and divided by the slope to yield the x-variable also known as the load P. It is important to note that Equation 3.34 provides the max strain felt by the cantilever beam at the fixed end which directly applies to this scenario since the strain gage is fastened at this location. Once the load was determined, torque was calculated by multiplying this measured load by moment arm *L*, which is the distance from the point of loading to the middle of the strain gage.

$$T = P\mathrm{L} \tag{3.36}$$

As for drag, the only value to be recorded was the drag strain measurement. Initially, the drag force was measured for the turbine housing alone (without blades) so that this value could later be subtracted from the overall drag (turbine housing and blades) yielding the drag force due to only the blades. Once a strain measurement was obtained, the weight pressing on the instruments was backed out using the initial instrument calibration. Again, this process comes from Section 3.5 where the strain value is substituted into the y-variable and divided by the slope to yield the x-variable or load

felt by the system. This load was then multiplied by gravity to obtain the overall drag force in Newtons, provided by the blades only.

3.7 Test Results

Due to the capabilities of the wind tunnel, only velocities up to approximately 26.8 m/s could be tested, which correspond to water speeds at full-scale of approximately 0.91 m/s or 3.0 ft/s. Consequently, to encompass the entire range of operating velocities for the water turbine (0.69 to 1.83 m/s or 2.0 to 6.0 ft/s), values must be extrapolated from the experimental curves found in this section.

Concerning torque, the raw data for each configuration and trial can be found in Appendix A. Figures 3.39 to Figure 3.45 are the plots of the torque versus speed curves for each turbine configuration. The legend of each plot shows the wind tunnel velocity for that specific turbine configuration. Due to the changes in daily parameters, the wind tunnel speeds vary; therefore, care should be taken when comparing two plots as the velocity values for each symbol are likely different.

When looking at varying only the difference in airfoil profile, Figures 3.39-3.41, it is evident that the NACA 653-018 produced the lowest maximum torque of 1.96 Nm. On the other hand, the NACA 0020 produced a slightly larger maximum torque of 3.7 Nm compared to the NACA 0022 which produced a maximum torque of 3.36 Nm. This data is matches the trends previously mentioned in Figure 3.2 when deciding which airfoils to test.

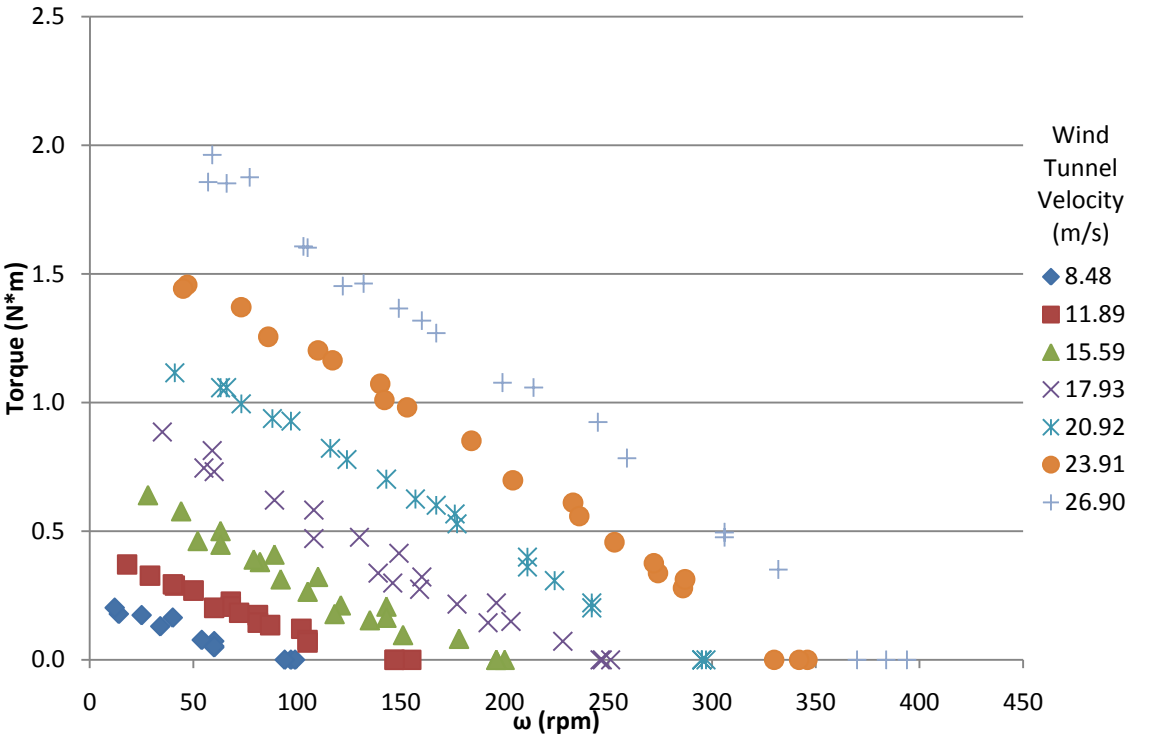

Figure 3.39. Torque/speed curves for NACA 653-018, three-bladed system with 48% solidity.

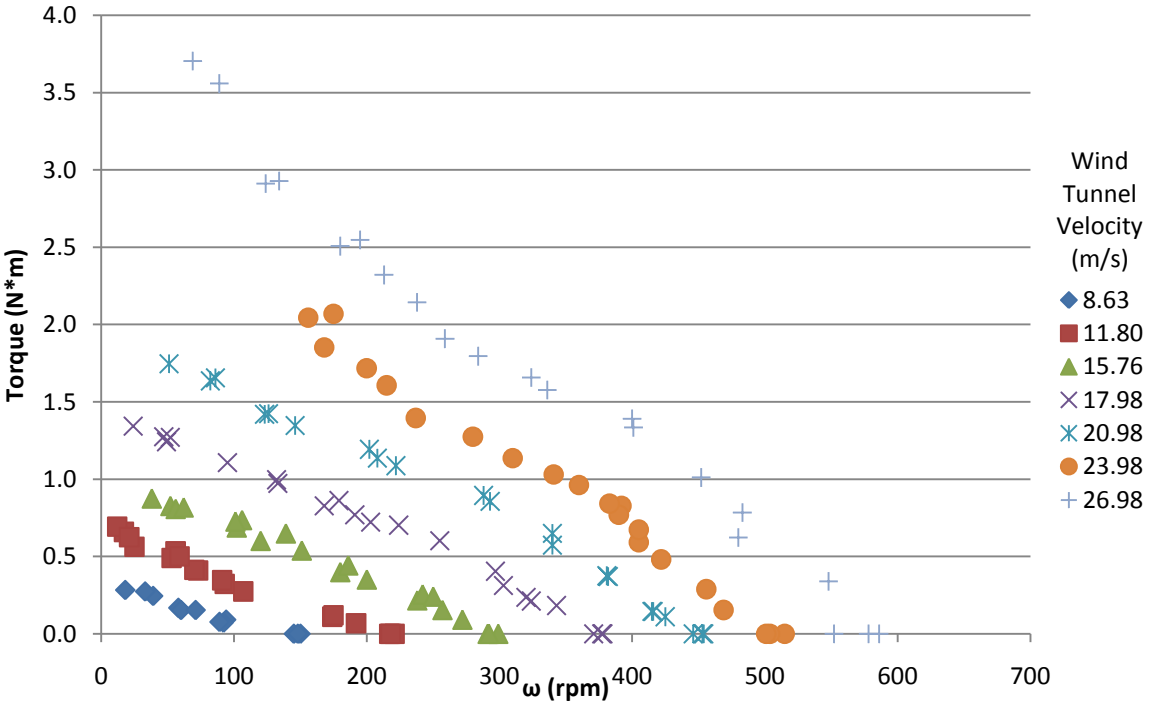

Figure 3.40. Torque/speed curves for NACA 0020, three-bladed system with 48% solidity.

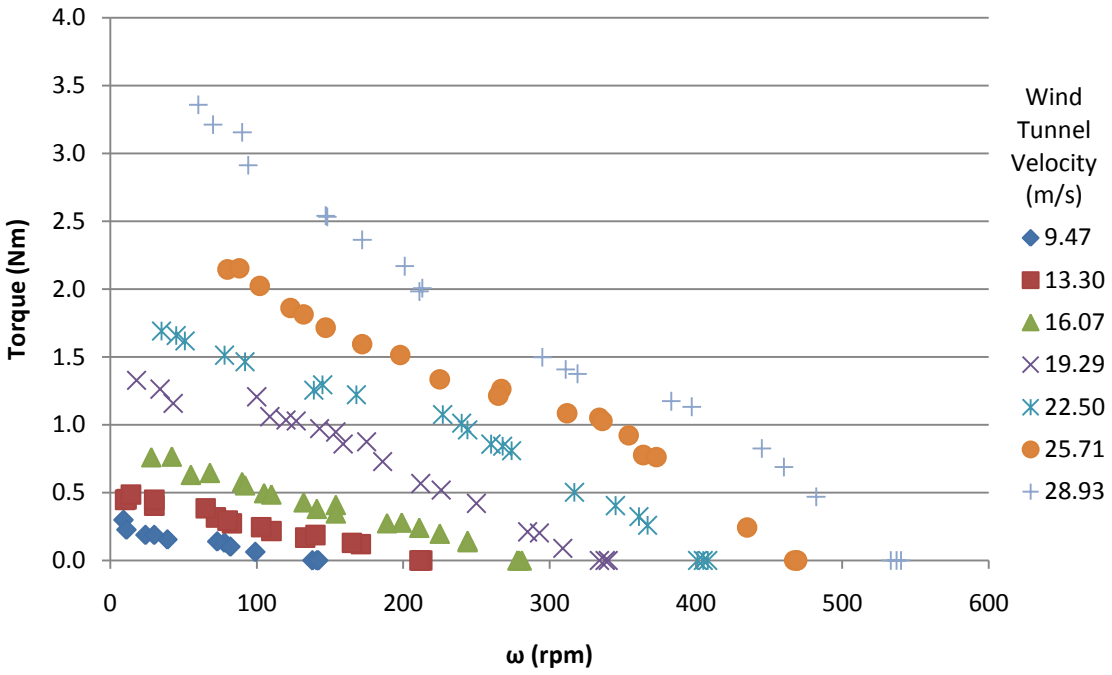

Figure 3.41. Torque/speed curves for NACA 0022, three-bladed system with 48% solidity.

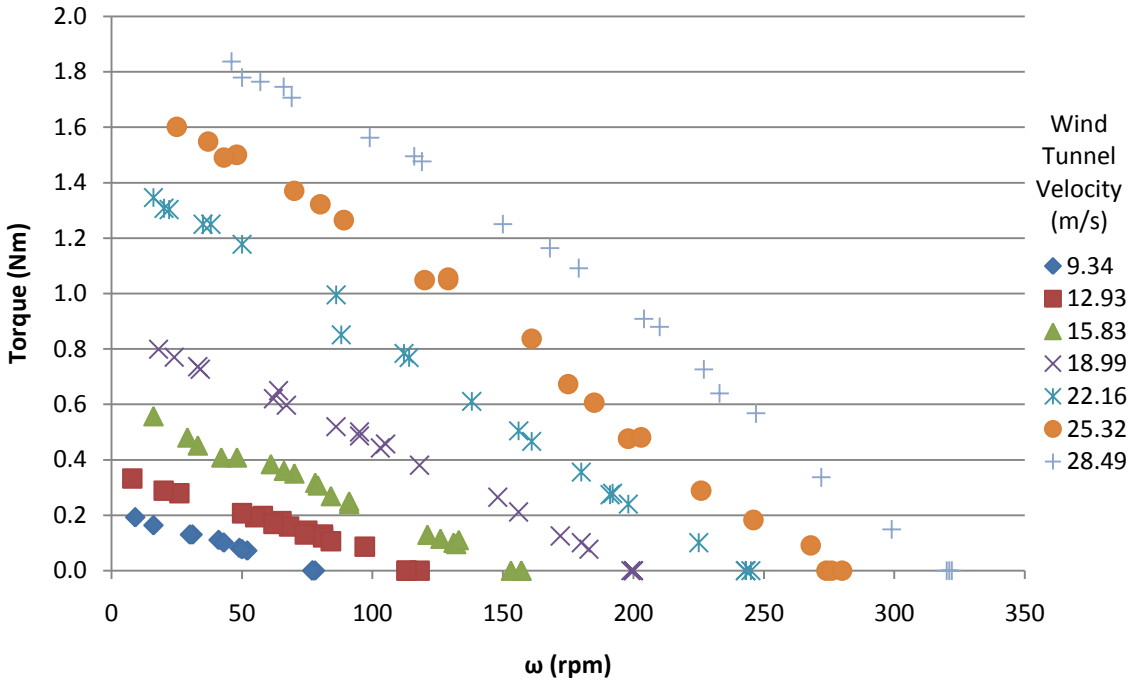

Figure 3.42. Torque/speed curves for NACA 0022, six-bladed system with 48% solidity.

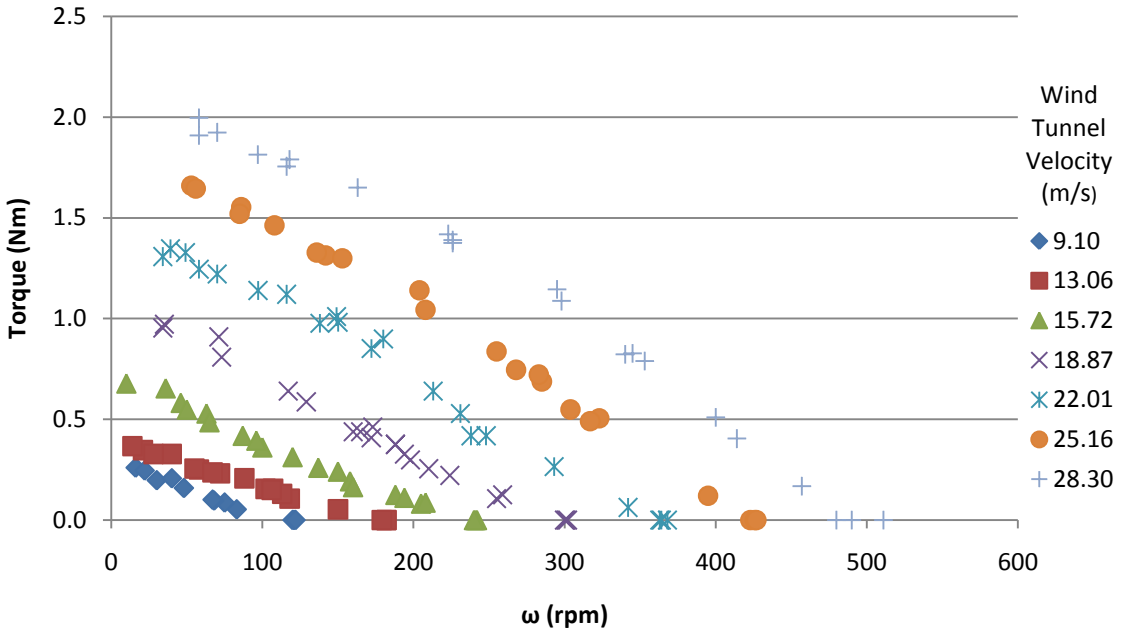

Figure 3.43. Torque/speed curves for NACA 0022, three-bladed system with 41% solidity.

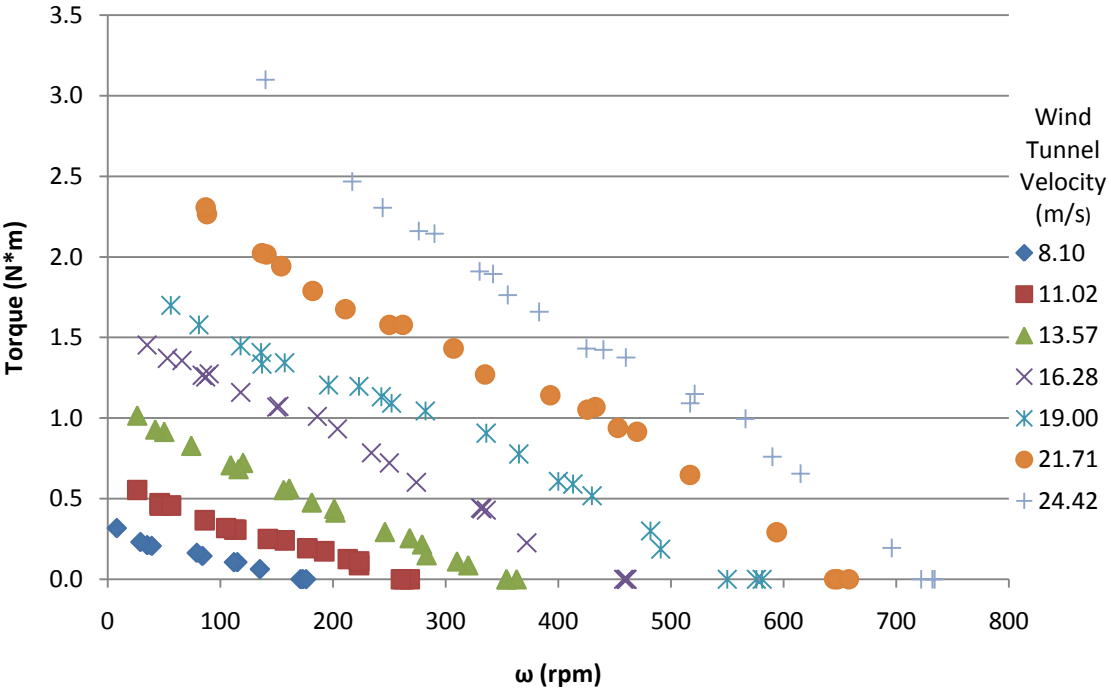

Figure 3.44. Torque/speed curves for NACA 0022, three-bladed system with 55% solidity.

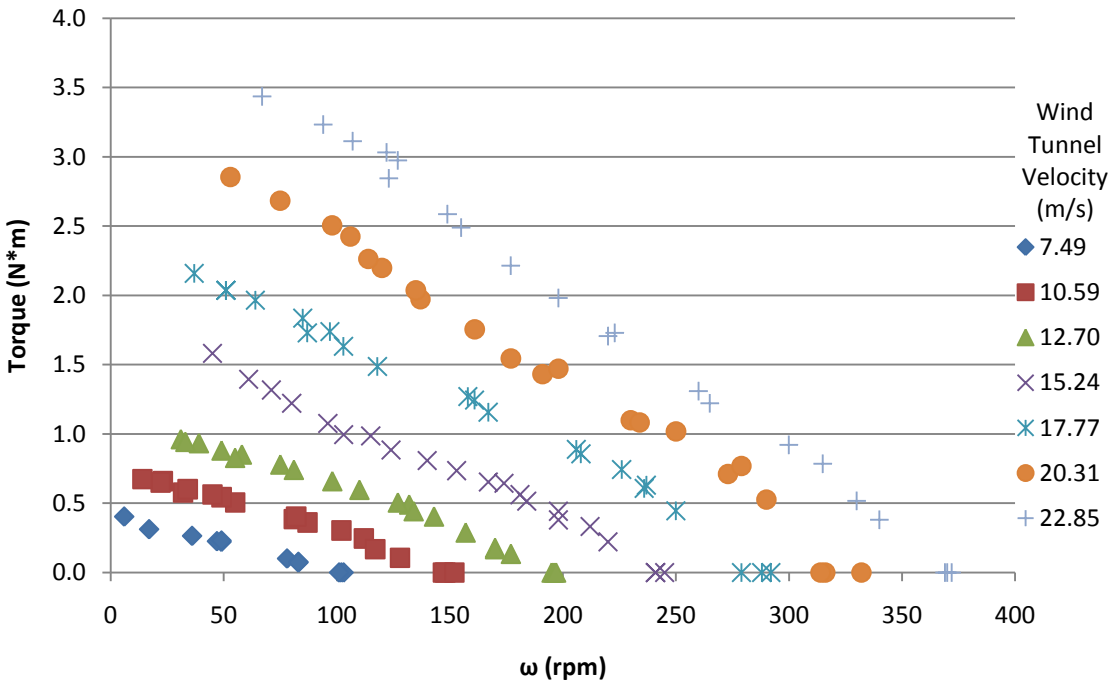

Figure 3.45. Torque/speed curves for NACA 0022, two-bladed system with 41% solidity.

When examining the effect of the number of blades per turbine, Figures 3.41 to 3.42 as well as 3.43 to 3.45, it can be seen that the NACA 0022, two-bladed system produced greater torque, 3.44 Nm, than the three-bladed, same solidity (41%) system which produced a max torque of 2.00Nm. On the other hand, the NACA 0022, three-bladed system (solidity of 48%) produced greater torque, 3.36 Nm, than the NACA 0022, six-bladed system with the same solidity which only produced 1.84 Nm of torque. Overall this study suggests that a two-bladed configuration would be the best choice for optimum performance. Also, this study validates the hypothesis that there exists some flow interference between blades which ultimately leads to a decline in turbine performance since each blade is not seeing the idealized uniform flow.

The final study compared the effects of varying solidity. Examining Figures 3.41 to 3.43 and 3.44, this study shows that the NACA 0022, three-bladed, 48% solidity configuration did the best, producing a torque of 3.36 Nm. The NACA 0022, three-bladed, 41% solidity configuration did the worst, producing a maximum torque of 2.00 Nm and the NACA 0022, three-bladed, 55% solidity configuration performed in between producing a maximum torque of 3.10 Nm. It is extremely important to note that the trends observed for maximum torque do not have to match the trends for maximum power. This is due to the fact that power is additionally based on the rotational speed of the turbine. Therefore, it is possible given a set value of torque for one configuration to produce more than another based on the angular velocity associated with that torque. Equation 3.36 shows the relationship between power and torque

$$P = T\omega \tag{3.37}$$

where T is torque in Nm, ω is the angular velocity in rad/s and P is power in Watts. This relationship was used to develop Figures 3.46 to 3.52. These figures show the power/speed curves generated from the torque/speed data. The actual raw data for power can also be seen in the tables in Appendix A. For convenience, the maximum power created by each turbine configuration, at each speed, was summarized in Table 3.4.

From these figures and with the aid of Table 3.4, the following observations can be made. When looking at varying only the airfoil profile, Figures 3.46-3.48, the NACA 653-018 produced the lowest maximum power output of 23.69W. Again, the NACA 0020 produced a slightly larger maximum power of 58.27 W compared to the NACA 0022 which produced a max power of 47.08 W.

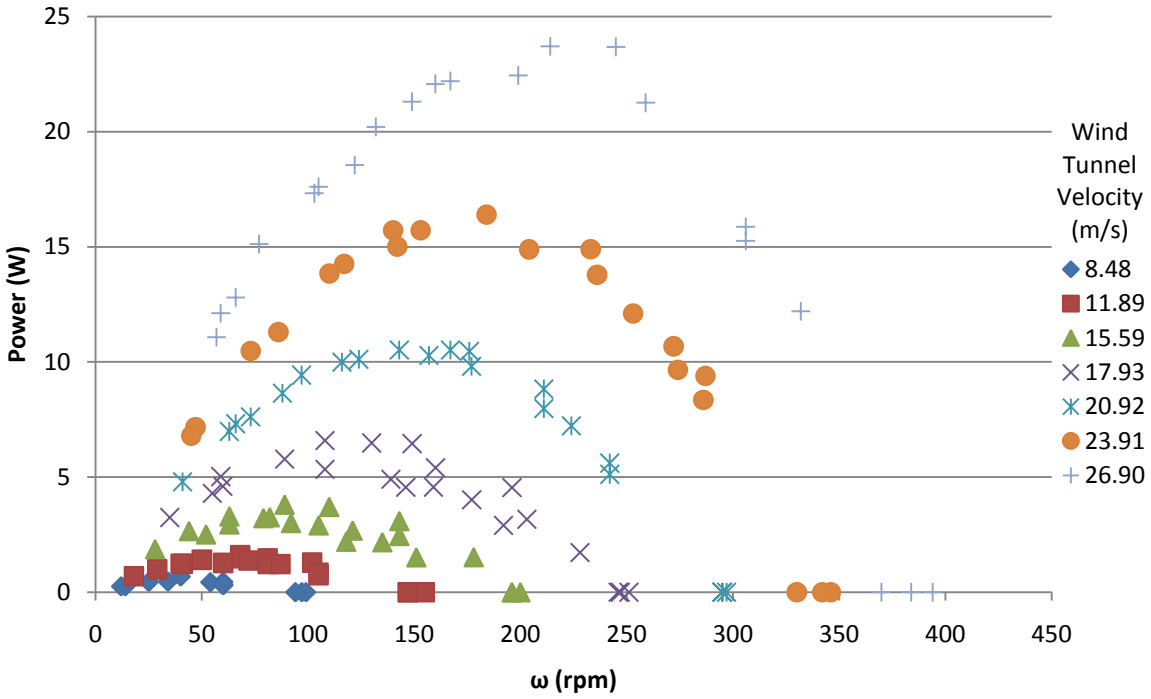

Figure 3.46. Power/speed curves for NACA 653-018, three-bladed system with 48% solidity.

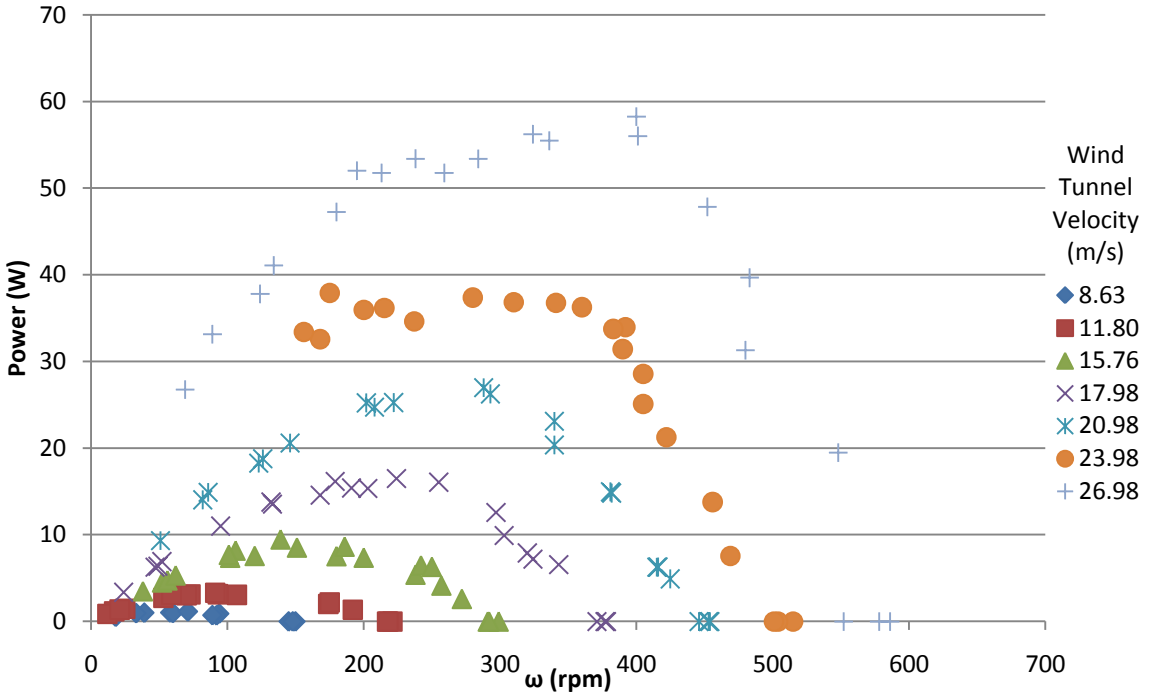

Figure 3.47. Power/speed curves for NACA 0020, three-bladed system with 48% solidity.

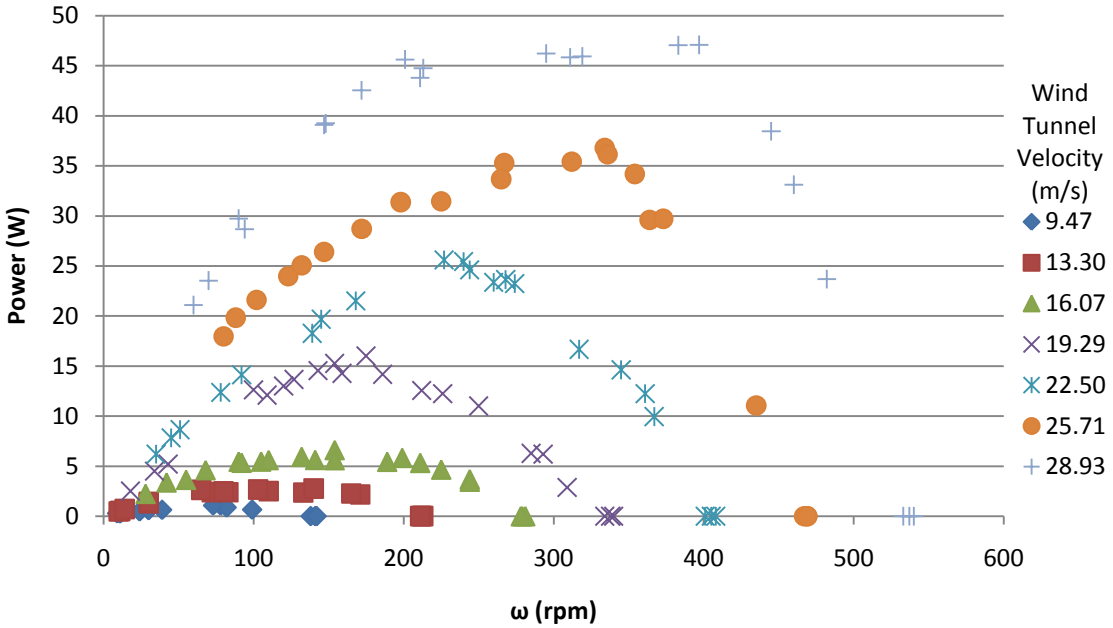

Figure 3.48. Power/speed curves for NACA 0022, three-bladed system with 48% solidity.

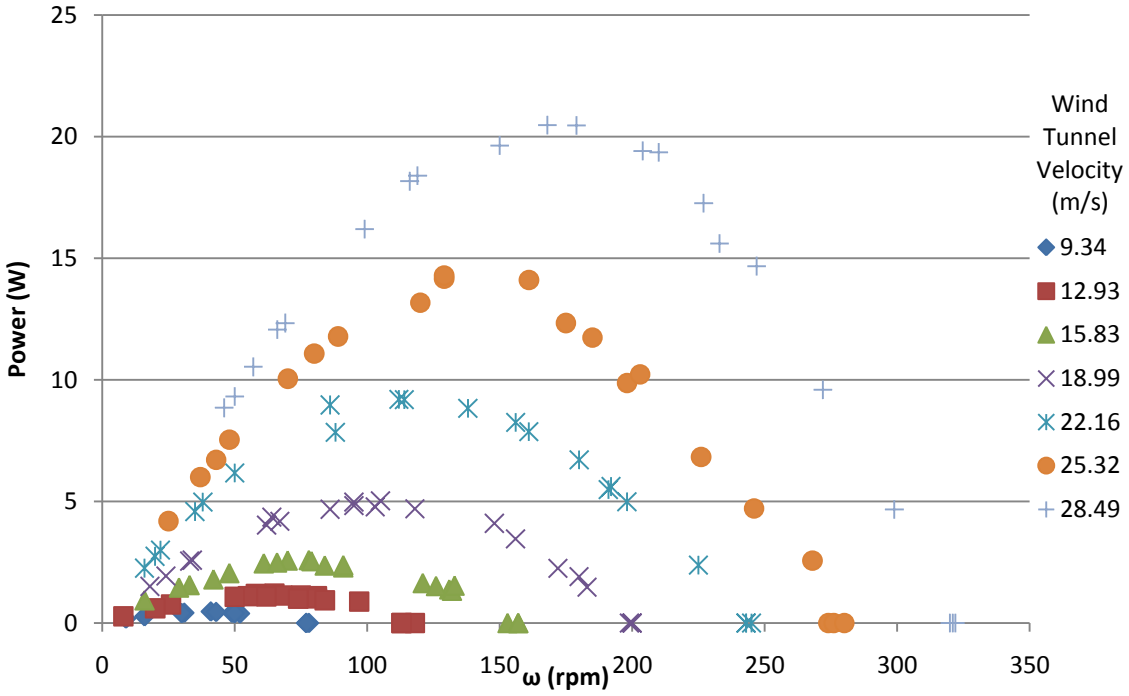

Figure 3.49. Power/speed curves for NACA 0022, six-bladed system with 48% solidity.

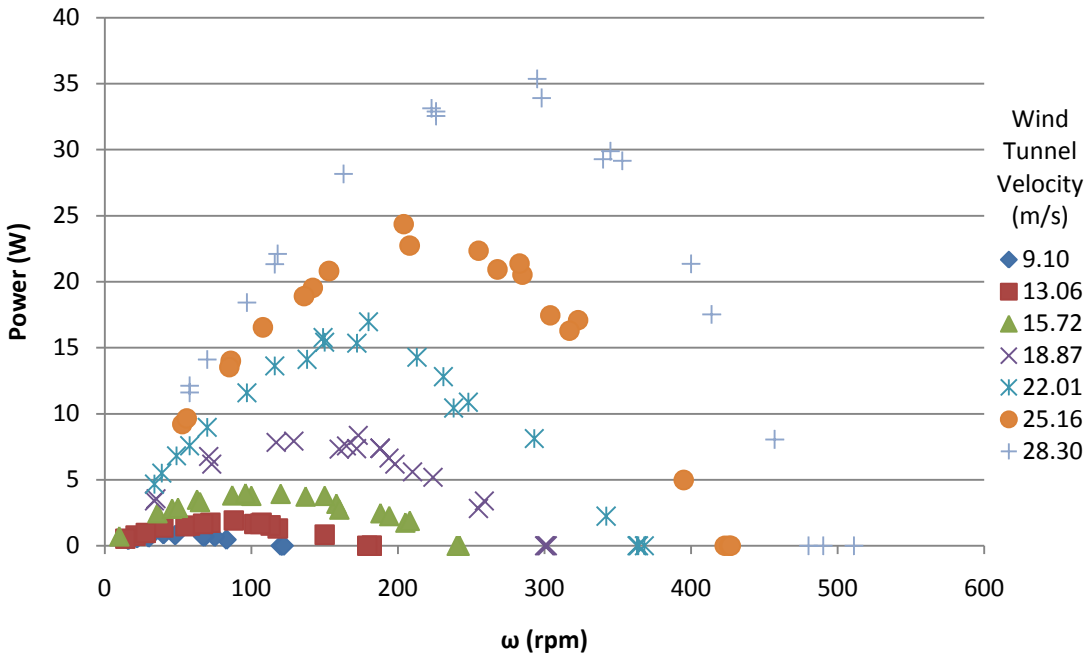

Figure 3.50. Power/speed curves for NACA 0022, three-bladed system with 41% solidity.

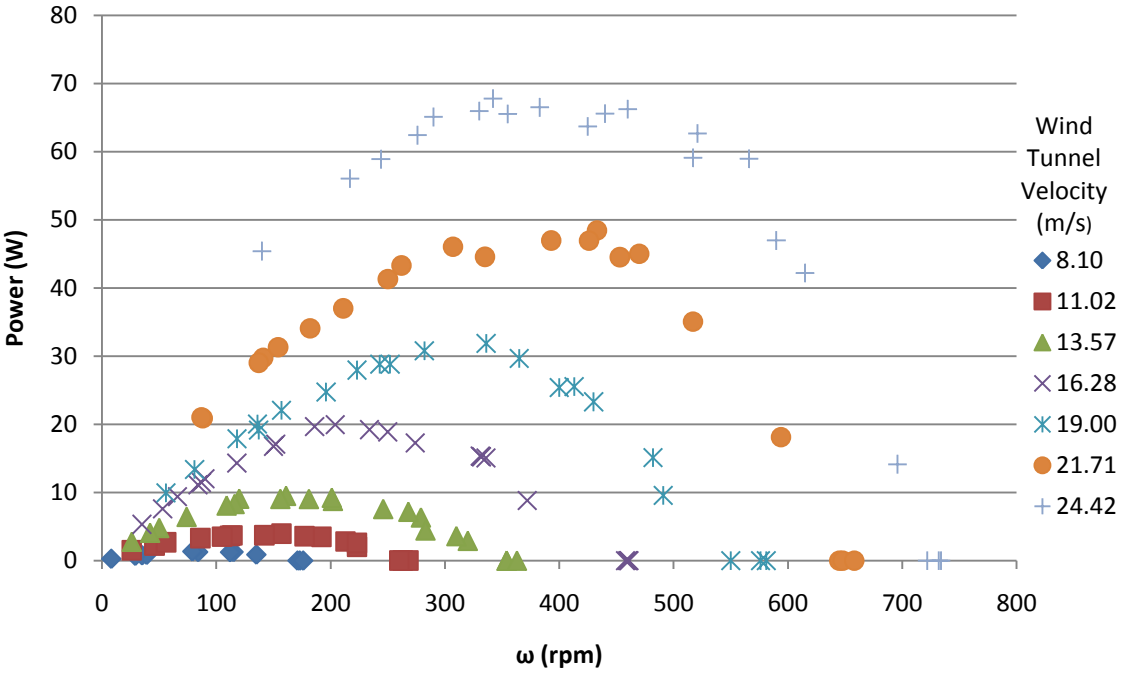

Figure 3.51. Power/speed curves for NACA 0022, three-bladed system with 55% solidity.

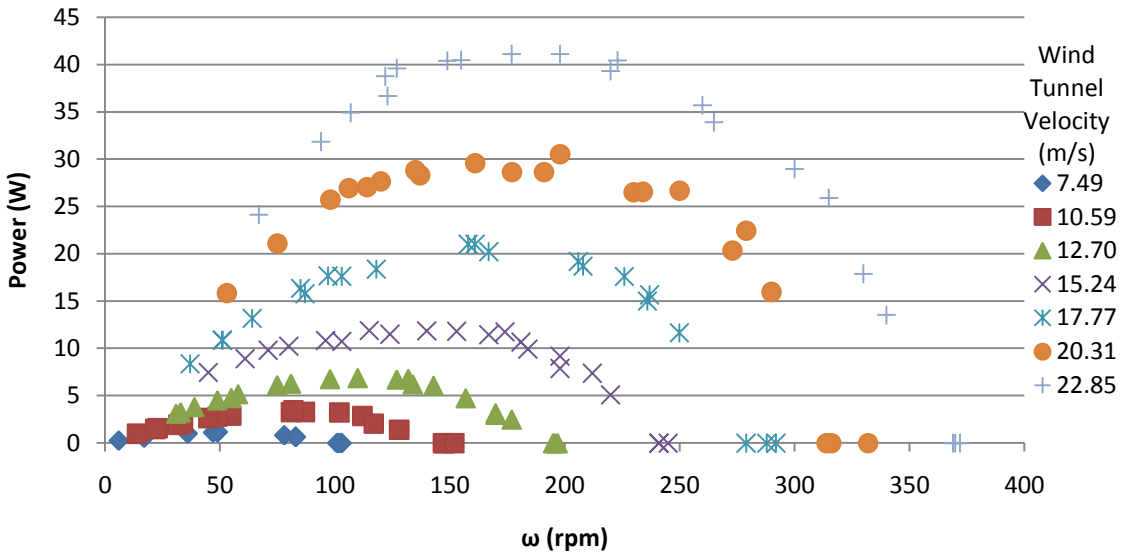

Figure 3.52. Power/speed curves for NACA 0022, two-bladed system with 41% solidity.

Table 3.4 Summary of Maximum Model Turbine Power in Watts for Variable Incoming Flow-speeds

Wind Tunnel Speed (m/s)	NACA 653018 (3 Blade) (48%)	NACA 0020 (3 Blade) (48%)	NACA 0022 (3 Blade) (48%)	NACA 0022 (6 Blade) (48%)	NACA 0022 (3 Blade) (41%)	NACA 0022 (3 Blade) (55%)	NACA 0022 (2 Blade) (41%)
8.1-9.5	0.5	1.1	1.1	0.5	0.9	1.4	1.2
11.0-13.3	1.6	3.3	2.8	1.2	1.9	4.0	3.5
13.6-16.1	3.8	9.5	6.6	2.6	4.0	9.5	6.9
19.0-22.5	6.6	16.5	16.0	5.0	8.4	19.7	11.9
21.7-22.5	10.5	27.0	25.6	9.2	17.0	31.9	21.0
21.7-25.7	16.4	37.9	36.8	14.3	24.4	48.4	30.5
24.4-28.9	23.7	58.3	47.1	20.5	35.4	67.8	41.1

Because this trend is identical to the torque, Figures 3.39-3.41, it is apparent that the rotating speed of each turbine was proportional to the torque and power produced.

When examining the effect of the number of blades per turbine, Figures 3.48 to 3.49 as well as Figures 3.50 to 3.52, it can be seen that the NACA 0022, two-bladed system produced a maximum power of 41.09 W whereas the three-bladed, same solidity (41%) system produced a max power of 35.36 W. On the other hand, the NACA 0022,

three-bladed system (solidity of 48%) produced a maximum power of 47.08 W whereas the NACA 0022, six-bladed system with the same solidity only produced 20.48 W of power. The trend from this blade number study also follows the trend found in Section 3.7 Figures 3.41, 3.42, 3.43 and 3.45 for torque.

Lastly, concerning solidity, comparing Figure 3.48 to Figures 3.50 and 3.51, the NACA 0022, three-bladed, 55% solidity configuration produced the greatest power of 67.78 W whereas the NACA 0022, three-bladed, 41% solidity configuration produced the lowest maximum power of 35.36 W. The NACA 0022, three-bladed, 48% solidity configuration produced a maximum power of 47.08 W. This trend does not agree with the corresponding trend found for torque/speed relationship, Section 3.7 Figures 3.41, 3.43 and 3.44. Consequently, this means that although the 55% solidity configuration produced a lower value of torque when compared to the 48% turbine, it was actually rotating much faster, thus, from Equation 3.36, more power was produced. As previously mentioned, each turbine configuration may have its uses based on specific design requirements. In other words, a customer might demand an explicit power output or maybe only one flow speed is available at a given site, thus making it appropriate to select a specific configuration. However, if the ultimate goal is to maximize power, the result simply that the optimum configuration from this set of studies would be a turbine utilizing 2 blades, a solidity of 55% and a NACA 0020 profile.

Next, each turbine configuration was tested to determine the drag force caused by the blades. Figures 3.53 to 3.59 show the resultant plots from the drag tests. The maximum drag created by each turbine configuration, at each speed, is also summarized in Table 3.5.

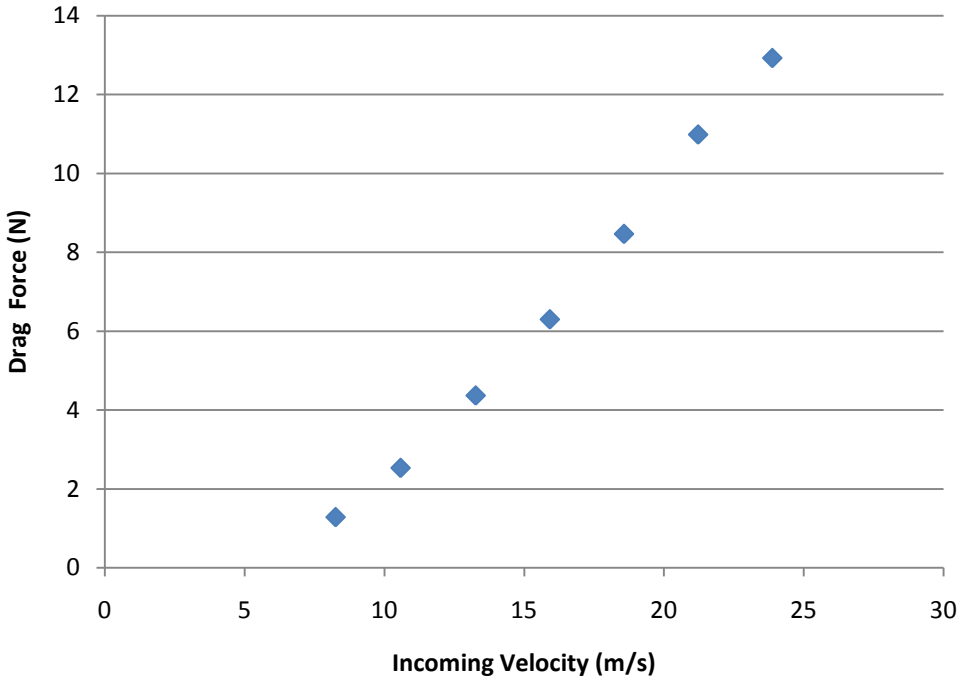

Figure 3.53. Drag vs incoming speed curves for NACA 653-018, three-bladed system with 48% solidity

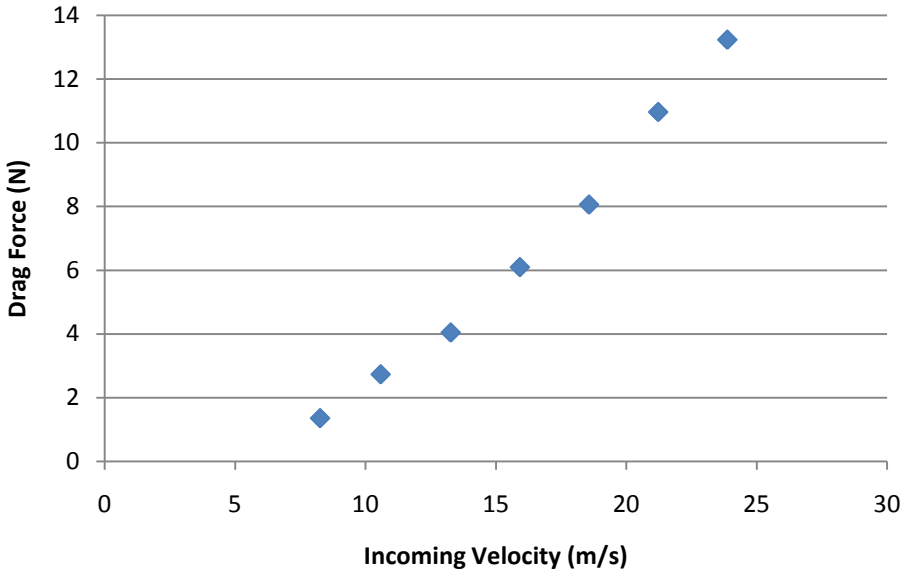

Figure 3.54. Drag vs. incoming velocity curves for NACA 0020, three-bladed system with 48% solidity

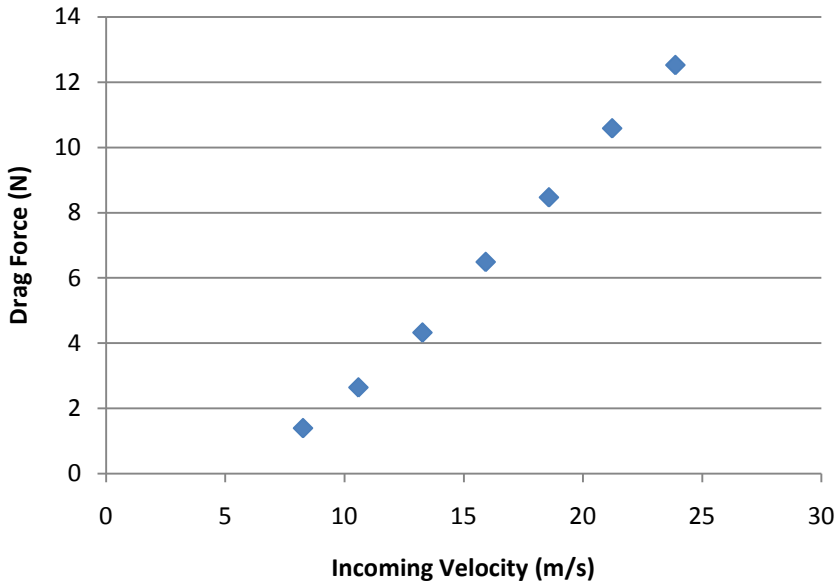

Figure 3.55. Drag vs. incoming velocity curves for NACA 0022, three-bladed system with 48% solidity

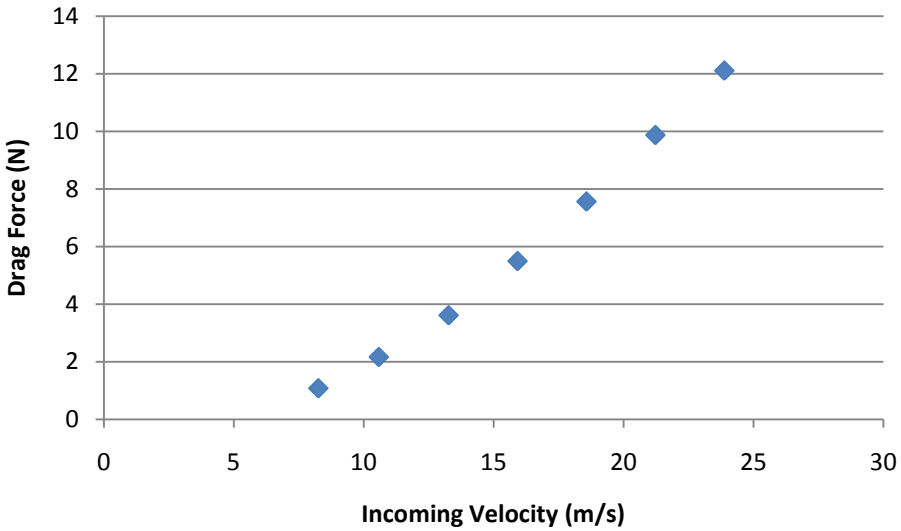

Figure 3.56. Drag vs. incoming velocity curves for NACA 0022, six-bladed system with 48% solidity

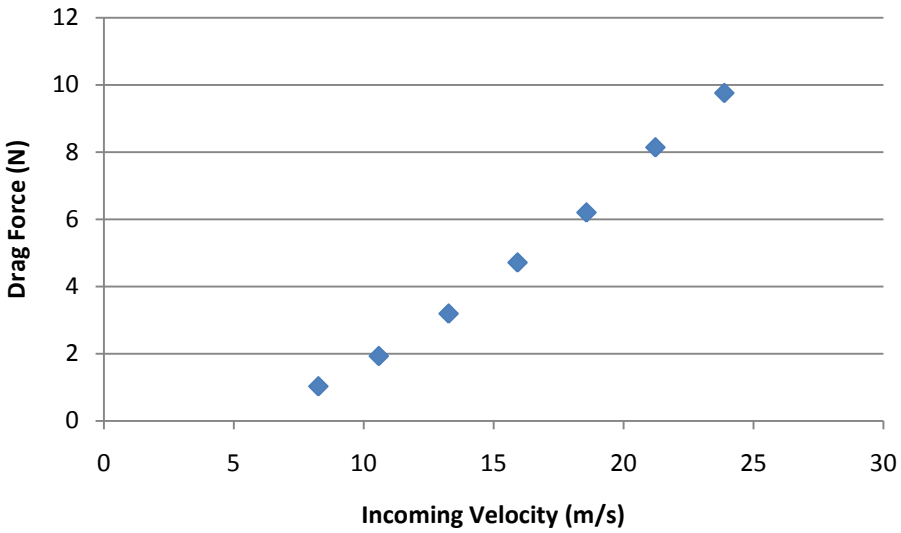

Figure 3.57. Drag vs. incoming velocity curves for NACA 0022, three-bladed system with 41% solidity

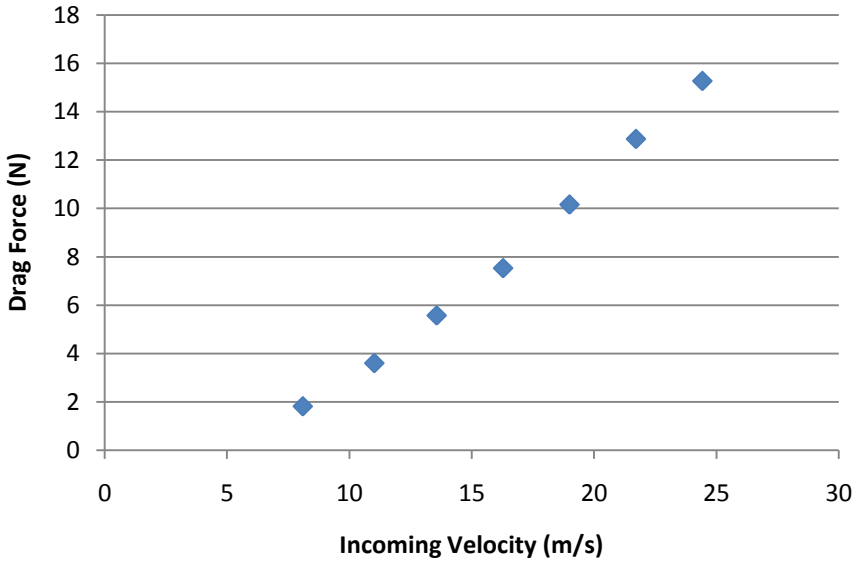

Figure 3.58. Drag vs. incoming velocity curves for NACA 0022, three-bladed system with 55% solidity

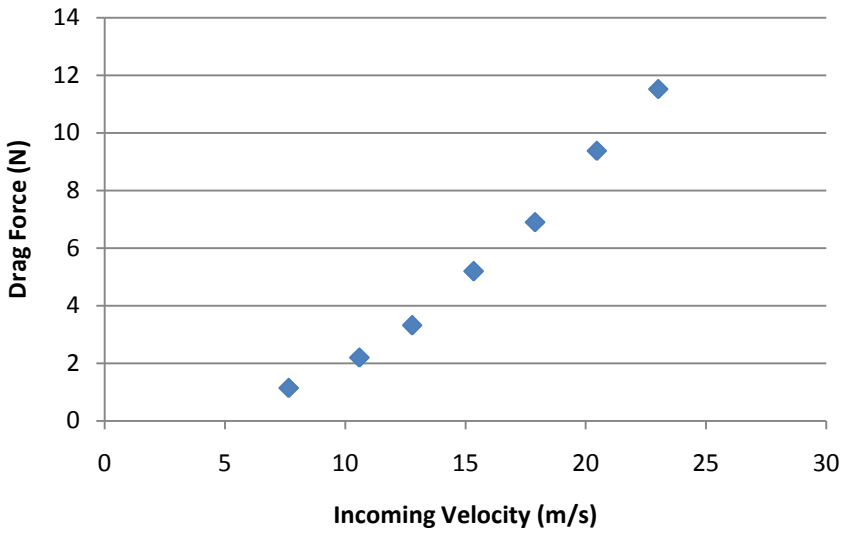

Figure 3.59. Drag vs. incoming velocity curves for NACA 0022, two-bladed system with 41% solidity

Table 3.5 Summary of Maximum Model Drag in Newtons for Variable Incoming Flow-speeds

Wind Tunnel Speed (m/s)	NACA 653018 (3 Blade) (48%)	NACA 0020 (3 Blade) (48%)	NACA 0022 (3 Blade) (48%)	NACA 0022 (6 Blade) (48%)	NACA 0022 (3 Blade) (41%)	NACA 0022 (3 Blade) (55%)	NACA 0022 (2 Blade) (41%)
7.7-8.3	1.3	1.4	1.4	1.1	1.0	1.8	1.1
10.6-11.0	2.5	2.7	2.6	2.2	1.9	3.6	2.2
12.8-13.6	4.4	4.0	4.3	3.6	3.2	5.6	3.3
15.3-16.3	6.3	6.1	6.5	5.5	4.7	7.5	5.2
17.9-19.0	8.5	8.1	8.5	7.6	6.2	10.2	6.9
20.5-21.7	11.0	11.0	10.6	9.9	8.1	12.9	9.4
23.0-24.4	12.9	13.2	12.5	12.1	9.8	15.3	11.5

As before, the first study concerned airfoil profile. For this study, each configuration consisted of three-blades and a 48% solidity. As can be seen in Table 3.5 and Figures 3.53 to 3.55, each of these configurations produced nearly equivalent drag forces at each incoming velocity, with the maximum drag produced ranging from 12.52 to 13.23 N. This result is expected since drag is proportional to the projected frontal blade area of the turbine blades. This also means that as long as solidity is held constant, the

airfoil profile does not have much of an impact on the drag force. Additionally, it can be seen from Figure 3.56 that the maximum drag force for the six-bladed turbine at the same solidity (48%) is 12 N, just short of the aforementioned range. Consequently, blade number has very little impact on the drag force when solidity is held constant. The last important result for this study shows that the maximum drag out of all configurations occurred for the turbine with maximum solidity. The 55% solidity turbine, Figure 3.58 produced a maximum drag force of 15.27 N, whereas the minimum drag force came from the 41% solidity configurations, Figures 3.57 and 3.59, with a corresponding maximum drag ranging from 9.76 to 11.52 N.

3.8 Uncertainty Analysis

When examining the plots in Section 3.7 and/or the raw data in Appendix A, the reader might be concerned with the efficiency of these systems given that previous research has shown the range of efficiencies for these turbines to be between 15-35%.[1-4] This was also a concern of the authors which was addressed. Due to design and operating conditions, not all helical turbines will reach the maximum efficiency limit of 35%. To reach this limit requires an optimal design with optimal flow conditions. However, it is expected that given a reasonable design and flow conditions, these turbines should fall within 15-35%. Table 3.6 summarizes the maximum efficiency of each of the tested configurations in percent.

There are several possible explanations for this shortfall; First, it is likely that there exists another extremely important variable that affects turbine performance which was not tested. This variable is the blade pitch.[2,8,13] Blade pitch refers to rotating the blades into or away from the rotor which causes a change in the angle of attack relative to

Table 3.6. Maximum Turbine Efficiency

	NACA 65_3018 (3 Blade) (48%)	NACA 0020 (3 Blade) (48%)	NACA 0022 (3 Blade) (48%)	NACA 0022 (6 Blade) (48%)	NACA 0022 (3 Blade) (41%)	NACA 0022 (3 Blade) (55%)	NACA 0022 (2 Blade) (41%)
Maximum Efficiency	3.8	9.2	6.8	2.7	4.7	14.0	11.3

the fluid. Since the angle of attack is directly related to the amount of power produced by the turbine, it is evident by again examining Figure 3.2 that changing the pitch of the blades could have a dramatic effect on the overall power production of the turbine.[13]In other words, if the angle of attack is controlled to be within the 5-15 degree range, wherein Figure 3.2 shows that the coefficient of lift is much greater than the coefficient of drag, more power will be produced thus making the turbine more efficient. From previous studies done by Gorlov and associates, it is expected that finding the optimal pitch angle for a turbine can raise the efficiency between 5% and 7%.[2]

Secondly, there always exists uncertainty in experimental measurements that should be accounted for. Since several measurements are compounded together into a final result, small uncertainties in each measurement can add up to large uncertainties in the final measured value of interest. Accordingly, an uncertainty analysis was conducted to capture the total uncertainty in this set of test measurements. It is important to note that this uncertainty analysis method is very conservative due to the assumption found between Equation 3.48 And 3.49.[20]

Beginning with efficiency η, defined as

$$\eta = \frac{P_H}{P_A} \tag{3.38}$$

where P_H stands for power harvested and P_A stands for power available. Equation 3.39 and 3.40 are the definitions for available power and harvested power.

$$P_A = \frac{1}{2}\rho A V^3 \tag{3.39}$$

$$P_H = T\omega \tag{3.40}$$

Here ρ is the density of the fluid, A is the frontal area of the turbine, V is the incoming flow-speed, T is the torque generated by the turbine, and ω is the angular velocity of the turbine. Thus efficiency is a function of torque, angular velocity, density, incoming velocity, and turbine area measurements.

$$\eta = \eta(T, \omega, \rho, V, A) \tag{3.41}$$

where each of the measured quantities can be represented in terms of their mean value plus or minus some uncertainty.

$$T = \bar{T} \pm \Delta T \tag{3.42}$$

$$\omega = \bar{\omega} \pm \Delta\omega \tag{3.43}$$

$$\rho = \bar{\rho} \pm \Delta\rho \tag{3.44}$$

$$V = \bar{V} \pm \Delta V \tag{3.45}$$

$$A = \bar{A} \pm \Delta A \tag{3.46}$$

Here, the bar represents the mean value and Δ represents the uncertainty. Substituting these values into the original efficiency function and performing a first order Taylor's series expansion yields Equation 3.47.

$$\eta(\bar{T} \pm \Delta T, \bar{\omega} \pm \Delta\omega, \bar{\rho} \pm \Delta\rho, \bar{V} \pm \Delta V, \bar{A} \pm \Delta A) =$$

$$\eta(\bar{T}, \bar{\omega}, \bar{\rho}, \bar{V}, \bar{A}) + \frac{\partial\eta}{\partial T}\Delta T + \frac{\partial\eta}{\partial\omega}\Delta\omega + \frac{\partial\eta}{\partial\rho}\Delta\rho + \frac{\partial\eta}{\partial V}\Delta V + \frac{\partial\eta}{\partial A}\Delta A \qquad (3.47)$$

Subtracting $\eta(\bar{T}, \bar{\omega}, \bar{\rho}, \bar{V}, \bar{A})$ from both sides yields Equation 3.48, a measure of the uncertainty in efficiency.

$$\Delta\eta = \frac{\partial\eta}{\partial T}\Delta T + \frac{\partial\eta}{\partial\omega}\Delta\omega + \frac{\partial\eta}{\partial\rho}\Delta\rho + \frac{\partial\eta}{\partial V}\Delta V + \frac{\partial\eta}{\partial A}\Delta A \qquad (3.48)$$

However, because the uncertainty in the individual estimates typically falls within the given $\pm$ range according to a Gaussian distribution, a better estimate of the uncertainty in η is seen in Equation 3.49.[20]

$$\Delta\eta = \sqrt{\left(\frac{\partial\eta}{\partial T}\Delta T\right)^2 + \left(\frac{\partial\eta}{\partial\omega}\Delta\omega\right)^2 + \left(\frac{\partial\eta}{\partial\rho}\Delta\rho\right)^2 + \left(\frac{\partial\eta}{\partial V}\Delta V\right)^2 + \left(\frac{\partial\eta}{\partial A}\Delta A\right)^2} \qquad (3.49)$$

At this point each partial derivative from Equation 3.50 is determined.

$$\frac{\partial\eta}{\partial T} = \frac{\omega}{\frac{1}{2}\rho AV^3}\frac{T}{T} = \frac{\eta}{T} \qquad (3.50)$$

$$\frac{\partial\eta}{\partial\omega} = \frac{T}{\frac{1}{2}\rho AV^3}\frac{\omega}{\omega} = \frac{\eta}{\omega} \qquad (3.51)$$

$$\frac{\partial\eta}{\partial\rho} = \frac{-T\omega}{\frac{1}{2}\rho^2 AV^4} = \left(\frac{-1}{\rho}\right)\left(\frac{T\omega}{\frac{1}{2}\rho AV^3}\right) = \frac{-\eta}{\rho} \qquad (3.52)$$

$$\frac{\partial\eta}{\partial V} = \frac{-3T\omega}{\frac{1}{2}\rho AV^4} = \left(\frac{-3}{V}\right)\left(\frac{T\omega}{\frac{1}{2}\rho AV^3}\right) = \frac{-3\eta}{V} \qquad (3.53)$$

$$\frac{\partial\eta}{\partial A} = \frac{-T\omega}{\frac{1}{2}\rho A^2V^4} = \left(\frac{-1}{A}\right)\left(\frac{T\omega}{\frac{1}{2}\rho AV^3}\right) = \frac{-\eta}{A} \qquad (3.54)$$

Substituting the results into Equation 3.48 and dividing by η yields Equation 3.55.

$$\frac{\Delta\eta}{\eta} = \left[\left(\frac{\Delta T}{T}\right)^2 + \left(\frac{\Delta\omega}{\omega}\right)^2 + \left(-1\frac{\Delta\rho}{\rho}\right)^2 + \left(-3\frac{\Delta V}{V}\right)^2 + \left(-1\frac{\Delta A}{A}\right)^2\right]^{0.5} \tag{3.55}$$

The torque, angular velocity, density and turbine area measurements are measured directly so those variables are solved; however, velocity is dependent on the manometer pressure reading and daily air density. Based on Bernoulli's equation,

$$\Delta V = \sqrt{\frac{2dP}{\rho}} \tag{3.56}$$

applying the same Taylor's series expansion as before, the uncertainty in velocity may be estimated as seen in Equation 3.57.

$$\Delta V = \sqrt{\left(\frac{\partial V}{\partial P}\Delta P\right)^2 + \left(\frac{\partial V}{\partial \rho}\Delta\rho\right)^2} \tag{3.57}$$

The same process as above is employed to determine the partial derivatives of each variable yielding Equations 3.58 and 3.59.

$$\frac{\partial V}{\partial P} = \left(\frac{1}{2dP}\right)\left(\sqrt{\frac{2dP}{\rho}}\right) = \frac{V}{2dP} \tag{3.58}$$

$$\frac{\partial V}{\partial \rho} = \left(\frac{-1}{2\rho}\right)\left(\sqrt{\frac{2P}{\rho}}\right) = \frac{-V}{2\rho} \tag{3.59}$$

Substituting these equations back into Equation 3.57 produces Equation 3.60.

$$\frac{\Delta V}{V} = \sqrt{\left(\frac{\Delta P}{2P}\right)^2 + \left(\frac{-\Delta\rho}{2\rho}\right)^2} \tag{3.60}$$

As mentioned previously, *P* is the manometer pressure which is read directly from the instrument however, once again, air density $\rho$is comprised of the ideal gas constant *R*, the barometric pressure *Pb* and the atmospheric temperature *Ta*. Thus, based on the ideal gas law, $\rho = \frac{P_b}{RT_a}$, the partial variables must again be solved. Equation 3.61 shows the relationship between air density and its variables.

$$\Delta\rho = \sqrt{\left(\frac{d\rho}{dR}\Delta R\right)^2 + \left(\frac{d\rho}{dP_b}\Delta P_b\right)^2 + \left(\frac{d\rho}{dT_a}\Delta T_a\right)^2} \tag{3.61}$$

Again, the partial derivative of each variable is taken as can be seen from Equation 3.62 to 3.64.

$$\frac{d\rho}{dR} = \frac{-P_b}{R^2T_a} = \frac{-\rho}{R} \tag{3.62}$$

$$\frac{d\rho}{dP_b} = \frac{1}{RT_a} = \frac{\rho}{P_b} \tag{3.63}$$

$$\frac{d\rho}{dT_a} = \frac{-RP_b}{{T_a}^2} = \frac{-\rho}{T_a} \tag{3.64}$$

These final variables are substituted into Equation 3.61 yielding Equation 3.65.

$$\frac{\Delta\rho}{\rho} = \left(\left(\frac{-\Delta R}{R}\right)^2 + \left(\frac{\Delta P_b}{P_b}\right)^2 + \left(\frac{-\Delta T_a}{T_a}\right)^2\right) \tag{3.65}$$

With the uncertainty process completed, Equation 3.60 and 3.65 are substituted back into Equation 3.55 yielding Equation 3.66, the final equation for uncertainty.

$$\frac{\Delta\eta}{\eta} = \left[\begin{array}{c}\left(\frac{\Delta T}{T}\right)^2 + \left(\frac{\Delta\omega}{\omega}\right)^2 + \left(-1\left(\left(\frac{-\Delta R}{R}\right)^2 + \left(\frac{\Delta P_b}{P_b}\right)^2 + \left(\frac{-\Delta T_a}{T_a}\right)^2\right)\right)^2 \\ + \left(-3\left(\sqrt{\left(\frac{\Delta P}{2P}\right)^2 + \left(\frac{-\Delta\rho}{2\rho}\right)^2}\right)\right)^2 + \left(-1\frac{\Delta A}{A}\right)^2\end{array}\right]^{0.5} \tag{3.66}$$

Appendix D was created, which is simply an extension of the raw data in Appendix A. These tables show the uncertainty value calculated, by Equation 3.66, for each efficiency value. Table 3.7 summarizes the maximum uncertainties in efficiencies from Appendix D. Additionally, Figures 3.60b to 3.66b were constructed to graphically display the uncertainty with associated error bars for the model power/speed curves which are Figures 3.60a to 3.66a.

3.9 Scaling Test Results

In order to complete the experimental objectives, the model results needed to be scaled back up to full-scale water conditions. The original Buckingham Pi analysis mentioned in Section 3.3 was employed. First, the nondimensional Reynolds number parameter, Equation 3.21, was matched. Equation 3.67 shows the solved form of Equation 3.21 which was used to determine the full-scale angular velocity.

$$\omega_p = \omega_m * \left[\frac{\mu_m}{\mu_p}\frac{\rho_p}{\rho_m}\frac{D_p}{D_m}\right] \tag{3.67}$$

Table 3.7 Summary of Maximum Efficiency Uncertainties in Percent

Wind Tunnel Speed (m/s)	NACA 653018 (3 Blade) (48%)	NACA 0020 (3 Blade) (48%)	NACA 0022 (3 Blade) (48%)	NACA 0022 (6 Blade) (48%)	NACA 0022 (3 Blade) (41%)	NACA 0022 (3 Blade) (55%)	NACA 0022 (2 Blade) (41%)
7.7-8.3	2.4	3.5	2.8	1.5	2.6	6.0	4.7
10.6-11.0	1.5	2.8	1.7	1.1	1.6	4.0	2.6
12.8-13.6	1.1	1.7	1.4	0.8	1.3	3.0	2.1
15.3-16.3	1.0	1.4	1.0	0.6	0.9	2.0	1.3
17.9-19.0	0.6	1.1	0.8	0.5	0.8	1.7	1.1
20.5-21.7	0.5	0.8	0.6	0.4	0.6	1.4	0.8
23.0-24.4	0.4	0.7	0.5	0.3	0.5	1.1	0.7

With this final bit of information, torque, power, and drag force were scaled using Equation 3.68-3.70 respectively. Appendix C contains the resultant tables for the scaled-up values.

$$T_p = T_m * \left[\frac{\rho_p}{\rho_m}\frac{\omega_p^2}{\omega_m^2}\frac{D_p^5}{D_m^5}\right] \tag{3.68}$$

$$P_p = P_m * \left[\frac{\rho_p}{\rho_m}\frac{\omega_p^3}{\omega_m^3}\frac{D_p^5}{D_m^5}\right] \tag{3.69}$$

$$F_{Dp} = F_{Dm} * \left[\frac{\rho_p}{\rho_m}\frac{\omega_p^2}{\omega_m^2}\frac{D_p^4}{D_m^4}\right] \tag{3.70}$$

With the abundance of data, it is useful to be able to understand the relationship between torque, power, and speed so that one may achieve a specific power output given a specific input load. Typically this load would be the sum of the resistances of the system used to convert this harvested power into a useful form. Accordingly, the following figures were created to understand this relationship. Even Figures 3.60 to 3.72, are the plots generated for the wind tunnel models whereas Figures 3.74 to 3.80 correspond to the full-scale results in water. Also, as previously mentioned odd Figures 3.61 to 3.73, are the error bar plots associated with the power versus angular velocity curves. These figures provide the range of efficiency values associated with each measurement. In conjunction the following set of figures are very beneficial. With a known incoming flow speed, figures labeled with an *a* can be used to determine the power range of the system. At this point, the user would typically pick a range of power outputs suitable for their needs.

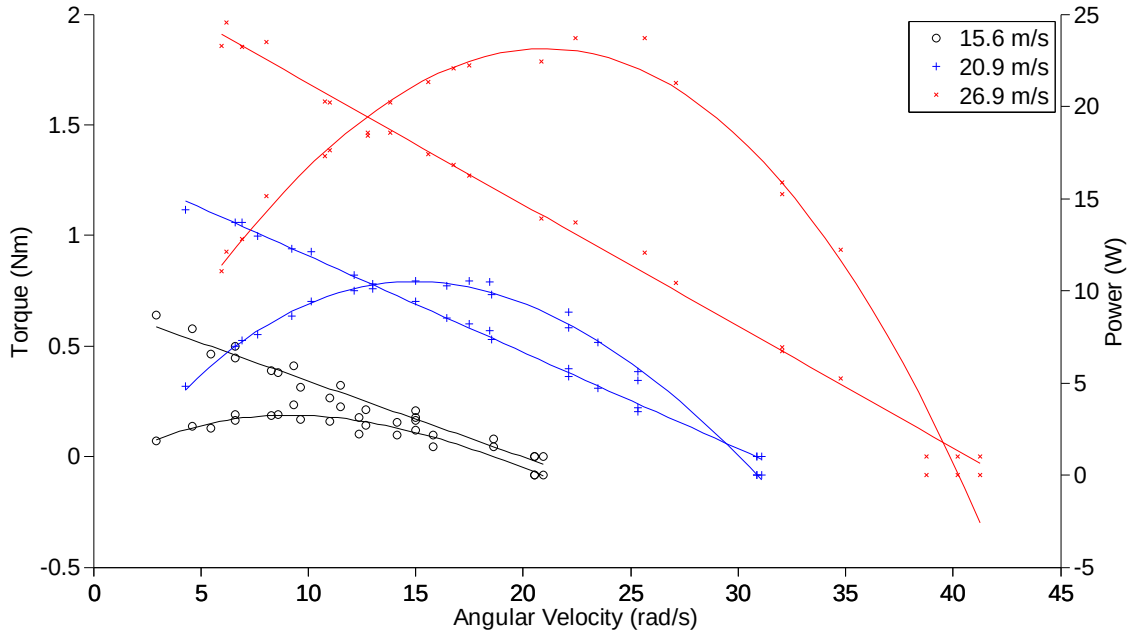

Figure 3.60. Model Torque/Speed curves superimposed with power/speed curves for NACA 653-018, three-bladed system with 48% solidity

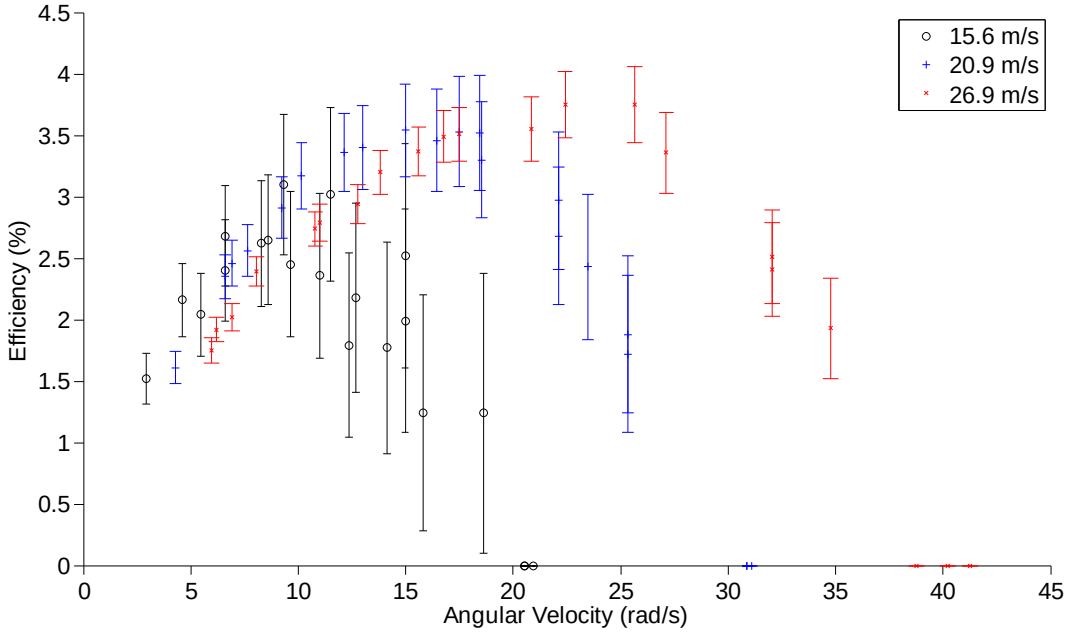

Figure 3.61. Model efficiency curves with uncertainty error bars for NACA 653-018, three-bladed system with 48% solidity

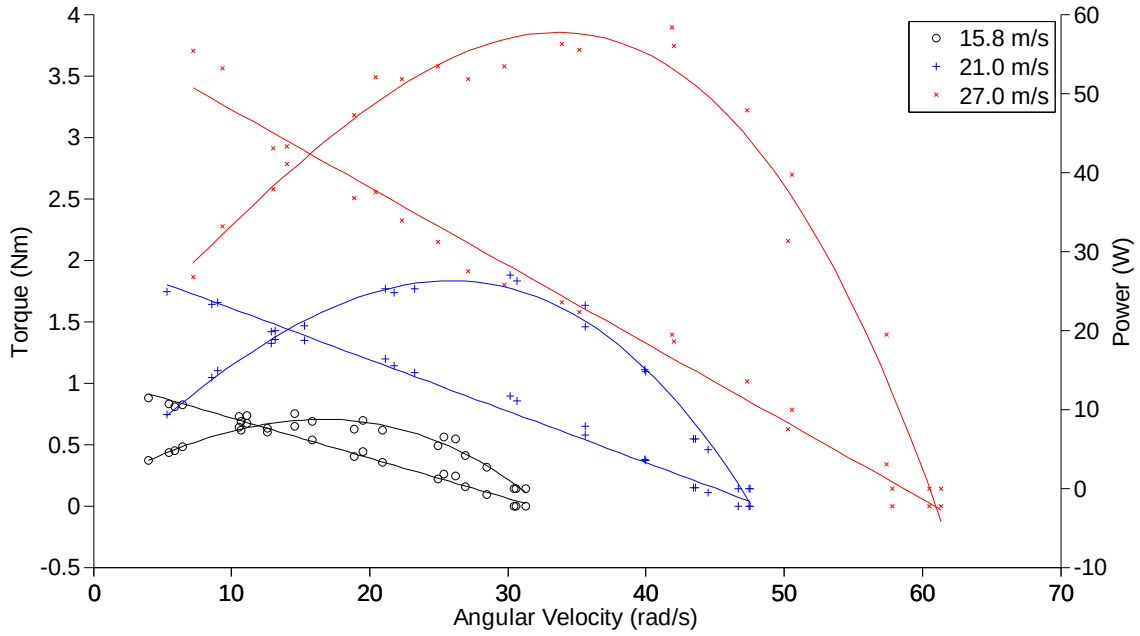

Figure 3.62. Model Torque/Speed curves superimposed with power/speed curves for NACA 0020, three-bladed system with 48% solidity

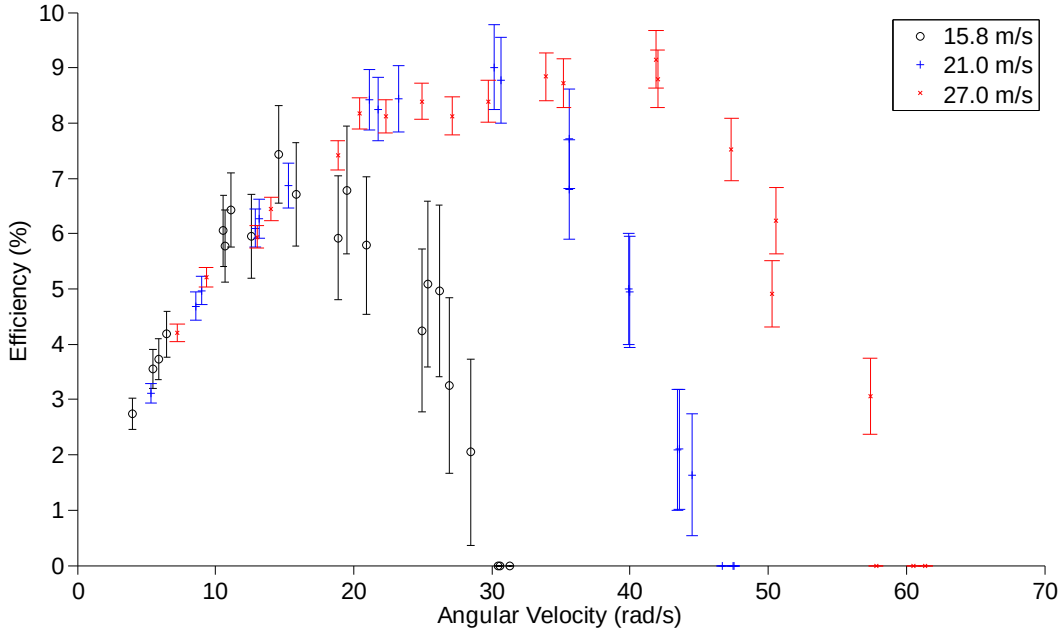

Figure 3.63. Model efficiency curves with uncertainty error bars for NACA 0020, three-bladed system with 48% solidity

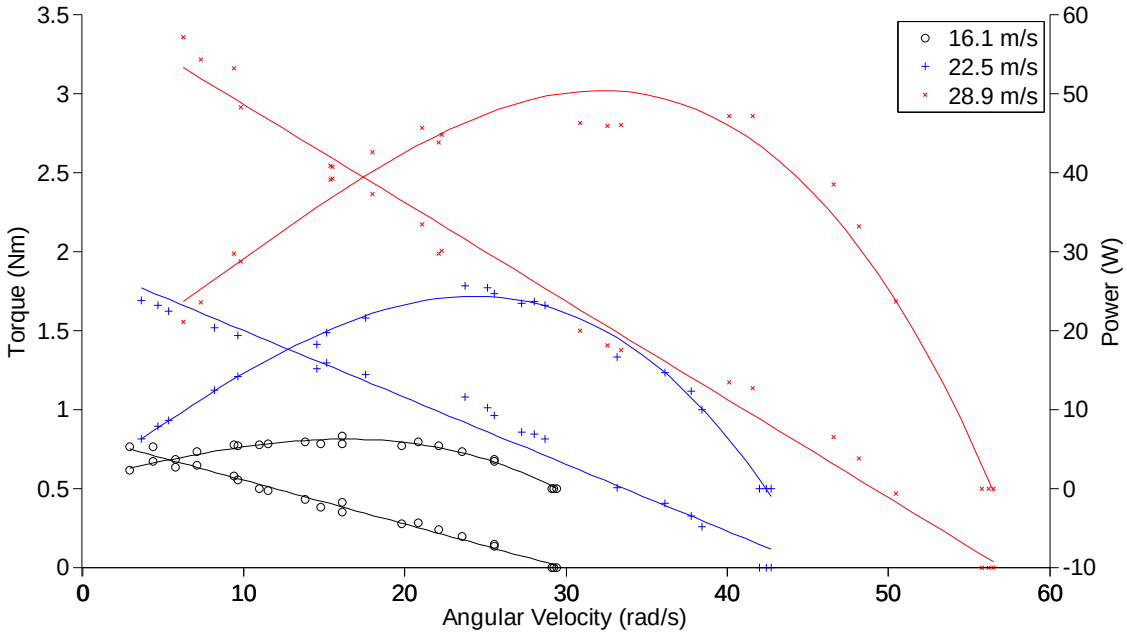

Figure 3.64. Model Torque/Speed curves superimposed with power/speed curves for NACA 0022, three-bladed system with 48% solidity

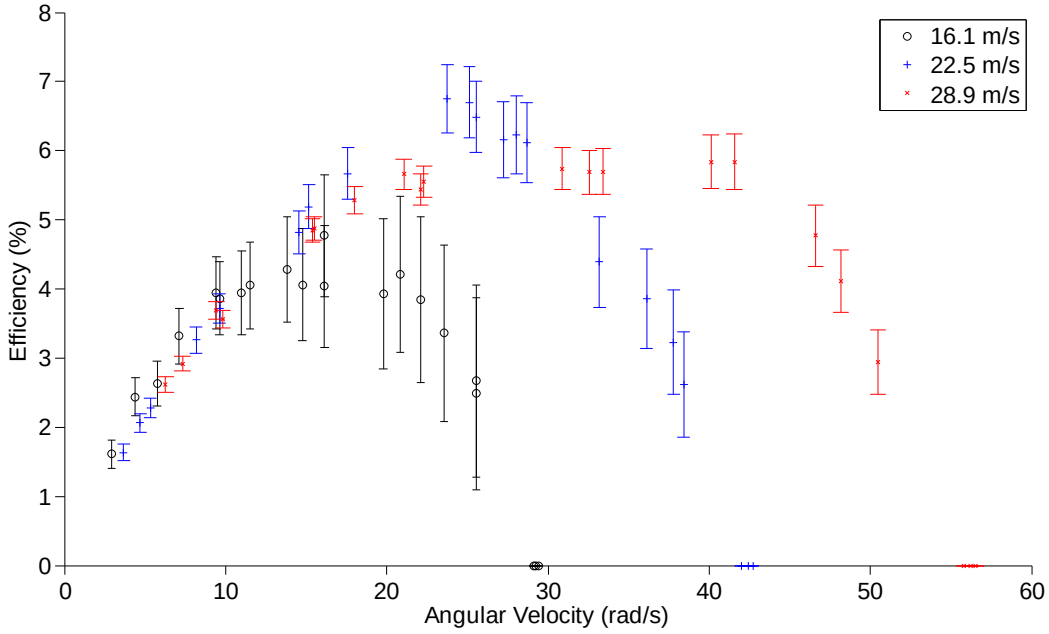

Figure 3.65. Model efficiency curves with uncertainty error bars for NACA 0022, three-bladed system with 48% solidity

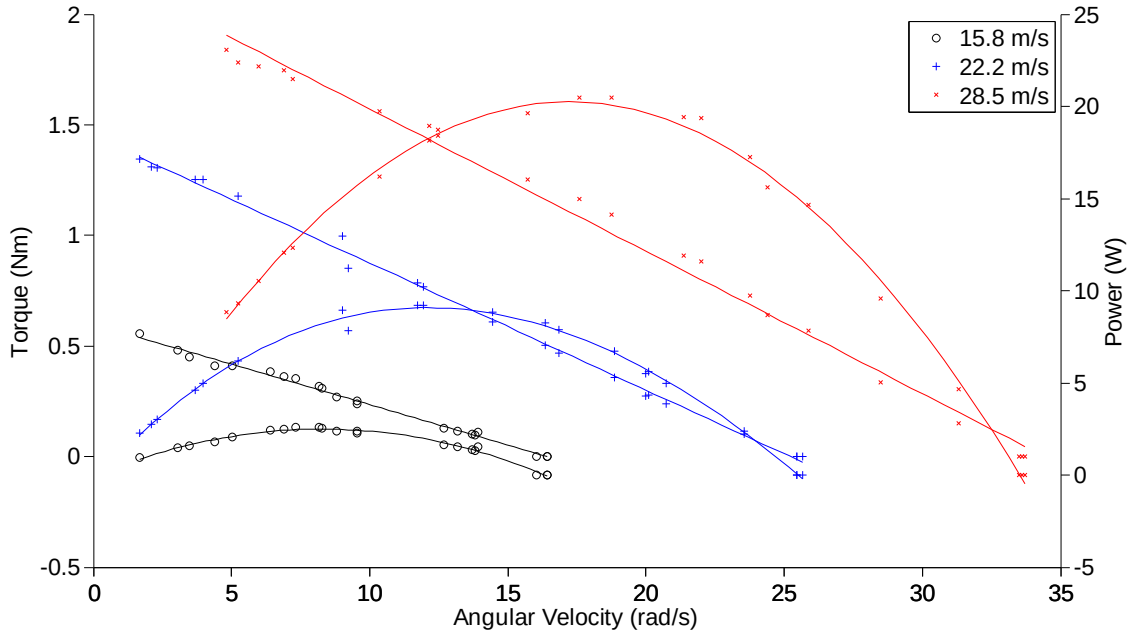

Figure 3.66. Model Torque/Speed curves superimposed with power/speed curves for NACA 0022, six-bladed system with 48% solidity

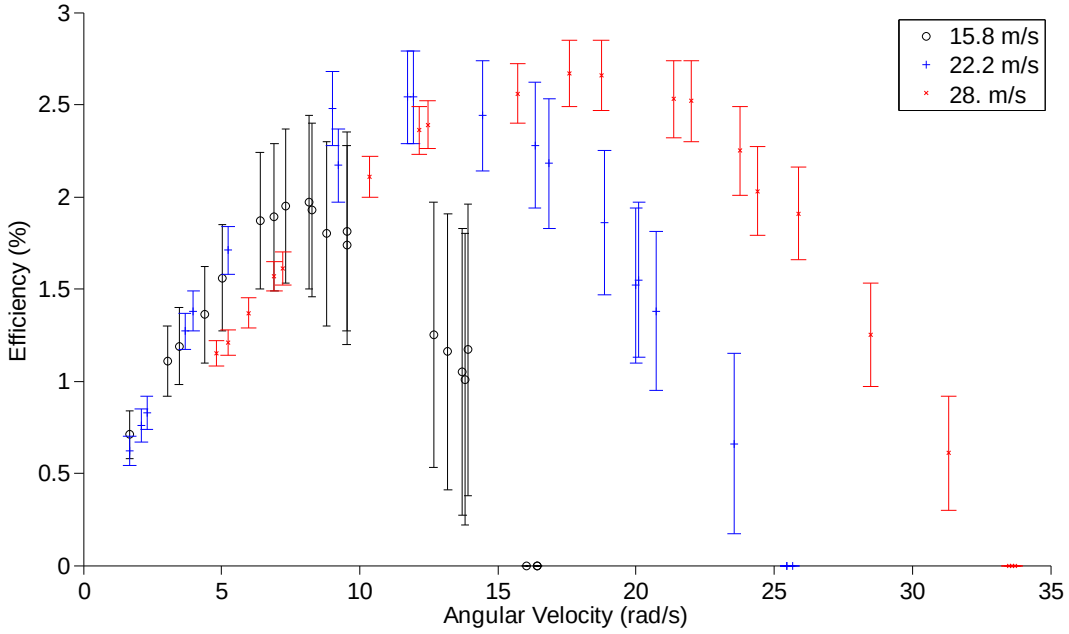

Figure 3.67. Model efficiency curves with uncertainty error bars for NACA 0022, six-bladed system with 48% solidity

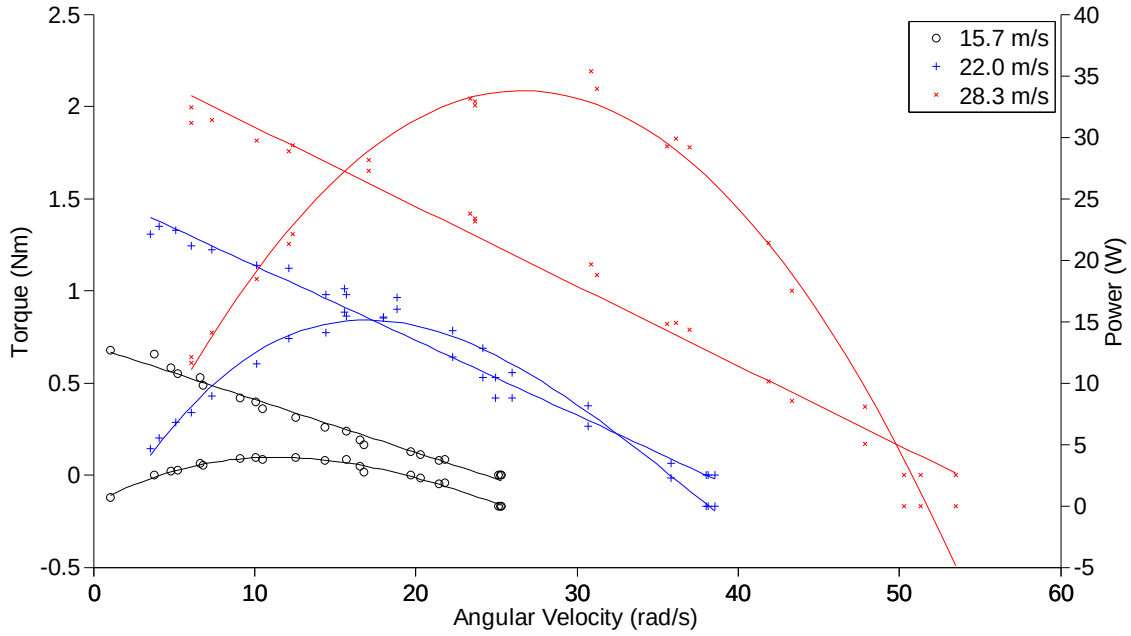

Figure 3.68. Model Torque/Speed curves superimposed with power/speed curves for NACA 0022, three-bladed system with 41% solidity

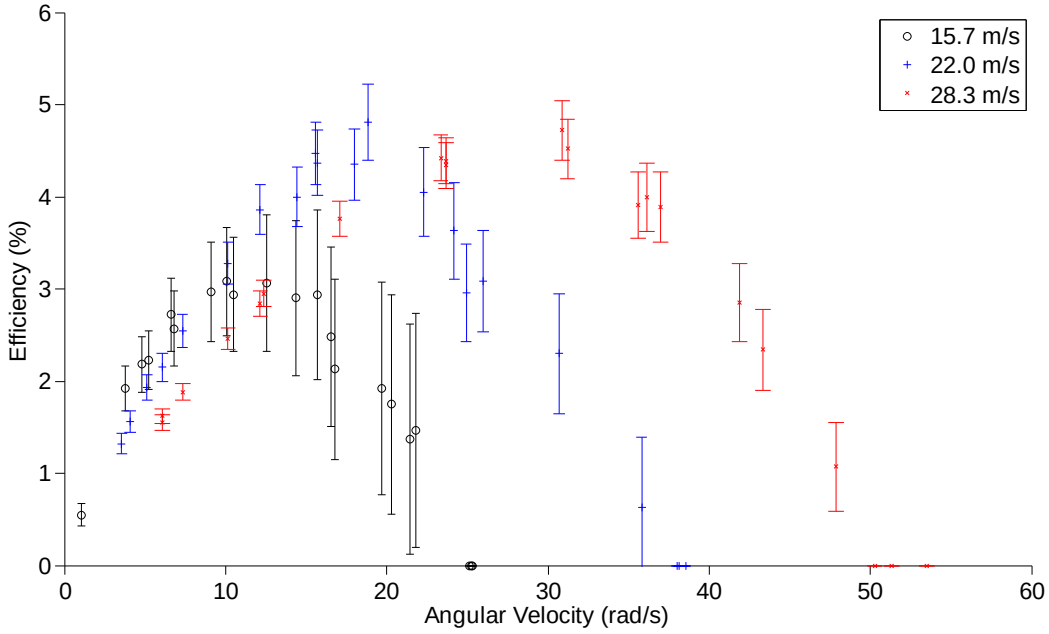

Figure 3.69. Model efficiency curves with uncertainty error bars for NACA 0022, three-bladed system with 41% solidity

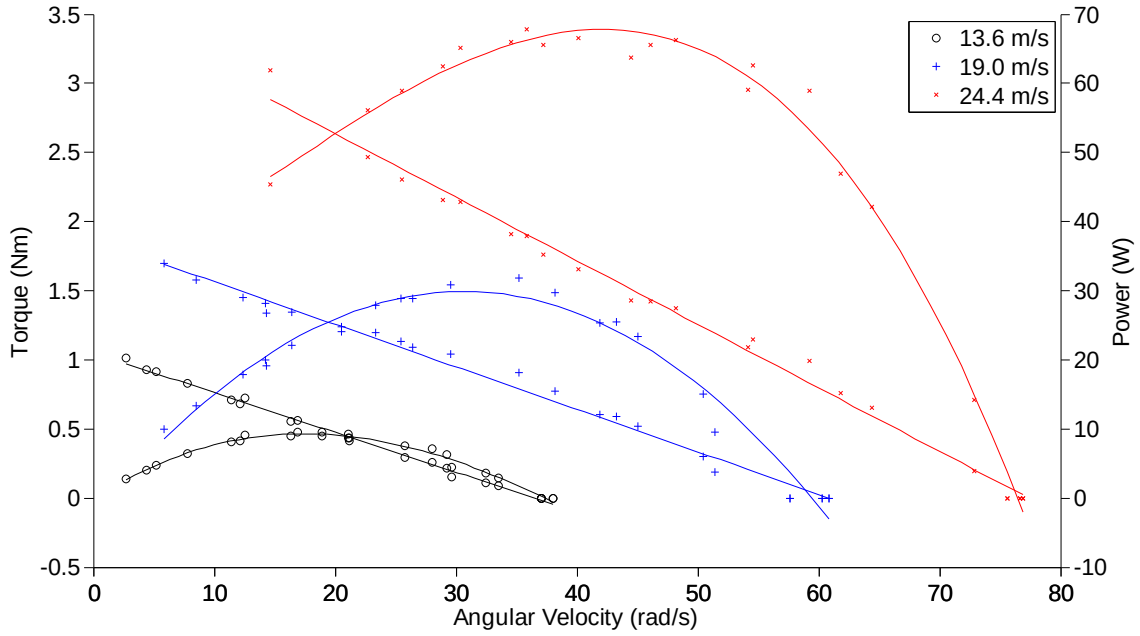

Figure 3.70. Model Torque/Speed curves superimposed with power/speed curves for NACA 0022, three-bladed system with 55% solidity

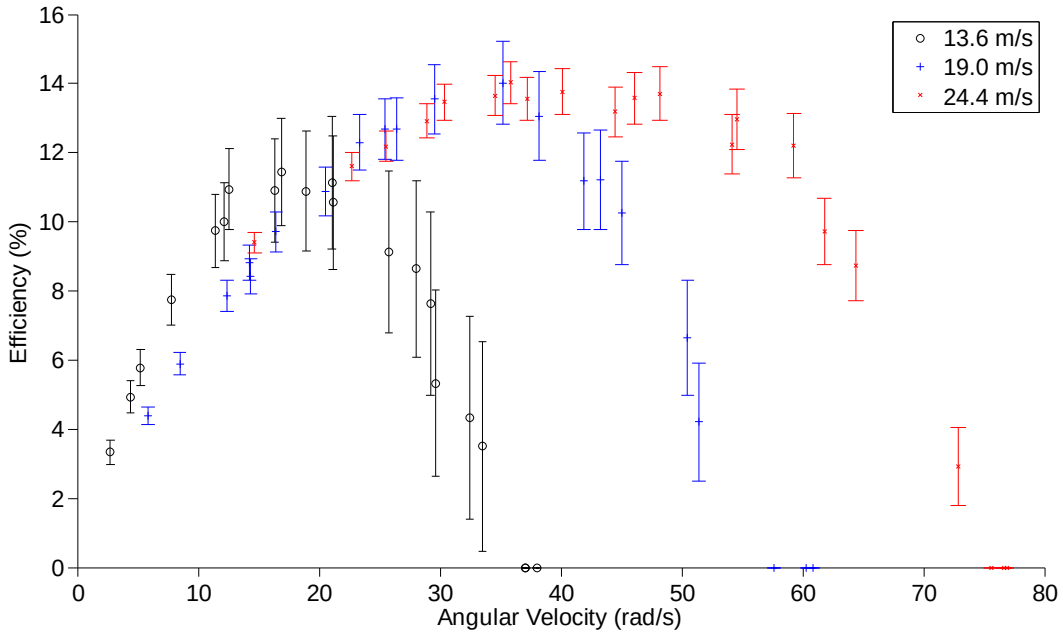

Figure 3.71. Model efficiency curves with uncertainty error bars for NACA 0022, three-bladed system with 55% solidity

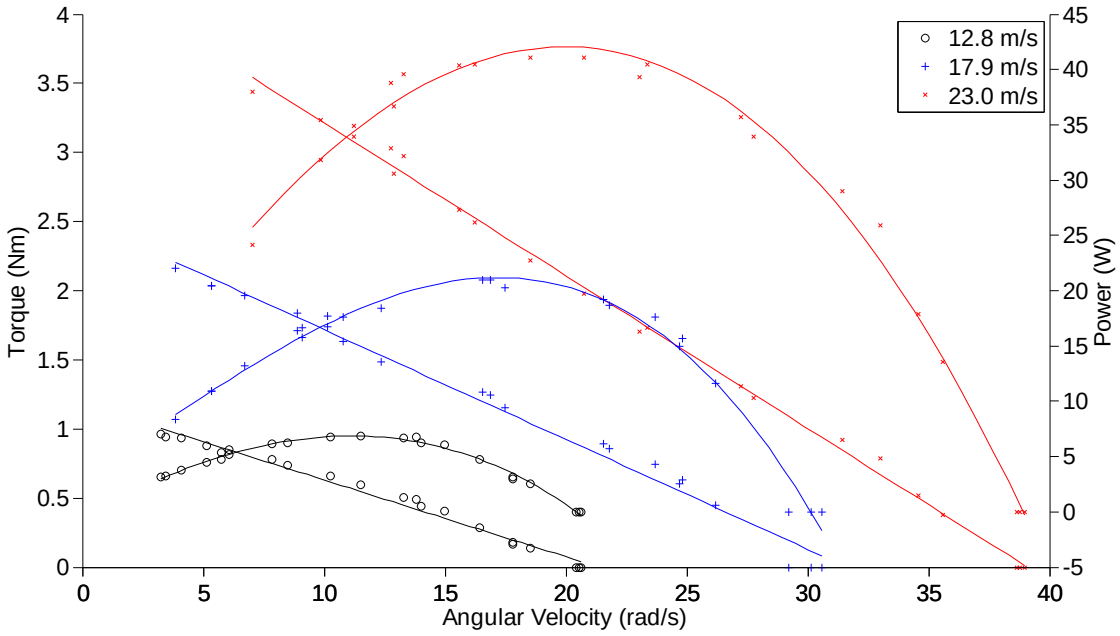

Figure 3.72. Model Torque/Speed curves superimposed with power/speed curves for NACA 0022, two-bladed system with 41% solidity

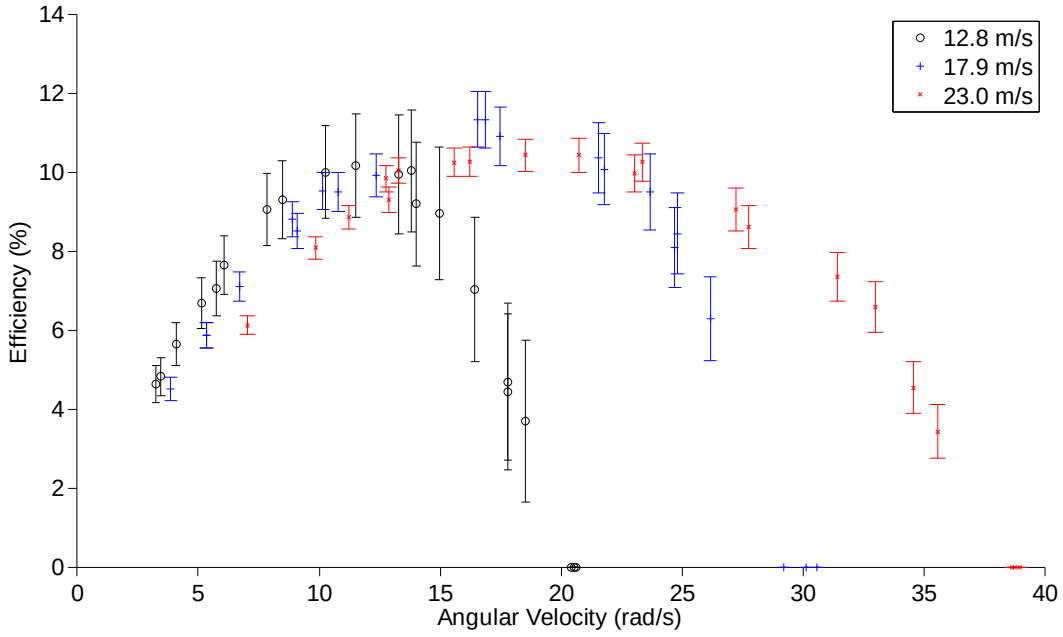

Figure 3.73. Model efficiency curves with uncertainty error bars for NACA 0022, two-bladed system with 41% solidity

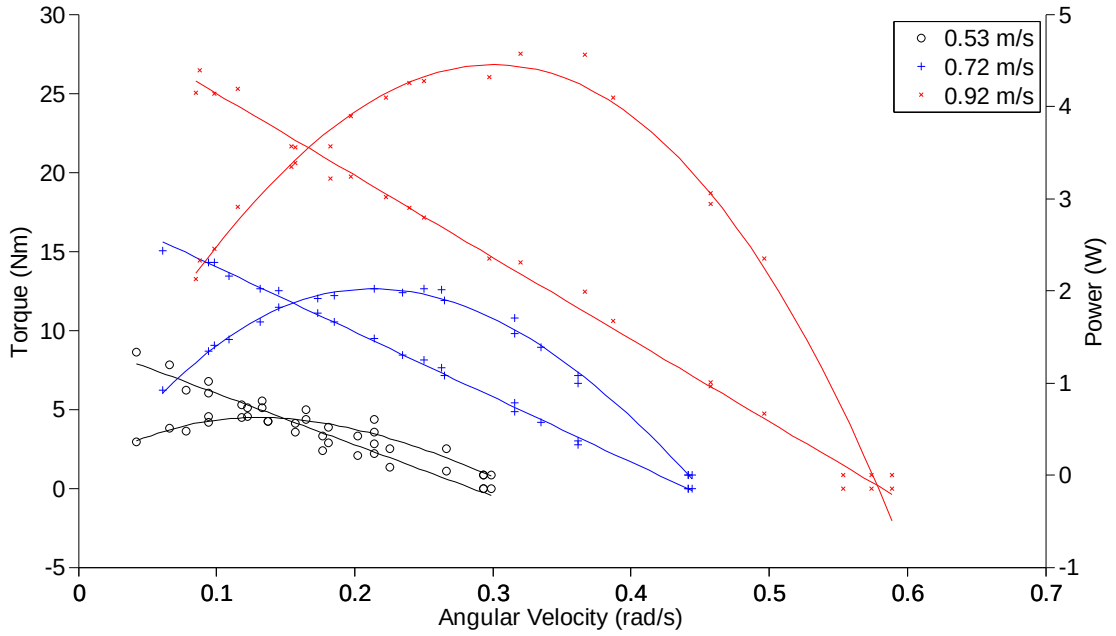

Figure 3.74. Full-scale Torque/Speed curves superimposed with power/speed curves for NACA 653-018, three-bladed system with 48% solidity

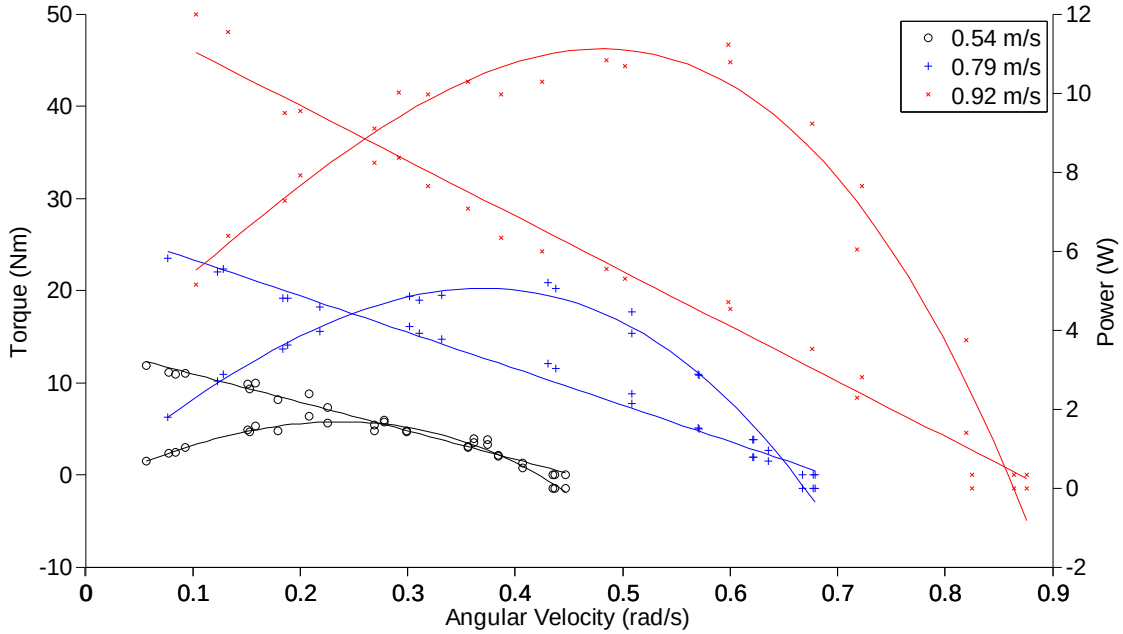

Figure 3.75. Full-scale Torque/Speed curves superimposed with power/speed curves for NACA 0020, three-bladed system with 48% solidity

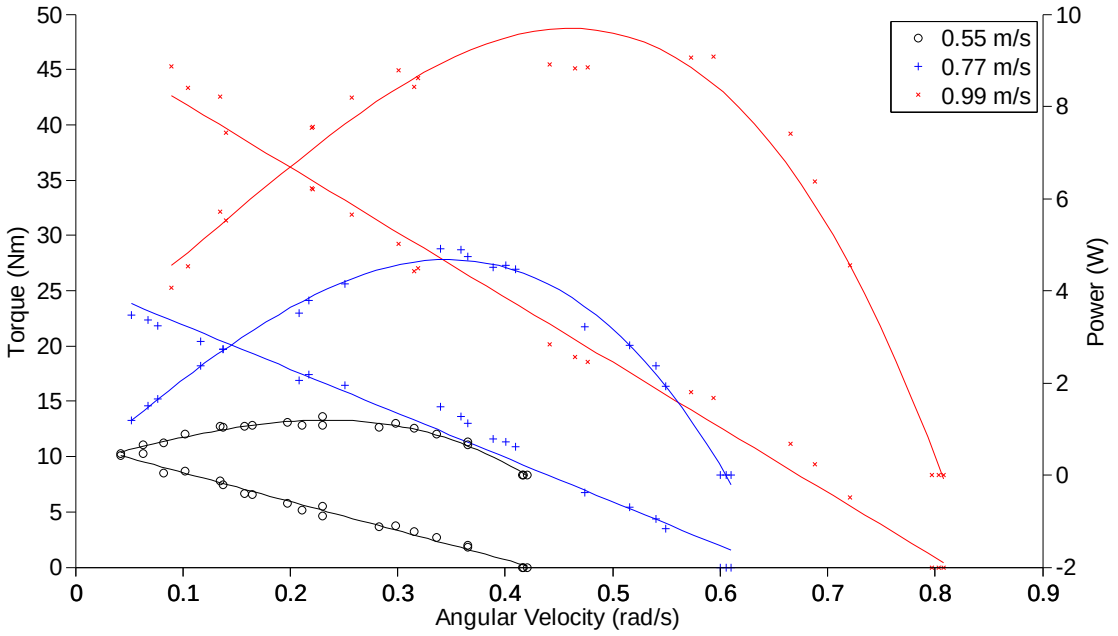

Figure 3.76. Full-scale Torque/Speed curves superimposed with power/speed curves for NACA 0022, three-bladed system with 48% solidity

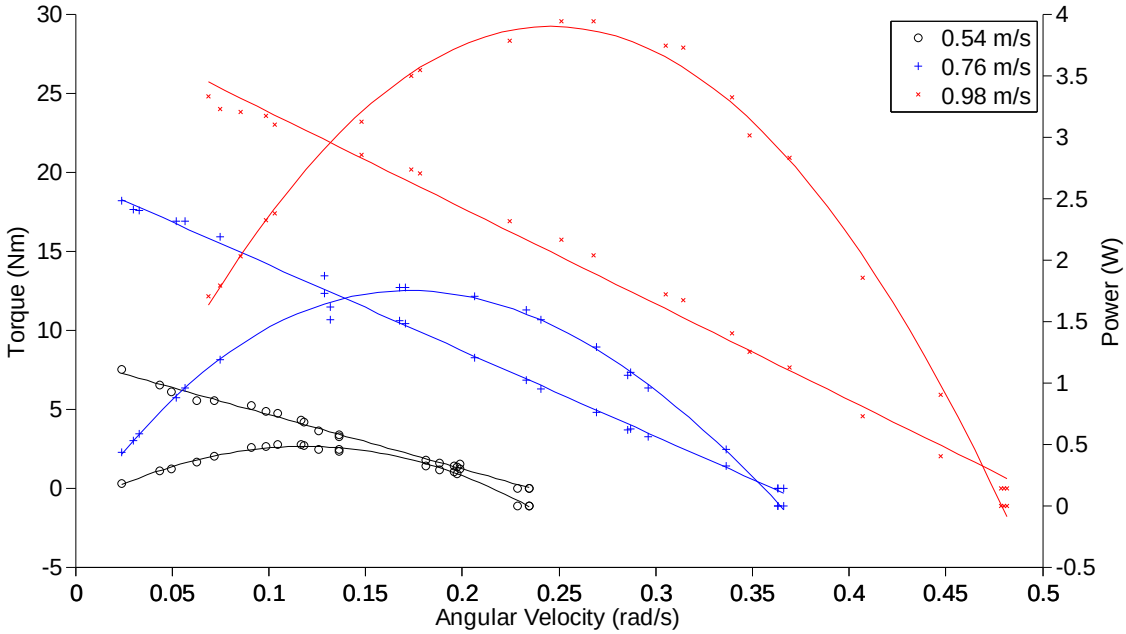

Figure 3.77. Full-scale Torque/Speed curves superimposed with power/speed curves for NACA 0022, six-bladed system with 48% solidity

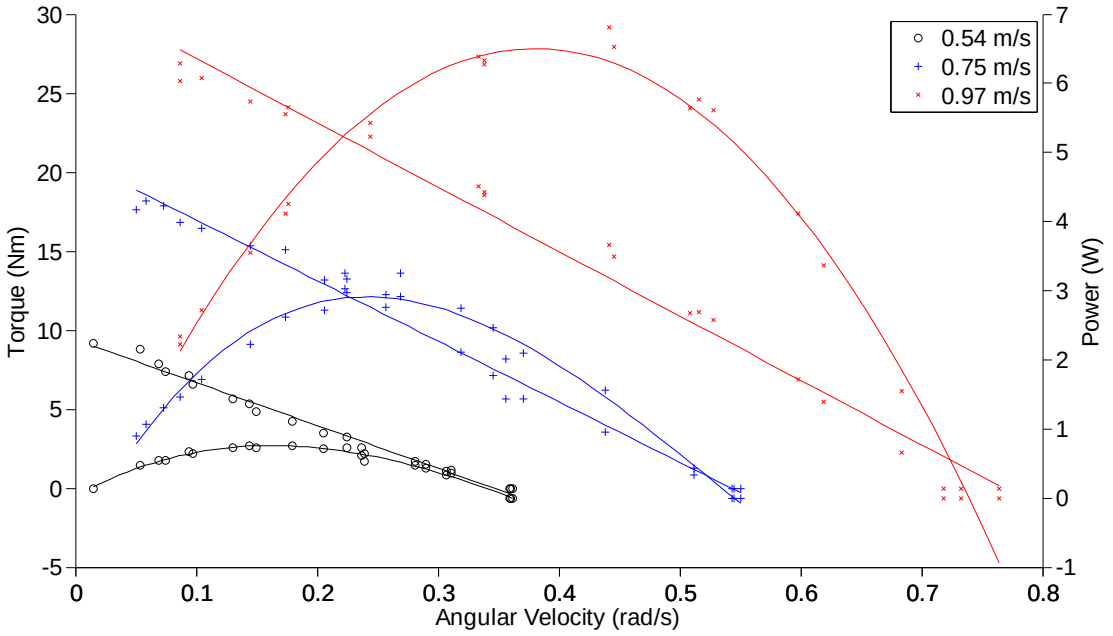

Figure 3.78. Full-scale Torque/Speed curves superimposed with power/speed curves for NACA 0022, three-bladed system with 41% solidity

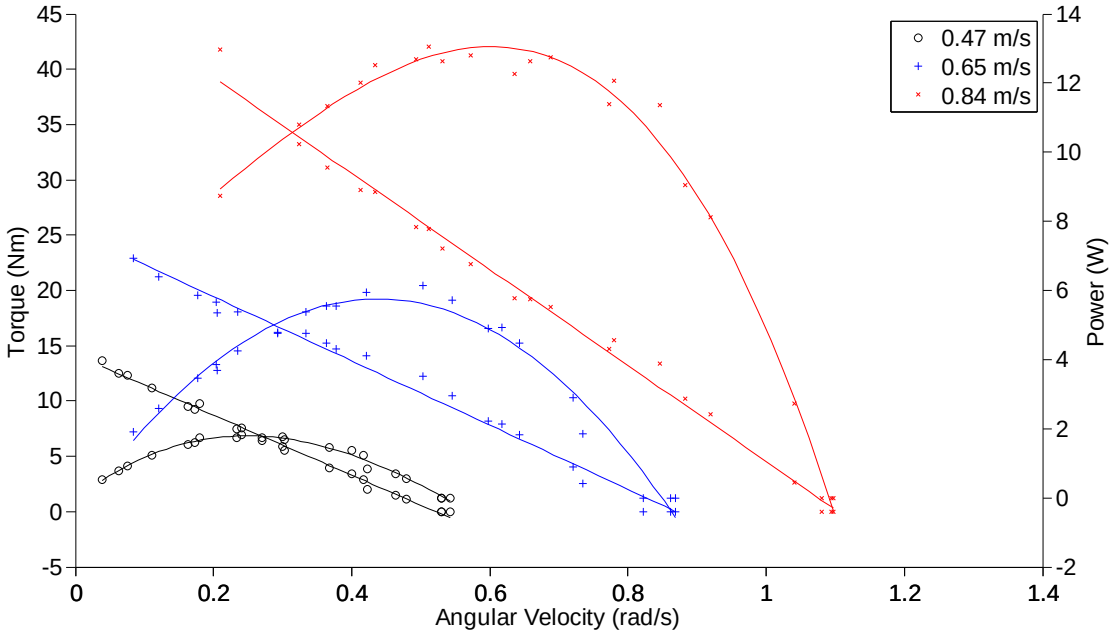

Figure 3.79. Full-scale Torque/Speed curves superimposed with power/speed curves for NACA 0022, three-bladed system with 55% solidity

After which, the associated error bar plot (labeled with a *b*) can be consulted to determine what angular velocities yield these power demands as well as the associated efficiencies. Once the ideal operating range is chosen, figures labeled with an *a* can be consulted again to find the range of torque values that match the needs of the design. Finally, this range of torque values can be used to design the power conversion system (i.e. the motor/generator/alternator) to ensure the design operates at optimum efficiencies thus meeting the initial goals for the power outputs. The scaled-up figures used to predict the performance in water, Figures 3.67 to 3.73, can be used the same way. These plots do not have associated error-bar plots to go with them due to the fact that the turbines were not tested in water but instead scaled from the wind tunnel test results. However, the efficiencies of both air and water configurations will match each other. Therefore, the efficiency versus angular velocity plots, Figures 3.60b to 3.66b, can be used synonymously in the same manner previously mentioned. It is important to recall that when using these figures the incoming flow-speeds vary between configurations. In these figures, the torque/speed data is represented by the straight lines on the plots whereas the power/speed data is represented by the parabolic shaped curves. Also, it should be noted that the data represented by asterisks symbolizes the highest flow-speed tested, which corresponds to a water flow-speed of approximately 0.91 m/s or 3.00 ft/s. Consequently, the data could be extrapolated to obtain power values for higher incoming flow-speeds.

From these figures, Table 3.8 was created summarizing the maximum power for each turbine after being scaled up to prototype dimensions. These values are specifically a result of the tests and are not adjusted from the uncertainty analysis.

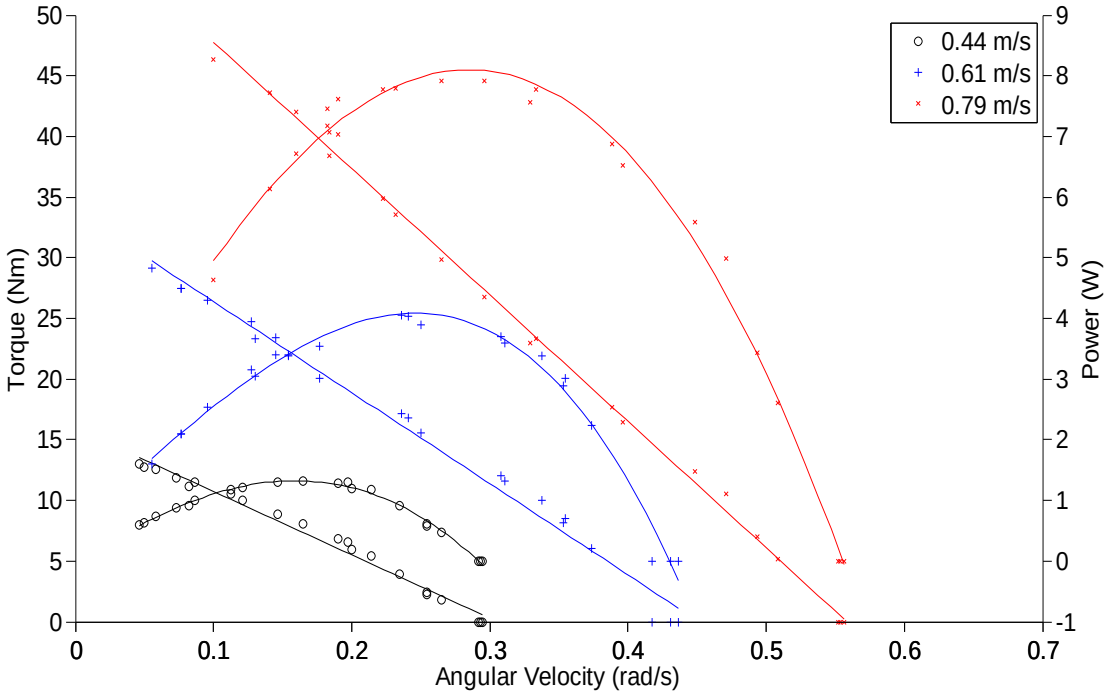

Figure 3.80. Full-scale Torque/Speed curves superimposed with power/speed curves for NACA 0022, two-bladed system with 41% solidity

Table 3.8 Summary of Maximum Prototype Turbine Power in Watts for Variable Incoming Flow-speeds

Water Channel Speed (m/s)	NACA 653018 (3 Blade) (48%)	NACA 0020 (3 Blade) (48%)	NACA 0022 (3 Blade) (48%)	NACA 0022 (6 Blade) (48%)	NACA 0022 (3 Blade) (41%)	NACA 0022 (3 Blade) (55%)	NACA 0022 (2 Blade) (41%)
0.2-.0.3	0.2	0.3	0.2	0.1	0.2	0.3	0.3
0.4-0.5	0.4	0.8	0.6	0.3	0.4	0.9	0.8
0.4-0.6	0.9	2.2	1.5	0.6	0.9	2.1	1.6
0.5-0.7	1.5	3.8	3.6	1.1	1.9	4.5	2.7
0.6-0.8	2.4	6.2	5.8	2.1	3.8	7.2	4.8
0.7-0.9	3.8	8.7	8.3	3.2	5.5	10.9	6.9
0.8-1.0	5.5	13.4	10.6	4.6	8.0	15.3	9.3

The experimental drag results were also scaled to prototype dimensions and water conditions using the same process. As discussed previously, drag force is effectively a function of solidity; the larger the solidity or frontal area of the turbine that is taken up by blades, the larger the drag force. Figures 3.74 to 3.80 show the trends for each configuration such that *Dp* stands for the drag force of the prototype and *Vp* stand for the incoming flow velocity of the prototype in water. As can be seen in these figures the drag force increases as incoming flow speed increases. Some of the figures show a linear relationship between these variables whereas others resemble a parabolic shape. The drag force ranged from about 30 Newtons, at the lowest speed for the lowest solidity to 500 N at the highest speed for the highest solidity. Again these plots cover only the range of incoming flow-speeds that were tested; therefore, the drag for higher speeds should be extrapolated if necessary by fitting a curve to the plot of interest.

From this set of data, Table 3.9 was created summarizing the maximum drag for each turbine after being scaled up to prototype dimensions.

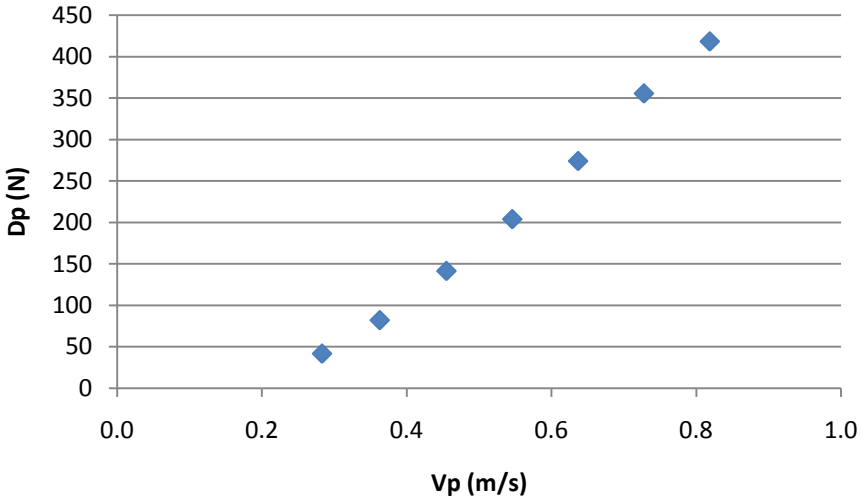

Figure 3.81. Water turbine drag vs. incoming velocity curve for NACA 653-018, three-bladed system with 48% solidity.

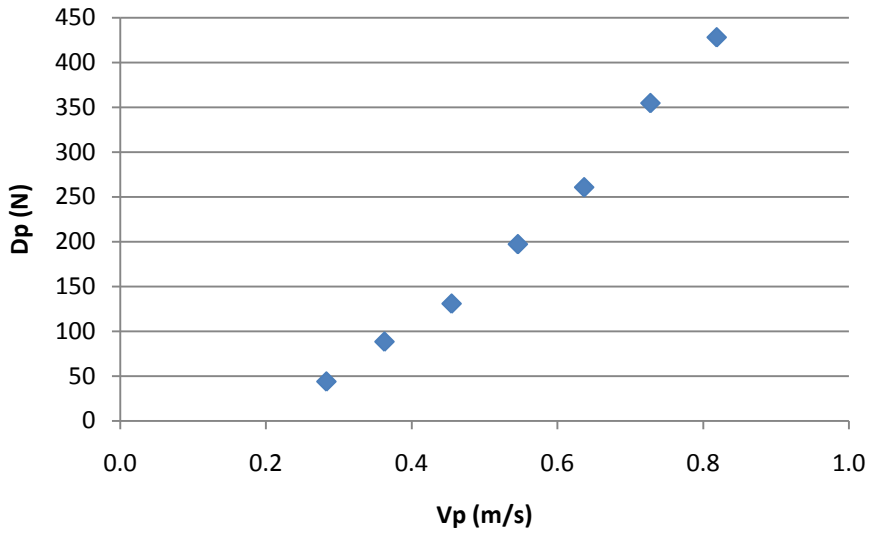

Figure 3.82. Water turbine drag vs. incoming velocity curve for NACA 0020, three-bladed system, 48% solidity

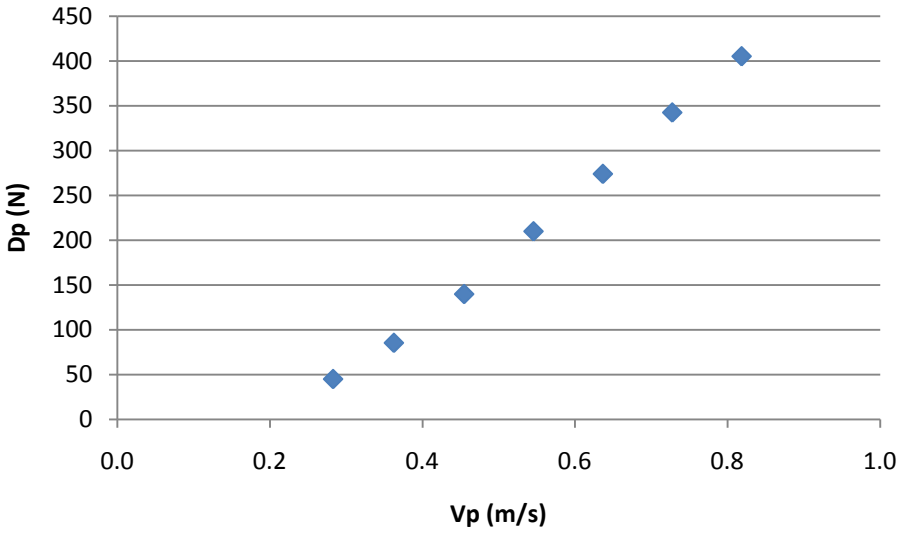

Figure 3.83. Water turbine drag vs. incoming velocity curve for NACA 0022, three-bladed system, 48% solidity

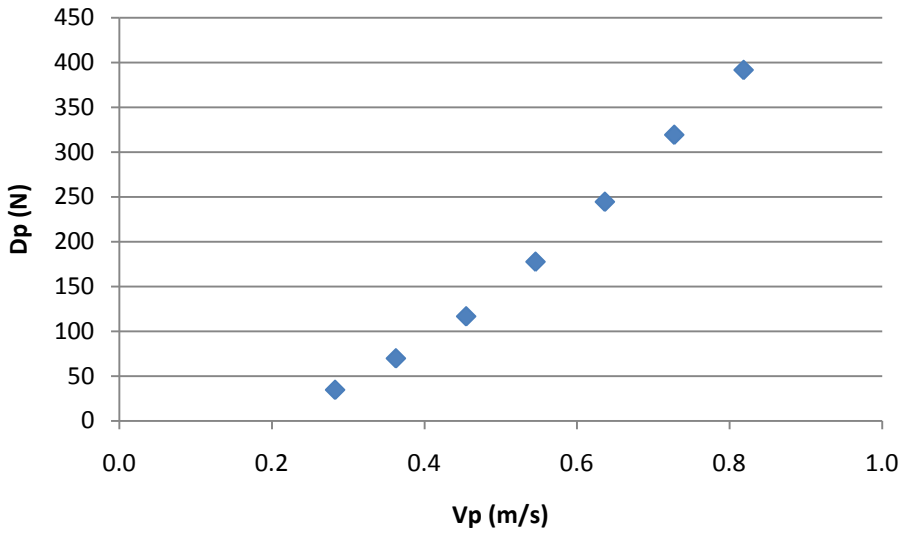

Figure 3.84. Water turbine drag vs. incoming velocity curve for NACA 0022, six-bladed system, 48% solidity

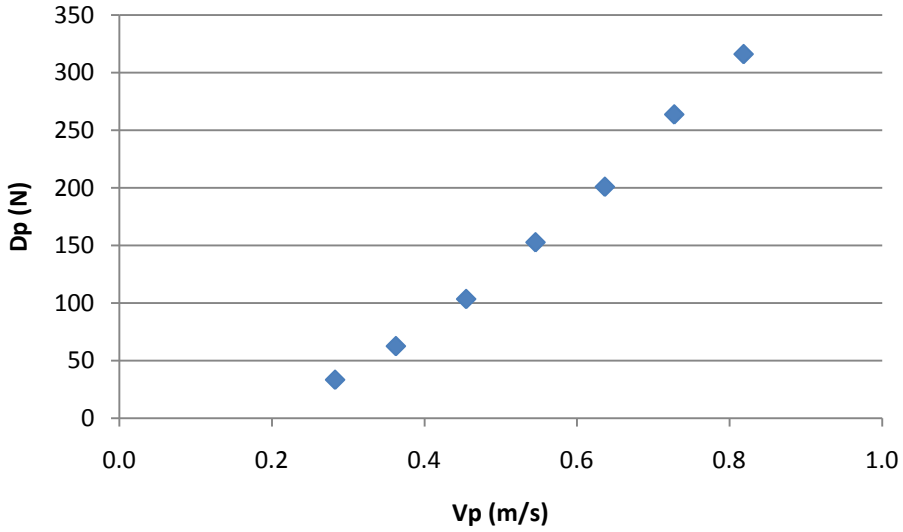

Figure 3.85. Water turbine drag vs. incoming velocity curve for NACA 0022, three-bladed system, 41% solidity

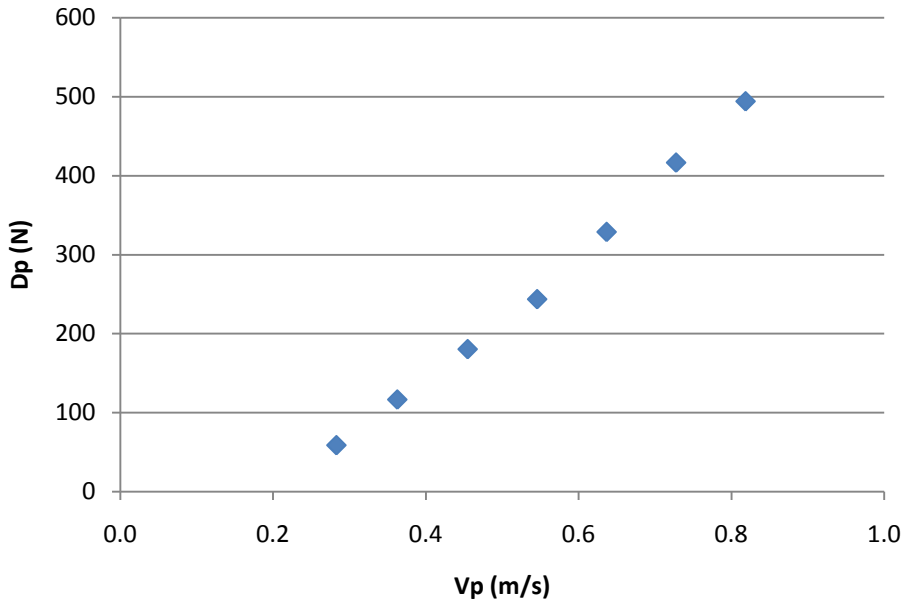

Figure 3.86. Water turbine drag vs. incoming velocity curve for NACA 0022, three-bladed system, 55% solidity

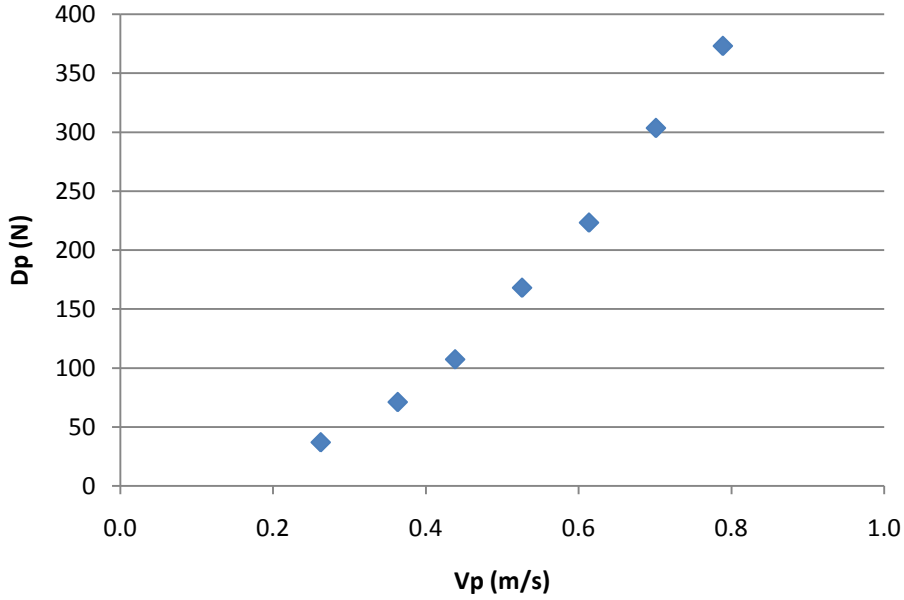

Figure 3.87. Water turbine drag vs. incoming velocity curve for NACA 0022, two-bladed system, 41% solidity

Table 3.9 Summary of Maximum Prototype Drag in Newtons for Variable Incoming Flow-speeds

Wind Tunnel Speed (m/s)	NACA 653018 (3 Blade) (48%)	NACA 0020 (3 Blade) (48%)	NACA 0022 (3 Blade) (48%)	NACA 0022 (6 Blade) (48%)	NACA 0022 (3 Blade) (41%)	NACA 0022 (3 Blade) (55%)	NACA 0022 (2 Blade) (41%)
0.28	42	44	45	35	33	59	37
0.37	82	88	85	70	62	117	71
0.45	141	131	140	117	103	180	107
0.55	204	197	210	178	153	244	168
0.64	274	261	274	245	201	329	223
0.72	355	355	342	319	264	417	303
0.81	418	428	405	392	316	494	373

3.10 Summary

This chapter covers a comprehensive experimental analysis for harvesting power from low-head, low-speed hydraulic sources. Three studies were conducted which examined the airfoil profile, the number of blades, and the turbine solidity. From this test matrix, seven model-sized turbine configurations were constructed. Extensive torque and drag force tests were conducted to compile a set of tables and figures for examination. Using these figures and tables a turbine configuration can be chosen and with a known load (i.e., alternator, motor, generator) and incoming velocity, the rotational velocity, drag force, and power output can be determined.

Depending on the application it can be observed that each turbine configuration has its useful applications based on natural environmental conditions and customer needs. If ones goal is to simply harvest a given amount of power other than the turbines maximum power capacity, a low solidity should be utilized. On the other hand, if one desires maximum power output, wherein the magnitude of the drag forces is not an issue it would be wisest to choose a turbine with a solidity around 55%. Consequently, using a combination of customer needs along with known equipment dimensions and capacities,

the equations and figures presented in this chapter can be used to determine the originally unknown outputs.

By choosing the best performing turbine from each study, it was determined that the configuration that would produce the most power and thus the highest efficiency would consists of two blades, a NACA 0020 profile, and a turbine solidity of 55%.

CHAPTER 4

CONCLUSIONS

4.1 Summary of Work

Several conclusions can be made from the computational and experimental work of this thesis. While not the original conclusions desired at the onset of the project, and given the fact that there remains a lack of harmony between the computational and experimental results, many important conclusions were made with respect to the modeling, analysis, and optimization of hydraulic turbines for low-head hydraulic sources. These conclusions are listed below.

1) The modeling and analysis of a hydraulic turbine with swept blades is both a very unique and complicated problem. Multiple input parameters greatly affect the performance of a turbine design. Furthermore each of these input parameters, such as incoming velocity, turbine size, cord length and number of blades influence other key parameters such as turbine frontal area and solidity. This greatly complicated the analysis process and compounded the number of test cases needed to fully understand the effects on performance of each input parameter.
2) The torque generated by the turbine is not solely a function of the tangential force acting on each of the blades. It is also a function of the angular momentum flux around the turbine circumference. For a complete

understanding of torque generation and energy transfer through the system, the conservation of momentum equation must be satisfied. Understanding of the downstream momentum loss is crucial in evaluating the energy produced by a turbine.

3) In spite of the simplifying assumptions, the model predicts the correct trends for turbine performance. The magnitudes of the computational results for torque generation, however, are consistently lower than the experimental results.
4) Peak performance of a discrete airfoil section for a given turbine configuration occurs when an airfoil profile exhibits a high coefficient of lift value at high angles of attack. This provides for a large lifting force at an angle of attack large enough to produce a significant force in the tangential direction. Current analysis indicates that a NACA0015 would optimize performance.
5) For rotational speeds close to, and equal to zero, the discrete sections at large angles of attack produce a large drag force. Much of this force is in the tangential direction and results in positive torque. This phenomenon increases the ability of the turbine to be self starting.
6) The computational analysis indicates that greater performance can be achieved at higher rotational speeds. At these higher rpm values, the angles of attack are shifted towards zero and thus are more favorable. While current tests do not demonstrate these effects, they provide insight into methods aimed at improving the efficiency of the turbine design.

7) Power increases as blade number decreases. This is thought to be due to flow interference. The fewer the number of blades, the more time the flow has to converge back to its original uniform condition for the next blade. The more that this flow represents the ideal, uniform case, the better the turbine will perform.
8) Power increases as solidity increases up until the point where flow is forced around the turbine instead of through. Out of the three solidities tested the 55 % solidity produced the largest power output.
9) Plotting the ratio C_l/C_d(where C_l and C_d stand for the coefficient of lift and drag respectively) for different airfoils appears to have a direct correlation on overall power output. As coefficient data vary greatly between sources, this decision on what data to use must be made with caution.[19,22,26-28,30,33]However, the trend suggests that the larger the area under the curve, the greater the power output. The peak efficiency of the NACA 65_3-018 was 3.8%, whereas the NACA 0022 peaked at 6.8% and the NACA 0020 peaked at 9.2%.
10) Power versus speed curve trends do not necessarily match torque versus speed curve trends. It is possible for a turbine to produce more power than another turbine producing the exact same torque values, depending on the rotational speed at which that torque is produced.
11) Drag force has a direct correlation with solidity. Although the exact relationship is not known, the drag force increases as solidity increases. Also, drag force appears to be relatively consistent between turbine configurations

with the same solidity. In other words, drag force is independent of the number of blades per turbine and the airfoil profile.

12) From the experimental work in this thesis the maximum power output from any turbine, at a scaled flow of 1 m/s (3ft/s) in water would be 15.29 W. This power would be generated by the NACA 0022, three-bladed, 55 % solidity turbine configuration.

4.2 Discrepancies Explained

Unfortunately discrepancies do exist between the initial goals of the project and the final outcomes in both the computational and experimental realms of this thesis. It has been noted that discrepancies exist between the predicted performance of the turbines and their actual performance. The models do, however, produce the correct trends. These differences are largely attributed to the assumptions made in the model. Concerning the experimental work, the overall turbine efficiencies ranged from 3-15% whereas this range was expected to be 20-30%. These differences can be attributed to measurement uncertainty, the lack of a pitch angle study as well as the lack of an optimal configuration at the optimal flow-speeds. Below is a summary of explanations for these differences.

- The major assumption that the turbine can be modeled by dividing it into multiple thin, but finite, discrete sections (which can be modeled as an airfoil profile in a 2D flow) introduces error by neglecting all 3D effects.
- Inherent error exists in the sources of the coefficients of lift and drag. Knowing the correct values for these coefficients is essential for correctly modeling the turbine performance. Any errors in this data will be compounded through the analysis.

- An assumed, simplified model of the downstream momentum loss is used. A more accurate model is desirable.
- Stall angles and coefficient of lift and drag values are a function of the direction of rotation. This effect, called hysteresis, is not accounted for in the code. This further contributes to the error in the coefficient of lift and drag data.
- The incoming flow vectors were assumed to be parallel to the direction of the incoming free stream velocity at each discrete section. Due to the pressure drop across the turbine, some of the flow will be forced around the turbine instead of through it. This effect will change both the magnitude and direction of these free stream velocity vectors.
- A simple model using a constant momentum deficit at each downstream location was used. This introduced error into both the direction and magnitude of the resultant velocity vectors on the downstream discrete sections. A better model of the momentum deficit could reduce these errors.
- An average resultant velocity vector, located at the center of lift, was used. This is an average of all the resultant velocity vectors that would be incident along the length of the cord. The accuracy of this assumption decreases with cord length.
- Effects from the twist of the blades or from the offset of one discrete section from those next to it were ignored.
- All experimental measurements need to be precise as measurement uncertainties add up quickly causing significant errors in the final readings. An uncertainty analysis was conducted in this study, which should be consulted in future testing to determine the most sensitive variables for uncertainty errors.

- A torque meter is desired for measuring torque accurately. Although torque was correctly transferred from the turbine to the cantilever beam in the experimental setup, the strain values used to ultimately calculate torque varied between 5-20 micro strain for each measurement. A torque meter would get rid of this fluctuation in results causing the end product to be more accurate.
- No experimental study was performed to determine the effect of pitch angle on turbine performance. This test was not possible with the given experimental setup as it is necessary to be able to control the pitch angle on the order of 0.1 degrees. In this case, the experimental setup used consisted of the blades being secured to the hub by a piece of all-thread running through holes drilled in the blades. Consequently, it is highly likely that the pitch angle for each blade was different from one another and not necessarily zero as it was assumed to be. Due to the setup the pitch angle likely varied plus or minus 5 degrees.

4.3 Future Work

Several structured recommendations can be made for future work that will likely increase the proficiency of the computational analysis as well as the efficiencies of the model turbines.

- An in-depth theoretical study of the conservation of momentum equation, with a focus on the resulting momentum deficit at the rear of the turbine would allow for good angular momentum deficit values a to be predicted, which would allow the code to be used to analyze cases where there is no experimental data available.
- A more in-depth study is needed concerning the coefficients of lift and drag used in the code. Accurate, repeatable data are needed for all angles of attack for each

airfoil shape that is to be analyzed. Further attempts to harmonize published sources of coefficients should be pursued.

- Further fluid dynamic study is needed to better understand and model the flow around each of the discrete sections, including modeling the flow that passed around, not through, the turbine frontal area, redirection and reduction of flow that had passed through the upstream portion of the turbine, and other currently unaccounted for flow phenomena.
- A model for the effects of the velocity gradient caused by boundary effects of the bed of the river or canal on the turbine should be developed and included in the full computational analysis.
- Better understanding of the 3D flow effects associated with these helically-swept blades and the amount of error introduced to the model by using a summation of 2D discrete sections is needed.
- An experimental study should be conducted on blade pitch. Research shows that blade pitch can affect turbine performance quite substantially, as changing the pitch affects the amount of flow through the turbine. In order to do this, the entire turbine (hubs included) should be designed in SolidWorks or some other design software and manufactured as a single unit, wherein the pitch angle could be explicitly specified. This would ensure that the pitch angle was accurate, as any small changes in this angle may substantially impact the performance.
- A further investigation should be conducted on the effect of solidity on turbine performance. Multiples solidities (48% and above) should be tested to determine the upper limit of solidity. It is expected that there will be a point where

performance drops significantly on both the high and low ends. With these values, a trend should be found to determine the very best solidity for this helical turbine design.

- Another experimental study should be conducted on an optimum airfoil to be used. With continued research, it appears that the NACA 0015 airfoil may prove to be the ideal candidate. The best way to begin this process would include plotting the ratio of C_l/C_d, and looking for the airfoils with the largest peak values.
- An experimental study should be conducted to investigate the recommended helical turbine configuration identified in this thesis. It is expected that a two bladed, NACA 0020, 55 % solidity turbine will produce the greatest efficiency when compared to those tested for this thesis.

APPENDIX A

RAW DATA TORQUE/SPEED TABLES

NACA 65-018 3 Bladed Turbine with 48% Solidity Trial 1									
F (Hz)	**U (m/s)**	**ω (rpm)**	**ω (rad/s)**	**Strain**	**T(N*m)**	**Tan Force (N)**	**P (W)**	**PA (W)**	**Eff (%)**
15	8.48	97	10.16	0	0.0000	0.0000	0.0000	20	0.00
15	8.48	60	6.28	15	0.0721	0.2104	0.4533	20	2.29
15	8.48	34	3.56	27	0.1299	0.3787	0.4624	20	2.33
15	8.48	14	1.47	37	0.1780	0.5190	0.2609	20	1.32
20	11.89	155	16.23	0	0.0000	0.0000	0.0000	55	0.00
20	11.89	102	10.68	25	0.1202	0.3507	1.2843	55	2.35
20	11.89	81	8.48	36	0.1731	0.5049	1.4687	55	2.69
20	11.89	68	7.12	47	0.2261	0.6592	1.6097	55	2.95
20	11.89	41	4.29	60	0.2886	0.8416	1.2390	55	2.27
20	11.89	29	3.04	68	0.3271	0.9538	0.9932	55	1.82
25	15.59	200	20.94	0	0.0000	0.0000	0.0000	123	0.00
25	15.59	178	18.64	17	0.0818	0.2384	1.5241	123	1.24
25	15.59	143	14.97	43	0.2068	0.6031	3.0970	123	2.52
25	15.59	89	9.32	85	0.4088	1.1922	3.8102	123	3.10
25	15.59	63	6.60	104	0.5002	1.4587	3.3000	123	2.68
25	15.59	44	4.61	120	0.5772	1.6832	2.6593	123	2.16
25	15.59	28	2.93	133	0.6397	1.8655	1.8756	123	1.52
30	17.93	251	26.28	0	0.0000	0.0000	0.0000	187	0.00
30	17.93	228	23.88	15	0.0721	0.2104	1.7225	187	0.92
30	17.93	196	20.53	46	0.2212	0.6452	4.5410	187	2.42
30	17.93	149	15.60	86	0.4136	1.2063	6.4539	187	3.45
30	17.93	108	11.31	121	0.5820	1.6972	6.5819	187	3.51
30	17.93	59	6.18	159	0.7647	2.2302	4.7249	187	2.52
30	17.93	35	3.67	184	0.8850	2.5808	3.2436	187	1.73
35	20.92	295	30.89	0	0.0000	0.0000	0.0000	297	0.00
35	20.92	242	25.34	46	0.2212	0.6452	5.6068	297	1.88
35	20.92	211	22.10	75	0.3607	1.0520	7.9704	297	2.68
35	20.92	176	18.43	118	0.5675	1.6551	10.4601	297	3.52
35	20.92	124	12.99	162	0.7792	2.2723	10.1176	297	3.40
35	20.92	97	10.16	193	0.9283	2.7071	9.4291	297	3.17
35	20.92	66	6.91	220	1.0581	3.0858	7.3132	297	2.46
40	23.91	330	34.56	0	0.0000	0.0000	0.0000	444	0.00
40	23.91	286	29.95	58	0.2790	0.8135	8.3547	444	1.88
40	23.91	253	26.49	95	0.4569	1.3325	12.1055	444	2.73
40	23.91	233	24.40	127	0.6108	1.7813	14.9039	444	3.36
40	23.91	153	16.02	204	0.9812	2.8614	15.7203	444	3.54
40	23.91	110	11.52	250	1.2024	3.5066	13.8507	444	3.12
40	23.91	47	4.92	303	1.4573	4.2500	7.1726	444	1.62

45	26.90	370	38.75	0	0.0000	0.0000	0.0000	632	0.00
45	26.90	332	34.77	73	0.3511	1.0239	12.2068	632	1.93
45	26.90	259	27.12	163	0.7840	2.2863	21.2631	632	3.36
45	26.90	199	20.84	224	1.0774	3.1419	22.4512	632	3.55
45	26.90	149	15.60	284	1.3659	3.9835	21.3130	632	3.37
45	26.90	105	11.00	333	1.6016	4.6708	17.6105	632	2.79
45	26.90	57	5.97	386	1.8565	5.4142	11.0816	632	1.75

NACA 65-018 3 Bladed Turbine with 48% Solidity Trial 2									
F (Hz)	**U (m/s)**	**ω (rpm)**	**ω (rad/s)**	**Strain**	**T(N*m)**	**Tan Force (N)**	**P (W)**	**PA (W)**	**Eff (%)**
15	8.48	99	10.37	0	0.0000	0.0000	0.0000	20	0.00
15	8.48	60	6.28	10	0.0481	0.1403	0.3022	20	1.53
15	8.48	54	5.65	16	0.0770	0.2244	0.4352	20	2.20
15	8.48	40	4.19	34	0.1635	0.4769	0.6850	20	3.46
20	11.89	147	15.39	0	0.0000	0.0000	0.0000	55	0.00
20	11.89	105	11.00	16	0.0770	0.2244	0.8462	55	1.55
20	11.89	81	8.48	30	0.1443	0.4208	1.2239	55	2.24
20	11.89	68	7.12	43	0.2068	0.6031	1.4727	55	2.70
20	11.89	50	5.24	56	0.2693	0.7855	1.4103	55	2.58
20	11.89	18	1.88	77	0.3703	1.0800	0.6981	55	1.28
25	15.59	196	20.53	0	0.0000	0.0000	0.0000	123	0.00
25	15.59	151	15.81	20	0.0962	0.2805	1.5211	123	1.24
25	15.59	135	14.14	32	0.1539	0.4488	2.1758	123	1.77
25	15.59	121	12.67	44	0.2116	0.6172	2.6815	123	2.18
25	15.59	110	11.52	67	0.3222	0.9398	3.7120	123	3.02
25	15.59	82	8.59	79	0.3800	1.1081	3.2627	123	2.65
25	15.59	63	6.60	93	0.4473	1.3044	2.9510	123	2.40
30	17.93	246	25.76	0	0.0000	0.0000	0.0000	187	0.00
30	17.93	192	20.11	30	0.1443	0.4208	2.9011	187	1.55
30	17.93	177	18.54	45	0.2164	0.6312	4.0117	187	2.14
30	17.93	160	16.76	67	0.3222	0.9398	5.3993	187	2.88
30	17.93	130	13.61	99	0.4762	1.3886	6.4821	187	3.46
30	17.93	89	9.32	129	0.6204	1.8094	5.7825	187	3.09
30	17.93	60	6.28	152	0.7311	2.1320	4.5934	187	2.45
35	20.92	295	30.89	0	0.0000	0.0000	0.0000	297	0.00
35	20.92	242	25.34	42	0.2020	0.5891	5.1192	297	1.72
35	20.92	211	22.10	83	0.3992	1.1642	8.8206	297	2.97
35	20.92	167	17.49	125	0.6012	1.7533	10.5139	297	3.53
35	20.92	116	12.15	171	0.8224	2.3985	9.9906	297	3.36
35	20.92	88	9.22	195	0.9379	2.7351	8.6428	297	2.91
35	20.92	63	6.60	220	1.0581	3.0858	6.9808	297	2.35

40	23.91	346	36.23	0	0.0000	0.0000	0.0000	444	0.00
40	23.91	274	28.69	70	0.3367	0.9818	9.6602	444	2.18
40	23.91	236	24.71	116	0.5579	1.6271	13.7882	444	3.11
40	23.91	184	19.27	177	0.8513	2.4827	16.4033	444	3.69
40	23.91	140	14.66	223	1.0725	3.1279	15.7243	444	3.54
40	23.91	117	12.25	242	1.1639	3.3944	14.2607	444	3.21
40	23.91	73	7.64	285	1.3707	3.9975	10.4787	444	2.36
45	26.90	394	41.26	0	0.0000	0.0000	0.0000	632	0.00
45	26.90	306	32.04	103	0.4954	1.4447	15.8744	632	2.51
45	26.90	245	25.66	192	0.9234	2.6931	23.6923	632	3.75
45	26.90	167	17.49	264	1.2697	3.7029	22.2054	632	3.51
45	26.90	132	13.82	304	1.4621	4.2640	20.2109	632	3.20
45	26.90	103	10.79	334	1.6064	4.6848	17.3270	632	2.74
45	26.90	77	8.06	390	1.8758	5.4703	15.1250	632	2.39

NACA 65-018 3 Bladed Turbine with 48% Solidity Trial 3									
F (Hz)	**U (m/s)**	**ω (rpm)**	**ω (rad/s)**	**Strain**	**T(N*m)**	**Tan Force (N)**	**P (W)**	**PA (W)**	**Eff (%)**
15	8.48	94	9.84	0	0.0000	0.0000	0.0000	20	0.00
15	8.48	60	6.28	11	0.0529	0.1543	0.3324	20	1.68
15	8.48	25	2.62	36	0.1731	0.5049	0.4533	20	2.29
15	8.48	12	1.26	42	0.2020	0.5891	0.2538	20	1.28
20	11.89	147	15.39	0	0.0000	0.0000	0.0000	55	0.00
20	11.89	105	11.00	14	0.0673	0.1964	0.7404	55	1.36
20	11.89	87	9.11	28	0.1347	0.3927	1.2269	55	2.25
20	11.89	72	7.54	38	0.1828	0.5330	1.3780	55	2.52
20	11.89	60	6.28	42	0.2020	0.5891	1.2692	55	2.32
20	11.89	40	4.19	61	0.2934	0.8556	1.2289	55	2.25
25	15.59	196	20.53	0	0.0000	0.0000	0.0000	123	0.00
25	15.59	143	14.97	34	0.1635	0.4769	2.4488	123	1.99
25	15.59	118	12.36	37	0.1780	0.5190	2.1990	123	1.79
25	15.59	105	11.00	55	0.2645	0.7714	2.9086	123	2.36
25	15.59	92	9.63	65	0.3126	0.9117	3.0119	123	2.45
25	15.59	79	8.27	81	0.3896	1.1361	3.2229	123	2.62
25	15.59	52	5.45	96	0.4617	1.3465	2.5143	123	2.04
30	17.93	247	25.87	0	0.0000	0.0000	0.0000	187	0.00
30	17.93	203	21.26	31	0.1491	0.4348	3.1695	187	1.69
30	17.93	159	16.65	57	0.2741	0.7995	4.5647	187	2.44
30	17.93	146	15.29	62	0.2982	0.8696	4.5591	187	2.43
30	17.93	139	14.56	70	0.3367	0.9818	4.9006	187	2.62
30	17.93	108	11.31	98	0.4713	1.3746	5.3308	187	2.85
30	17.93	55	5.76	155	0.7455	2.1741	4.2937	187	2.29

35	20.92	297	31.10	0	0.0000	0.0000	0.0000	297	0.00
35	20.92	224	23.46	64	0.3078	0.8977	7.2205	297	2.43
35	20.92	177	18.54	110	0.5291	1.5429	9.8063	297	3.30
35	20.92	157	16.44	130	0.6253	1.8234	10.2797	297	3.46
35	20.92	143	14.97	146	0.7022	2.0478	10.5155	297	3.54
35	20.92	73	7.64	207	0.9956	2.9034	7.6108	297	2.56
35	20.92	41	4.29	232	1.1158	3.2541	4.7908	297	1.61
40	23.91	342	35.81	0	0.0000	0.0000	0.0000	444	0.00
40	23.91	287	30.05	65	0.3126	0.9117	9.3958	444	2.12
40	23.91	272	28.48	78	0.3752	1.0941	10.6857	444	2.41
40	23.91	204	21.36	145	0.6974	2.0338	14.8983	444	3.36
40	23.91	142	14.87	210	1.0100	2.9455	15.0192	444	3.38
40	23.91	86	9.01	261	1.2553	3.6609	11.3052	444	2.55
40	23.91	45	4.71	300	1.4429	4.2079	6.7994	444	1.53
45	26.90	384	40.21	0	0.0000	0.0000	0.0000	632	0.00
45	26.90	306	32.04	99	0.4762	1.3886	15.2579	632	2.41
45	26.90	214	22.41	220	1.0581	3.0858	23.7124	632	3.75
45	26.90	160	16.76	274	1.3178	3.8432	22.0805	632	3.49
45	26.90	122	12.78	302	1.4525	4.2359	18.5569	632	2.94
45	26.90	66	6.91	385	1.8517	5.4001	12.7980	632	2.02
45	26.90	59	6.18	408	1.9623	5.7227	12.1241	632	1.92

NACA 0020 3 Bladed Turbine with 48% Solidity Trial 1									
F (Hz)	**U (m/s)**	**ω (rpm)**	**ω (rad/s)**	**Strain**	**T(N*m)**	**Tan Force (N)**	**P (W)**	**PA (W)**	**Eff (%)**
15	8.63	150	15.71	0	0.0000	0.0000	0.0000	21	0.00
15	8.63	94	9.84	19	0.0914	0.2665	0.8995	21	4.31
15	8.63	58	6.07	35	0.1683	0.4909	1.0224	21	4.90
15	8.63	39	4.08	51	0.2453	0.7153	1.0018	21	4.80
20	11.80	221	23.14	0	0.0000	0.0000	0.0000	53	0.00
20	11.80	174	18.22	23	0.1106	0.3226	2.0157	53	3.79
20	11.80	107	11.21	57	0.2741	0.7995	3.0718	53	5.77
20	11.80	73	7.64	85	0.4088	1.1922	3.1252	53	5.87
20	11.80	56	5.86	111	0.5339	1.5569	3.1308	53	5.88
20	11.80	17	1.78	137	0.6589	1.9216	1.1730	53	2.20
25	15.76	299	31.31	0	0.0000	0.0000	0.0000	127	0.00
25	15.76	257	26.91	32	0.1539	0.4488	4.1421	127	3.26
25	15.76	238	24.92	45	0.2164	0.6312	5.3942	127	4.25
25	15.76	180	18.85	83	0.3992	1.1642	7.5247	127	5.92
25	15.76	139	14.56	135	0.6493	1.8936	9.4512	127	7.44
25	15.76	106	11.10	153	0.7359	2.1460	8.1684	127	6.43
25	15.76	52	5.45	172	0.8273	2.4125	4.5048	127	3.55

30	17.98	377	39.48	0	0.0000	0.0000	0.0000	189	0.00
30	17.98	320	33.51	49	0.2357	0.6873	7.8974	189	4.19
30	17.98	297	31.10	84	0.4040	1.1782	12.5654	189	6.66
30	17.98	224	23.46	146	0.7022	2.0478	16.4718	189	8.73
30	17.98	191	20.00	160	0.7695	2.2442	15.3919	189	8.16
30	17.98	133	13.93	202	0.9715	2.8333	13.5314	189	7.17
30	17.98	52	5.45	264	1.2697	3.7029	6.9143	189	3.67
35	20.98	453	47.44	0	0.0000	0.0000	0.0000	300	0.00
35	20.98	425	44.51	23	0.1106	0.3226	4.9233	300	1.64
35	20.98	382	40.00	77	0.3703	1.0800	14.8147	300	4.95
35	20.98	288	30.16	186	0.8946	2.6089	26.9802	300	9.01
35	20.98	208	21.78	236	1.1351	3.3102	24.7238	300	8.25
35	20.98	123	12.88	295	1.4188	4.1378	18.2754	300	6.10
35	20.98	86	9.01	344	1.6545	4.8251	14.9003	300	4.97
40	23.98	515	53.93	0	0.0000	0.0000	0.0000	447	0.00
40	23.98	405	42.41	123	0.5916	1.7252	25.0899	447	5.61
40	23.98	392	41.05	172	0.8273	2.4125	33.9589	447	7.60
40	23.98	360	37.70	200	0.9619	2.8053	36.2637	447	8.11
40	23.98	280	29.32	265	1.2745	3.7170	37.3717	447	8.36
40	23.98	215	22.51	334	1.6064	4.6848	36.1680	447	8.09
40	23.98	175	18.33	430	2.0681	6.0313	37.9006	447	8.48
45	26.98	552	57.81	0	0.0000	0.0000	0.0000	637	0.00
45	26.98	480	50.27	77	0.6228	1.8162	31.3046	637	4.92
45	26.98	401	41.99	165	1.3345	3.8919	56.0408	637	8.80
45	26.98	259	27.12	236	1.9088	5.5666	51.7711	637	8.13
45	26.98	180	18.85	310	2.5073	7.3121	47.2618	637	7.42
45	26.98	124	12.99	360	2.9117	8.4915	37.8094	637	5.94
45	26.98	69	7.23	458	3.7044	10.8030	26.7664	637	4.20

NACA 0020 3 Bladed Turbine with 48% Solidity Trial 2									
F (Hz)	**U (m/s)**	**ω (rpm)**	**ω (rad/s)**	**Strain**	**T(N*m)**	**Tan Force (N)**	**P (W)**	**PA (W)**	**Eff (%)**
15	8.63	145	15.18	0	0.0000	0.0000	0.0000	21	0.00
15	8.63	92	9.63	15	0.0721	0.2104	0.6951	21	3.33
15	8.63	60	6.28	32	0.1539	0.4488	0.9670	21	4.63
15	8.63	33	3.46	57	0.2741	0.7995	0.9474	21	4.54
20	11.80	217	22.72	0	0.0000	0.0000	0.0000	53	0.00
20	11.80	175	18.33	25	0.1202	0.3507	2.2035	53	4.14
20	11.80	93	9.74	67	0.3222	0.9398	3.1383	53	5.90
20	11.80	53	5.55	102	0.4906	1.4307	2.7228	53	5.12
20	11.80	25	2.62	117	0.5627	1.6411	1.4732	53	2.77
20	11.80	12	1.26	144	0.6926	2.0198	0.8703	53	1.64

25	15.76	291	30.47	0	0.0000	0.0000	0.0000	127	0.00
25	15.76	242	25.34	53	0.2549	0.7434	6.4600	127	5.09
25	15.76	200	20.94	73	0.3511	1.0239	7.3535	127	5.79
25	15.76	151	15.81	112	0.5387	1.5709	8.5179	127	6.71
25	15.76	102	10.68	143	0.6878	2.0058	7.3464	127	5.78
25	15.76	56	5.86	168	0.8080	2.3564	4.7385	127	3.73
25	15.76	38	3.98	182	0.8754	2.5528	3.4833	127	2.74
30	17.98	378	39.58	0	0.0000	0.0000	0.0000	189	0.00
30	17.98	324	33.93	44	0.2116	0.6172	7.1802	189	3.81
30	17.98	303	31.73	65	0.3126	0.9117	9.9196	189	5.26
30	17.98	203	21.26	150	0.7214	2.1039	15.3365	189	8.13
30	17.98	179	18.74	179	0.8609	2.5107	16.1378	189	8.56
30	17.98	132	13.82	207	0.9956	2.9034	13.7621	189	7.30
30	17.98	47	4.92	265	1.2745	3.7170	6.2731	189	3.33
35	20.98	454	47.54	0	0.0000	0.0000	0.0000	300	0.00
35	20.98	416	43.56	30	0.1443	0.4208	6.2857	300	2.10
35	20.98	340	35.60	135	0.6493	1.8936	23.1181	300	7.72
35	20.98	293	30.68	178	0.8561	2.4967	26.2680	300	8.77
35	20.98	202	21.15	248	1.1928	3.4785	25.2314	300	8.42
35	20.98	126	13.19	296	1.4236	4.1518	18.7846	300	6.27
35	20.98	51	5.34	363	1.7459	5.0915	9.3243	300	3.11
40	23.98	504	52.78	0	0.0000	0.0000	0.0000	447	0.00
40	23.98	469	49.11	32	0.1539	0.4488	7.5590	447	1.69
40	23.98	456	47.75	60	0.2886	0.8416	13.7802	447	3.08
40	23.98	422	44.19	100	0.4810	1.4026	21.2545	447	4.75
40	23.98	390	40.84	160	0.7695	2.2442	31.4285	447	7.03
40	23.98	310	32.46	236	1.1351	3.3102	36.8479	447	8.24
40	23.98	200	20.94	357	1.7170	5.0074	35.9615	447	8.04
45	26.98	578	60.53	0	0.0000	0.0000	0.0000	637	0.00
45	26.98	452	47.33	125	1.0110	2.9484	47.8547	637	7.52
45	26.98	336	35.19	195	1.5772	4.5995	55.4945	637	8.72
45	26.98	238	24.92	265	2.1434	6.2507	53.4194	637	8.39
45	26.98	195	20.42	315	2.5478	7.4300	52.0261	637	8.17
45	26.98	134	14.03	362	2.9279	8.5386	41.0856	637	6.45
45	26.98	89	9.32	440	3.5588	10.3785	33.1679	637	5.21

NACA 0020 3 Bladed Turbine with 48% Solidity Trial 3									
F (Hz)	**U (m/s)**	**ω (rpm)**	**ω (rad/s)**	**Strain**	**T(N*m)**	**Tan Force (N)**	**P (W)**	**PA (W)**	**Eff (%)**
15	8.63	148	15.50	0	0.0000	0.0000	0.0000	21	0.00
15	8.63	89	9.32	16	0.0770	0.2244	0.7172	21	3.44
15	8.63	71	7.44	32	0.1539	0.4488	1.1443	21	5.48

15	8.63	18	1.88	59	0.2838	0.8276	0.5349	21	2.56
20	11.80	218	22.83	0	0.0000	0.0000	0.0000	53	0.00
20	11.80	192	20.11	14	0.0673	0.1964	1.3538	53	2.54
20	11.80	91	9.53	72	0.3463	1.0099	3.3000	53	6.20
20	11.80	70	7.33	86	0.4136	1.2063	3.0320	53	5.70
20	11.80	59	6.18	104	0.5002	1.4587	3.0905	53	5.81
20	11.80	21	2.20	130	0.6253	1.8234	1.3750	53	2.58
25	15.76	292	30.58	0	0.0000	0.0000	0.0000	127	0.00
25	15.76	272	28.48	19	0.0914	0.2665	2.6029	127	2.05
25	15.76	250	26.18	50	0.2405	0.7013	6.2958	127	4.96
25	15.76	186	19.48	92	0.4425	1.2904	8.6187	127	6.79
25	15.76	120	12.57	125	0.6012	1.7533	7.5549	127	5.95
25	15.76	101	10.58	151	0.7263	2.1180	7.6813	127	6.05
25	15.76	62	6.49	170	0.8176	2.3845	5.3086	127	4.18
30	17.98	371	38.85	0	0.0000	0.0000	0.0000	189	0.00
30	17.98	343	35.92	38	0.1828	0.5330	6.5647	189	3.48
30	17.98	255	26.70	125	0.6012	1.7533	16.0542	189	8.51
30	17.98	168	17.59	172	0.8273	2.4125	14.5538	189	7.72
30	17.98	95	9.95	230	1.1062	3.2261	11.0050	189	5.83
30	17.98	49	5.13	258	1.2409	3.6188	6.3673	189	3.38
30	17.98	24	2.51	279	1.3419	3.9133	3.3725	189	1.79
35	20.98	446	46.70	0	0.0000	0.0000	0.0000	300	0.00
35	20.98	415	43.46	30	0.1443	0.4208	6.2706	300	2.09
35	20.98	381	39.90	78	0.3752	1.0941	14.9678	300	5.00
35	20.98	340	35.60	119	0.5723	1.6691	20.3782	300	6.80
35	20.98	222	23.25	226	1.0870	3.1699	25.2697	300	8.44
35	20.98	146	15.29	280	1.3467	3.9274	20.5897	300	6.87
35	20.98	82	8.59	340	1.6353	4.7689	14.0421	300	4.69
40	23.98	501	52.46	0	0.0000	0.0000	0.0000	447	0.00
40	23.98	405	42.41	140	0.6733	1.9637	28.5576	447	6.39
40	23.98	383	40.11	175	0.8417	2.4546	33.7579	447	7.55
40	23.98	341	35.71	214	1.0293	3.0016	36.7542	447	8.22
40	23.98	237	24.82	290	1.3948	4.0676	34.6167	447	7.74
40	23.98	168	17.59	385	1.8517	5.4001	32.5769	447	7.29
40	23.98	156	16.34	425	2.0441	5.9612	33.3928	447	7.47
45	26.98	586	61.37	0	0.0000	0.0000	0.0000	637	0.00
45	26.98	548	57.39	42	0.3397	0.9907	19.4942	637	3.06
45	26.98	483	50.58	97	0.7845	2.2880	39.6821	637	6.23
45	26.98	400	41.89	172	1.3912	4.0570	58.2726	637	9.15
45	26.98	324	33.93	205	1.6581	4.8354	56.2568	637	8.84
45	26.98	284	29.74	222	1.7956	5.2364	53.4007	637	8.39

45	26.98	213	22.31	287	2.3213	6.7696	51.7771	637	8.13

NACA-0022 3 Bladed Turbine with 48% Solidity Trial 1									
F (Hz)	**U (m/s)**	**ω (rpm)**	**ω (rad/s)**	**Strain**	**T(N*m)**	**Tan Force (N)**	**P (W)**	**PA (W)**	**Eff (%)**
15	9.47	138	14.45	0	0.0000	0.0000	0.0000	28	0.00
15	9.47	99	10.37	13	0.0625	0.1823	0.6482	28	2.30
15	9.47	78	8.17	27	0.1299	0.3787	1.0607	28	3.76
15	9.47	9	0.94	62	0.2982	0.8696	0.2810	28	1.00
20	13.30	212	22.20	0	0.0000	0.0000	0.0000	78	0.00
20	13.30	133	13.93	35	0.1683	0.4909	2.3445	78	3.00
20	13.30	110	11.52	45	0.2164	0.6312	2.4931	78	3.19
20	13.30	83	8.69	57	0.2741	0.7995	2.3828	78	3.05
20	13.30	72	7.54	66	0.3174	0.9257	2.3934	78	3.06
20	13.30	11	1.15	94	0.4521	1.3185	0.5208	78	0.67
25	16.07	279	29.22	0	0.0000	0.0000	0.0000	138	0.00
25	16.07	225	23.56	41	0.1972	0.5751	4.6463	138	3.36
25	16.07	199	20.84	58	0.2790	0.8135	5.8133	138	4.21
25	16.07	154	16.13	85	0.4088	1.1922	6.5929	138	4.77
25	16.07	90	9.42	120	0.5772	1.6832	5.4395	138	3.94
25	16.07	68	7.12	134	0.6445	1.8795	4.5894	138	3.32
25	16.07	28	2.93	158	0.7599	2.2162	2.2282	138	1.61
30	19.29	340	35.60	0	0.0000	0.0000	0.0000	239	0.00
30	19.29	309	32.36	11	0.0890	0.2595	2.8789	239	1.21
30	19.29	285	29.85	26	0.2103	0.6133	6.2762	239	2.63
30	19.29	186	19.48	90	0.7279	2.1229	14.1785	239	5.94
30	19.29	159	16.65	106	0.8573	2.5003	14.2751	239	5.98
30	19.29	120	12.57	128	1.0353	3.0192	13.0097	239	5.45
30	19.29	43	4.50	143	1.1566	3.3730	5.2081	239	2.18
35	22.50	401	41.99	0	0.0000	0.0000	0.0000	379	0.00
35	22.50	345	36.13	50	0.4044	1.1794	14.6105	379	3.86
35	22.50	274	28.69	100	0.8088	2.3587	23.2074	379	6.12
35	22.50	244	25.55	119	0.9625	2.8069	24.5931	379	6.49
35	22.50	168	17.59	151	1.2213	3.5617	21.4863	379	5.67
35	22.50	78	8.17	187	1.5125	4.4108	12.3541	379	3.26
35	22.50	35	3.67	209	1.6904	4.9298	6.1957	379	1.63
40	25.71	467	48.90	0	0.0000	0.0000	0.0000	566	0.00
40	25.71	364	38.12	96	0.7765	2.2644	29.5971	566	5.23
40	25.71	334	34.98	130	1.0515	3.0664	36.7761	566	6.50
40	25.71	267	27.96	156	1.2617	3.6796	35.2786	566	6.24
40	25.71	198	20.73	187	1.5125	4.4108	31.3605	566	5.54
40	25.71	123	12.88	230	1.8603	5.4251	23.9612	566	4.24

40	25.71	80	8.38	265	2.1434	6.2507	17.9561	566	3.17
45	28.93	533	55.82	0	0.0000	0.0000	0.0000	805	0.00
45	28.93	460	48.17	85	0.6875	2.0049	33.1171	805	4.11
45	28.93	397	41.57	140	1.1323	3.3022	47.0754	805	5.84
45	28.93	319	33.41	170	1.3750	4.0099	45.9320	805	5.70
45	28.93	213	22.31	248	2.0059	5.8497	44.7411	805	5.55
45	28.93	172	18.01	292	2.3617	6.8875	42.5390	805	5.28
45	28.93	94	9.84	360	2.9117	8.4915	28.6620	805	3.56

NACA-0022 3 Bladed Turbine with 48% Solidity Trial 2									
F (Hz)	**U (m/s)**	**ω (rpm)**	**ω (rad/s)**	**Strain**	**T(N*m)**	**Tan Force (N)**	**P (W)**	**PA (W)**	**Eff (%)**
15	9.47	141	14.77	0	0.0000	0.0000	0.0000	28	0.00
15	9.47	82	8.59	21	0.1010	0.2946	0.8673	28	3.07
15	9.47	39	4.08	32	0.1539	0.4488	0.6286	28	2.23
15	9.47	24	2.51	39	0.1876	0.5470	0.4714	28	1.67
20	13.30	213	22.31	0	0.0000	0.0000	0.0000	78	0.00
20	13.30	171	17.91	25	0.1202	0.3507	2.1532	78	2.75
20	13.30	103	10.79	51	0.2453	0.7153	2.6457	78	3.38
20	13.30	80	8.38	61	0.2934	0.8556	2.4579	78	3.14
20	13.30	30	3.14	84	0.4040	1.1782	1.2692	78	1.62
20	13.30	10	1.05	93	0.4473	1.3044	0.4684	78	0.60
25	16.07	281	29.43	0	0.0000	0.0000	0.0000	138	0.00
25	16.07	244	25.55	30	0.1443	0.4208	3.6868	138	2.67
25	16.07	189	19.79	57	0.2741	0.7995	5.4259	138	3.93
25	16.07	141	14.77	79	0.3800	1.1081	5.6103	138	4.06
25	16.07	105	11.00	103	0.4954	1.4447	5.4471	138	3.94
25	16.07	92	9.63	115	0.5531	1.6130	5.3287	138	3.86
25	16.07	55	5.76	131	0.6301	1.8374	3.6289	138	2.63
30	19.29	338	35.40	0	0.0000	0.0000	0.0000	239	0.00
30	19.29	293	30.68	25	0.2022	0.5897	6.2042	239	2.60
30	19.29	226	23.67	64	0.5176	1.5096	12.2508	239	5.13
30	19.29	212	22.20	70	0.5662	1.6511	12.5693	239	5.27
30	19.29	154	16.13	117	0.9463	2.7597	15.2610	239	6.39
30	19.29	100	10.47	149	1.2051	3.5145	12.6201	239	5.29
30	19.29	18	1.88	164	1.3265	3.8683	2.5003	239	1.05
35	22.50	408	42.73	0	0.0000	0.0000	0.0000	379	0.00
35	22.50	361	37.80	40	0.3235	0.9435	12.2305	379	3.23
35	22.50	317	33.20	62	0.5015	1.4624	16.6466	379	4.39
35	22.50	260	27.23	106	0.8573	2.5003	23.3429	379	6.16
35	22.50	240	25.13	125	1.0110	2.9484	25.4096	379	6.70
35	22.50	139	14.56	155	1.2537	3.6560	18.2483	379	4.82

35	22.50	51	5.34	200	1.6176	4.7175	8.6392	379	2.28
40	25.71	469	49.11	0	0.0000	0.0000	0.0000	566	0.00
40	25.71	435	45.55	30	0.2426	0.7076	11.0532	566	1.95
40	25.71	373	39.06	94	0.7603	2.2172	29.6970	566	5.25
40	25.71	312	32.67	134	1.0838	3.1607	35.4108	566	6.26
40	25.71	225	23.56	165	1.3345	3.8919	31.4443	566	5.56
40	25.71	147	15.39	212	1.7147	5.0005	26.3954	566	4.67
40	25.71	102	10.68	250	2.0220	5.8969	21.5981	566	3.82
45	28.93	540	56.55	0	0.0000	0.0000	0.0000	805	0.00
45	28.93	383	40.11	145	1.1728	3.4202	47.0373	805	5.84
45	28.93	295	30.89	185	1.4963	4.3637	46.2242	805	5.74
45	28.93	201	21.05	268	2.1676	6.3214	45.6254	805	5.66
45	28.93	147	15.39	314	2.5397	7.4064	39.0951	805	4.85
45	28.93	90	9.42	390	3.1544	9.1991	29.7292	805	3.69
45	28.93	60	6.28	415	3.3566	9.7888	21.0899	805	2.62

NACA-0022 3 Bladed Turbine with 48% Solidity Trial 3									
F (Hz)	**U (m/s)**	**ω (rpm)**	**ω (rad/s)**	**Strain**	**T(N*m)**	**Tan Force (N)**	**P (W)**	**PA (W)**	**Eff (%)**
15	9.47	142	14.87	0	0.0000	0.0000	0.0000	28	0.00
15	9.47	73	7.64	29	0.1395	0.4068	1.0663	28	3.78
15	9.47	30	3.14	39	0.1876	0.5470	0.5893	28	2.09
15	9.47	11	1.15	47	0.2261	0.6592	0.2604	28	0.92
20	13.30	211	22.10	0	0.0000	0.0000	0.0000	78	0.00
20	13.30	165	17.28	27	0.1299	0.3787	2.2438	78	2.87
20	13.30	140	14.66	39	0.1876	0.5470	2.7500	78	3.52
20	13.30	65	6.81	80	0.3848	1.1221	2.6190	78	3.35
20	13.30	30	3.14	93	0.4473	1.3044	1.4052	78	1.80
20	13.30	14	1.47	101	0.4858	1.4167	0.7122	78	0.91
25	16.07	278	29.11	0	0.0000	0.0000	0.0000	138	0.00
25	16.07	244	25.55	28	0.1347	0.3927	3.4410	138	2.49
25	16.07	211	22.10	50	0.2405	0.7013	5.3136	138	3.85
25	16.07	154	16.13	72	0.3463	1.0099	5.5846	138	4.04
25	16.07	132	13.82	89	0.4281	1.2483	5.9170	138	4.28
25	16.07	110	11.52	101	0.4858	1.4167	5.5957	138	4.05
25	16.07	42	4.40	159	0.7647	2.2302	3.3635	138	2.44
30	19.29	334	34.98	0	0.0000	0.0000	0.0000	239	0.00
30	19.29	250	26.18	52	0.4206	1.2265	11.0108	239	4.61
30	19.29	175	18.33	108	0.8735	2.5474	16.0080	239	6.71
30	19.29	143	14.97	120	0.9706	2.8305	14.5343	239	6.09
30	19.29	127	13.30	127	1.0272	2.9956	13.6610	239	5.72
30	19.29	109	11.41	131	1.0595	3.0899	12.0941	239	5.07

30	19.29	34	3.56	156	1.2617	3.6796	4.4924	239	1.88
35	22.50	405	42.41	0	0.0000	0.0000	0.0000	379	0.00
35	22.50	367	38.43	32	0.2588	0.7548	9.9470	379	2.62
35	22.50	268	28.06	104	0.8412	2.4531	23.6072	379	6.23
35	22.50	227	23.77	133	1.0757	3.1371	25.5713	379	6.75
35	22.50	145	15.18	160	1.2941	3.7740	19.6501	379	5.19
35	22.50	92	9.63	181	1.4639	4.2693	14.1040	379	3.72
35	22.50	45	4.71	205	1.6581	4.8354	7.8134	379	2.06
40	25.71	469	49.11	0	0.0000	0.0000	0.0000	566	0.00
40	25.71	354	37.07	114	0.9220	2.6890	34.1809	566	6.04
40	25.71	336	35.19	127	1.0272	2.9956	36.1426	566	6.39
40	25.71	265	27.75	150	1.2132	3.5381	33.6677	566	5.95
40	25.71	172	18.01	197	1.5934	4.6467	28.6992	566	5.07
40	25.71	132	13.82	224	1.8117	5.2836	25.0437	566	4.43
40	25.71	88	9.22	266	2.1514	6.2742	19.8262	566	3.50
45	28.93	537	56.23	0	0.0000	0.0000	0.0000	805	0.00
45	28.93	482	50.47	58	0.4691	1.3681	23.6783	805	2.94
45	28.93	445	46.60	102	0.8250	2.4059	38.4447	805	4.77
45	28.93	311	32.57	174	1.4073	4.1042	45.8338	805	5.69
45	28.93	211	22.10	245	1.9816	5.7789	43.7849	805	5.44
45	28.93	148	15.50	313	2.5316	7.3829	39.2357	805	4.87
45	28.93	70	7.33	397	3.2110	9.3642	23.5377	805	2.92

NACA-0022 6 Bladed Turbine with 48% Solidity Trial 1									
F (Hz)	**U (m/s)**	**ω (rpm)**	**ω (rad/s)**	**Strain**	**T(N*m)**	**Tan Force (N)**	**P (W)**	**PA (W)**	**Eff (%)**
15	9.34	77	8.06	0	0.0000	0.0000	0.0000	27	0.00
15	9.34	52	5.45	15	0.0721	0.2104	0.3929	27	1.45
15	9.34	31	3.25	27	0.1299	0.3787	0.4216	27	1.56
15	9.34	9	0.94	40	0.1924	0.5611	0.1813	27	0.67
20	12.93	118	12.36	0	0.0000	0.0000	0.0000	72	0.00
20	12.93	81	8.48	27	0.1299	0.3787	1.1015	72	1.53
20	12.93	75	7.85	30	0.1443	0.4208	1.1332	72	1.58
20	12.93	65	6.81	37	0.1780	0.5190	1.2113	72	1.68
20	12.93	58	6.07	41	0.1972	0.5751	1.1977	72	1.67
20	12.93	26	2.72	58	0.2790	0.8135	0.7595	72	1.06
25	15.83	153	16.02	0	0.0000	0.0000	0.0000	132	0.00
25	15.83	131	13.72	21	0.1010	0.2946	1.3856	132	1.05
25	15.83	121	12.67	27	0.1299	0.3787	1.6455	132	1.25
25	15.83	78	8.17	66	0.3174	0.9257	2.5929	132	1.97
25	15.83	70	7.33	73	0.3511	1.0239	2.5737	132	1.95
25	15.83	42	4.40	85	0.4088	1.1922	1.7981	132	1.36

25	15.83	33	3.46	94	0.4521	1.3185	1.5624	132	1.19
30	18.99	200	20.94	0	0.0000	0.0000	0.0000	228	0.00
30	18.99	172	18.01	26	0.1251	0.3647	2.2524	228	0.99
30	18.99	156	16.34	44	0.2116	0.6172	3.4571	228	1.52
30	18.99	118	12.36	79	0.3800	1.1081	4.6951	228	2.06
30	18.99	95	9.95	101	0.4858	1.4167	4.8326	228	2.12
30	18.99	62	6.49	129	0.6204	1.8094	4.0283	228	1.77
30	18.99	33	3.46	153	0.7359	2.1460	2.5430	228	1.12
35	22.16	245	25.66	0	0.0000	0.0000	0.0000	362	0.00
35	22.16	198	20.73	50	0.2405	0.7013	4.9863	362	1.38
35	22.16	156	16.34	105	0.5050	1.4728	8.2500	362	2.28
35	22.16	114	11.94	160	0.7695	2.2442	9.1868	362	2.54
35	22.16	88	9.22	177	0.8513	2.4827	7.8450	362	2.17
35	22.16	35	3.67	260	1.2505	3.6468	4.5833	362	1.27
35	22.16	22	2.30	271	1.3034	3.8011	3.0028	362	0.83
40	25.32	274	28.69	0	0.0000	0.0000	0.0000	540	0.00
40	25.32	226	23.67	60	0.2886	0.8416	6.8297	540	1.27
40	25.32	198	20.73	99	0.4762	1.3886	9.8728	540	1.83
40	25.32	175	18.33	140	0.6733	1.9637	12.3397	540	2.29
40	25.32	120	12.57	218	1.0485	3.0577	13.1758	540	2.44
40	25.32	80	8.38	275	1.3226	3.8572	11.0806	540	2.05
40	25.32	48	5.03	312	1.5006	4.3762	7.5428	540	1.40
45	28.49	320	33.51	0	0.0000	0.0000	0.0000	768	0.00
45	28.49	227	23.77	151	0.7263	2.1180	17.2640	768	2.25
45	28.49	210	21.99	183	0.8802	2.5668	19.3557	768	2.52
45	28.49	179	18.74	227	1.0918	3.1840	20.4653	768	2.66
45	28.49	119	12.46	307	1.4766	4.3061	18.4003	768	2.39
45	28.49	69	7.23	355	1.7074	4.9793	12.3372	768	1.61
45	28.49	50	5.24	370	1.7796	5.1897	9.3177	768	1.21

NACA-0022 6 Bladed Turbine with 48% Solidity Trial 2									
F (Hz)	**U (m/s)**	**ω (rpm)**	**ω (rad/s)**	**Strain**	**T(N*m)**	**Tan Force (N)**	**P (W)**	**PA (W)**	**Eff (%)**
15	9.34	78	8.17	0	0.0000	0.0000	0.0000	27	0.00
15	9.34	49	5.13	17	0.0818	0.2384	0.4196	27	1.55
15	9.34	41	4.29	23	0.1106	0.3226	0.4750	27	1.75
15	9.34	16	1.68	34	0.1635	0.4769	0.2740	27	1.01
20	12.93	113	11.83	0	0.0000	0.0000	0.0000	72	0.00
20	12.93	97	10.16	18	0.0866	0.2525	0.8794	72	1.22
20	12.93	81	8.48	25	0.1202	0.3507	1.0199	72	1.42
20	12.93	68	7.12	33	0.1587	0.4629	1.1302	72	1.57
20	12.93	55	5.76	40	0.1924	0.5611	1.1081	72	1.54

20	12.93	8	0.84	69	0.3319	0.9678	0.2780	72	0.39
25	15.83	157	16.44	0	0.0000	0.0000	0.0000	132	0.00
25	15.83	132	13.82	20	0.0962	0.2805	1.3297	132	1.01
25	15.83	126	13.19	24	0.1154	0.3366	1.5231	132	1.16
25	15.83	91	9.53	50	0.2405	0.7013	2.2917	132	1.74
25	15.83	79	8.27	64	0.3078	0.8977	2.5465	132	1.93
25	15.83	61	6.39	80	0.3848	1.1221	2.4579	132	1.87
25	15.83	16	1.68	116	0.5579	1.6271	0.9348	132	0.71
30	18.99	199	20.84	0	0.0000	0.0000	0.0000	228	0.00
30	18.99	183	19.16	16	0.0770	0.2244	1.4747	228	0.65
30	18.99	105	11.00	95	0.4569	1.3325	5.0240	228	2.21
30	18.99	86	9.01	108	0.5194	1.5148	4.6780	228	2.05
30	18.99	67	7.02	124	0.5964	1.7393	4.1844	228	1.84
30	18.99	34	3.56	151	0.7263	2.1180	2.5858	228	1.14
30	18.99	24	2.51	160	0.7695	2.2442	1.9341	228	0.85
35	22.16	243	25.45	0	0.0000	0.0000	0.0000	362	0.00
35	22.16	225	23.56	21	0.1010	0.2946	2.3798	362	0.66
35	22.16	191	20.00	57	0.2741	0.7995	5.4834	362	1.52
35	22.16	161	16.86	97	0.4665	1.3606	7.8657	362	2.18
35	22.16	112	11.73	163	0.7840	2.2863	9.1949	362	2.54
35	22.16	50	5.24	245	1.1784	3.4364	6.1699	362	1.71
35	22.16	20	2.09	272	1.3082	3.8152	2.7399	362	0.76
40	25.32	276	28.90	0	0.0000	0.0000	0.0000	540	0.00
40	25.32	246	25.76	38	0.1828	0.5330	4.7082	540	0.87
40	25.32	185	19.37	126	0.6060	1.7673	11.7404	540	2.18
40	25.32	161	16.86	174	0.8369	2.4406	14.1096	540	2.61
40	25.32	129	13.51	218	1.0485	3.0577	14.1640	540	2.62
40	25.32	70	7.33	285	1.3707	3.9975	10.0481	540	1.86
40	25.32	37	3.87	322	1.5487	4.5165	6.0006	540	1.11
45	28.49	321	33.62	0	0.0000	0.0000	0.0000	768	0.00
45	28.49	299	31.31	31	0.1491	0.4348	4.6684	768	0.61
45	28.49	272	28.48	70	0.3367	0.9818	9.5897	768	1.25
45	28.49	247	25.87	118	0.5675	1.6551	14.6797	768	1.91
45	28.49	150	15.71	260	1.2505	3.6468	19.6428	768	2.56
45	28.49	99	10.37	325	1.5631	4.5586	16.2053	768	2.11
45	28.49	57	5.97	367	1.7651	5.1477	10.5361	768	1.37

NACA-0022 6 Bladed Turbine with 48% Solidity Trial 3									
F (Hz)	**U (m/s)**	**ω (rpm)**	**ω (rad/s)**	**Strain**	**T(N*m)**	**Tan Force (N)**	**P (W)**	**PA (W)**	**Eff (%)**
15	9.34	77	8.06	0	0.0000	0.0000	0.0000	27	0.00
15	9.34	50	5.24	16	0.0770	0.2244	0.4029	27	1.49

15	9.34	43	4.50	21	0.1010	0.2946	0.4548	27	1.68
15	9.34	30	3.14	27	0.1299	0.3787	0.4080	27	1.51
20	12.93	113	11.83	0	0.0000	0.0000	0.0000	72	0.00
20	12.93	84	8.80	22	0.1058	0.3086	0.9308	72	1.29
20	12.93	74	7.75	27	0.1299	0.3787	1.0063	72	1.40
20	12.93	62	6.49	35	0.1683	0.4909	1.0929	72	1.52
20	12.93	50	5.24	43	0.2068	0.6031	1.0829	72	1.51
20	12.93	20	2.09	60	0.2886	0.8416	0.6044	72	0.84
25	15.83	157	16.44	0	0.0000	0.0000	0.0000	132	0.00
25	15.83	133	13.93	23	0.1106	0.3226	1.5407	132	1.17
25	15.83	91	9.53	52	0.2501	0.7294	2.3833	132	1.81
25	15.83	84	8.80	56	0.2693	0.7855	2.3692	132	1.80
25	15.83	66	6.91	75	0.3607	1.0520	2.4931	132	1.89
25	15.83	48	5.03	85	0.4088	1.1922	2.0549	132	1.56
25	15.83	29	3.04	100	0.4810	1.4026	1.4606	132	1.11
30	18.99	200	20.94	0	0.0000	0.0000	0.0000	228	0.00
30	18.99	180	18.85	21	0.1010	0.2946	1.9038	228	0.84
30	18.99	148	15.50	55	0.2645	0.7714	4.0998	228	1.80
30	18.99	103	10.79	92	0.4425	1.2904	4.7727	228	2.10
30	18.99	95	9.95	104	0.5002	1.4587	4.9762	228	2.19
30	18.99	64	6.70	135	0.6493	1.8936	4.3516	228	1.91
30	18.99	18	1.88	166	0.7984	2.3284	1.5049	228	0.66
35	22.16	243	25.45	0	0.0000	0.0000	0.0000	362	0.00
35	22.16	192	20.11	58	0.2790	0.8135	5.6088	362	1.55
35	22.16	180	18.85	74	0.3559	1.0379	6.7088	362	1.86
35	22.16	138	14.45	127	0.6108	1.7813	8.8272	362	2.44
35	22.16	86	9.01	207	0.9956	2.9034	8.9662	362	2.48
35	22.16	38	3.98	260	1.2505	3.6468	4.9762	362	1.38
35	22.16	16	1.68	280	1.3467	3.9274	2.2564	362	0.62
40	25.32	280	29.32	0	0.0000	0.0000	0.0000	540	0.00
40	25.32	268	28.06	19	0.0914	0.2665	2.5646	540	0.48
40	25.32	203	21.26	100	0.4810	1.4026	10.2243	540	1.89
40	25.32	129	13.51	220	1.0581	3.0858	14.2939	540	2.65
40	25.32	89	9.32	263	1.2649	3.6889	11.7892	540	2.18
40	25.32	43	4.50	310	1.4910	4.3482	6.7138	540	1.24
40	25.32	25	2.62	333	1.6016	4.6708	4.1930	540	0.78
45	28.49	322	33.72	0	0.0000	0.0000	0.0000	768	0.00
45	28.49	233	24.40	133	0.6397	1.8655	15.6080	768	2.03
45	28.49	204	21.36	189	0.9090	2.6510	19.4192	768	2.53
45	28.49	168	17.59	242	1.1639	3.3944	20.4769	768	2.67
45	28.49	116	12.15	311	1.4958	4.3622	18.1701	768	2.36

45	28.49	66	6.91	363	1.7459	5.0915	12.0667	768	1.57
45	28.49	46	4.82	382	1.8373	5.3580	8.8503	768	1.15

NACA-0022 3 Bladed Turbine with 41% Solidity Trial 1									
F (Hz)	**U (m/s)**	**ω (rpm)**	**ω (rad/s)**	**Strain**	**T(N*m)**	**Tan Force (N)**	**P (W)**	**PA (W)**	**Eff (%)**
15	9.10	121	12.67	0	0.0000	0.0000	0.0000	25	0.00
15	9.10	83	8.69	11	0.0529	0.1543	0.4598	25	1.84
15	9.10	30	3.14	41	0.1972	0.5751	0.6195	25	2.48
15	9.10	16	1.68	54	0.2597	0.7574	0.4352	25	1.75
20	13.06	182	19.06	0	0.0000	0.0000	0.0000	74	0.00
20	13.06	150	15.71	11	0.0529	0.1543	0.8310	74	1.13
20	13.06	107	11.21	32	0.1539	0.4488	1.7245	74	2.34
20	13.06	88	9.22	43	0.2068	0.6031	1.9059	74	2.59
20	13.06	58	6.07	52	0.2501	0.7294	1.5190	74	2.06
20	13.06	40	4.19	68	0.3271	0.9538	1.3700	74	1.86
25	15.72	242	25.34	0	0.0000	0.0000	0.0000	129	0.00
25	15.72	205	21.47	17	0.0818	0.2384	1.7553	129	1.37
25	15.72	188	19.69	26	0.1251	0.3647	2.4619	129	1.92
25	15.72	158	16.55	40	0.1924	0.5611	3.1831	129	2.48
25	15.72	100	10.47	75	0.3607	1.0520	3.7775	129	2.94
25	15.72	63	6.60	110	0.5291	1.5429	3.4904	129	2.72
25	15.72	36	3.77	136	0.6541	1.9076	2.4659	129	1.92
30	18.87	301	31.52	0	0.0000	0.0000	0.0000	222	0.00
30	18.87	259	27.12	26	0.1251	0.3647	3.3917	222	1.53
30	18.87	194	20.32	68	0.3271	0.9538	6.6443	222	2.99
30	18.87	188	19.69	78	0.3752	1.0941	7.3857	222	3.33
30	18.87	173	18.12	96	0.4617	1.3465	8.3648	222	3.77
30	18.87	129	13.51	122	0.5868	1.7112	7.9266	222	3.57
30	18.87	71	7.44	189	0.9090	2.6510	6.7586	222	3.04
35	22.01	363	38.01	0	0.0000	0.0000	0.0000	353	0.00
35	22.01	342	35.81	13	0.0625	0.1823	2.2393	353	0.63
35	22.01	248	25.97	87	0.4184	1.2203	10.8670	353	3.08
35	22.01	150	15.71	204	0.9812	2.8614	15.4121	353	4.37
35	22.01	97	10.16	237	1.1399	3.3242	11.5787	353	3.28
35	22.01	58	6.07	259	1.2457	3.6328	7.5660	353	2.15
35	22.01	34	3.56	272	1.3082	3.8152	4.6579	353	1.32
40	25.16	423	44.30	0	0.0000	0.0000	0.0000	527	0.00
40	25.16	304	31.83	114	0.5483	1.5990	17.4549	527	3.32
40	25.16	285	29.85	143	0.6878	2.0058	20.5267	527	3.90
40	25.16	268	28.06	155	0.7455	2.1741	20.9221	527	3.97
40	25.16	204	21.36	237	1.1399	3.3242	24.3510	527	4.62

40	25.16	142	14.87	273	1.3130	3.8292	19.5250	527	3.71
40	25.16	108	11.31	304	1.4621	4.2640	16.5362	527	3.14
45	28.30	511	53.51	0	0.0000	0.0000	0.0000	750	0.00
45	28.30	414	43.35	84	0.4040	1.1782	17.5153	750	2.34
45	28.30	345	36.13	172	0.8273	2.4125	29.8873	750	3.99
45	28.30	295	30.89	238	1.1447	3.3383	35.3621	750	4.72
45	28.30	226	23.67	289	1.3900	4.0536	32.8962	750	4.39
45	28.30	118	12.36	372	1.7892	5.2178	22.1087	750	2.95
45	28.30	70	7.33	400	1.9238	5.6105	14.1025	750	1.88

NACA-0022 3 Bladed Turbine with 41% Solidity Trial 2									
F (Hz)	**U (m/s)**	**ω (rpm)**	**ω (rad/s)**	**Strain**	**T(N*m)**	**Tan Force (N)**	**P (W)**	**PA (W)**	**Eff (%)**
15	9.10	120	12.57	0	0.0000	0.0000	0.0000	25	0.00
15	9.10	75	7.85	18	0.0866	0.2525	0.6799	25	2.73
15	9.10	68	7.12	20	0.0962	0.2805	0.6850	25	2.75
15	9.10	48	5.03	33	0.1587	0.4629	0.7978	25	3.20
20	13.06	182	19.06	0	0.0000	0.0000	0.0000	74	0.00
20	13.06	118	12.36	22	0.1058	0.3086	1.3075	74	1.77
20	13.06	102	10.68	32	0.1539	0.4488	1.6440	74	2.23
20	13.06	72	7.54	48	0.2309	0.6733	1.7407	74	2.36
20	13.06	55	5.76	53	0.2549	0.7434	1.4682	74	1.99
20	13.06	21	2.20	72	0.3463	1.0099	0.7615	74	1.03
25	15.72	241	25.24	0	0.0000	0.0000	0.0000	129	0.00
25	15.72	194	20.32	23	0.1106	0.3226	2.2473	129	1.75
25	15.72	160	16.76	34	0.1635	0.4769	2.7399	129	2.13
25	15.72	150	15.71	50	0.2405	0.7013	3.7775	129	2.94
25	15.72	120	12.57	65	0.3126	0.9117	3.9286	129	3.06
25	15.72	87	9.11	87	0.4184	1.2203	3.8122	129	2.97
25	15.72	46	4.82	121	0.5820	1.6972	2.8034	129	2.18
30	18.87	300	31.42	0	0.0000	0.0000	0.0000	222	0.00
30	18.87	255	26.70	22	0.1058	0.3086	2.8255	222	1.27
30	18.87	210	21.99	53	0.2549	0.7434	5.6058	222	2.52
30	18.87	188	19.69	78	0.3752	1.0941	7.3857	222	3.33
30	18.87	160	16.76	91	0.4377	1.2764	7.3333	222	3.30
30	18.87	73	7.64	168	0.8080	2.3564	6.1769	222	2.78
30	18.87	35	3.67	202	0.9715	2.8333	3.5609	222	1.60
35	22.01	364	38.12	0	0.0000	0.0000	0.0000	353	0.00
35	22.01	293	30.68	55	0.2645	0.7714	8.1165	353	2.30
35	22.01	231	24.19	110	0.5291	1.5429	12.7980	353	3.63
35	22.01	180	18.85	187	0.8994	2.6229	16.9533	353	4.81
35	22.01	149	15.60	210	1.0100	2.9455	15.7596	353	4.47

35	22.01	116	12.15	233	1.1206	3.2681	13.6130	353	3.86
35	22.01	49	5.13	276	1.3275	3.8713	6.8115	353	1.93
40	25.16	426	44.61	0	0.0000	0.0000	0.0000	527	0.00
40	25.16	395	41.36	25	0.1202	0.3507	4.9737	527	0.94
40	25.16	323	33.82	105	0.5050	1.4728	17.0817	527	3.24
40	25.16	208	21.78	217	1.0437	3.0437	22.7333	527	4.32
40	25.16	136	14.24	276	1.3275	3.8713	18.9055	527	3.59
40	25.16	86	9.01	323	1.5535	4.5305	13.9907	527	2.66
40	25.16	53	5.55	345	1.6593	4.8391	9.2095	527	1.75
45	28.30	490	51.31	0	0.0000	0.0000	0.0000	750	0.00
45	28.30	457	47.86	35	0.1683	0.4909	8.0561	750	1.07
45	28.30	400	41.89	106	0.5098	1.4868	21.3553	750	2.85
45	28.30	340	35.60	171	0.8224	2.3985	29.2829	750	3.91
45	28.30	223	23.35	295	1.4188	4.1378	33.1334	750	4.42
45	28.30	116	12.15	365	1.7555	5.1196	21.3250	750	2.84
45	28.30	58	6.07	397	1.9094	5.5684	11.5973	750	1.55

NACA-0022 3 Bladed Turbine with 41% Solidity Trial 3									
F (Hz)	**U (m/s)**	**ω (rpm)**	**ω (rad/s)**	**Strain**	**T(N*m)**	**Tan Force (N)**	**P (W)**	**PA (W)**	**Eff (%)**
15	9.10	122	12.78	0	0.0000	0.0000	0.0000	25	0.00
15	9.10	67	7.02	21	0.1010	0.2946	0.7087	25	2.84
15	9.10	40	4.19	43	0.2068	0.6031	0.8663	25	3.47
15	9.10	22	2.30	51	0.2453	0.7153	0.5651	25	2.27
20	13.06	179	18.74	0	0.0000	0.0000	0.0000	74	0.00
20	13.06	113	11.83	27	0.1299	0.3787	1.5367	74	2.09
20	13.06	106	11.10	31	0.1491	0.4348	1.6550	74	2.25
20	13.06	67	7.02	49	0.2357	0.6873	1.6535	74	2.24
20	13.06	28	2.93	68	0.3271	0.9538	0.9590	74	1.30
20	13.06	14	1.47	76	0.3655	1.0660	0.5359	74	0.73
25	15.72	240	25.13	0	0.0000	0.0000	0.0000	129	0.00
25	15.72	208	21.78	18	0.0866	0.2525	1.8857	129	1.47
25	15.72	137	14.35	54	0.2597	0.7574	3.7261	129	2.90
25	15.72	96	10.05	82	0.3944	1.1502	3.9648	129	3.08
25	15.72	65	6.81	101	0.4858	1.4167	3.3065	129	2.57
25	15.72	50	5.24	114	0.5483	1.5990	2.8709	129	2.23
25	15.72	10	1.05	141	0.6782	1.9777	0.7102	129	0.55
30	18.87	302	31.63	0	0.0000	0.0000	0.0000	222	0.00
30	18.87	224	23.46	46	0.2212	0.6452	5.1897	222	2.34
30	18.87	198	20.73	62	0.2982	0.8696	6.1830	222	2.78
30	18.87	172	18.01	85	0.4088	1.1922	7.3635	222	3.32
30	18.87	165	17.28	91	0.4377	1.2764	7.5625	222	3.40

30	18.87	117	12.25	133	0.6397	1.8655	7.8375	222	3.53
30	18.87	34	3.56	198	0.9523	2.7772	3.3907	222	1.53
35	22.01	368	38.54	0	0.0000	0.0000	0.0000	353	0.00
35	22.01	238	24.92	87	0.4184	1.2203	10.4288	353	2.96
35	22.01	213	22.31	133	0.6397	1.8655	14.2682	353	4.05
35	22.01	172	18.01	177	0.8513	2.4827	15.3335	353	4.35
35	22.01	138	14.45	203	0.9764	2.8473	14.1096	353	4.00
35	22.01	70	7.33	254	1.2216	3.5627	8.9551	353	2.54
35	22.01	39	4.08	280	1.3467	3.9274	5.5000	353	1.56
40	25.16	427	44.72	0	0.0000	0.0000	0.0000	527	0.00
40	25.16	317	33.20	102	0.4906	1.4307	16.2854	527	3.09
40	25.16	283	29.64	150	0.7214	2.1039	21.3804	527	4.06
40	25.16	255	26.70	174	0.8369	2.4406	22.3475	527	4.24
40	25.16	153	16.02	270	1.2986	3.7871	20.8063	527	3.95
40	25.16	85	8.90	316	1.5198	4.4323	13.5284	527	2.57
40	25.16	56	5.86	342	1.6449	4.7970	9.6461	527	1.83
45	28.30	480	50.27	0	0.0000	0.0000	0.0000	750	0.00
45	28.30	353	36.97	164	0.7888	2.3003	29.1580	750	3.89
45	28.30	298	31.21	226	1.0870	3.1699	33.9206	750	4.52
45	28.30	226	23.67	286	1.3756	4.0115	32.5547	750	4.34
45	28.30	163	17.07	343	1.6497	4.8110	28.1592	750	3.76
45	28.30	97	10.16	377	1.8132	5.2879	18.4184	750	2.46
45	28.30	58	6.07	415	1.9960	5.8209	12.1231	750	1.62

NACA-0022 3 Bladed Turbine with 55% Solidity Trial 1									
F (Hz)	**U (m/s)**	**ω (rpm)**	**ω (rad/s)**	**Strain**	**T(N*m)**	**Tan Force (N)**	**P (W)**	**PA (W)**	**Eff (%)**
15	8.10	171	17.91	0	0.0000	0.0000	0.0000	18	0.00
15	8.10	115	12.04	22	0.1058	0.3086	1.2743	18	7.23
15	8.10	84	8.80	30	0.1443	0.4208	1.2692	18	7.20
15	8.10	8	0.84	66	0.3174	0.9257	0.2659	18	1.51
20	11.02	263	27.54	0	0.0000	0.0000	0.0000	44	0.00
20	11.02	223	23.35	18	0.0866	0.2525	2.0217	44	4.55
20	11.02	213	22.31	26	0.1251	0.3647	2.7893	44	6.28
20	11.02	157	16.44	50	0.2405	0.7013	3.9537	44	8.91
20	11.02	112	11.73	64	0.3078	0.8977	3.6102	44	8.13
20	11.02	46	4.82	98	0.4713	1.3746	2.2705	44	5.11
25	13.57	354	37.07	0	0.0000	0.0000	0.0000	83	0.00
25	13.57	320	33.51	18	0.0866	0.2525	2.9011	83	3.50
25	13.57	279	29.22	45	0.2164	0.6312	6.3235	83	7.63
25	13.57	202	21.15	86	0.4136	1.2063	8.7496	83	10.56
25	13.57	161	16.86	117	0.5627	1.6411	9.4875	83	11.45

25	13.57	120	12.57	150	0.7214	2.1039	9.0659	83	10.94
25	13.57	26	2.72	211	1.0148	2.9596	2.7631	83	3.34
30	16.28	458	47.96	0	0.0000	0.0000	0.0000	143	0.00
30	16.28	332	34.77	91	0.4377	1.2764	15.2166	143	10.63
30	16.28	250	26.18	150	0.7214	2.1039	18.8873	143	13.19
30	16.28	186	19.48	210	1.0100	2.9455	19.6730	143	13.74
30	16.28	152	15.92	223	1.0725	3.1279	17.0721	143	11.93
30	16.28	90	9.42	265	1.2745	3.7170	12.0123	143	8.39
30	16.28	66	6.91	282	1.3563	3.9554	9.3742	143	6.55
35	19.00	576	60.32	0	0.0000	0.0000	0.0000	227	0.00
35	19.00	491	51.42	23	0.1860	0.5425	9.5650	227	4.21
35	19.00	400	41.89	75	0.6066	1.7691	25.4096	227	11.18
35	19.00	282	29.53	129	1.0434	3.0428	30.8116	227	13.55
35	19.00	196	20.53	149	1.2051	3.5145	24.7354	227	10.88
35	19.00	137	14.35	165	1.3345	3.8919	19.1461	227	8.42
35	19.00	81	8.48	195	1.5772	4.5995	13.3781	227	5.89
40	21.71	645	67.54	0	0.0000	0.0000	0.0000	339	0.00
40	21.71	594	62.20	36	0.2912	0.8491	18.1119	339	5.34
40	21.71	433	45.34	132	1.0676	3.1135	48.4103	339	14.27
40	21.71	393	41.15	141	1.1404	3.3258	46.9340	339	13.83
40	21.71	250	26.18	195	1.5772	4.5995	41.2905	339	12.17
40	21.71	141	14.77	249	2.0139	5.8733	29.7368	339	8.76
40	21.71	88	9.22	280	2.2647	6.6045	20.8697	339	6.15
45	24.42	722	75.61	0	0.0000	0.0000	0.0000	483	0.00
45	24.42	696	72.88	24	0.1941	0.5661	14.1480	483	2.93
45	24.42	615	64.40	81	0.6551	1.9106	42.1926	483	8.73
45	24.42	521	54.56	142	1.1485	3.3494	62.6617	483	12.97
45	24.42	440	46.08	176	1.4235	4.1514	65.5905	483	13.58
45	24.42	383	40.11	205	1.6581	4.8354	66.5010	483	13.76
45	24.42	330	34.56	236	1.9088	5.5666	65.9632	483	13.65

NACA-0022 3 Bladed Turbine with 55% Solidity Trial 2									
F (Hz)	**U (m/s)**	**ω (rpm)**	**ω (rad/s)**	**Strain**	**T(N*m)**	**Tan Force (N)**	**P(W)**	**PA (W)**	**Eff(%)**
15	8.10	173	18.12	0	0.0000	0.0000	0.0000	18	0.00
15	8.10	112	11.73	22	0.1058	0.3086	1.2410	18	7.04
15	8.10	79	8.27	34	0.1635	0.4769	1.3528	18	7.68
15	8.10	35	3.67	44	0.2116	0.6172	0.7756	18	4.40
20	11.02	268	28.06	0	0.0000	0.0000	0.0000	44	0.00
20	11.02	192	20.11	36	0.1731	0.5049	3.4813	44	7.84
20	11.02	114	11.94	64	0.3078	0.8977	3.6747	44	8.28
20	11.02	86	9.01	76	0.3655	1.0660	3.2919	44	7.41

20	11.02	46	4.82	95	0.4569	1.3325	2.2010	44	4.96
20	11.02	26	2.72	115	0.5531	1.6130	1.5059	44	3.39
25	13.57	354	37.07	0	0.0000	0.0000	0.0000	83	0.00
25	13.57	283	29.64	31	0.1491	0.4348	4.4186	83	5.33
25	13.57	268	28.06	53	0.2549	0.7434	7.1540	83	8.64
25	13.57	201	21.05	91	0.4377	1.2764	9.2125	83	11.12
25	13.57	156	16.34	115	0.5531	1.6130	9.0357	83	10.91
25	13.57	116	12.15	142	0.6830	1.9917	8.2963	83	10.01
25	13.57	50	5.24	190	0.9138	2.6650	4.7848	83	5.78
30	16.28	461	48.28	0	0.0000	0.0000	0.0000	143	0.00
30	16.28	372	38.96	47	0.2261	0.6592	8.8060	143	6.15
30	16.28	336	35.19	89	0.4281	1.2483	15.0615	143	10.52
30	16.28	234	24.50	163	0.7840	2.2863	19.2107	143	13.42
30	16.28	150	15.71	222	1.0677	3.1138	16.7719	143	11.72
30	16.28	84	8.80	263	1.2649	3.6889	11.1269	143	7.77
30	16.28	35	3.67	302	1.4525	4.2359	5.3237	143	3.72
35	19.00	550	57.60	0	0.0000	0.0000	0.0000	227	0.00
35	19.00	413	43.25	73	0.5904	1.7219	25.5358	227	11.23
35	19.00	252	26.39	135	1.0919	3.1843	28.8144	227	12.68
35	19.00	223	23.35	148	1.1970	3.4909	27.9539	227	12.30
35	19.00	157	16.44	166	1.3426	3.9155	22.0741	227	9.71
35	19.00	118	12.36	179	1.4478	4.2221	17.8900	227	7.87
35	19.00	56	5.86	210	1.6985	4.9534	9.9605	227	4.38
40	21.71	648	67.86	0	0.0000	0.0000	0.0000	339	0.00
40	21.71	517	54.14	80	0.6470	1.8870	35.0313	339	10.32
40	21.71	453	47.44	116	0.9382	2.7361	44.5074	339	13.12
40	21.71	335	35.08	157	1.2698	3.7032	44.5472	339	13.13
40	21.71	262	27.44	195	1.5772	4.5995	43.2725	339	12.75
40	21.71	211	22.10	207	1.6742	4.8826	36.9938	339	10.90
40	21.71	137	14.35	250	2.0220	5.8969	29.0092	339	8.55
45	24.42	732	76.65	0	0.0000	0.0000	0.0000	483	0.00
45	24.42	566	59.27	123	0.9948	2.9013	58.9654	483	12.20
45	24.42	460	48.17	170	1.3750	4.0099	66.2342	483	13.71
45	24.42	355	37.18	218	1.7632	5.1421	65.5482	483	13.57
45	24.42	276	28.90	267	2.1595	6.2978	62.4160	483	12.92
45	24.42	217	22.72	305	2.4669	7.1942	56.0577	483	11.60
45	24.42	140	14.66	383	3.0977	9.0340	45.4153	483	9.40

NACA-0022 3 Bladed Turbine with 55% Solidity Trial 3									
F (Hz)	**U (m/s)**	**ω (rpm)**	**ω (rad/s)**	**Strain**	**T(N*m)**	**Tan Force (N)**	**P(W)**	**PA (W)**	**Eff(%)**
15	8.10	176	18.43	0	0.0000	0.0000	0.0000	18	0.00

15	8.10	135	14.14	13	0.0625	0.1823	0.8839	18	5.02
15	8.10	39	4.08	43	0.2068	0.6031	0.8446	18	4.79
15	8.10	29	3.04	48	0.2309	0.6733	0.7011	18	3.98
20	11.02	260	27.23	0	0.0000	0.0000	0.0000	44	0.00
20	11.02	223	23.35	23	0.1106	0.3226	2.5833	44	5.82
20	11.02	177	18.54	40	0.1924	0.5611	3.5659	44	8.03
20	11.02	142	14.87	52	0.2501	0.7294	3.7190	44	8.38
20	11.02	105	11.00	66	0.3174	0.9257	3.4904	44	7.86
20	11.02	56	5.86	95	0.4569	1.3325	2.6795	44	6.04
25	13.57	363	38.01	0	0.0000	0.0000	0.0000	83	0.00
25	13.57	310	32.46	23	0.1106	0.3226	3.5911	83	4.33
25	13.57	246	25.76	61	0.2934	0.8556	7.5580	83	9.12
25	13.57	181	18.95	99	0.4762	1.3886	9.0251	83	10.89
25	13.57	109	11.41	147	0.7070	2.0619	8.0702	83	9.74
25	13.57	74	7.75	172	0.8273	2.4125	6.4106	83	7.74
25	13.57	42	4.40	193	0.9283	2.7071	4.0827	83	4.93
30	16.28	460	48.17	0	0.0000	0.0000	0.0000	143	0.00
30	16.28	331	34.66	92	0.4425	1.2904	15.3375	143	10.71
30	16.28	274	28.69	125	0.6012	1.7533	17.2504	143	12.05
30	16.28	204	21.36	194	0.9331	2.7211	19.9329	143	13.92
30	16.28	118	12.36	241	1.1591	3.3803	14.3231	143	10.01
30	16.28	87	9.11	261	1.2553	3.6609	11.4367	143	7.99
30	16.28	53	5.55	285	1.3707	3.9975	7.6078	143	5.31
35	19.00	581	60.84	0	0.0000	0.0000	0.0000	227	0.00
35	19.00	482	50.47	37	0.2993	0.8727	15.1051	227	6.64
35	19.00	430	45.03	64	0.5176	1.5096	23.3090	227	10.25
35	19.00	365	38.22	96	0.7765	2.2644	29.6784	227	13.06
35	19.00	336	35.19	112	0.9059	2.6418	31.8737	227	14.02
35	19.00	243	25.45	140	1.1323	3.3022	28.8144	227	12.68
35	19.00	136	14.24	174	1.4073	4.1042	20.0431	227	8.82
40	21.71	658	68.91	0	0.0000	0.0000	0.0000	339	0.00
40	21.71	470	49.22	113	0.9140	2.6654	44.9834	339	13.26
40	21.71	426	44.61	130	1.0515	3.0664	46.9060	339	13.82
40	21.71	307	32.15	177	1.4316	4.1750	46.0243	339	13.56
40	21.71	182	19.06	221	1.7875	5.2128	34.0674	339	10.04
40	21.71	154	16.13	240	1.9411	5.6610	31.3046	339	9.23
40	21.71	87	9.11	285	2.3051	6.7224	21.0010	339	6.19
45	24.42	734	76.86	0	0.0000	0.0000	0.0000	483	0.00
45	24.42	590	61.78	94	0.7603	2.2172	46.9738	483	9.72
45	24.42	517	54.14	135	1.0919	3.1843	59.1153	483	12.24
45	24.42	425	44.51	177	1.4316	4.1750	63.7145	483	13.19

45	24.42	342	35.81	234	1.8926	5.5195	67.7825	483	14.03
45	24.42	290	30.37	265	2.1434	6.2507	65.0908	483	13.47
45	24.42	244	25.55	285	2.3051	6.7224	58.8994	483	12.19

NACA-0022 2 Bladed Turbine with 41% Solidity Trial 1									
F (Hz)	**U (m/s)**	**ω (rpm)**	**ω (rad/s)**	**Strain**	**T(N*m)**	**Tan Force (N)**	**P(W)**	**PA (W)**	**Eff(%)**
15	7.65	102	10.68	0	0.0000	0.0000	0.0000	14	0.00
15	7.65	78	8.17	21	0.1010	0.2946	0.8250	14	5.94
15	7.65	49	5.13	46	0.2212	0.6452	1.1353	14	8.18
15	7.65	6	0.63	84	0.4040	1.1782	0.2538	14	1.83
20	10.59	148	15.50	0	0.0000	0.0000	0.0000	39	0.00
20	10.59	110	11.52	51	0.2453	0.7153	2.8255	39	7.20
20	10.59	81	8.48	80	0.3848	1.1221	3.2637	39	8.31
20	10.59	55	5.76	105	0.5050	1.4728	2.9086	39	7.41
20	10.59	32	3.35	120	0.5772	1.6832	1.9341	39	4.93
20	10.59	23	2.41	137	0.6589	1.9216	1.5870	39	4.04
25	12.79	195	20.42	0	0.0000	0.0000	0.0000	68	0.00
25	12.79	170	17.80	37	0.1780	0.5190	3.1680	68	4.69
25	12.79	143	14.97	84	0.4040	1.1782	6.0500	68	8.95
25	12.79	110	11.52	124	0.5964	1.7393	6.8699	68	10.16
25	12.79	75	7.85	162	0.7792	2.2723	6.1195	68	9.05
25	12.79	58	6.07	177	0.8513	2.4827	5.1706	68	7.65
25	12.79	31	3.25	200	0.9619	2.8053	3.1227	68	4.62
30	15.34	241	25.24	0	0.0000	0.0000	0.0000	117	0.00
30	15.34	198	20.73	79	0.3800	1.1081	7.8783	117	6.75
30	15.34	181	18.95	117	0.5627	1.6411	10.6660	117	9.13
30	15.34	153	16.02	153	0.7359	2.1460	11.7902	117	10.09
30	15.34	115	12.04	205	0.9860	2.8754	11.8738	117	10.17
30	15.34	96	10.05	224	1.0774	3.1419	10.8307	117	9.27
30	15.34	71	7.44	274	1.3178	3.8432	9.7982	117	8.39
35	17.90	292	30.58	0	0.0000	0.0000	0.0000	185	0.00
35	17.90	236	24.71	75	0.6066	1.7691	14.9916	185	8.08
35	17.90	206	21.57	110	0.8897	2.5946	19.1927	185	10.35
35	17.90	158	16.55	157	1.2698	3.7032	21.0103	185	11.33
35	17.90	118	12.36	184	1.4882	4.3401	18.3897	185	9.91
35	17.90	97	10.16	215	1.7389	5.0713	17.6639	185	9.52
35	17.90	64	6.70	243	1.9654	5.7317	13.1723	185	7.10
40	20.46	316	33.09	0	0.0000	0.0000	0.0000	277	0.00
40	20.46	290	30.37	65	0.5257	1.5332	15.9657	277	5.77
40	20.46	230	24.09	136	1.1000	3.2079	26.4937	277	9.57
40	20.46	191	20.00	177	1.4316	4.1750	28.6340	277	10.34

40	20.46	137	14.35	244	1.9735	5.7553	28.3130	277	10.23
40	20.46	120	12.57	272	2.2000	6.4158	27.6456	277	9.99
40	20.46	75	7.85	332	2.6853	7.8310	21.0899	277	7.62
45	23.01	370	38.75	0	0.0000	0.0000	0.0000	394	0.00
45	23.01	315	32.99	97	0.7845	2.2880	25.8796	394	6.57
45	23.01	265	27.75	151	1.2213	3.5617	33.8921	394	8.60
45	23.01	220	23.04	211	1.7066	4.9769	39.3171	394	9.97
45	23.01	155	16.23	308	2.4911	7.2649	40.4351	394	10.26
45	23.01	123	12.88	352	2.8470	8.3028	36.6711	394	9.30
45	23.01	107	11.21	385	3.1139	9.0811	34.8916	394	8.85

NACA-0022 2 Bladed Turbine with 41% Solidity Trial 2									
F (Hz)	**U (m/s)**	**ω (rpm)**	**ω (rad/s)**	**Strain**	**T(N*m)**	**Tan Force (N)**	**P(W)**	**PA (W)**	**Eff(%)**
15	7.65	103	10.79	0	0.0000	0.0000	0.0000	14	0.00
15	7.65	83	8.69	16	0.0770	0.2244	0.6689	14	4.82
15	7.65	47	4.92	47	0.2261	0.6592	1.1126	14	8.02
15	7.65	36	3.77	55	0.2645	0.7714	0.9973	14	7.18
20	10.59	147	15.39	0	0.0000	0.0000	0.0000	39	0.00
20	10.59	117	12.25	35	0.1683	0.4909	2.0625	39	5.25
20	10.59	87	9.11	75	0.3607	1.0520	3.2864	39	8.37
20	10.59	49	5.13	113	0.5435	1.5850	2.7888	39	7.10
20	10.59	34	3.56	125	0.6012	1.7533	2.1406	39	5.45
20	10.59	22	2.30	135	0.6493	1.8936	1.4959	39	3.81
25	12.79	196	20.53	0	0.0000	0.0000	0.0000	68	0.00
25	12.79	177	18.54	28	0.1347	0.3927	2.4961	68	3.69
25	12.79	170	17.80	35	0.1683	0.4909	2.9968	68	4.43
25	12.79	132	13.82	102	0.4906	1.4307	6.7813	68	10.03
25	12.79	98	10.26	137	0.6589	1.9216	6.7622	68	10.00
25	12.79	49	5.13	183	0.8802	2.5668	4.5163	68	6.68
25	12.79	39	4.08	194	0.9331	2.7211	3.8107	68	5.64
30	15.34	241	25.24	0	0.0000	0.0000	0.0000	117	0.00
30	15.34	184	19.27	107	0.5146	1.5008	9.9161	117	8.49
30	15.34	167	17.49	136	0.6541	1.9076	11.4392	117	9.79
30	15.34	140	14.66	168	0.8080	2.3564	11.8461	117	10.14
30	15.34	103	10.79	207	0.9956	2.9034	10.7386	117	9.19
30	15.34	80	8.38	254	1.2216	3.5627	10.2344	117	8.76
30	15.34	45	4.71	329	1.5824	4.6147	7.4567	117	6.38
35	17.90	288	30.16	0	0.0000	0.0000	0.0000	185	0.00
35	17.90	250	26.18	55	0.4448	1.2973	11.6460	185	6.28
35	17.90	226	23.67	92	0.7441	2.1700	17.6105	185	9.49
35	17.90	161	16.86	154	1.2456	3.6325	21.0002	185	11.32

35	17.90	103	10.79	202	1.6338	4.7647	17.6224	185	9.50
35	17.90	85	8.90	227	1.8360	5.3543	16.3426	185	8.81
35	17.90	51	5.34	252	2.0382	5.9440	10.8855	185	5.87
40	20.46	314	32.88	0	0.0000	0.0000	0.0000	277	0.00
40	20.46	273	28.59	88	0.7118	2.0757	20.3480	277	7.35
40	20.46	234	24.50	134	1.0838	3.1607	26.5581	277	9.59
40	20.46	177	18.54	191	1.5448	4.5052	28.6340	277	10.34
40	20.46	114	11.94	280	2.2647	6.6045	27.0358	277	9.77
40	20.46	98	10.26	310	2.5073	7.3121	25.7314	277	9.29
40	20.46	53	5.55	353	2.8551	8.3264	15.8462	277	5.72
45	23.01	372	38.96	0	0.0000	0.0000	0.0000	394	0.00
45	23.01	330	34.56	64	0.5176	1.5096	17.8883	394	4.54
45	23.01	260	27.23	162	1.3103	3.8212	35.6750	394	9.05
45	23.01	198	20.73	245	1.9816	5.7789	41.0873	394	10.42
45	23.01	149	15.60	320	2.5882	7.5480	40.3843	394	10.24
45	23.01	127	13.30	368	2.9764	8.6802	39.5847	394	10.04
45	23.01	94	9.84	400	3.2352	9.4350	31.8466	394	8.08

NACA-0022 2 Bladed Turbine with 41% Solidity Trial 3									
F (Hz)	**U (m/s)**	**ω (rpm)**	**ω (rad/s)**	**Strain**	**T(N*m)**	**Tan Force (N)**	**P(W)**	**PA (W)**	**Eff(%)**
15	7.65	101	10.58	0	0.0000	0.0000	0.0000	14	0.00
15	7.65	83	8.69	15	0.0721	0.2104	0.6271	14	4.52
15	7.65	49	5.13	48	0.2309	0.6733	1.1846	14	8.53
15	7.65	17	1.78	65	0.3126	0.9117	0.5565	14	4.01
20	10.59	152	15.92	0	0.0000	0.0000	0.0000	39	0.00
20	10.59	128	13.40	22	0.1058	0.3086	1.4183	39	3.61
20	10.59	102	10.68	63	0.3030	0.8837	3.2365	39	8.24
20	10.59	82	8.59	84	0.4040	1.1782	3.4692	39	8.84
20	10.59	45	4.71	117	0.5627	1.6411	2.6518	39	6.75
20	10.59	14	1.47	140	0.6733	1.9637	0.9872	39	2.51
25	12.79	197	20.63	0	0.0000	0.0000	0.0000	68	0.00
25	12.79	157	16.44	60	0.2886	0.8416	4.7445	68	7.02
25	12.79	134	14.03	92	0.4425	1.2904	6.2091	68	9.19
25	12.79	127	13.30	105	0.5050	1.4728	6.7163	68	9.94
25	12.79	81	8.48	154	0.7407	2.1601	6.2827	68	9.29
25	12.79	55	5.76	172	0.8273	2.4125	4.7646	68	7.05
25	12.79	33	3.46	196	0.9427	2.7492	3.2577	68	4.82
30	15.34	245	25.66	0	0.0000	0.0000	0.0000	117	0.00
30	15.34	220	23.04	46	0.2212	0.6452	5.0971	117	4.36
30	15.34	212	22.20	69	0.3319	0.9678	7.3676	117	6.31
30	15.34	198	20.73	92	0.4425	1.2904	9.1747	117	7.86

30	15.34	174	18.22	134	0.6445	1.8795	11.7434	117	10.05
30	15.34	124	12.99	184	0.8850	2.5808	11.4916	117	9.84
30	15.34	61	6.39	290	1.3948	4.0676	8.9098	117	7.63
35	17.90	279	29.22	0	0.0000	0.0000	0.0000	185	0.00
35	17.90	237	24.82	78	0.6309	1.8398	15.6574	185	8.44
35	17.90	208	21.78	106	0.8573	2.5003	18.6743	185	10.07
35	17.90	167	17.49	143	1.1566	3.3730	20.2269	185	10.91
35	17.90	87	9.11	214	1.7309	5.0477	15.7692	185	8.50
35	17.90	51	5.34	252	2.0382	5.9440	10.8855	185	5.87
35	17.90	37	3.87	267	2.1595	6.2978	8.3674	185	4.51
40	20.46	332	34.77	0	0.0000	0.0000	0.0000	277	0.00
40	20.46	279	29.22	95	0.7684	2.2408	22.4493	277	8.11
40	20.46	250	26.18	126	1.0191	2.9720	26.6800	277	9.64
40	20.46	198	20.73	182	1.4720	4.2929	30.5220	277	11.02
40	20.46	161	16.86	217	1.7551	5.1185	29.5911	277	10.69
40	20.46	135	14.14	252	2.0382	5.9440	28.8144	277	10.41
40	20.46	106	11.10	300	2.4264	7.0762	26.9341	277	9.73
45	23.01	369	38.64	0	0.0000	0.0000	0.0000	394	0.00
45	23.01	340	35.60	47	0.3801	1.1086	13.5348	394	3.43
45	23.01	300	31.42	114	0.9220	2.6890	28.9669	394	7.35
45	23.01	223	23.35	214	1.7309	5.0477	40.4198	394	10.25
45	23.01	177	18.54	274	2.2161	6.4629	41.0771	394	10.42
45	23.01	122	12.78	375	3.0330	8.8453	38.7496	394	9.83
45	23.01	67	7.02	425	3.4375	10.0246	24.1179	394	6.12

APPENDIX B

RAW DATA DRAG TABLES

NACA-65-018 3 Bladed Turbine with 48% Solidity

F (Hz)	U (m/s)	Strain Gage (AVG)	Strain Gage Blade Only	Drag (kg)	Drag Force (N)
15	8.25	110.5	80	0.13	1.29
20	10.58	213	157.5	0.26	2.53
25	13.27	360.5	271.5	0.45	4.37
30	15.92	517.5	391.5	0.64	6.30
35	18.57	702	526	0.86	8.46
40	21.23	913.5	682.5	1.12	10.98
45	23.88	1103	803	1.32	12.92

NACA-0020 3 Bladed Turbine with 48% Solidity					
F (Hz)	U (m/s)	Strain Gage (AVG)	Strain Gage Blade Only	Drag (kg)	Drag Force (N)
15	8.25	114.5	84	0.14	1.35
20	10.58	225	169.5	0.28	2.73
25	13.27	340	251	0.41	4.04
30	15.92	504.5	378.5	0.62	6.09
35	18.57	676.5	500.5	0.82	8.05
40	21.23	912	681	1.12	10.96
45	23.88	1122	822	1.35	13.23

NACA-0022 3 Bladed Turbine with 48% Solidity					
F (Hz)	U (m/s)	Strain Gage (AVG)	Strain Gage Blade Only	Drag (kg)	Drag Force (N)
15	8.25	117	86.5	0.14	1.39
20	10.58	219.5	164	0.27	2.64
25	13.27	357.5	268.5	0.44	4.32
30	15.92	529	403	0.66	6.49
35	18.57	702	526	0.86	8.46
40	21.23	888.5	657.5	1.08	10.58
45	23.88	1078	778	1.28	12.52

NACA-0022 6 Bladed Turbine with 48% Solidity					
F (Hz)	U (m/s)	Strain Gage (AVG)	Strain Gage Blade Only	Drag (kg)	Drag Force (N)
15	8.25	97	66.5	0.11	1.07
20	10.58	189.5	134	0.22	2.16
25	13.27	313	224	0.37	3.60
30	15.92	467	341	0.56	5.49
35	18.57	645.5	469.5	0.77	7.56
40	21.23	844	613	1.01	9.86
45	23.88	1052	752	1.23	12.10

NACA-0022 3 Bladed Turbine with 41% Solidity					
F (Hz)	**U (m/s)**	**Strain Gage (AVG)**	**Strain Gage Blade Only**	**Drag (kg)**	**Drag Force (N)**
15	8.25	94.5	64	0.10	1.03
20	10.58	175.5	120	0.20	1.93
25	13.27	287.5	198.5	0.33	3.19
30	15.92	419	293	0.48	4.72
35	18.57	561.5	385.5	0.63	6.20
40	21.23	737	506	0.83	8.14
45	23.88	906.5	606.5	0.99	9.76

NACA-0022 3 Bladed Turbine with 55% Solidity					
F (Hz)	**U (m/s)**	**Strain Gage (AVG)**	**Strain Gage Blade Only**	**Drag (kg)**	**Drag Force (N)**
15	8.10	143.5	113	0.19	1.82
20	11.02	279.5	224	0.37	3.60
25	13.57	435.5	346.5	0.57	5.58
30	16.28	594	468	0.77	7.53
35	19.00	807.5	631.5	1.04	10.16
40	21.71	1031	800	1.31	12.87
45	24.42	1249	949	1.56	15.27

NACA-0022 2 Bladed Turbine with 41% Solidity					
F (Hz)	**U (m/s)**	**Strain Gage (AVG)**	**Strain Gage Blade Only**	**Drag (kg)**	**Drag Force (N)**
15	7.65	101.5	71	0.12	1.14
20	10.59	192	136.5	0.22	2.20
25	12.79	295	206	0.34	3.32
30	15.34	448.5	322.5	0.53	5.19
35	17.90	604.5	428.5	0.70	6.90
40	20.46	813.5	582.5	0.96	9.37
45	23.01	1016	716	1.17	11.52

APPENDIX C

SCALED TORQUE/POWER TABLES

NACA 65-018 3 Bladed Turbine with 48% Solidity												
ω_m (rad/s)	ω_p (rad/s)	V_m (m/s)	V_p (m/s)	Vel_m (ND)	Vel_p (ND)	Re	T_m (Nm)	T_p (Nm)	P_m (W)	P_p (W)	PA (W)	Eff (%)
10.16	0.15	8.48	0.29	3.29	3.29	1E+5	0.00	0.00	0.00	0.00	4.56	0.00
6.28	0.09	8.48	0.29	5.31	5.31	1E+5	0.07	1.16	0.45	0.10	4.56	2.29
3.56	0.05	8.48	0.29	9.38	9.38	1E+5	0.13	2.09	0.46	0.11	4.56	2.33
1.47	0.02	8.48	0.29	22.77	22.77	1E+5	0.18	2.87	0.26	0.06	4.56	1.32
16.23	0.23	11.89	0.41	2.88	2.88	2E+5	0.00	0.00	0.00	0.00	12.57	0.00
10.68	0.15	11.89	0.41	4.38	4.38	2E+5	0.12	1.94	1.28	0.30	12.57	2.35
8.48	0.12	11.89	0.41	5.52	5.52	2E+5	0.17	2.79	1.47	0.34	12.57	2.69
7.12	0.10	11.89	0.41	6.57	6.57	2E+5	0.23	3.64	1.61	0.37	12.57	2.95
4.29	0.06	11.89	0.41	10.90	10.90	2E+5	0.29	4.65	1.24	0.29	12.57	2.27
3.04	0.04	11.89	0.41	15.41	15.41	2E+5	0.33	5.27	0.99	0.23	12.57	1.82
20.94	0.30	15.59	0.53	2.93	2.93	2E+5	0.00	0.00	0.00	0.00	28.33	0.00
18.64	0.27	15.59	0.53	3.29	3.29	2E+5	0.08	1.32	1.52	0.35	28.33	1.24
14.97	0.21	15.59	0.53	4.10	4.10	2E+5	0.21	3.33	3.10	0.71	28.33	2.52
9.32	0.13	15.59	0.53	6.59	6.59	2E+5	0.41	6.59	3.81	0.88	28.33	3.10
6.60	0.09	15.59	0.53	9.30	9.30	2E+5	0.50	8.06	3.30	0.76	28.33	2.68
4.61	0.07	15.59	0.53	13.32	13.32	2E+5	0.58	9.30	2.66	0.61	28.33	2.16
2.93	0.04	15.59	0.53	20.93	20.93	2E+5	0.64	10.31	1.88	0.43	28.33	1.52
26.28	0.38	17.93	0.61	2.69	2.69	3E+5	0.00	0.00	0.00	0.00	43.12	0.00
23.88	0.34	17.93	0.61	2.96	2.96	3E+5	0.07	1.16	1.72	0.40	43.12	0.92
20.53	0.29	17.93	0.61	3.44	3.44	3E+5	0.22	3.57	4.54	1.05	43.12	2.42
15.60	0.22	17.93	0.61	4.52	4.52	3E+5	0.41	6.67	6.45	1.49	43.12	3.45
11.31	0.16	17.93	0.61	6.24	6.24	3E+5	0.58	9.38	6.58	1.52	43.12	3.51
6.18	0.09	17.93	0.61	11.43	11.43	3E+5	0.76	12.33	4.72	1.09	43.12	2.52
3.67	0.05	17.93	0.61	19.26	19.26	3E+5	0.88	14.27	3.24	0.75	43.12	1.73
30.89	0.44	20.92	0.72	2.67	2.67	3E+5	0.00	0.00	0.00	0.00	68.48	0.00
25.34	0.36	20.92	0.72	3.25	3.25	3E+5	0.22	3.57	5.61	1.29	68.48	1.88
22.10	0.32	20.92	0.72	3.73	3.73	3E+5	0.36	5.81	7.97	1.83	68.48	2.68
18.43	0.26	20.92	0.72	4.47	4.47	3E+5	0.57	9.15	10.46	2.41	68.48	3.52
12.99	0.19	20.92	0.72	6.34	6.34	3E+5	0.78	12.56	10.12	2.33	68.48	3.40
10.16	0.15	20.92	0.72	8.11	8.11	3E+5	0.93	14.96	9.43	2.17	68.48	3.17
6.91	0.10	20.92	0.72	11.92	11.92	3E+5	1.06	17.06	7.31	1.68	68.48	2.46
34.56	0.49	23.91	0.82	2.72	2.72	4E+5	0.00	0.00	0.00	0.00	102.21	0.00
29.95	0.43	23.91	0.82	3.14	3.14	4E+5	0.28	4.50	8.35	1.92	102.21	1.88
26.49	0.38	23.91	0.82	3.55	3.55	4E+5	0.46	7.37	12.11	2.79	102.21	2.73
24.40	0.35	23.91	0.82	3.86	3.86	4E+5	0.61	9.85	14.90	3.43	102.21	3.36
16.02	0.23	23.91	0.82	5.87	5.87	4E+5	0.98	15.82	15.72	3.62	102.21	3.54
11.52	0.16	23.91	0.82	8.17	8.17	4E+5	1.20	19.38	13.85	3.19	102.21	3.12
4.92	0.07	23.91	0.82	19.12	19.12	4E+5	1.46	23.49	7.17	1.65	102.21	1.62
38.75	0.55	26.90	0.92	2.73	2.73	4E+5	0.00	0.00	0.00	0.00	145.54	0.00

34.77	0.50	26.90	0.92	3.05	3.05	4E+5	0.35	5.66	12.21	2.81	145.54	1.93
27.12	0.39	26.90	0.92	3.90	3.90	4E+5	0.78	12.64	21.26	4.89	145.54	3.36
20.84	0.30	26.90	0.92	5.08	5.08	4E+5	1.08	17.37	22.45	5.17	145.54	3.55
15.60	0.22	26.90	0.92	6.79	6.79	4E+5	1.37	22.02	21.31	4.91	145.54	3.37
11.00	0.16	26.90	0.92	9.63	9.63	4E+5	1.60	25.82	17.61	4.05	145.54	2.79
5.97	0.09	26.90	0.92	17.74	17.74	4E+5	1.86	29.93	11.08	2.55	145.54	1.75
10.37	0.15	8.48	0.29	3.22	3.22	1E+5	0.00	0.00	0.00	0.00	4.56	0.00
6.28	0.09	8.48	0.29	5.31	5.31	1E+5	0.05	0.78	0.30	0.07	4.56	1.53
5.65	0.08	8.48	0.29	5.90	5.90	1E+5	0.08	1.24	0.44	0.10	4.56	2.20
4.19	0.06	8.48	0.29	7.97	7.97	1E+5	0.16	2.64	0.68	0.16	4.56	3.46
15.39	0.22	11.89	0.41	3.04	3.04	2E+5	0.00	0.00	0.00	0.00	12.57	0.00
11.00	0.16	11.89	0.41	4.26	4.26	2E+5	0.08	1.24	0.85	0.19	12.57	1.55
8.48	0.12	11.89	0.41	5.52	5.52	2E+5	0.14	2.33	1.22	0.28	12.57	2.24
7.12	0.10	11.89	0.41	6.57	6.57	2E+5	0.21	3.33	1.47	0.34	12.57	2.70
5.24	0.07	11.89	0.41	8.94	8.94	2E+5	0.27	4.34	1.41	0.32	12.57	2.58
1.88	0.03	11.89	0.41	24.83	24.83	2E+5	0.37	5.97	0.70	0.16	12.57	1.28
20.53	0.29	15.59	0.53	2.99	2.99	2E+5	0.00	0.00	0.00	0.00	28.33	0.00
15.81	0.23	15.59	0.53	3.88	3.88	2E+5	0.10	1.55	1.52	0.35	28.33	1.24
14.14	0.20	15.59	0.53	4.34	4.34	2E+5	0.15	2.48	2.18	0.50	28.33	1.77
12.67	0.18	15.59	0.53	4.84	4.84	2E+5	0.21	3.41	2.68	0.62	28.33	2.18
11.52	0.16	15.59	0.53	5.33	5.33	2E+5	0.32	5.19	3.71	0.85	28.33	3.02
8.59	0.12	15.59	0.53	7.15	7.15	2E+5	0.38	6.12	3.26	0.75	28.33	2.65
6.60	0.09	15.59	0.53	9.30	9.30	2E+5	0.45	7.21	2.95	0.68	28.33	2.40
25.76	0.37	17.93	0.61	2.74	2.74	3E+5	0.00	0.00	0.00	0.00	43.12	0.00
20.11	0.29	17.93	0.61	3.51	3.51	3E+5	0.14	2.33	2.90	0.67	43.12	1.55
18.54	0.26	17.93	0.61	3.81	3.81	3E+5	0.22	3.49	4.01	0.92	43.12	2.14
16.76	0.24	17.93	0.61	4.21	4.21	3E+5	0.32	5.19	5.40	1.24	43.12	2.88
13.61	0.19	17.93	0.61	5.19	5.19	3E+5	0.48	7.68	6.48	1.49	43.12	3.46
9.32	0.13	17.93	0.61	7.57	7.57	3E+5	0.62	10.00	5.78	1.33	43.12	3.09
6.28	0.09	17.93	0.61	11.24	11.24	3E+5	0.73	11.78	4.59	1.06	43.12	2.45
30.89	0.44	20.92	0.72	2.67	2.67	3E+5	0.00	0.00	0.00	0.00	68.48	0.00
25.34	0.36	20.92	0.72	3.25	3.25	3E+5	0.20	3.26	5.12	1.18	68.48	1.72
22.10	0.32	20.92	0.72	3.73	3.73	3E+5	0.40	6.43	8.82	2.03	68.48	2.97
17.49	0.25	20.92	0.72	4.71	4.71	3E+5	0.60	9.69	10.51	2.42	68.48	3.53
12.15	0.17	20.92	0.72	6.78	6.78	3E+5	0.82	13.26	9.99	2.30	68.48	3.36
9.22	0.13	20.92	0.72	8.94	8.94	3E+5	0.94	15.12	8.64	1.99	68.48	2.91
6.60	0.09	20.92	0.72	12.48	12.48	3E+5	1.06	17.06	6.98	1.61	68.48	2.35
36.23	0.52	23.91	0.82	2.60	2.60	4E+5	0.00	0.00	0.00	0.00	102.21	0.00
28.69	0.41	23.91	0.82	3.28	3.28	4E+5	0.34	5.43	9.66	2.22	102.21	2.18
24.71	0.35	23.91	0.82	3.81	3.81	4E+5	0.56	8.99	13.79	3.17	102.21	3.11
19.27	0.28	23.91	0.82	4.89	4.89	4E+5	0.85	13.72	16.40	3.78	102.21	3.69

14.66	0.21	23.91	0.82	6.42	6.42	4E+5	1.07	17.29	15.72	3.62	102.21	3.54
12.25	0.17	23.91	0.82	7.68	7.68	4E+5	1.16	18.76	14.26	3.28	102.21	3.21
7.64	0.11	23.91	0.82	12.31	12.31	4E+5	1.37	22.10	10.48	2.41	102.21	2.36
41.26	0.59	26.90	0.92	2.57	2.57	4E+5	0.00	0.00	0.00	0.00	145.54	0.00
32.04	0.46	26.90	0.92	3.30	3.30	4E+5	0.50	7.99	15.87	3.65	145.54	2.51
25.66	0.37	26.90	0.92	4.13	4.13	4E+5	0.92	14.89	23.69	5.45	145.54	3.75
17.49	0.25	26.90	0.92	6.06	6.06	4E+5	1.27	20.47	22.21	5.11	145.54	3.51
13.82	0.20	26.90	0.92	7.66	7.66	4E+5	1.46	23.57	20.21	4.65	145.54	3.20
10.79	0.15	26.90	0.92	9.82	9.82	4E+5	1.61	25.89	17.33	3.99	145.54	2.74
8.06	0.12	26.90	0.92	13.13	13.13	4E+5	1.88	30.24	15.12	3.48	145.54	2.39
9.84	0.14	8.48	0.29	3.39	3.39	1E+5	0.00	0.00	0.00	0.00	4.56	0.00
6.28	0.09	8.48	0.29	5.31	5.31	1E+5	0.05	0.85	0.33	0.08	4.56	1.68
2.62	0.04	8.48	0.29	12.75	12.75	1E+5	0.17	2.79	0.45	0.10	4.56	2.29
1.26	0.02	8.48	0.29	26.57	26.57	1E+5	0.20	3.26	0.25	0.06	4.56	1.28
15.39	0.22	11.89	0.41	3.04	3.04	2E+5	0.00	0.00	0.00	0.00	12.57	0.00
11.00	0.16	11.89	0.41	4.26	4.26	2E+5	0.07	1.09	0.74	0.17	12.57	1.36
9.11	0.13	11.89	0.41	5.14	5.14	2E+5	0.13	2.17	1.23	0.28	12.57	2.25
7.54	0.11	11.89	0.41	6.21	6.21	2E+5	0.18	2.95	1.38	0.32	12.57	2.52
6.28	0.09	11.89	0.41	7.45	7.45	2E+5	0.20	3.26	1.27	0.29	12.57	2.32
4.19	0.06	11.89	0.41	11.17	11.17	2E+5	0.29	4.73	1.23	0.28	12.57	2.25
20.53	0.29	15.59	0.53	2.99	2.99	2E+5	0.00	0.00	0.00	0.00	28.33	0.00
14.97	0.21	15.59	0.53	4.10	4.10	2E+5	0.16	2.64	2.45	0.56	28.33	1.99
12.36	0.18	15.59	0.53	4.97	4.97	2E+5	0.18	2.87	2.20	0.51	28.33	1.79
11.00	0.16	15.59	0.53	5.58	5.58	2E+5	0.26	4.26	2.91	0.67	28.33	2.36
9.63	0.14	15.59	0.53	6.37	6.37	2E+5	0.31	5.04	3.01	0.69	28.33	2.45
8.27	0.12	15.59	0.53	7.42	7.42	2E+5	0.39	6.28	3.22	0.74	28.33	2.62
5.45	0.08	15.59	0.53	11.27	11.27	2E+5	0.46	7.44	2.51	0.58	28.33	2.04
25.87	0.37	17.93	0.61	2.73	2.73	3E+5	0.00	0.00	0.00	0.00	43.12	0.00
21.26	0.30	17.93	0.61	3.32	3.32	3E+5	0.15	2.40	3.17	0.73	43.12	1.69
16.65	0.24	17.93	0.61	4.24	4.24	3E+5	0.27	4.42	4.56	1.05	43.12	2.44
15.29	0.22	17.93	0.61	4.62	4.62	3E+5	0.30	4.81	4.56	1.05	43.12	2.43
14.56	0.21	17.93	0.61	4.85	4.85	3E+5	0.34	5.43	4.90	1.13	43.12	2.62
11.31	0.16	17.93	0.61	6.24	6.24	3E+5	0.47	7.60	5.33	1.23	43.12	2.85
5.76	0.08	17.93	0.61	12.26	12.26	3E+5	0.75	12.02	4.29	0.99	43.12	2.29
31.10	0.44	20.92	0.72	2.65	2.65	3E+5	0.00	0.00	0.00	0.00	68.48	0.00
23.46	0.34	20.92	0.72	3.51	3.51	3E+5	0.31	4.96	7.22	1.66	68.48	2.43
18.54	0.26	20.92	0.72	4.44	4.44	3E+5	0.53	8.53	9.81	2.26	68.48	3.30
16.44	0.23	20.92	0.72	5.01	5.01	3E+5	0.63	10.08	10.28	2.37	68.48	3.46
14.97	0.21	20.92	0.72	5.50	5.50	3E+5	0.70	11.32	10.52	2.42	68.48	3.54
7.64	0.11	20.92	0.72	10.77	10.77	3E+5	1.00	16.05	7.61	1.75	68.48	2.56
4.29	0.06	20.92	0.72	19.18	19.18	3E+5	1.12	17.99	4.79	1.10	68.48	1.61

35.81	0.51	23.91	0.82	2.63	2.63	4E+5	0.00	0.00	0.00	0.00	102.21	0.00
30.05	0.43	23.91	0.82	3.13	3.13	4E+5	0.31	5.04	9.40	2.16	102.21	2.12
28.48	0.41	23.91	0.82	3.30	3.30	4E+5	0.38	6.05	10.69	2.46	102.21	2.41
21.36	0.31	23.91	0.82	4.41	4.41	4E+5	0.70	11.24	14.90	3.43	102.21	3.36
14.87	0.21	23.91	0.82	6.33	6.33	4E+5	1.01	16.28	15.02	3.46	102.21	3.38
9.01	0.13	23.91	0.82	10.45	10.45	4E+5	1.26	20.24	11.31	2.60	102.21	2.55
4.71	0.07	23.91	0.82	19.97	19.97	4E+5	1.44	23.26	6.80	1.57	102.21	1.53
40.21	0.57	26.90	0.92	2.63	2.63	4E+5	0.00	0.00	0.00	0.00	145.54	0.00
32.04	0.46	26.90	0.92	3.30	3.30	4E+5	0.48	7.68	15.26	3.51	145.54	2.41
22.41	0.32	26.90	0.92	4.73	4.73	4E+5	1.06	17.06	23.71	5.46	145.54	3.75
16.76	0.24	26.90	0.92	6.32	6.32	4E+5	1.32	21.24	22.08	5.08	145.54	3.49
12.78	0.18	26.90	0.92	8.29	8.29	4E+5	1.45	23.41	18.56	4.27	145.54	2.94
6.91	0.10	26.90	0.92	15.32	15.32	4E+5	1.85	29.85	12.80	2.95	145.54	2.02
6.18	0.09	26.90	0.92	17.14	17.14	4E+5	1.96	31.63	12.12	2.79	145.54	1.92

NACA 0020 3 Bladed Turbine with 48% Solidity												
ω_m (rad/s)	**ω_p (rad/s)**	**V_m (m/s)**	**V_p (m/s)**	**Vel_m (ND)**	**Vel_p (ND)**	**Re**	**T_m (Nm)**	**T_p (Nm)**	**P_m (W)**	**P_p (W)**	**PA (W)**	**Eff (%)**
15.71	0.22	8.63	0.30	2.16	2.16	1E+5	0.00	0.00	0.00	0.00	4.81	0.00
9.84	0.14	8.63	0.30	3.45	3.45	1E+5	0.09	1.48	0.90	0.21	4.81	4.31
6.07	0.09	8.63	0.30	5.60	5.60	1E+5	0.17	2.72	1.02	0.24	4.81	4.90
4.08	0.06	8.63	0.30	8.32	8.32	1E+5	0.25	3.96	1.00	0.23	4.81	4.80
23.14	0.33	11.80	0.40	2.01	2.01	2E+5	0.00	0.00	0.00	0.00	12.28	0.00
18.22	0.26	11.80	0.40	2.55	2.55	2E+5	0.11	1.79	2.02	0.46	12.28	3.79
11.21	0.16	11.80	0.40	4.14	4.14	2E+5	0.27	4.43	3.07	0.71	12.28	5.77
7.64	0.11	11.80	0.40	6.08	6.08	2E+5	0.41	6.60	3.13	0.72	12.28	5.87
5.86	0.08	11.80	0.40	7.92	7.92	2E+5	0.53	8.62	3.13	0.72	12.28	5.88
1.78	0.03	11.80	0.40	26.09	26.09	2E+5	0.66	10.64	1.17	0.27	12.28	2.20
31.31	0.45	15.76	0.54	1.98	1.98	3E+5	0.00	0.00	0.00	0.00	29.29	0.00
26.91	0.38	15.76	0.54	2.31	2.31	3E+5	0.15	2.49	4.14	0.96	29.29	3.26
24.92	0.36	15.76	0.54	2.49	2.49	3E+5	0.22	3.50	5.39	1.24	29.29	4.25
18.85	0.27	15.76	0.54	3.29	3.29	3E+5	0.40	6.45	7.52	1.74	29.29	5.92
14.56	0.21	15.76	0.54	4.26	4.26	3E+5	0.65	10.49	9.45	2.18	29.29	7.44
11.10	0.16	15.76	0.54	5.59	5.59	3E+5	0.74	11.89	8.17	1.88	29.29	6.43
5.45	0.08	15.76	0.54	11.40	11.40	3E+5	0.83	13.36	4.50	1.04	29.29	3.55
39.48	0.56	17.98	0.62	1.79	1.79	3E+5	0.00	0.00	0.00	0.00	43.51	0.00
33.51	0.48	17.98	0.62	2.11	2.11	3E+5	0.24	3.81	7.90	1.82	43.51	4.19
31.10	0.44	17.98	0.62	2.28	2.28	3E+5	0.40	6.53	12.57	2.90	43.51	6.66
23.46	0.34	17.98	0.62	3.02	3.02	3E+5	0.70	11.34	16.47	3.80	43.51	8.73
20.00	0.29	17.98	0.62	3.54	3.54	3E+5	0.77	12.43	15.39	3.55	43.51	8.16
13.93	0.20	17.98	0.62	5.08	5.08	3E+5	0.97	15.69	13.53	3.12	43.51	7.17

5.45	0.08	17.98	0.62	13.00	13.00	3E+5	1.27	20.51	6.91	1.59	43.51	3.67
47.44	0.68	20.98	0.72	1.74	1.74	3E+5	0.00	0.00	0.00	0.00	69.09	0.00
44.51	0.64	20.98	0.72	1.86	1.86	3E+5	0.11	1.79	4.92	1.14	69.09	1.64
40.00	0.57	20.98	0.72	2.07	2.07	3E+5	0.37	5.98	14.81	3.42	69.09	4.95
30.16	0.43	20.98	0.72	2.74	2.74	3E+5	0.89	14.45	26.98	6.22	69.09	9.01
21.78	0.31	20.98	0.72	3.79	3.79	3E+5	1.14	18.33	24.72	5.70	69.09	8.25
12.88	0.18	20.98	0.72	6.41	6.41	3E+5	1.42	22.92	18.28	4.22	69.09	6.10
9.01	0.13	20.98	0.72	9.17	9.17	3E+5	1.65	26.72	14.90	3.44	69.09	4.97
53.93	0.77	23.98	0.82	1.75	1.75	4E+5	0.00	0.00	0.00	0.00	103.13	0.00
42.41	0.61	23.98	0.82	2.23	2.23	4E+5	0.59	9.56	25.09	5.79	103.13	5.61
41.05	0.59	23.98	0.82	2.30	2.30	4E+5	0.83	13.36	33.96	7.83	103.13	7.60
37.70	0.54	23.98	0.82	2.50	2.50	4E+5	0.96	15.54	36.26	8.36	103.13	8.11
29.32	0.42	23.98	0.82	3.22	3.22	4E+5	1.27	20.59	37.37	8.62	103.13	8.36
22.51	0.32	23.98	0.82	4.19	4.19	4E+5	1.61	25.95	36.17	8.34	103.13	8.09
18.33	0.26	23.98	0.82	5.15	5.15	4E+5	2.07	33.40	37.90	8.74	103.13	8.48
57.81	0.83	26.98	0.92	1.84	1.84	4E+5	0.00	0.00	0.00	0.00	146.85	0.00
50.27	0.72	26.98	0.92	2.11	2.11	4E+5	0.62	10.06	31.30	7.22	146.85	4.92
41.99	0.60	26.98	0.92	2.53	2.53	4E+5	1.33	21.56	56.04	12.93	146.85	8.80
27.12	0.39	26.98	0.92	3.92	3.92	4E+5	1.91	30.83	51.77	11.94	146.85	8.13
18.85	0.27	26.98	0.92	5.63	5.63	4E+5	2.51	40.50	47.26	10.90	146.85	7.42
12.99	0.19	26.98	0.92	8.18	8.18	4E+5	2.91	47.03	37.81	8.72	146.85	5.94
7.23	0.10	26.98	0.92	14.70	14.70	4E+5	3.70	59.83	26.77	6.17	146.85	4.20
15.18	0.22	8.63	0.30	2.24	2.24	1E+5	0.00	0.00	0.00	0.00	4.81	0.00
9.63	0.14	8.63	0.30	3.53	3.53	1E+5	0.07	1.17	0.70	0.16	4.81	3.33
6.28	0.09	8.63	0.30	5.41	5.41	1E+5	0.15	2.49	0.97	0.22	4.81	4.63
3.46	0.05	8.63	0.30	9.84	9.84	1E+5	0.27	4.43	0.95	0.22	4.81	4.54
22.72	0.32	11.80	0.40	2.04	2.04	2E+5	0.00	0.00	0.00	0.00	12.28	0.00
18.33	0.26	11.80	0.40	2.53	2.53	2E+5	0.12	1.94	2.20	0.51	12.28	4.14
9.74	0.14	11.80	0.40	4.77	4.77	2E+5	0.32	5.20	3.14	0.72	12.28	5.90
5.55	0.08	11.80	0.40	8.37	8.37	2E+5	0.49	7.92	2.72	0.63	12.28	5.12
2.62	0.04	11.80	0.40	17.74	17.74	2E+5	0.56	9.09	1.47	0.34	12.28	2.77
1.26	0.02	11.80	0.40	36.96	36.96	2E+5	0.69	11.19	0.87	0.20	12.28	1.64
30.47	0.44	15.76	0.54	2.04	2.04	3E+5	0.00	0.00	0.00	0.00	29.29	0.00
25.34	0.36	15.76	0.54	2.45	2.45	3E+5	0.25	4.12	6.46	1.49	29.29	5.09
20.94	0.30	15.76	0.54	2.96	2.96	3E+5	0.35	5.67	7.35	1.70	29.29	5.79
15.81	0.23	15.76	0.54	3.92	3.92	3E+5	0.54	8.70	8.52	1.96	29.29	6.71
10.68	0.15	15.76	0.54	5.81	5.81	3E+5	0.69	11.11	7.35	1.69	29.29	5.78
5.86	0.08	15.76	0.54	10.58	10.58	3E+5	0.81	13.05	4.74	1.09	29.29	3.73
3.98	0.06	15.76	0.54	15.60	15.60	3E+5	0.88	14.14	3.48	0.80	29.29	2.74
39.58	0.57	17.98	0.62	1.79	1.79	3E+5	0.00	0.00	0.00	0.00	43.51	0.00
33.93	0.48	17.98	0.62	2.09	2.09	3E+5	0.21	3.42	7.18	1.66	43.51	3.81

31.73	0.45	17.98	0.62	2.23	2.23	3E+5	0.31	5.05	9.92	2.29	43.51	5.26
21.26	0.30	17.98	0.62	3.33	3.33	3E+5	0.72	11.65	15.34	3.54	43.51	8.13
18.74	0.27	17.98	0.62	3.78	3.78	3E+5	0.86	13.91	16.14	3.72	43.51	8.56
13.82	0.20	17.98	0.62	5.12	5.12	3E+5	1.00	16.08	13.76	3.17	43.51	7.30
4.92	0.07	17.98	0.62	14.39	14.39	3E+5	1.27	20.59	6.27	1.45	43.51	3.33
47.54	0.68	20.98	0.72	1.74	1.74	3E+5	0.00	0.00	0.00	0.00	69.09	0.00
43.56	0.62	20.98	0.72	1.90	1.90	3E+5	0.14	2.33	6.29	1.45	69.09	2.10
35.60	0.51	20.98	0.72	2.32	2.32	3E+5	0.65	10.49	23.12	5.33	69.09	7.72
30.68	0.44	20.98	0.72	2.69	2.69	3E+5	0.86	13.83	26.27	6.06	69.09	8.77
21.15	0.30	20.98	0.72	3.91	3.91	3E+5	1.19	19.27	25.23	5.82	69.09	8.42
13.19	0.19	20.98	0.72	6.26	6.26	3E+5	1.42	22.99	18.78	4.33	69.09	6.27
5.34	0.08	20.98	0.72	15.47	15.47	3E+5	1.75	28.20	9.32	2.15	69.09	3.11
52.78	0.75	23.98	0.82	1.79	1.79	4E+5	0.00	0.00	0.00	0.00	103.13	0.00
49.11	0.70	23.98	0.82	1.92	1.92	4E+5	0.15	2.49	7.56	1.74	103.13	1.69
47.75	0.68	23.98	0.82	1.98	1.98	4E+5	0.29	4.66	13.78	3.18	103.13	3.08
44.19	0.63	23.98	0.82	2.14	2.14	4E+5	0.48	7.77	21.25	4.90	103.13	4.75
40.84	0.58	23.98	0.82	2.31	2.31	4E+5	0.77	12.43	31.43	7.25	103.13	7.03
32.46	0.46	23.98	0.82	2.91	2.91	4E+5	1.14	18.33	36.85	8.50	103.13	8.24
20.94	0.30	23.98	0.82	4.51	4.51	4E+5	1.72	27.73	35.96	8.30	103.13	8.04
60.53	0.86	26.98	0.92	1.75	1.75	4E+5	0.00	0.00	0.00	0.00	146.85	0.00
47.33	0.68	26.98	0.92	2.24	2.24	4E+5	1.01	16.33	47.85	11.04	146.85	7.52
35.19	0.50	26.98	0.92	3.02	3.02	4E+5	1.58	25.47	55.49	12.80	146.85	8.72
24.92	0.36	26.98	0.92	4.26	4.26	4E+5	2.14	34.62	53.42	12.32	146.85	8.39
20.42	0.29	26.98	0.92	5.20	5.20	4E+5	2.55	41.15	52.03	12.00	146.85	8.17
14.03	0.20	26.98	0.92	7.57	7.57	4E+5	2.93	47.29	41.09	9.48	146.85	6.45
9.32	0.13	26.98	0.92	11.40	11.40	4E+5	3.56	57.48	33.17	7.65	146.85	5.21
15.50	0.22	8.63	0.30	2.19	2.19	1E+5	0.00	0.00	0.00	0.00	4.81	0.00
9.32	0.13	8.63	0.30	3.65	3.65	1E+5	0.08	1.24	0.72	0.17	4.81	3.44
7.44	0.11	8.63	0.30	4.57	4.57	1E+5	0.15	2.49	1.14	0.26	4.81	5.48
1.88	0.03	8.63	0.30	18.03	18.03	1E+5	0.28	4.58	0.53	0.12	4.81	2.56
22.83	0.33	11.80	0.40	2.03	2.03	2E+5	0.00	0.00	0.00	0.00	12.28	0.00
20.11	0.29	11.80	0.40	2.31	2.31	2E+5	0.07	1.09	1.35	0.31	12.28	2.54
9.53	0.14	11.80	0.40	4.87	4.87	2E+5	0.35	5.59	3.30	0.76	12.28	6.20
7.33	0.10	11.80	0.40	6.34	6.34	2E+5	0.41	6.68	3.03	0.70	12.28	5.70
6.18	0.09	11.80	0.40	7.52	7.52	2E+5	0.50	8.08	3.09	0.71	12.28	5.81
2.20	0.03	11.80	0.40	21.12	21.12	2E+5	0.63	10.10	1.37	0.32	12.28	2.58
30.58	0.44	15.76	0.54	2.03	2.03	3E+5	0.00	0.00	0.00	0.00	29.29	0.00
28.48	0.41	15.76	0.54	2.18	2.18	3E+5	0.09	1.48	2.60	0.60	29.29	2.05
26.18	0.37	15.76	0.54	2.37	2.37	3E+5	0.24	3.88	6.30	1.45	29.29	4.96
19.48	0.28	15.76	0.54	3.19	3.19	3E+5	0.44	7.15	8.62	1.99	29.29	6.79
12.57	0.18	15.76	0.54	4.94	4.94	3E+5	0.60	9.71	7.55	1.74	29.29	5.95

10.58	0.15	15.76	0.54	5.87	5.87	3E+5	0.73	11.73	7.68	1.77	29.29	6.05
6.49	0.09	15.76	0.54	9.56	9.56	3E+5	0.82	13.21	5.31	1.22	29.29	4.18
38.85	0.55	17.98	0.62	1.82	1.82	3E+5	0.00	0.00	0.00	0.00	43.51	0.00
35.92	0.51	17.98	0.62	1.97	1.97	3E+5	0.18	2.95	6.56	1.51	43.51	3.48
26.70	0.38	17.98	0.62	2.65	2.65	3E+5	0.60	9.71	16.05	3.70	43.51	8.51
17.59	0.25	17.98	0.62	4.02	4.02	3E+5	0.83	13.36	14.55	3.36	43.51	7.72
9.95	0.14	17.98	0.62	7.12	7.12	3E+5	1.11	17.87	11.01	2.54	43.51	5.83
5.13	0.07	17.98	0.62	13.80	13.80	3E+5	1.24	20.04	6.37	1.47	43.51	3.38
2.51	0.04	17.98	0.62	28.17	28.17	3E+5	1.34	21.67	3.37	0.78	43.51	1.79
46.70	0.67	20.98	0.72	1.77	1.77	3E+5	0.00	0.00	0.00	0.00	69.09	0.00
43.46	0.62	20.98	0.72	1.90	1.90	3E+5	0.14	2.33	6.27	1.45	69.09	2.09
39.90	0.57	20.98	0.72	2.07	2.07	3E+5	0.38	6.06	14.97	3.45	69.09	5.00
35.60	0.51	20.98	0.72	2.32	2.32	3E+5	0.57	9.24	20.38	4.70	69.09	6.80
23.25	0.33	20.98	0.72	3.55	3.55	3E+5	1.09	17.56	25.27	5.83	69.09	8.44
15.29	0.22	20.98	0.72	5.40	5.40	3E+5	1.35	21.75	20.59	4.75	69.09	6.87
8.59	0.12	20.98	0.72	9.62	9.62	3E+5	1.64	26.41	14.04	3.24	69.09	4.69
52.46	0.75	23.98	0.82	1.80	1.80	4E+5	0.00	0.00	0.00	0.00	103.13	0.00
42.41	0.61	23.98	0.82	2.23	2.23	4E+5	0.67	10.88	28.56	6.59	103.13	6.39
40.11	0.57	23.98	0.82	2.35	2.35	4E+5	0.84	13.59	33.76	7.79	103.13	7.55
35.71	0.51	23.98	0.82	2.64	2.64	4E+5	1.03	16.62	36.75	8.48	103.13	8.22
24.82	0.35	23.98	0.82	3.80	3.80	4E+5	1.39	22.53	34.62	7.98	103.13	7.74
17.59	0.25	23.98	0.82	5.37	5.37	4E+5	1.85	29.91	32.58	7.51	103.13	7.29
16.34	0.23	23.98	0.82	5.78	5.78	4E+5	2.04	33.02	33.39	7.70	103.13	7.47
61.37	0.88	26.98	0.92	1.73	1.73	4E+5	0.00	0.00	0.00	0.00	146.85	0.00
57.39	0.82	26.98	0.92	1.85	1.85	4E+5	0.34	5.49	19.49	4.50	146.85	3.06
50.58	0.72	26.98	0.92	2.10	2.10	4E+5	0.78	12.67	39.68	9.15	146.85	6.23
41.89	0.60	26.98	0.92	2.54	2.54	4E+5	1.39	22.47	58.27	13.44	146.85	9.15
33.93	0.48	26.98	0.92	3.13	3.13	4E+5	1.66	26.78	56.26	12.98	146.85	8.84
29.74	0.42	26.98	0.92	3.57	3.57	4E+5	1.80	29.00	53.40	12.32	146.85	8.39
22.31	0.32	26.98	0.92	4.76	4.76	4E+5	2.32	37.49	51.78	11.94	146.85	8.13

NACA-0022 3 Bladed Turbine with 48% Solidity												
ω_m (rad/s)	**ω_p (rad/s)**	**V_m (m/s)**	**V_p (m/s)**	**Vel_m (ND)**	**Vel_p (ND)**	**Re**	**T_m (Nm)**	**T_p (Nm)**	**P_m (W)**	**P_p (W)**	**PA (W)**	**Eff (%)**
14.45	0.21	9.47	0.32	2.58	2.58	2E+5	0.00	0.00	0.00	0.00	6.34	0.00
10.37	0.15	9.47	0.32	3.59	3.59	2E+5	0.06	0.98	0.65	0.15	6.34	2.30
8.17	0.12	9.47	0.32	4.56	4.56	2E+5	0.13	2.04	1.06	0.24	6.34	3.76
0.94	0.01	9.47	0.32	39.54	39.54	2E+5	0.30	4.69	0.28	0.06	6.34	1.00
22.20	0.32	13.30	0.46	2.36	2.36	2E+5	0.00	0.00	0.00	0.00	17.58	0.00
13.93	0.20	13.30	0.46	3.76	3.76	2E+5	0.17	2.65	2.34	0.53	17.58	3.00
11.52	0.16	13.30	0.46	4.54	4.54	2E+5	0.22	3.41	2.49	0.56	17.58	3.19

8.69	0.12	13.30	0.46	6.02	6.02	2E+5	0.27	4.32	2.38	0.54	17.58	3.05
7.54	0.11	13.30	0.46	6.94	6.94	2E+5	0.32	5.00	2.39	0.54	17.58	3.06
1.15	0.02	13.30	0.46	45.44	45.44	2E+5	0.45	7.12	0.52	0.12	17.58	0.67
29.22	0.42	16.07	0.55	2.17	2.17	3E+5	0.00	0.00	0.00	0.00	31.05	0.00
23.56	0.34	16.07	0.55	2.69	2.69	3E+5	0.20	3.10	4.65	1.04	31.05	3.36
20.84	0.30	16.07	0.55	3.04	3.04	3E+5	0.28	4.39	5.81	1.31	31.05	4.21
16.13	0.23	16.07	0.55	3.92	3.92	3E+5	0.41	6.44	6.59	1.48	31.05	4.77
9.42	0.13	16.07	0.55	6.71	6.71	3E+5	0.58	9.09	5.44	1.22	31.05	3.94
7.12	0.10	16.07	0.55	8.89	8.89	3E+5	0.64	10.15	4.59	1.03	31.05	3.32
2.93	0.04	16.07	0.55	21.58	21.58	3E+5	0.76	11.96	2.23	0.50	31.05	1.61
35.60	0.51	19.29	0.66	2.13	2.13	3E+5	0.00	0.00	0.00	0.00	53.65	0.00
32.36	0.46	19.29	0.66	2.35	2.35	3E+5	0.09	1.40	2.88	0.65	53.65	1.21
29.85	0.43	19.29	0.66	2.54	2.54	3E+5	0.21	3.31	6.28	1.41	53.65	2.63
19.48	0.28	19.29	0.66	3.90	3.90	3E+5	0.73	11.46	14.18	3.19	53.65	5.94
16.65	0.24	19.29	0.66	4.56	4.56	3E+5	0.86	13.50	14.28	3.21	53.65	5.98
12.57	0.18	19.29	0.66	6.04	6.04	3E+5	1.04	16.30	13.01	2.92	53.65	5.45
4.50	0.06	19.29	0.66	16.86	16.86	3E+5	1.16	18.21	5.21	1.17	53.65	2.18
41.99	0.60	22.50	0.77	2.11	2.11	4E+5	0.00	0.00	0.00	0.00	85.20	0.00
36.13	0.52	22.50	0.77	2.45	2.45	4E+5	0.40	6.37	14.61	3.28	85.20	3.86
28.69	0.41	22.50	0.77	3.09	3.09	4E+5	0.81	12.73	23.21	5.22	85.20	6.12
25.55	0.36	22.50	0.77	3.47	3.47	4E+5	0.96	15.15	24.59	5.53	85.20	6.49
17.59	0.25	22.50	0.77	5.04	5.04	4E+5	1.22	19.23	21.49	4.83	85.20	5.67
8.17	0.12	22.50	0.77	10.84	10.84	4E+5	1.51	23.81	12.35	2.78	85.20	3.26
3.67	0.05	22.50	0.77	24.17	24.17	4E+5	1.69	26.61	6.20	1.39	85.20	1.63
48.90	0.70	25.71	0.88	2.07	2.07	4E+5	0.00	0.00	0.00	0.00	127.17	0.00
38.12	0.54	25.71	0.88	2.66	2.66	4E+5	0.78	12.22	29.60	6.65	127.17	5.23
34.98	0.50	25.71	0.88	2.89	2.89	4E+5	1.05	16.55	36.78	8.27	127.17	6.50
27.96	0.40	25.71	0.88	3.62	3.62	4E+5	1.26	19.86	35.28	7.93	127.17	6.24
20.73	0.30	25.71	0.88	4.88	4.88	4E+5	1.51	23.81	31.36	7.05	127.17	5.54
12.88	0.18	25.71	0.88	7.86	7.86	4E+5	1.86	29.28	23.96	5.39	127.17	4.24
8.38	0.12	25.71	0.88	12.08	12.08	4E+5	2.14	33.74	17.96	4.04	127.17	3.17
55.82	0.80	28.93	0.99	2.04	2.04	5E+5	0.00	0.00	0.00	0.00	181.07	0.00
48.17	0.69	28.93	0.99	2.36	2.36	5E+5	0.69	10.82	33.12	7.45	181.07	4.11
41.57	0.59	28.93	0.99	2.74	2.74	5E+5	1.13	17.82	47.08	10.58	181.07	5.84
33.41	0.48	28.93	0.99	3.41	3.41	5E+5	1.37	21.64	45.93	10.33	181.07	5.70
22.31	0.32	28.93	0.99	5.11	5.11	5E+5	2.01	31.57	44.74	10.06	181.07	5.55
18.01	0.26	28.93	0.99	6.32	6.32	5E+5	2.36	37.18	42.54	9.56	181.07	5.28
9.84	0.14	28.93	0.99	11.57	11.57	5E+5	2.91	45.83	28.66	6.44	181.07	3.56
14.77	0.21	9.47	0.32	2.52	2.52	2E+5	0.00	0.00	0.00	0.00	6.34	0.00
8.59	0.12	9.47	0.32	4.34	4.34	2E+5	0.10	1.59	0.87	0.19	6.34	3.07
4.08	0.06	9.47	0.32	9.12	9.12	2E+5	0.15	2.42	0.63	0.14	6.34	2.23

2.51	0.04	9.47	0.32	14.83	14.83	2E+5	0.19	2.95	0.47	0.11	6.34	1.67
22.31	0.32	13.30	0.46	2.35	2.35	2E+5	0.00	0.00	0.00	0.00	17.58	0.00
17.91	0.26	13.30	0.46	2.92	2.92	2E+5	0.12	1.89	2.15	0.48	17.58	2.75
10.79	0.15	13.30	0.46	4.85	4.85	2E+5	0.25	3.86	2.65	0.59	17.58	3.38
8.38	0.12	13.30	0.46	6.25	6.25	2E+5	0.29	4.62	2.46	0.55	17.58	3.14
3.14	0.04	13.30	0.46	16.66	16.66	2E+5	0.40	6.36	1.27	0.29	17.58	1.62
1.05	0.01	13.30	0.46	49.99	49.99	2E+5	0.45	7.04	0.47	0.11	17.58	0.60
29.43	0.42	16.07	0.55	2.15	2.15	3E+5	0.00	0.00	0.00	0.00	31.05	0.00
25.55	0.36	16.07	0.55	2.48	2.48	3E+5	0.14	2.27	3.69	0.83	31.05	2.67
19.79	0.28	16.07	0.55	3.20	3.20	3E+5	0.27	4.32	5.43	1.22	31.05	3.93
14.77	0.21	16.07	0.55	4.29	4.29	3E+5	0.38	5.98	5.61	1.26	31.05	4.06
11.00	0.16	16.07	0.55	5.75	5.75	3E+5	0.50	7.80	5.45	1.22	31.05	3.94
9.63	0.14	16.07	0.55	6.57	6.57	3E+5	0.55	8.71	5.33	1.20	31.05	3.86
5.76	0.08	16.07	0.55	10.99	10.99	3E+5	0.63	9.92	3.63	0.82	31.05	2.63
35.40	0.51	19.29	0.66	2.15	2.15	3E+5	0.00	0.00	0.00	0.00	53.65	0.00
30.68	0.44	19.29	0.66	2.47	2.47	3E+5	0.20	3.18	6.20	1.39	53.65	2.60
23.67	0.34	19.29	0.66	3.21	3.21	3E+5	0.52	8.15	12.25	2.75	53.65	5.13
22.20	0.32	19.29	0.66	3.42	3.42	3E+5	0.57	8.91	12.57	2.83	53.65	5.27
16.13	0.23	19.29	0.66	4.71	4.71	3E+5	0.95	14.90	15.26	3.43	53.65	6.39
10.47	0.15	19.29	0.66	7.25	7.25	3E+5	1.21	18.97	12.62	2.84	53.65	5.29
1.88	0.03	19.29	0.66	40.28	40.28	3E+5	1.33	20.88	2.50	0.56	53.65	1.05
42.73	0.61	22.50	0.77	2.07	2.07	4E+5	0.00	0.00	0.00	0.00	85.20	0.00
37.80	0.54	22.50	0.77	2.34	2.34	4E+5	0.32	5.09	12.23	2.75	85.20	3.23
33.20	0.47	22.50	0.77	2.67	2.67	4E+5	0.50	7.89	16.65	3.74	85.20	4.39
27.23	0.39	22.50	0.77	3.25	3.25	4E+5	0.86	13.50	23.34	5.25	85.20	6.16
25.13	0.36	22.50	0.77	3.52	3.52	4E+5	1.01	15.91	25.41	5.71	85.20	6.70
14.56	0.21	22.50	0.77	6.09	6.09	4E+5	1.25	19.73	18.25	4.10	85.20	4.82
5.34	0.08	22.50	0.77	16.59	16.59	4E+5	1.62	25.46	8.64	1.94	85.20	2.28
49.11	0.70	25.71	0.88	2.06	2.06	4E+5	0.00	0.00	0.00	0.00	127.17	0.00
45.55	0.65	25.71	0.88	2.22	2.22	4E+5	0.24	3.82	11.05	2.48	127.17	1.95
39.06	0.56	25.71	0.88	2.59	2.59	4E+5	0.76	11.97	29.70	6.68	127.17	5.25
32.67	0.47	25.71	0.88	3.10	3.10	4E+5	1.08	17.06	35.41	7.96	127.17	6.26
23.56	0.34	25.71	0.88	4.30	4.30	4E+5	1.33	21.01	31.44	7.07	127.17	5.56
15.39	0.22	25.71	0.88	6.58	6.58	4E+5	1.71	26.99	26.40	5.93	127.17	4.67
10.68	0.15	25.71	0.88	9.48	9.48	4E+5	2.02	31.83	21.60	4.86	127.17	3.82
56.55	0.81	28.93	0.99	2.01	2.01	5E+5	0.00	0.00	0.00	0.00	181.07	0.00
40.11	0.57	28.93	0.99	2.84	2.84	5E+5	1.17	18.46	47.04	10.57	181.07	5.84
30.89	0.44	28.93	0.99	3.69	3.69	5E+5	1.50	23.55	46.22	10.39	181.07	5.74
21.05	0.30	28.93	0.99	5.41	5.41	5E+5	2.17	34.12	45.63	10.26	181.07	5.66
15.39	0.22	28.93	0.99	7.40	7.40	5E+5	2.54	39.98	39.10	8.79	181.07	4.85
9.42	0.13	28.93	0.99	12.08	12.08	5E+5	3.15	49.65	29.73	6.68	181.07	3.69

6.28	0.09	28.93	0.99	18.13	18.13	5E+5	3.36	52.84	21.09	4.74	181.07	2.62
14.87	0.21	9.47	0.32	2.51	2.51	2E+5	0.00	0.00	0.00	0.00	6.34	0.00
7.64	0.11	9.47	0.32	4.87	4.87	2E+5	0.14	2.20	1.07	0.24	6.34	3.78
3.14	0.04	9.47	0.32	11.86	11.86	2E+5	0.19	2.95	0.59	0.13	6.34	2.09
1.15	0.02	9.47	0.32	32.35	32.35	2E+5	0.23	3.56	0.26	0.06	6.34	0.92
22.10	0.32	13.30	0.46	2.37	2.37	2E+5	0.00	0.00	0.00	0.00	17.58	0.00
17.28	0.25	13.30	0.46	3.03	3.03	2E+5	0.13	2.04	2.24	0.50	17.58	2.87
14.66	0.21	13.30	0.46	3.57	3.57	2E+5	0.19	2.95	2.75	0.62	17.58	3.52
6.81	0.10	13.30	0.46	7.69	7.69	2E+5	0.38	6.06	2.62	0.59	17.58	3.35
3.14	0.04	13.30	0.46	16.66	16.66	2E+5	0.45	7.04	1.41	0.32	17.58	1.80
1.47	0.02	13.30	0.46	35.70	35.70	2E+5	0.49	7.65	0.71	0.16	17.58	0.91
29.11	0.42	16.07	0.55	2.17	2.17	3E+5	0.00	0.00	0.00	0.00	31.05	0.00
25.55	0.36	16.07	0.55	2.48	2.48	3E+5	0.13	2.12	3.44	0.77	31.05	2.49
22.10	0.32	16.07	0.55	2.86	2.86	3E+5	0.24	3.79	5.31	1.19	31.05	3.85
16.13	0.23	16.07	0.55	3.92	3.92	3E+5	0.35	5.45	5.58	1.26	31.05	4.04
13.82	0.20	16.07	0.55	4.58	4.58	3E+5	0.43	6.74	5.92	1.33	31.05	4.28
11.52	0.16	16.07	0.55	5.49	5.49	3E+5	0.49	7.65	5.60	1.26	31.05	4.05
4.40	0.06	16.07	0.55	14.39	14.39	3E+5	0.76	12.04	3.36	0.76	31.05	2.44
34.98	0.50	19.29	0.66	2.17	2.17	3E+5	0.00	0.00	0.00	0.00	53.65	0.00
26.18	0.37	19.29	0.66	2.90	2.90	3E+5	0.42	6.62	11.01	2.48	53.65	4.61
18.33	0.26	19.29	0.66	4.14	4.14	3E+5	0.87	13.75	16.01	3.60	53.65	6.71
14.97	0.21	19.29	0.66	5.07	5.07	3E+5	0.97	15.28	14.53	3.27	53.65	6.09
13.30	0.19	19.29	0.66	5.71	5.71	3E+5	1.03	16.17	13.66	3.07	53.65	5.72
11.41	0.16	19.29	0.66	6.65	6.65	3E+5	1.06	16.68	12.09	2.72	53.65	5.07
3.56	0.05	19.29	0.66	21.33	21.33	3E+5	1.26	19.86	4.49	1.01	53.65	1.88
42.41	0.61	22.50	0.77	2.09	2.09	4E+5	0.00	0.00	0.00	0.00	85.20	0.00
38.43	0.55	22.50	0.77	2.30	2.30	4E+5	0.26	4.07	9.95	2.24	85.20	2.62
28.06	0.40	22.50	0.77	3.16	3.16	4E+5	0.84	13.24	23.61	5.31	85.20	6.23
23.77	0.34	22.50	0.77	3.73	3.73	4E+5	1.08	16.93	25.57	5.75	85.20	6.75
15.18	0.22	22.50	0.77	5.83	5.83	4E+5	1.29	20.37	19.65	4.42	85.20	5.19
9.63	0.14	22.50	0.77	9.19	9.19	4E+5	1.46	23.04	14.10	3.17	85.20	3.72
4.71	0.07	22.50	0.77	18.80	18.80	4E+5	1.66	26.10	7.81	1.76	85.20	2.06
49.11	0.70	25.71	0.88	2.06	2.06	4E+5	0.00	0.00	0.00	0.00	127.17	0.00
37.07	0.53	25.71	0.88	2.73	2.73	4E+5	0.92	14.51	34.18	7.68	127.17	6.04
35.19	0.50	25.71	0.88	2.88	2.88	4E+5	1.03	16.17	36.14	8.13	127.17	6.39
27.75	0.40	25.71	0.88	3.65	3.65	4E+5	1.21	19.10	33.67	7.57	127.17	5.95
18.01	0.26	25.71	0.88	5.62	5.62	4E+5	1.59	25.08	28.70	6.45	127.17	5.07
13.82	0.20	25.71	0.88	7.32	7.32	4E+5	1.81	28.52	25.04	5.63	127.17	4.43
9.22	0.13	25.71	0.88	10.99	10.99	4E+5	2.15	33.87	19.83	4.46	127.17	3.50
56.23	0.80	28.93	0.99	2.03	2.03	5E+5	0.00	0.00	0.00	0.00	181.07	0.00
50.47	0.72	28.93	0.99	2.26	2.26	5E+5	0.47	7.38	23.68	5.32	181.07	2.94

46.60	0.67	28.93	0.99	2.44	2.44	5E+5	0.82	12.99	38.44	8.64	181.07	4.77
32.57	0.47	28.93	0.99	3.50	3.50	5E+5	1.41	22.15	45.83	10.30	181.07	5.69
22.10	0.32	28.93	0.99	5.15	5.15	5E+5	1.98	31.19	43.78	9.84	181.07	5.44
15.50	0.22	28.93	0.99	7.35	7.35	5E+5	2.53	39.85	39.24	8.82	181.07	4.87
7.33	0.10	28.93	0.99	15.54	15.54	5E+5	3.21	50.55	23.54	5.29	181.07	2.92

NACA-0022 6 Bladed Turbine with 48% Solidity												
ω_m (rad/s)	ω_p (rad/s)	V_m (m/s)	V_p (m/s)	Vel_m (ND)	Vel_p (ND)	Re	T_m (Nm)	T_p (Nm)	P_m (W)	P_p (W)	PA (W)	Eff (%)
8.06	0.12	9.34	0.32	4.56	4.56	1E+5	0.00	0.00	0.00	0.00	6.10	0.00
5.45	0.08	9.34	0.32	6.75	6.75	1E+5	0.07	1.14	0.39	0.09	6.10	1.45
3.25	0.05	9.34	0.32	11.33	11.33	1E+5	0.13	2.05	0.42	0.09	6.10	1.56
0.94	0.01	9.34	0.32	39.02	39.02	1E+5	0.19	3.03	0.18	0.04	6.10	0.67
12.36	0.18	12.93	0.44	4.12	4.12	2E+5	0.00	0.00	0.00	0.00	16.18	0.00
8.48	0.12	12.93	0.44	6.00	6.00	2E+5	0.13	2.05	1.10	0.25	16.18	1.53
7.85	0.11	12.93	0.44	6.48	6.48	2E+5	0.14	2.27	1.13	0.25	16.18	1.58
6.81	0.10	12.93	0.44	7.48	7.48	2E+5	0.18	2.80	1.21	0.27	16.18	1.68
6.07	0.09	12.93	0.44	8.38	8.38	2E+5	0.20	3.11	1.20	0.27	16.18	1.67
2.72	0.04	12.93	0.44	18.70	18.70	2E+5	0.28	4.40	0.76	0.17	16.18	1.06
16.02	0.23	15.83	0.54	3.89	3.89	3E+5	0.00	0.00	0.00	0.00	29.64	0.00
13.72	0.20	15.83	0.54	4.54	4.54	3E+5	0.10	1.59	1.39	0.31	29.64	1.05
12.67	0.18	15.83	0.54	4.92	4.92	3E+5	0.13	2.05	1.65	0.37	29.64	1.25
8.17	0.12	15.83	0.54	7.63	7.63	3E+5	0.32	5.00	2.59	0.58	29.64	1.97
7.33	0.10	15.83	0.54	8.50	8.50	3E+5	0.35	5.53	2.57	0.58	29.64	1.95
4.40	0.06	15.83	0.54	14.17	14.17	3E+5	0.41	6.44	1.80	0.40	29.64	1.36
3.46	0.05	15.83	0.54	18.03	18.03	3E+5	0.45	7.12	1.56	0.35	29.64	1.19
20.94	0.30	18.99	0.65	3.57	3.57	3E+5	0.00	0.00	0.00	0.00	51.23	0.00
18.01	0.26	18.99	0.65	4.15	4.15	3E+5	0.13	1.97	2.25	0.51	51.23	0.99
16.34	0.23	18.99	0.65	4.58	4.58	3E+5	0.21	3.33	3.46	0.78	51.23	1.52
12.36	0.18	18.99	0.65	6.05	6.05	3E+5	0.38	5.99	4.70	1.06	51.23	2.06
9.95	0.14	18.99	0.65	7.52	7.52	3E+5	0.49	7.65	4.83	1.09	51.23	2.12
6.49	0.09	18.99	0.65	11.52	11.52	3E+5	0.62	9.78	4.03	0.91	51.23	1.77
3.46	0.05	18.99	0.65	21.64	21.64	3E+5	0.74	11.59	2.54	0.57	51.23	1.12
25.66	0.37	22.16	0.76	3.40	3.40	4E+5	0.00	0.00	0.00	0.00	81.35	0.00
20.73	0.30	22.16	0.76	4.21	4.21	4E+5	0.24	3.79	4.99	1.12	81.35	1.38
16.34	0.23	22.16	0.76	5.34	5.34	4E+5	0.51	7.96	8.25	1.86	81.35	2.28
11.94	0.17	22.16	0.76	7.31	7.31	4E+5	0.77	12.12	9.19	2.07	81.35	2.54
9.22	0.13	22.16	0.76	9.47	9.47	4E+5	0.85	13.41	7.85	1.77	81.35	2.17
3.67	0.05	22.16	0.76	23.80	23.80	4E+5	1.25	19.70	4.58	1.03	81.35	1.27
2.30	0.03	22.16	0.76	37.86	37.86	4E+5	1.30	20.54	3.00	0.68	81.35	0.83
28.69	0.41	25.32	0.87	3.47	3.47	4E+5	0.00	0.00	0.00	0.00	121.43	0.00

23.67	0.34	25.32	0.87	4.21	4.21	4E+5	0.29	4.55	6.83	1.54	121.43	1.27
20.73	0.30	25.32	0.87	4.81	4.81	4E+5	0.48	7.50	9.87	2.22	121.43	1.83
18.33	0.26	25.32	0.87	5.44	5.44	4E+5	0.67	10.61	12.34	2.78	121.43	2.29
12.57	0.18	25.32	0.87	7.93	7.93	4E+5	1.05	16.52	13.18	2.96	121.43	2.44
8.38	0.12	25.32	0.87	11.90	11.90	4E+5	1.32	20.84	11.08	2.49	121.43	2.05
5.03	0.07	25.32	0.87	19.83	19.83	4E+5	1.50	23.64	7.54	1.70	121.43	1.40
33.51	0.48	28.49	0.98	3.35	3.35	5E+5	0.00	0.00	0.00	0.00	172.89	0.00
23.77	0.34	28.49	0.98	4.72	4.72	5E+5	0.73	11.44	17.26	3.88	172.89	2.25
21.99	0.31	28.49	0.98	5.10	5.10	5E+5	0.88	13.87	19.36	4.36	172.89	2.52
18.74	0.27	28.49	0.98	5.98	5.98	5E+5	1.09	17.20	20.47	4.60	172.89	2.66
12.46	0.18	28.49	0.98	9.00	9.00	5E+5	1.48	23.26	18.40	4.14	172.89	2.39
7.23	0.10	28.49	0.98	15.52	15.52	5E+5	1.71	26.90	12.34	2.78	172.89	1.61
5.24	0.07	28.49	0.98	21.42	21.42	5E+5	1.78	28.04	9.32	2.10	172.89	1.21
8.17	0.12	9.34	0.32	4.50	4.50	1E+5	0.00	0.00	0.00	0.00	6.10	0.00
5.13	0.07	9.34	0.32	7.17	7.17	1E+5	0.08	1.29	0.42	0.09	6.10	1.55
4.29	0.06	9.34	0.32	8.57	8.57	1E+5	0.11	1.74	0.47	0.11	6.10	1.75
1.68	0.02	9.34	0.32	21.95	21.95	1E+5	0.16	2.58	0.27	0.06	6.10	1.01
11.83	0.17	12.93	0.44	4.30	4.30	2E+5	0.00	0.00	0.00	0.00	16.18	0.00
10.16	0.15	12.93	0.44	5.01	5.01	2E+5	0.09	1.36	0.88	0.20	16.18	1.22
8.48	0.12	12.93	0.44	6.00	6.00	2E+5	0.12	1.89	1.02	0.23	16.18	1.42
7.12	0.10	12.93	0.44	7.15	7.15	2E+5	0.16	2.50	1.13	0.25	16.18	1.57
5.76	0.08	12.93	0.44	8.84	8.84	2E+5	0.19	3.03	1.11	0.25	16.18	1.54
0.84	0.01	12.93	0.44	60.77	60.77	2E+5	0.33	5.23	0.28	0.06	16.18	0.39
16.44	0.23	15.83	0.54	3.79	3.79	3E+5	0.00	0.00	0.00	0.00	29.64	0.00
13.82	0.20	15.83	0.54	4.51	4.51	3E+5	0.10	1.52	1.33	0.30	29.64	1.01
13.19	0.19	15.83	0.54	4.72	4.72	3E+5	0.12	1.82	1.52	0.34	29.64	1.16
9.53	0.14	15.83	0.54	6.54	6.54	3E+5	0.24	3.79	2.29	0.52	29.64	1.74
8.27	0.12	15.83	0.54	7.53	7.53	3E+5	0.31	4.85	2.55	0.57	29.64	1.93
6.39	0.09	15.83	0.54	9.75	9.75	3E+5	0.38	6.06	2.46	0.55	29.64	1.87
1.68	0.02	15.83	0.54	37.19	37.19	3E+5	0.56	8.79	0.93	0.21	29.64	0.71
20.84	0.30	18.99	0.65	3.59	3.59	3E+5	0.00	0.00	0.00	0.00	51.23	0.00
19.16	0.27	18.99	0.65	3.90	3.90	3E+5	0.08	1.21	1.47	0.33	51.23	0.65
11.00	0.16	18.99	0.65	6.80	6.80	3E+5	0.46	7.20	5.02	1.13	51.23	2.21
9.01	0.13	18.99	0.65	8.30	8.30	3E+5	0.52	8.18	4.68	1.05	51.23	2.05
7.02	0.10	18.99	0.65	10.66	10.66	3E+5	0.60	9.40	4.18	0.94	51.23	1.84
3.56	0.05	18.99	0.65	21.00	21.00	3E+5	0.73	11.44	2.59	0.58	51.23	1.14
2.51	0.04	18.99	0.65	29.75	29.75	3E+5	0.77	12.12	1.93	0.44	51.23	0.85
25.45	0.36	22.16	0.76	3.43	3.43	4E+5	0.00	0.00	0.00	0.00	81.35	0.00
23.56	0.34	22.16	0.76	3.70	3.70	4E+5	0.10	1.59	2.38	0.54	81.35	0.66
20.00	0.29	22.16	0.76	4.36	4.36	4E+5	0.27	4.32	5.48	1.23	81.35	1.52
16.86	0.24	22.16	0.76	5.17	5.17	4E+5	0.47	7.35	7.87	1.77	81.35	2.18

11.73	0.17	22.16	0.76	7.44	7.44	4E+5	0.78	12.35	9.19	2.07	81.35	2.54
5.24	0.07	22.16	0.76	16.66	16.66	4E+5	1.18	18.57	6.17	1.39	81.35	1.71
2.09	0.03	22.16	0.76	41.65	41.65	4E+5	1.31	20.61	2.74	0.62	81.35	0.76
28.90	0.41	25.32	0.87	3.45	3.45	4E+5	0.00	0.00	0.00	0.00	121.43	0.00
25.76	0.37	25.32	0.87	3.87	3.87	4E+5	0.18	2.88	4.71	1.06	121.43	0.87
19.37	0.28	25.32	0.87	5.15	5.15	4E+5	0.61	9.55	11.74	2.64	121.43	2.18
16.86	0.24	25.32	0.87	5.91	5.91	4E+5	0.84	13.19	14.11	3.17	121.43	2.61
13.51	0.19	25.32	0.87	7.38	7.38	4E+5	1.05	16.52	14.16	3.19	121.43	2.62
7.33	0.10	25.32	0.87	13.60	13.60	4E+5	1.37	21.60	10.05	2.26	121.43	1.86
3.87	0.06	25.32	0.87	25.73	25.73	4E+5	1.55	24.40	6.00	1.35	121.43	1.11
33.62	0.48	28.49	0.98	3.34	3.34	5E+5	0.00	0.00	0.00	0.00	172.89	0.00
31.31	0.45	28.49	0.98	3.58	3.58	5E+5	0.15	2.35	4.67	1.05	172.89	0.61
28.48	0.41	28.49	0.98	3.94	3.94	5E+5	0.34	5.30	9.59	2.16	172.89	1.25
25.87	0.37	28.49	0.98	4.34	4.34	5E+5	0.57	8.94	14.68	3.30	172.89	1.91
15.71	0.22	28.49	0.98	7.14	7.14	5E+5	1.25	19.70	19.64	4.42	172.89	2.56
10.37	0.15	28.49	0.98	10.82	10.82	5E+5	1.56	24.63	16.21	3.65	172.89	2.11
5.97	0.09	28.49	0.98	18.79	18.79	5E+5	1.77	27.81	10.54	2.37	172.89	1.37
8.06	0.12	9.34	0.32	4.56	4.56	1E+5	0.00	0.00	0.00	0.00	6.10	0.00
5.24	0.07	9.34	0.32	7.02	7.02	1E+5	0.08	1.21	0.40	0.09	6.10	1.49
4.50	0.06	9.34	0.32	8.17	8.17	1E+5	0.10	1.59	0.45	0.10	6.10	1.68
3.14	0.04	9.34	0.32	11.71	11.71	1E+5	0.13	2.05	0.41	0.09	6.10	1.51
11.83	0.17	12.93	0.44	4.30	4.30	2E+5	0.00	0.00	0.00	0.00	16.18	0.00
8.80	0.13	12.93	0.44	5.79	5.79	2E+5	0.11	1.67	0.93	0.21	16.18	1.29
7.75	0.11	12.93	0.44	6.57	6.57	2E+5	0.13	2.05	1.01	0.23	16.18	1.40
6.49	0.09	12.93	0.44	7.84	7.84	2E+5	0.17	2.65	1.09	0.25	16.18	1.52
5.24	0.07	12.93	0.44	9.72	9.72	2E+5	0.21	3.26	1.08	0.24	16.18	1.51
2.09	0.03	12.93	0.44	24.31	24.31	2E+5	0.29	4.55	0.60	0.14	16.18	0.84
16.44	0.23	15.83	0.54	3.79	3.79	3E+5	0.00	0.00	0.00	0.00	29.64	0.00
13.93	0.20	15.83	0.54	4.47	4.47	3E+5	0.11	1.74	1.54	0.35	29.64	1.17
9.53	0.14	15.83	0.54	6.54	6.54	3E+5	0.25	3.94	2.38	0.54	29.64	1.81
8.80	0.13	15.83	0.54	7.08	7.08	3E+5	0.27	4.24	2.37	0.53	29.64	1.80
6.91	0.10	15.83	0.54	9.01	9.01	3E+5	0.36	5.68	2.49	0.56	29.64	1.89
5.03	0.07	15.83	0.54	12.40	12.40	3E+5	0.41	6.44	2.05	0.46	29.64	1.56
3.04	0.04	15.83	0.54	20.52	20.52	3E+5	0.48	7.58	1.46	0.33	29.64	1.11
20.94	0.30	18.99	0.65	3.57	3.57	3E+5	0.00	0.00	0.00	0.00	51.23	0.00
18.85	0.27	18.99	0.65	3.97	3.97	3E+5	0.10	1.59	1.90	0.43	51.23	0.84
15.50	0.22	18.99	0.65	4.82	4.82	3E+5	0.26	4.17	4.10	0.92	51.23	1.80
10.79	0.15	18.99	0.65	6.93	6.93	3E+5	0.44	6.97	4.77	1.07	51.23	2.10
9.95	0.14	18.99	0.65	7.52	7.52	3E+5	0.50	7.88	4.98	1.12	51.23	2.19
6.70	0.10	18.99	0.65	11.16	11.16	3E+5	0.65	10.23	4.35	0.98	51.23	1.91
1.88	0.03	18.99	0.65	39.66	39.66	3E+5	0.80	12.58	1.50	0.34	51.23	0.66

25.45	0.36	22.16	0.76	3.43	3.43	4E+5	0.00	0.00	0.00	0.00	81.35	0.00
20.11	0.29	22.16	0.76	4.34	4.34	4E+5	0.28	4.40	5.61	1.26	81.35	1.55
18.85	0.27	22.16	0.76	4.63	4.63	4E+5	0.36	5.61	6.71	1.51	81.35	1.86
14.45	0.21	22.16	0.76	6.04	6.04	4E+5	0.61	9.62	8.83	1.99	81.35	2.44
9.01	0.13	22.16	0.76	9.69	9.69	4E+5	1.00	15.69	8.97	2.02	81.35	2.48
3.98	0.06	22.16	0.76	21.92	21.92	4E+5	1.25	19.70	4.98	1.12	81.35	1.38
1.68	0.02	22.16	0.76	52.06	52.06	4E+5	1.35	21.22	2.26	0.51	81.35	0.62
29.32	0.42	25.32	0.87	3.40	3.40	4E+5	0.00	0.00	0.00	0.00	121.43	0.00
28.06	0.40	25.32	0.87	3.55	3.55	4E+5	0.09	1.44	2.56	0.58	121.43	0.48
21.26	0.30	25.32	0.87	4.69	4.69	4E+5	0.48	7.58	10.22	2.30	121.43	1.89
13.51	0.19	25.32	0.87	7.38	7.38	4E+5	1.06	16.67	14.29	3.22	121.43	2.65
9.32	0.13	25.32	0.87	10.70	10.70	4E+5	1.26	19.93	11.79	2.65	121.43	2.18
4.50	0.06	25.32	0.87	22.14	22.14	4E+5	1.49	23.49	6.71	1.51	121.43	1.24
2.62	0.04	25.32	0.87	38.08	38.08	4E+5	1.60	25.23	4.19	0.94	121.43	0.78
33.72	0.48	28.49	0.98	3.33	3.33	5E+5	0.00	0.00	0.00	0.00	172.89	0.00
24.40	0.35	28.49	0.98	4.60	4.60	5E+5	0.64	10.08	15.61	3.51	172.89	2.03
21.36	0.31	28.49	0.98	5.25	5.25	5E+5	0.91	14.32	19.42	4.37	172.89	2.53
17.59	0.25	28.49	0.98	6.37	6.37	5E+5	1.16	18.34	20.48	4.61	172.89	2.66
12.15	0.17	28.49	0.98	9.23	9.23	5E+5	1.50	23.57	18.17	4.09	172.89	2.36
6.91	0.10	28.49	0.98	16.23	16.23	5E+5	1.75	27.51	12.07	2.72	172.89	1.57
4.82	0.07	28.49	0.98	23.28	23.28	5E+5	1.84	28.95	8.85	1.99	172.89	1.15

NACA-0022 3 Bladed Turbine with 41% Solidity												
ω_m (rad/s)	**ω_p (rad/s)**	**V_m (m/s)**	**V_p (m/s)**	**Vel_m (ND)**	**Vel_p (ND)**	**Re**	**$T_{m(Nm)}$**	**T_p (Nm)**	**P_m (W)**	**P_p (W)**	**PA (W)**	**Eff (%)**
12.67	0.18	9.10	0.31	2.83	2.83	1E+5	0.00	0.00	0.00	0.00	5.64	0.00
8.69	0.12	9.10	0.31	4.12	4.12	1E+5	0.05	0.84	0.46	0.10	5.64	1.84
3.14	0.04	9.10	0.31	11.41	11.41	1E+5	0.20	3.12	0.62	0.14	5.64	2.48
1.68	0.02	9.10	0.31	21.39	21.39	1E+5	0.26	4.11	0.44	0.10	5.64	1.75
19.06	0.27	13.06	0.45	2.70	2.70	2E+5	0.00	0.00	0.00	0.00	16.67	0.00
15.71	0.22	13.06	0.45	3.27	3.27	2E+5	0.05	0.84	0.83	0.19	16.67	1.13
11.21	0.16	13.06	0.45	4.59	4.59	2E+5	0.15	2.44	1.72	0.39	16.67	2.34
9.22	0.13	13.06	0.45	5.58	5.58	2E+5	0.21	3.28	1.91	0.43	16.67	2.59
6.07	0.09	13.06	0.45	8.47	8.47	2E+5	0.25	3.96	1.52	0.34	16.67	2.06
4.19	0.06	13.06	0.45	12.28	12.28	2E+5	0.33	5.18	1.37	0.31	16.67	1.86
25.34	0.36	15.72	0.54	2.44	2.44	3E+5	0.00	0.00	0.00	0.00	29.08	0.00
21.47	0.31	15.72	0.54	2.88	2.88	3E+5	0.08	1.30	1.76	0.40	29.08	1.37
19.69	0.28	15.72	0.54	3.14	3.14	3E+5	0.13	1.98	2.46	0.56	29.08	1.92
16.55	0.24	15.72	0.54	3.74	3.74	3E+5	0.19	3.05	3.18	0.72	29.08	2.48
10.47	0.15	15.72	0.54	5.91	5.91	3E+5	0.36	5.71	3.78	0.85	29.08	2.94
6.60	0.09	15.72	0.54	9.38	9.38	3E+5	0.53	8.38	3.49	0.79	29.08	2.72

3.77	0.05	15.72	0.54	16.42	16.42	3E+5	0.65	10.36	2.47	0.56	29.08	1.92
31.52	0.45	18.87	0.65	2.36	2.36	3E+5	0.00	0.00	0.00	0.00	50.26	0.00
27.12	0.39	18.87	0.65	2.74	2.74	3E+5	0.13	1.98	3.39	0.77	50.26	1.53
20.32	0.29	18.87	0.65	3.66	3.66	3E+5	0.33	5.18	6.64	1.50	50.26	2.99
19.69	0.28	18.87	0.65	3.77	3.77	3E+5	0.38	5.94	7.39	1.67	50.26	3.33
18.12	0.26	18.87	0.65	4.10	4.10	3E+5	0.46	7.31	8.36	1.89	50.26	3.77
13.51	0.19	18.87	0.65	5.50	5.50	3E+5	0.59	9.30	7.93	1.79	50.26	3.57
7.44	0.11	18.87	0.65	9.99	9.99	3E+5	0.91	14.40	6.76	1.53	50.26	3.04
38.01	0.54	22.01	0.75	2.28	2.28	4E+5	0.00	0.00	0.00	0.00	79.80	0.00
35.81	0.51	22.01	0.75	2.42	2.42	4E+5	0.06	0.99	2.24	0.51	79.80	0.63
25.97	0.37	22.01	0.75	3.34	3.34	4E+5	0.42	6.63	10.87	2.46	79.80	3.08
15.71	0.22	22.01	0.75	5.52	5.52	4E+5	0.98	15.54	15.41	3.49	79.80	4.37
10.16	0.15	22.01	0.75	8.53	8.53	4E+5	1.14	18.06	11.58	2.62	79.80	3.28
6.07	0.09	22.01	0.75	14.27	14.27	4E+5	1.25	19.74	7.57	1.71	79.80	2.15
3.56	0.05	22.01	0.75	24.34	24.34	4E+5	1.31	20.73	4.66	1.05	79.80	1.32
44.30	0.63	25.16	0.86	2.24	2.24	4E+5	0.00	0.00	0.00	0.00	119.12	0.00
31.83	0.45	25.16	0.86	3.11	3.11	4E+5	0.55	8.69	17.45	3.95	119.12	3.32
29.85	0.43	25.16	0.86	3.32	3.32	4E+5	0.69	10.90	20.53	4.64	119.12	3.90
28.06	0.40	25.16	0.86	3.53	3.53	4E+5	0.75	11.81	20.92	4.73	119.12	3.97
21.36	0.31	25.16	0.86	4.64	4.64	4E+5	1.14	18.06	24.35	5.51	119.12	4.63
14.87	0.21	25.16	0.86	6.66	6.66	4E+5	1.31	20.80	19.52	4.42	119.12	3.71
11.31	0.16	25.16	0.86	8.76	8.76	4E+5	1.46	23.16	16.54	3.74	119.12	3.14
53.51	0.76	28.30	0.97	2.08	2.08	5E+5	0.00	0.00	0.00	0.00	169.61	0.00
43.35	0.62	28.30	0.97	2.57	2.57	5E+5	0.40	6.40	17.52	3.96	169.61	2.34
36.13	0.52	28.30	0.97	3.08	3.08	5E+5	0.83	13.11	29.89	6.76	169.61	3.99
30.89	0.44	28.30	0.97	3.61	3.61	5E+5	1.14	18.14	35.36	8.00	169.61	4.72
23.67	0.34	28.30	0.97	4.71	4.71	5E+5	1.39	22.02	32.90	7.44	169.61	4.39
12.36	0.18	28.30	0.97	9.02	9.02	5E+5	1.79	28.35	22.11	5.00	169.61	2.95
7.33	0.10	28.30	0.97	15.20	15.20	5E+5	1.92	30.48	14.10	3.19	169.61	1.88
12.57	0.18	9.10	0.31	2.85	2.85	1E+5	0.00	0.00	0.00	0.00	5.64	0.00
7.85	0.11	9.10	0.31	4.56	4.56	1E+5	0.09	1.37	0.68	0.15	5.64	2.73
7.12	0.10	9.10	0.31	5.03	5.03	1E+5	0.10	1.52	0.68	0.15	5.64	2.75
5.03	0.07	9.10	0.31	7.13	7.13	1E+5	0.16	2.51	0.80	0.18	5.64	3.20
19.06	0.27	13.06	0.45	2.70	2.70	2E+5	0.00	0.00	0.00	0.00	16.67	0.00
12.36	0.18	13.06	0.45	4.16	4.16	2E+5	0.11	1.68	1.31	0.30	16.67	1.78
10.68	0.15	13.06	0.45	4.81	4.81	2E+5	0.15	2.44	1.64	0.37	16.67	2.23
7.54	0.11	13.06	0.45	6.82	6.82	2E+5	0.23	3.66	1.74	0.39	16.67	2.36
5.76	0.08	13.06	0.45	8.93	8.93	2E+5	0.25	4.04	1.47	0.33	16.67	1.99
2.20	0.03	13.06	0.45	23.38	23.38	2E+5	0.35	5.49	0.76	0.17	16.67	1.03
25.24	0.36	15.72	0.54	2.45	2.45	3E+5	0.00	0.00	0.00	0.00	29.08	0.00
20.32	0.29	15.72	0.54	3.05	3.05	3E+5	0.11	1.75	2.25	0.51	29.08	1.75

16.76	0.24	15.72	0.54	3.69	3.69	3E+5	0.16	2.59	2.74	0.62	29.08	2.13
15.71	0.22	15.72	0.54	3.94	3.94	3E+5	0.24	3.81	3.78	0.85	29.08	2.94
12.57	0.18	15.72	0.54	4.93	4.93	3E+5	0.31	4.95	3.93	0.89	29.08	3.06
9.11	0.13	15.72	0.54	6.80	6.80	3E+5	0.42	6.63	3.81	0.86	29.08	2.97
4.82	0.07	15.72	0.54	12.85	12.85	3E+5	0.58	9.22	2.80	0.63	29.08	2.18
31.42	0.45	18.87	0.65	2.36	2.36	3E+5	0.00	0.00	0.00	0.00	50.26	0.00
26.70	0.38	18.87	0.65	2.78	2.78	3E+5	0.11	1.68	2.83	0.64	50.26	1.27
21.99	0.31	18.87	0.65	3.38	3.38	3E+5	0.25	4.04	5.61	1.27	50.26	2.52
19.69	0.28	18.87	0.65	3.77	3.77	3E+5	0.38	5.94	7.39	1.67	50.26	3.33
16.76	0.24	18.87	0.65	4.43	4.43	3E+5	0.44	6.93	7.33	1.66	50.26	3.30
7.64	0.11	18.87	0.65	9.72	9.72	3E+5	0.81	12.80	6.18	1.40	50.26	2.78
3.67	0.05	18.87	0.65	20.27	20.27	3E+5	0.97	15.39	3.56	0.81	50.26	1.60
38.12	0.54	22.01	0.75	2.27	2.27	4E+5	0.00	0.00	0.00	0.00	79.80	0.00
30.68	0.44	22.01	0.75	2.82	2.82	4E+5	0.26	4.19	8.12	1.84	79.80	2.30
24.19	0.35	22.01	0.75	3.58	3.58	4E+5	0.53	8.38	12.80	2.90	79.80	3.63
18.85	0.27	22.01	0.75	4.60	4.60	4E+5	0.90	14.25	16.95	3.84	79.80	4.81
15.60	0.22	22.01	0.75	5.55	5.55	4E+5	1.01	16.00	15.76	3.57	79.80	4.47
12.15	0.17	22.01	0.75	7.14	7.14	4E+5	1.12	17.75	13.61	3.08	79.80	3.86
5.13	0.07	22.01	0.75	16.89	16.89	4E+5	1.33	21.03	6.81	1.54	79.80	1.93
44.61	0.64	25.16	0.86	2.22	2.22	4E+5	0.00	0.00	0.00	0.00	119.12	0.00
41.36	0.59	25.16	0.86	2.39	2.39	4E+5	0.12	1.90	4.97	1.13	119.12	0.94
33.82	0.48	25.16	0.86	2.93	2.93	4E+5	0.51	8.00	17.08	3.86	119.12	3.24
21.78	0.31	25.16	0.86	4.55	4.55	4E+5	1.04	16.54	22.73	5.14	119.12	4.32
14.24	0.20	25.16	0.86	6.96	6.96	4E+5	1.33	21.03	18.91	4.28	119.12	3.59
9.01	0.13	25.16	0.86	11.00	11.00	4E+5	1.55	24.61	13.99	3.17	119.12	2.66
5.55	0.08	25.16	0.86	17.85	17.85	4E+5	1.66	26.29	9.21	2.08	119.12	1.75
51.31	0.73	28.30	0.97	2.17	2.17	5E+5	0.00	0.00	0.00	0.00	169.61	0.00
47.86	0.68	28.30	0.97	2.33	2.33	5E+5	0.17	2.67	8.06	1.82	169.61	1.07
41.89	0.60	28.30	0.97	2.66	2.66	5E+5	0.51	8.08	21.36	4.83	169.61	2.85
35.60	0.51	28.30	0.97	3.13	3.13	5E+5	0.82	13.03	29.28	6.63	169.61	3.91
23.35	0.33	28.30	0.97	4.77	4.77	5E+5	1.42	22.48	33.13	7.50	169.61	4.42
12.15	0.17	28.30	0.97	9.17	9.17	5E+5	1.76	27.81	21.33	4.82	169.61	2.84
6.07	0.09	28.30	0.97	18.35	18.35	5E+5	1.91	30.25	11.60	2.62	169.61	1.55
12.78	0.18	9.10	0.31	2.81	2.81	1E+5	0.00	0.00	0.00	0.00	5.64	0.00
7.02	0.10	9.10	0.31	5.11	5.11	1E+5	0.10	1.60	0.71	0.16	5.64	2.84
4.19	0.06	9.10	0.31	8.56	8.56	1E+5	0.21	3.28	0.87	0.20	5.64	3.47
2.30	0.03	9.10	0.31	15.56	15.56	1E+5	0.25	3.89	0.57	0.13	5.64	2.27
18.74	0.27	13.06	0.45	2.74	2.74	2E+5	0.00	0.00	0.00	0.00	16.67	0.00
11.83	0.17	13.06	0.45	4.35	4.35	2E+5	0.13	2.06	1.54	0.35	16.67	2.09
11.10	0.16	13.06	0.45	4.63	4.63	2E+5	0.15	2.36	1.66	0.37	16.67	2.25
7.02	0.10	13.06	0.45	7.33	7.33	2E+5	0.24	3.73	1.65	0.37	16.67	2.24

2.93	0.04	13.06	0.45	17.54	17.54	2E+5	0.33	5.18	0.96	0.22	16.67	1.30
1.47	0.02	13.06	0.45	35.07	35.07	2E+5	0.37	5.79	0.54	0.12	16.67	0.73
25.13	0.36	15.72	0.54	2.46	2.46	3E+5	0.00	0.00	0.00	0.00	29.08	0.00
21.78	0.31	15.72	0.54	2.84	2.84	3E+5	0.09	1.37	1.89	0.43	29.08	1.47
14.35	0.20	15.72	0.54	4.32	4.32	3E+5	0.26	4.11	3.73	0.84	29.08	2.90
10.05	0.14	15.72	0.54	6.16	6.16	3E+5	0.39	6.25	3.96	0.90	29.08	3.08
6.81	0.10	15.72	0.54	9.10	9.10	3E+5	0.49	7.70	3.31	0.75	29.08	2.57
5.24	0.07	15.72	0.54	11.82	11.82	3E+5	0.55	8.69	2.87	0.65	29.08	2.23
1.05	0.01	15.72	0.54	59.12	59.12	3E+5	0.68	10.74	0.71	0.16	29.08	0.55
31.63	0.45	18.87	0.65	2.35	2.35	3E+5	0.00	0.00	0.00	0.00	50.26	0.00
23.46	0.34	18.87	0.65	3.17	3.17	3E+5	0.22	3.50	5.19	1.17	50.26	2.34
20.73	0.30	18.87	0.65	3.58	3.58	3E+5	0.30	4.72	6.18	1.40	50.26	2.78
18.01	0.26	18.87	0.65	4.12	4.12	3E+5	0.41	6.48	7.36	1.67	50.26	3.32
17.28	0.25	18.87	0.65	4.30	4.30	3E+5	0.44	6.93	7.56	1.71	50.26	3.40
12.25	0.17	18.87	0.65	6.06	6.06	3E+5	0.64	10.13	7.84	1.77	50.26	3.53
3.56	0.05	18.87	0.65	20.87	20.87	3E+5	0.95	15.09	3.39	0.77	50.26	1.53
38.54	0.55	22.01	0.75	2.25	2.25	4E+5	0.00	0.00	0.00	0.00	79.80	0.00
24.92	0.36	22.01	0.75	3.48	3.48	4E+5	0.42	6.63	10.43	2.36	79.80	2.96
22.31	0.32	22.01	0.75	3.89	3.89	4E+5	0.64	10.13	14.27	3.23	79.80	4.05
18.01	0.26	22.01	0.75	4.81	4.81	4E+5	0.85	13.49	15.33	3.47	79.80	4.35
14.45	0.21	22.01	0.75	6.00	6.00	4E+5	0.98	15.47	14.11	3.19	79.80	4.00
7.33	0.10	22.01	0.75	11.82	11.82	4E+5	1.22	19.35	8.96	2.03	79.80	2.54
4.08	0.06	22.01	0.75	21.22	21.22	4E+5	1.35	21.34	5.50	1.24	79.80	1.56
44.72	0.64	25.16	0.86	2.22	2.22	4E+5	0.00	0.00	0.00	0.00	119.12	0.00
33.20	0.47	25.16	0.86	2.98	2.98	4E+5	0.49	7.77	16.29	3.68	119.12	3.09
29.64	0.42	25.16	0.86	3.34	3.34	4E+5	0.72	11.43	21.38	4.84	119.12	4.06
26.70	0.38	25.16	0.86	3.71	3.71	4E+5	0.84	13.26	22.35	5.06	119.12	4.24
16.02	0.23	25.16	0.86	6.18	6.18	4E+5	1.30	20.57	20.81	4.71	119.12	3.95
8.90	0.13	25.16	0.86	11.13	11.13	4E+5	1.52	24.08	13.53	3.06	119.12	2.57
5.86	0.08	25.16	0.86	16.89	16.89	4E+5	1.64	26.06	9.65	2.18	119.12	1.83
50.27	0.72	28.30	0.97	2.22	2.22	5E+5	0.00	0.00	0.00	0.00	169.61	0.00
36.97	0.53	28.30	0.97	3.01	3.01	5E+5	0.79	12.50	29.16	6.60	169.61	3.89
31.21	0.45	28.30	0.97	3.57	3.57	5E+5	1.09	17.22	33.92	7.67	169.61	4.52
23.67	0.34	28.30	0.97	4.71	4.71	5E+5	1.38	21.79	32.55	7.37	169.61	4.34
17.07	0.24	28.30	0.97	6.53	6.53	5E+5	1.65	26.14	28.16	6.37	169.61	3.76
10.16	0.15	28.30	0.97	10.97	10.97	5E+5	1.81	28.73	18.42	4.17	169.61	2.46
6.07	0.09	28.30	0.97	18.35	18.35	5E+5	2.00	31.62	12.12	2.74	169.61	1.62

NACA-0022 3 Bladed Turbine with 55% Solidity												
ω_m (rad/s)	**ω_p (rad/s)**	**V_m (m/s)**	**V_p (m/s)**	**Vel_m (ND)**	**Vel_p (ND)**	**Re**	**T_m (Nm)**	**T_p (Nm)**	**P_m (W)**	**P_p (W)**	**PA (W)**	**Eff (%)**

17.91	0.26	8.10	0.28	1.78	1.78	1E+5	0.00	0.00	0.00	0.00	3.97	0.00
12.04	0.17	8.10	0.28	2.65	2.65	1E+5	0.11	1.67	1.27	0.29	3.97	7.23
8.80	0.13	8.10	0.28	3.62	3.62	1E+5	0.14	2.28	1.27	0.29	3.97	7.20
0.84	0.01	8.10	0.28	38.06	38.06	1E+5	0.32	5.01	0.27	0.06	3.97	1.51
27.54	0.39	11.02	0.38	1.58	1.58	2E+5	0.00	0.00	0.00	0.00	10.01	0.00
23.35	0.33	11.02	0.38	1.86	1.86	2E+5	0.09	1.37	2.02	0.46	10.01	4.55
22.31	0.32	11.02	0.38	1.95	1.95	2E+5	0.13	1.98	2.79	0.63	10.01	6.28
16.44	0.23	11.02	0.38	2.64	2.64	2E+5	0.24	3.80	3.95	0.89	10.01	8.91
11.73	0.17	11.02	0.38	3.70	3.70	2E+5	0.31	4.86	3.61	0.81	10.01	8.13
4.82	0.07	11.02	0.38	9.01	9.01	2E+5	0.47	7.44	2.27	0.51	10.01	5.11
37.07	0.53	13.57	0.47	1.44	1.44	2E+5	0.00	0.00	0.00	0.00	18.68	0.00
33.51	0.48	13.57	0.47	1.59	1.59	2E+5	0.09	1.37	2.90	0.65	18.68	3.50
29.22	0.42	13.57	0.47	1.83	1.83	2E+5	0.22	3.42	6.32	1.43	18.68	7.63
21.15	0.30	13.57	0.47	2.53	2.53	2E+5	0.41	6.53	8.75	1.97	18.68	10.56
16.86	0.24	13.57	0.47	3.17	3.17	2E+5	0.56	8.89	9.49	2.14	18.68	11.45
12.57	0.18	13.57	0.47	4.25	4.25	2E+5	0.72	11.39	9.07	2.04	18.68	10.94
2.72	0.04	13.57	0.47	19.62	19.62	2E+5	1.01	16.02	2.76	0.62	18.68	3.34
47.96	0.68	16.28	0.56	1.34	1.34	3E+5	0.00	0.00	0.00	0.00	32.28	0.00
34.77	0.50	16.28	0.56	1.84	1.84	3E+5	0.44	6.91	15.22	3.43	32.28	10.63
26.18	0.37	16.28	0.56	2.45	2.45	3E+5	0.72	11.39	18.89	4.26	32.28	13.19
19.48	0.28	16.28	0.56	3.29	3.29	3E+5	1.01	15.95	19.67	4.44	32.28	13.74
15.92	0.23	16.28	0.56	4.03	4.03	3E+5	1.07	16.94	17.07	3.85	32.28	11.93
9.42	0.13	16.28	0.56	6.80	6.80	3E+5	1.27	20.12	12.01	2.71	32.28	8.39
6.91	0.10	16.28	0.56	9.27	9.27	3E+5	1.36	21.42	9.37	2.11	32.28	6.55
60.32	0.86	19.00	0.65	1.24	1.24	3E+5	0.00	0.00	0.00	0.00	51.26	0.00
51.42	0.73	19.00	0.65	1.45	1.45	3E+5	0.19	2.94	9.57	2.16	51.26	4.21
41.89	0.60	19.00	0.65	1.79	1.79	3E+5	0.61	9.58	25.41	5.73	51.26	11.18
29.53	0.42	19.00	0.65	2.53	2.53	3E+5	1.04	16.48	30.81	6.95	51.26	13.55
20.53	0.29	19.00	0.65	3.64	3.64	3E+5	1.21	19.03	24.74	5.58	51.26	10.88
14.35	0.20	19.00	0.65	5.21	5.21	3E+5	1.33	21.07	19.15	4.32	51.26	8.42
8.48	0.12	19.00	0.65	8.82	8.82	3E+5	1.58	24.90	13.38	3.02	51.26	5.89
67.54	0.96	21.71	0.74	1.27	1.27	3E+5	0.00	0.00	0.00	0.00	76.52	0.00
62.20	0.89	21.71	0.74	1.37	1.37	3E+5	0.29	4.60	18.11	4.08	76.52	5.34
45.34	0.65	21.71	0.74	1.88	1.88	3E+5	1.07	16.86	48.41	10.92	76.52	14.27
41.15	0.59	21.71	0.74	2.08	2.08	3E+5	1.14	18.01	46.93	10.58	76.52	13.83
26.18	0.37	21.71	0.74	3.26	3.26	3E+5	1.58	24.90	41.29	9.31	76.52	12.17
14.77	0.21	21.71	0.74	5.79	5.79	3E+5	2.01	31.80	29.74	6.71	76.52	8.76
9.22	0.13	21.71	0.74	9.27	9.27	3E+5	2.26	35.76	20.87	4.71	76.52	6.15
75.61	1.08	24.42	0.84	1.27	1.27	4E+5	0.00	0.00	0.00	0.00	108.95	0.00
72.88	1.04	24.42	0.84	1.32	1.32	4E+5	0.19	3.06	14.15	3.19	108.95	2.93
64.40	0.92	24.42	0.84	1.49	1.49	4E+5	0.66	10.34	42.19	9.51	108.95	8.73

54.56	0.78	24.42	0.84	1.76	1.76	4E+5	1.15	18.14	62.66	14.13	108.95	12.97
46.08	0.66	24.42	0.84	2.09	2.09	4E+5	1.42	22.48	65.59	14.79	108.95	13.58
40.11	0.57	24.42	0.84	2.40	2.40	4E+5	1.66	26.18	66.50	15.00	108.95	13.76
34.56	0.49	24.42	0.84	2.78	2.78	4E+5	1.91	30.14	65.96	14.88	108.95	13.65
18.12	0.26	8.10	0.28	1.76	1.76	1E+5	0.00	0.00	0.00	0.00	3.97	0.00
11.73	0.17	8.10	0.28	2.72	2.72	1E+5	0.11	1.67	1.24	0.28	3.97	7.04
8.27	0.12	8.10	0.28	3.85	3.85	1E+5	0.16	2.58	1.35	0.31	3.97	7.68
3.67	0.05	8.10	0.28	8.70	8.70	1E+5	0.21	3.34	0.78	0.17	3.97	4.40
28.06	0.40	11.02	0.38	1.55	1.55	2E+5	0.00	0.00	0.00	0.00	10.01	0.00
20.11	0.29	11.02	0.38	2.16	2.16	2E+5	0.17	2.73	3.48	0.79	10.01	7.84
11.94	0.17	11.02	0.38	3.63	3.63	2E+5	0.31	4.86	3.67	0.83	10.01	8.28
9.01	0.13	11.02	0.38	4.82	4.82	2E+5	0.37	5.77	3.29	0.74	10.01	7.41
4.82	0.07	11.02	0.38	9.01	9.01	2E+5	0.46	7.21	2.20	0.50	10.01	4.96
2.72	0.04	11.02	0.38	15.94	15.94	2E+5	0.55	8.73	1.51	0.34	10.01	3.39
37.07	0.53	13.57	0.47	1.44	1.44	2E+5	0.00	0.00	0.00	0.00	18.68	0.00
29.64	0.42	13.57	0.47	1.80	1.80	2E+5	0.15	2.35	4.42	1.00	18.68	5.33
28.06	0.40	13.57	0.47	1.90	1.90	2E+5	0.25	4.02	7.15	1.61	18.68	8.64
21.05	0.30	13.57	0.47	2.54	2.54	2E+5	0.44	6.91	9.21	2.08	18.68	11.12
16.34	0.23	13.57	0.47	3.27	3.27	2E+5	0.55	8.73	9.04	2.04	18.68	10.91
12.15	0.17	13.57	0.47	4.40	4.40	2E+5	0.68	10.78	8.30	1.87	18.68	10.01
5.24	0.07	13.57	0.47	10.20	10.20	2E+5	0.91	14.43	4.78	1.08	18.68	5.78
48.28	0.69	16.28	0.56	1.33	1.33	3E+5	0.00	0.00	0.00	0.00	32.28	0.00
38.96	0.56	16.28	0.56	1.65	1.65	3E+5	0.23	3.57	8.81	1.99	32.28	6.15
35.19	0.50	16.28	0.56	1.82	1.82	3E+5	0.43	6.76	15.06	3.40	32.28	10.52
24.50	0.35	16.28	0.56	2.62	2.62	3E+5	0.78	12.38	19.21	4.33	32.28	13.42
15.71	0.22	16.28	0.56	4.08	4.08	3E+5	1.07	16.86	16.77	3.78	32.28	11.72
8.80	0.13	16.28	0.56	7.29	7.29	3E+5	1.26	19.97	11.13	2.51	32.28	7.77
3.67	0.05	16.28	0.56	17.49	17.49	3E+5	1.45	22.94	5.32	1.20	32.28	3.72
57.60	0.82	19.00	0.65	1.30	1.30	3E+5	0.00	0.00	0.00	0.00	51.26	0.00
43.25	0.62	19.00	0.65	1.73	1.73	3E+5	0.59	9.32	25.54	5.76	51.26	11.23
26.39	0.38	19.00	0.65	2.83	2.83	3E+5	1.09	17.24	28.81	6.50	51.26	12.68
23.35	0.33	19.00	0.65	3.20	3.20	3E+5	1.20	18.90	27.95	6.30	51.26	12.30
16.44	0.23	19.00	0.65	4.55	4.55	3E+5	1.34	21.20	22.07	4.98	51.26	9.71
12.36	0.18	19.00	0.65	6.05	6.05	3E+5	1.45	22.86	17.89	4.03	51.26	7.87
5.86	0.08	19.00	0.65	12.75	12.75	3E+5	1.70	26.82	9.96	2.25	51.26	4.38
67.86	0.97	21.71	0.74	1.26	1.26	3E+5	0.00	0.00	0.00	0.00	76.52	0.00
54.14	0.77	21.71	0.74	1.58	1.58	3E+5	0.65	10.22	35.03	7.90	76.52	10.32
47.44	0.68	21.71	0.74	1.80	1.80	3E+5	0.94	14.81	44.51	10.04	76.52	13.12
35.08	0.50	21.71	0.74	2.44	2.44	3E+5	1.27	20.05	44.55	10.05	76.52	13.13
27.44	0.39	21.71	0.74	3.12	3.12	3E+5	1.58	24.90	43.27	9.76	76.52	12.75
22.10	0.32	21.71	0.74	3.87	3.87	3E+5	1.67	26.44	36.99	8.34	76.52	10.90

14.35	0.20	21.71	0.74	5.96	5.96	3E+5	2.02	31.93	29.01	6.54	76.52	8.55
76.65	1.09	24.42	0.84	1.25	1.25	4E+5	0.00	0.00	0.00	0.00	108.95	0.00
59.27	0.85	24.42	0.84	1.62	1.62	4E+5	0.99	15.71	58.97	13.30	108.95	12.20
48.17	0.69	24.42	0.84	2.00	2.00	4E+5	1.38	21.71	66.23	14.94	108.95	13.71
37.18	0.53	24.42	0.84	2.59	2.59	4E+5	1.76	27.84	65.55	14.78	108.95	13.57
28.90	0.41	24.42	0.84	3.33	3.33	4E+5	2.16	34.10	62.42	14.08	108.95	12.92
22.72	0.32	24.42	0.84	4.23	4.23	4E+5	2.47	38.95	56.06	12.64	108.95	11.60
14.66	0.21	24.42	0.84	6.56	6.56	4E+5	3.10	48.91	45.42	10.24	108.95	9.40
18.43	0.26	8.10	0.28	1.73	1.73	1E+5	0.00	0.00	0.00	0.00	3.97	0.00
14.14	0.20	8.10	0.28	2.26	2.26	1E+5	0.06	0.99	0.88	0.20	3.97	5.02
4.08	0.06	8.10	0.28	7.81	7.81	1E+5	0.21	3.27	0.84	0.19	3.97	4.79
3.04	0.04	8.10	0.28	10.50	10.50	1E+5	0.23	3.65	0.70	0.16	3.97	3.98
27.23	0.39	11.02	0.38	1.59	1.59	2E+5	0.00	0.00	0.00	0.00	10.01	0.00
23.35	0.33	11.02	0.38	1.86	1.86	2E+5	0.11	1.75	2.58	0.58	10.01	5.82
18.54	0.26	11.02	0.38	2.34	2.34	2E+5	0.19	3.04	3.57	0.80	10.01	8.03
14.87	0.21	11.02	0.38	2.92	2.92	2E+5	0.25	3.95	3.72	0.84	10.01	8.38
11.00	0.16	11.02	0.38	3.95	3.95	2E+5	0.32	5.01	3.49	0.79	10.01	7.86
5.86	0.08	11.02	0.38	7.40	7.40	2E+5	0.46	7.21	2.68	0.60	10.01	6.04
38.01	0.54	13.57	0.47	1.41	1.41	2E+5	0.00	0.00	0.00	0.00	18.68	0.00
32.46	0.46	13.57	0.47	1.65	1.65	2E+5	0.11	1.75	3.59	0.81	18.68	4.33
25.76	0.37	13.57	0.47	2.07	2.07	2E+5	0.29	4.63	7.56	1.70	18.68	9.12
18.95	0.27	13.57	0.47	2.82	2.82	2E+5	0.48	7.52	9.03	2.04	18.68	10.89
11.41	0.16	13.57	0.47	4.68	4.68	2E+5	0.71	11.16	8.07	1.82	18.68	9.74
7.75	0.11	13.57	0.47	6.89	6.89	2E+5	0.83	13.06	6.41	1.45	18.68	7.74
4.40	0.06	13.57	0.47	12.15	12.15	2E+5	0.93	14.66	4.08	0.92	18.68	4.93
48.17	0.69	16.28	0.56	1.33	1.33	3E+5	0.00	0.00	0.00	0.00	32.28	0.00
34.66	0.50	16.28	0.56	1.85	1.85	3E+5	0.44	6.99	15.34	3.46	32.28	10.71
28.69	0.41	16.28	0.56	2.23	2.23	3E+5	0.60	9.49	17.25	3.89	32.28	12.05
21.36	0.31	16.28	0.56	3.00	3.00	3E+5	0.93	14.73	19.93	4.50	32.28	13.92
12.36	0.18	16.28	0.56	5.19	5.19	3E+5	1.16	18.30	14.32	3.23	32.28	10.01
9.11	0.13	16.28	0.56	7.04	7.04	3E+5	1.26	19.82	11.44	2.58	32.28	7.99
5.55	0.08	16.28	0.56	11.55	11.55	3E+5	1.37	21.64	7.61	1.72	32.28	5.31
60.84	0.87	19.00	0.65	1.23	1.23	3E+5	0.00	0.00	0.00	0.00	51.26	0.00
50.47	0.72	19.00	0.65	1.48	1.48	3E+5	0.30	4.73	15.11	3.41	51.26	6.64
45.03	0.64	19.00	0.65	1.66	1.66	3E+5	0.52	8.17	23.31	5.26	51.26	10.25
38.22	0.55	19.00	0.65	1.96	1.96	3E+5	0.78	12.26	29.68	6.69	51.26	13.06
35.19	0.50	19.00	0.65	2.13	2.13	3E+5	0.91	14.30	31.87	7.19	51.26	14.02
25.45	0.36	19.00	0.65	2.94	2.94	3E+5	1.13	17.88	28.81	6.50	51.26	12.68
14.24	0.20	19.00	0.65	5.25	5.25	3E+5	1.41	22.22	20.04	4.52	51.26	8.82
68.91	0.98	21.71	0.74	1.24	1.24	3E+5	0.00	0.00	0.00	0.00	76.52	0.00
49.22	0.70	21.71	0.74	1.74	1.74	3E+5	0.91	14.43	44.98	10.14	76.52	13.26

44.61	0.64	21.71	0.74	1.92	1.92	3E+5	1.05	16.60	46.91	10.58	76.52	13.82
32.15	0.46	21.71	0.74	2.66	2.66	3E+5	1.43	22.61	46.02	10.38	76.52	13.56
19.06	0.27	21.71	0.74	4.48	4.48	3E+5	1.79	28.23	34.07	7.68	76.52	10.04
16.13	0.23	21.71	0.74	5.30	5.30	3E+5	1.94	30.65	31.30	7.06	76.52	9.23
9.11	0.13	21.71	0.74	9.38	9.38	3E+5	2.31	36.40	21.00	4.74	76.52	6.19
76.86	1.10	24.42	0.84	1.25	1.25	4E+5	0.00	0.00	0.00	0.00	108.95	0.00
61.78	0.88	24.42	0.84	1.56	1.56	4E+5	0.76	12.01	46.97	10.59	108.95	9.72
54.14	0.77	24.42	0.84	1.78	1.78	4E+5	1.09	17.24	59.12	13.33	108.95	12.24
44.51	0.64	24.42	0.84	2.16	2.16	4E+5	1.43	22.61	63.71	14.37	108.95	13.19
35.81	0.51	24.42	0.84	2.68	2.68	4E+5	1.89	29.88	67.78	15.29	108.95	14.03
30.37	0.43	24.42	0.84	3.17	3.17	4E+5	2.14	33.85	65.09	14.68	108.95	13.47
25.55	0.36	24.42	0.84	3.76	3.76	4E+5	2.31	36.40	58.90	13.28	108.95	12.19

NACA-0022 2 Bladed Turbine with 41% Solidity												
ω_m (rad/s)	**ω_p (rad/s)**	**V_m (m/s)**	**V_p (m/s)**	**Vel_m (ND)**	**Vel_p (ND)**	**Re**	**T_m (Nm)**	**T_p (Nm)**	**P_m (W)**	**P_p (W)**	**PA (W)**	**Eff (%)**
10.68	0.15	7.49	0.26	2.76	2.76	1E+5	0.00	0.00	0.00	0.00	3.14	0.00
8.17	0.12	7.49	0.26	3.61	3.61	1E+5	0.10	1.60	0.82	0.19	3.14	5.94
5.13	0.07	7.49	0.26	5.75	5.75	1E+5	0.22	3.51	1.14	0.26	3.14	8.18
0.63	0.01	7.49	0.26	46.93	46.93	1E+5	0.40	6.41	0.25	0.06	3.14	1.83
15.50	0.22	10.59	0.36	2.69	2.69	2E+5	0.00	0.00	0.00	0.00	8.89	0.00
11.52	0.16	10.59	0.36	3.62	3.62	2E+5	0.25	3.89	2.83	0.64	8.89	7.20
8.48	0.12	10.59	0.36	4.92	4.92	2E+5	0.38	6.10	3.26	0.74	8.89	8.31
5.76	0.08	10.59	0.36	7.24	7.24	2E+5	0.51	8.01	2.91	0.66	8.89	7.41
3.35	0.05	10.59	0.36	12.45	12.45	2E+5	0.58	9.15	1.93	0.44	8.89	4.93
2.41	0.03	10.59	0.36	17.32	17.32	2E+5	0.66	10.45	1.59	0.36	8.89	4.04
20.42	0.29	12.70	0.44	2.45	2.45	2E+5	0.00	0.00	0.00	0.00	15.31	0.00
17.80	0.25	12.70	0.44	2.81	2.81	2E+5	0.18	2.82	3.17	0.72	15.31	4.69
14.97	0.21	12.70	0.44	3.34	3.34	2E+5	0.40	6.41	6.05	1.37	15.31	8.95
11.52	0.16	12.70	0.44	4.34	4.34	2E+5	0.60	9.46	6.87	1.56	15.31	10.16
7.85	0.11	12.70	0.44	6.36	6.36	2E+5	0.78	12.36	6.12	1.39	15.31	9.05
6.07	0.09	12.70	0.44	8.23	8.23	2E+5	0.85	13.50	5.17	1.17	15.31	7.65
3.25	0.05	12.70	0.44	15.40	15.40	2E+5	0.96	15.25	3.12	0.71	15.31	4.62
25.24	0.36	15.24	0.52	2.38	2.38	2E+5	0.00	0.00	0.00	0.00	26.45	0.00
20.73	0.30	15.24	0.52	2.89	2.89	2E+5	0.38	6.03	7.88	1.78	26.45	6.74
18.95	0.27	15.24	0.52	3.16	3.16	2E+5	0.56	8.92	10.67	2.42	26.45	9.13
16.02	0.23	15.24	0.52	3.74	3.74	2E+5	0.74	11.67	11.79	2.67	26.45	10.09
12.04	0.17	15.24	0.52	4.98	4.98	2E+5	0.99	15.63	11.87	2.69	26.45	10.17
10.05	0.14	15.24	0.52	5.97	5.97	2E+5	1.08	17.08	10.83	2.45	26.45	9.27
7.44	0.11	15.24	0.52	8.07	8.07	2E+5	1.32	20.90	9.80	2.22	26.45	8.39
30.58	0.44	17.77	0.61	2.29	2.29	3E+5	0.00	0.00	0.00	0.00	42.00	0.00

24.71	0.35	17.77	0.61	2.83	2.83	3E+5	0.61	9.62	14.99	3.39	42.00	8.08
21.57	0.31	17.77	0.61	3.24	3.24	3E+5	0.89	14.11	19.19	4.35	42.00	10.35
16.55	0.24	17.77	0.61	4.23	4.23	3E+5	1.27	20.13	21.01	4.76	42.00	11.33
12.36	0.18	17.77	0.61	5.66	5.66	3E+5	1.49	23.60	18.39	4.16	42.00	9.91
10.16	0.15	17.77	0.61	6.89	6.89	3E+5	1.74	27.57	17.66	4.00	42.00	9.52
6.70	0.10	17.77	0.61	10.44	10.44	3E+5	1.97	31.16	13.17	2.98	42.00	7.10
33.09	0.47	20.31	0.70	2.42	2.42	3E+5	0.00	0.00	0.00	0.00	62.70	0.00
30.37	0.43	20.31	0.70	2.63	2.63	3E+5	0.53	8.34	15.97	3.62	62.70	5.77
24.09	0.34	20.31	0.70	3.32	3.32	3E+5	1.10	17.44	26.49	6.00	62.70	9.57
20.00	0.29	20.31	0.70	4.00	4.00	3E+5	1.43	22.70	28.63	6.48	62.70	10.34
14.35	0.20	20.31	0.70	5.57	5.57	3E+5	1.97	31.29	28.31	6.41	62.70	10.23
12.57	0.18	20.31	0.70	6.36	6.36	3E+5	2.20	34.88	27.65	6.26	62.70	9.99
7.85	0.11	20.31	0.70	10.18	10.18	3E+5	2.69	42.58	21.09	4.78	62.70	7.62
38.75	0.55	22.85	0.78	2.32	2.32	4E+5	0.00	0.00	0.00	0.00	89.27	0.00
32.99	0.47	22.85	0.78	2.73	2.73	4E+5	0.78	12.44	25.88	5.86	89.27	6.56
27.75	0.40	22.85	0.78	3.24	3.24	4E+5	1.22	19.37	33.89	7.68	89.27	8.60
23.04	0.33	22.85	0.78	3.91	3.91	4E+5	1.71	27.06	39.32	8.90	89.27	9.97
16.23	0.23	22.85	0.78	5.54	5.54	4E+5	2.49	39.50	40.44	9.16	89.27	10.26
12.88	0.18	22.85	0.78	6.99	6.99	4E+5	2.85	45.14	36.67	8.30	89.27	9.30
11.21	0.16	22.85	0.78	8.03	8.03	4E+5	3.11	49.38	34.89	7.90	89.27	8.85
10.79	0.15	7.49	0.26	2.73	2.73	1E+5	0.00	0.00	0.00	0.00	3.14	0.00
8.69	0.12	7.49	0.26	3.39	3.39	1E+5	0.08	1.22	0.67	0.15	3.14	4.82
4.92	0.07	7.49	0.26	5.99	5.99	1E+5	0.23	3.59	1.11	0.25	3.14	8.02
3.77	0.05	7.49	0.26	7.82	7.82	1E+5	0.26	4.19	1.00	0.23	3.14	7.18
15.39	0.22	10.59	0.36	2.71	2.71	2E+5	0.00	0.00	0.00	0.00	8.89	0.00
12.25	0.17	10.59	0.36	3.40	3.40	2E+5	0.17	2.67	2.06	0.47	8.89	5.25
9.11	0.13	10.59	0.36	4.58	4.58	2E+5	0.36	5.72	3.29	0.74	8.89	8.37
5.13	0.07	10.59	0.36	8.13	8.13	2E+5	0.54	8.62	2.79	0.63	8.89	7.10
3.56	0.05	10.59	0.36	11.71	11.71	2E+5	0.60	9.53	2.14	0.48	8.89	5.45
2.30	0.03	10.59	0.36	18.10	18.10	2E+5	0.65	10.30	1.50	0.34	8.89	3.81
20.53	0.29	12.70	0.44	2.44	2.44	2E+5	0.00	0.00	0.00	0.00	15.31	0.00
18.54	0.26	12.70	0.44	2.70	2.70	2E+5	0.13	2.14	2.50	0.57	15.31	3.69
17.80	0.25	12.70	0.44	2.81	2.81	2E+5	0.17	2.67	3.00	0.68	15.31	4.43
13.82	0.20	12.70	0.44	3.62	3.62	2E+5	0.49	7.78	6.78	1.54	15.31	10.03
10.26	0.15	12.70	0.44	4.87	4.87	2E+5	0.66	10.45	6.76	1.53	15.31	10.00
5.13	0.07	12.70	0.44	9.74	9.74	2E+5	0.88	13.96	4.52	1.02	15.31	6.68
4.08	0.06	12.70	0.44	12.24	12.24	2E+5	0.93	14.80	3.81	0.86	15.31	5.64
25.24	0.36	15.24	0.52	2.38	2.38	2E+5	0.00	0.00	0.00	0.00	26.45	0.00
19.27	0.28	15.24	0.52	3.11	3.11	2E+5	0.51	8.16	9.92	2.25	26.45	8.49
17.49	0.25	15.24	0.52	3.43	3.43	2E+5	0.65	10.37	11.44	2.59	26.45	9.79
14.66	0.21	15.24	0.52	4.09	4.09	2E+5	0.81	12.81	11.85	2.68	26.45	10.14

10.79	0.15	15.24	0.52	5.56	5.56	2E+5	1.00	15.79	10.74	2.43	26.45	9.19
8.38	0.12	15.24	0.52	7.16	7.16	2E+5	1.22	19.37	10.23	2.32	26.45	8.76
4.71	0.07	15.24	0.52	12.73	12.73	2E+5	1.58	25.09	7.46	1.69	26.45	6.38
30.16	0.43	17.77	0.61	2.32	2.32	3E+5	0.00	0.00	0.00	0.00	42.00	0.00
26.18	0.37	17.77	0.61	2.67	2.67	3E+5	0.44	7.05	11.65	2.64	42.00	6.28
23.67	0.34	17.77	0.61	2.96	2.96	3E+5	0.74	11.80	17.61	3.99	42.00	9.49
16.86	0.24	17.77	0.61	4.15	4.15	3E+5	1.25	19.75	21.00	4.76	42.00	11.32
10.79	0.15	17.77	0.61	6.49	6.49	3E+5	1.63	25.91	17.62	3.99	42.00	9.50
8.90	0.13	17.77	0.61	7.86	7.86	3E+5	1.84	29.11	16.34	3.70	42.00	8.81
5.34	0.08	17.77	0.61	13.10	13.10	3E+5	2.04	32.32	10.89	2.47	42.00	5.87
32.88	0.47	20.31	0.70	2.43	2.43	3E+5	0.00	0.00	0.00	0.00	62.70	0.00
28.59	0.41	20.31	0.70	2.80	2.80	3E+5	0.71	11.29	20.35	4.61	62.70	7.35
24.50	0.35	20.31	0.70	3.26	3.26	3E+5	1.08	17.19	26.56	6.01	62.70	9.59
18.54	0.26	20.31	0.70	4.31	4.31	3E+5	1.54	24.50	28.63	6.48	62.70	10.34
11.94	0.17	20.31	0.70	6.70	6.70	3E+5	2.26	35.91	27.04	6.12	62.70	9.76
10.26	0.15	20.31	0.70	7.79	7.79	3E+5	2.51	39.76	25.73	5.83	62.70	9.29
5.55	0.08	20.31	0.70	14.41	14.41	3E+5	2.86	45.27	15.85	3.59	62.70	5.72
38.96	0.56	22.85	0.78	2.31	2.31	4E+5	0.00	0.00	0.00	0.00	89.27	0.00
34.56	0.49	22.85	0.78	2.60	2.60	4E+5	0.52	8.21	17.89	4.05	89.27	4.54
27.23	0.39	22.85	0.78	3.30	3.30	4E+5	1.31	20.78	35.68	8.08	89.27	9.05
20.73	0.30	22.85	0.78	4.34	4.34	4E+5	1.98	31.42	41.09	9.30	89.27	10.42
15.60	0.22	22.85	0.78	5.77	5.77	4E+5	2.59	41.04	40.38	9.15	89.27	10.24
13.30	0.19	22.85	0.78	6.77	6.77	4E+5	2.98	47.20	39.58	8.96	89.27	10.04
9.84	0.14	22.85	0.78	9.14	9.14	4E+5	3.24	51.30	31.85	7.21	89.27	8.08
10.58	0.15	7.49	0.26	2.79	2.79	1E+5	0.00	0.00	0.00	0.00	3.14	0.00
8.69	0.12	7.49	0.26	3.39	3.39	1E+5	0.07	1.14	0.63	0.14	3.14	4.52
5.13	0.07	7.49	0.26	5.75	5.75	1E+5	0.23	3.66	1.18	0.27	3.14	8.53
1.78	0.03	7.49	0.26	16.57	16.57	1E+5	0.31	4.96	0.56	0.13	3.14	4.01
15.92	0.23	10.59	0.36	2.62	2.62	2E+5	0.00	0.00	0.00	0.00	8.89	0.00
13.40	0.19	10.59	0.36	3.11	3.11	2E+5	0.11	1.68	1.42	0.32	8.89	3.61
10.68	0.15	10.59	0.36	3.90	3.90	2E+5	0.30	4.80	3.24	0.73	8.89	8.24
8.59	0.12	10.59	0.36	4.86	4.86	2E+5	0.40	6.41	3.47	0.79	8.89	8.84
4.71	0.07	10.59	0.36	8.85	8.85	2E+5	0.56	8.92	2.65	0.60	8.89	6.75
1.47	0.02	10.59	0.36	28.45	28.45	2E+5	0.67	10.68	0.99	0.22	8.89	2.51
20.63	0.29	12.70	0.44	2.42	2.42	2E+5	0.00	0.00	0.00	0.00	15.31	0.00
16.44	0.23	12.70	0.44	3.04	3.04	2E+5	0.29	4.58	4.74	1.07	15.31	7.02
14.03	0.20	12.70	0.44	3.56	3.56	2E+5	0.44	7.02	6.21	1.41	15.31	9.19
13.30	0.19	12.70	0.44	3.76	3.76	2E+5	0.51	8.01	6.72	1.52	15.31	9.94
8.48	0.12	12.70	0.44	5.89	5.89	2E+5	0.74	11.75	6.28	1.42	15.31	9.29
5.76	0.08	12.70	0.44	8.68	8.68	2E+5	0.83	13.12	4.76	1.08	15.31	7.05
3.46	0.05	12.70	0.44	14.46	14.46	2E+5	0.94	14.95	3.26	0.74	15.31	4.82

25.66	0.37	15.24	0.52	2.34	2.34	2E+5	0.00	0.00	0.00	0.00	26.45	0.00
23.04	0.33	15.24	0.52	2.60	2.60	2E+5	0.22	3.51	5.10	1.15	26.45	4.36
22.20	0.32	15.24	0.52	2.70	2.70	2E+5	0.33	5.26	7.37	1.67	26.45	6.31
20.73	0.30	15.24	0.52	2.89	2.89	2E+5	0.44	7.02	9.17	2.08	26.45	7.85
18.22	0.26	15.24	0.52	3.29	3.29	2E+5	0.64	10.22	11.74	2.66	26.45	10.05
12.99	0.19	15.24	0.52	4.62	4.62	2E+5	0.89	14.03	11.49	2.60	26.45	9.84
6.39	0.09	15.24	0.52	9.39	9.39	2E+5	1.39	22.12	8.91	2.02	26.45	7.63
29.22	0.42	17.77	0.61	2.40	2.40	3E+5	0.00	0.00	0.00	0.00	42.00	0.00
24.82	0.35	17.77	0.61	2.82	2.82	3E+5	0.63	10.00	15.66	3.55	42.00	8.44
21.78	0.31	17.77	0.61	3.21	3.21	3E+5	0.86	13.59	18.67	4.23	42.00	10.07
17.49	0.25	17.77	0.61	4.00	4.00	3E+5	1.16	18.34	20.23	4.58	42.00	10.91
9.11	0.13	17.77	0.61	7.68	7.68	3E+5	1.73	27.45	15.77	3.57	42.00	8.50
5.34	0.08	17.77	0.61	13.10	13.10	3E+5	2.04	32.32	10.89	2.47	42.00	5.87
3.87	0.06	17.77	0.61	18.06	18.06	3E+5	2.16	34.24	8.37	1.89	42.00	4.51
34.77	0.50	20.31	0.70	2.30	2.30	3E+5	0.00	0.00	0.00	0.00	62.70	0.00
29.22	0.42	20.31	0.70	2.74	2.74	3E+5	0.77	12.18	22.45	5.08	62.70	8.11
26.18	0.37	20.31	0.70	3.05	3.05	3E+5	1.02	16.16	26.68	6.04	62.70	9.64
20.73	0.30	20.31	0.70	3.86	3.86	3E+5	1.47	23.34	30.52	6.91	62.70	11.02
16.86	0.24	20.31	0.70	4.74	4.74	3E+5	1.76	27.83	29.59	6.70	62.70	10.69
14.14	0.20	20.31	0.70	5.66	5.66	3E+5	2.04	32.32	28.81	6.53	62.70	10.41
11.10	0.16	20.31	0.70	7.20	7.20	3E+5	2.43	38.47	26.93	6.10	62.70	9.73
38.64	0.55	22.85	0.78	2.33	2.33	4E+5	0.00	0.00	0.00	0.00	89.27	0.00
35.60	0.51	22.85	0.78	2.53	2.53	4E+5	0.38	6.03	13.53	3.07	89.27	3.43
31.42	0.45	22.85	0.78	2.86	2.86	4E+5	0.92	14.62	28.97	6.56	89.27	7.35
23.35	0.33	22.85	0.78	3.85	3.85	4E+5	1.73	27.45	40.42	9.15	89.27	10.25
18.54	0.26	22.85	0.78	4.85	4.85	4E+5	2.22	35.14	41.08	9.30	89.27	10.42
12.78	0.18	22.85	0.78	7.04	7.04	4E+5	3.03	48.09	38.75	8.78	89.27	9.83
7.02	0.10	22.85	0.78	12.82	12.82	4E+5	3.44	54.51	24.12	5.46	89.27	6.12

APPENDIX D

SCALED DRAG TABLES

NACA 65-018 3 Bladed Turbine with 48% Solidity					
Vm (m/s)	**Vp (m/s)**	**Rem**	**Rep**	**Dm (N)**	**Dp (N)**
8.25	0.2829	131906	131906	1.29	41.66
10.58	0.3626	169069	169069	2.53	82.02
13.27	0.4547	212015	212015	4.37	141.39
15.92	0.5456	254418	254418	6.30	203.88
18.57	0.6366	296821	296821	8.46	273.92
21.23	0.7275	339224	339224	10.98	355.42
23.88	0.8185	381627	381627	12.92	418.18

NACA 0020 3 Bladed Turbine with 48% Solidity					
Vm (m/s)	**Vp (m/s)**	**Rem**	**Rep**	**Dm (N)**	**Dp (N)**
8.25	0.2829	131906	131906	1.35	43.74
10.58	0.3626	169069	169069	2.73	88.27
13.27	0.4547	212015	212015	4.04	130.71
15.92	0.5456	254418	254418	6.09	197.11
18.57	0.6366	296821	296821	8.05	260.64
21.23	0.7275	339224	339224	10.96	354.64
23.88	0.8185	381627	381627	13.23	428.07

NACA 0022 3 Bladed Turbine with 48% Solidity					
Vm (m/s)	**Vp (m/s)**	**Rem**	**Rep**	**Dm (N)**	**Dp (N)**
8.25	0.2829	131906	131906	1.39	45.05
10.58	0.3626	169069	169069	2.64	85.41
13.27	0.4547	212015	212015	4.32	139.83
15.92	0.5456	254418	254418	6.49	209.87
18.57	0.6366	296821	296821	8.46	273.92
21.23	0.7275	339224	339224	10.58	342.40
23.88	0.8185	381627	381627	12.52	405.16

NACA 0022 6 Bladed Turbine with 48% Solidity					
Vm (m/s)	**Vp (m/s)**	**Rem**	**Rep**	**Dm (N)**	**Dp (N)**
8.25	0.2829	131906	131906	1.07	34.63
10.58	0.3626	169069	169069	2.16	69.78
13.27	0.4547	212015	212015	3.60	116.65
15.92	0.5456	254418	254418	5.49	177.58
18.57	0.6366	296821	296821	7.56	244.50
21.23	0.7275	339224	339224	9.86	319.23
23.88	0.8185	381627	381627	12.10	391.62

NACA 0022 3 Bladed Turbine with 41% Solidity					
Vm (m/s)	**Vp (m/s)**	**Rem**	**Rep**	**Dm (N)**	**Dp (N)**
8.25	0.2829	131906	131906	1.03	33.33
10.58	0.3626	169069	169069	1.93	62.49
13.27	0.4547	212015	212015	3.19	103.37
15.92	0.5456	254418	254418	4.72	152.58
18.57	0.6366	296821	296821	6.20	200.76
21.23	0.7275	339224	339224	8.14	263.51
23.88	0.8185	381627	381627	9.76	315.84

NACA 0022 3 Bladed Turbine with 55% Solidity					
Vm (m/s)	**Vp (m/s)**	**Rem**	**Rep**	**Dm (N)**	**Dp (N)**
8.25	0.2829	131906	131906	1.82	58.85
10.58	0.3626	169069	169069	3.60	116.65
13.27	0.4547	212015	212015	5.58	180.45
15.92	0.5456	254418	254418	7.53	243.72
18.57	0.6366	296821	296821	10.16	328.86
21.23	0.7275	339224	339224	12.87	416.61
23.88	0.8185	381627	381627	15.27	494.21

NACA 0022 2 Bladed Turbine with 41% Solidity					
Vm (m/s)	**Vp (m/s)**	**Rem**	**Rep**	**Dm (N)**	**Dp (N)**
7.65	0.2623	122283	122283	1.14	36.97
10.59	0.3631	169294	169294	2.20	71.08
12.79	0.4382	204335	204335	3.32	107.28
15.34	0.5259	245202	245202	5.19	167.95
17.90	0.6135	286068	286068	6.90	223.15
20.46	0.7012	326935	326935	9.37	303.35
23.01	0.7888	367802	367802	11.52	372.87

APPENDIX E

EFFICIENCY UNCERTAINTY TABLES

NACA 65_3-018 3 BLADES, 48% SOLIDITY					
PA (W)	Efficiency (%)	del_rho	del_V	del_η	del_η*eff
20	0.00	0.0018	0.1358		
20	2.29	0.0018	0.1358	1.0413	2.38
20	2.33	0.0018	0.1358	0.5825	1.36
20	1.32	0.0018	0.1358	0.4458	0.59
55	0.00	0.0018	0.0691		
55	2.35	0.0018	0.0691	0.6245	1.47
55	2.69	0.0018	0.0691	0.4344	1.17
55	2.95	0.0018	0.0691	0.3338	0.98
55	2.27	0.0018	0.0691	0.2651	0.60
55	1.82	0.0018	0.0691	0.2397	0.44
123	0.00	0.0018	0.0402		
123	1.24	0.0018	0.0402	0.9175	1.14
123	2.52	0.0018	0.0402	0.3633	0.91
123	3.10	0.0018	0.0402	0.1855	0.57
123	2.68	0.0018	0.0402	0.1540	0.41
123	2.16	0.0018	0.0402	0.1381	0.30
123	1.52	0.0018	0.0402	0.1367	0.21
187	0.00	0.0018	0.0304		
187	0.92	0.0018	0.0304	1.0397	0.96
187	2.42	0.0018	0.0304	0.3395	0.82
187	3.45	0.0018	0.0304	0.1825	0.63
187	3.51	0.0018	0.0304	0.1311	0.46
187	2.52	0.0018	0.0304	0.1046	0.26
187	1.73	0.0018	0.0304	0.1021	0.18
297	0.00	0.0018	0.0223		
297	1.88	0.0018	0.0223	0.3395	0.64
297	2.68	0.0018	0.0223	0.2087	0.56
297	3.52	0.0018	0.0223	0.1335	0.47
297	3.40	0.0018	0.0223	0.0988	0.34
297	3.17	0.0018	0.0223	0.0847	0.27
297	2.46	0.0018	0.0223	0.0782	0.19
444	0.00	0.0018	0.0171		
444	1.88	0.0018	0.0171	0.2694	0.51
444	2.73	0.0018	0.0171	0.1651	0.45
444	3.36	0.0018	0.0171	0.1241	0.42
444	3.54	0.0018	0.0171	0.0790	0.28
444	3.12	0.0018	0.0171	0.0666	0.21
444	1.62	0.0018	0.0171	0.0674	0.11
632	0.00	0.0018	0.0135		

632	1.93	0.0018	0.0135	0.2143	0.41
632	3.36	0.0018	0.0135	0.0972	0.33
632	3.55	0.0018	0.0135	0.0720	0.26
632	3.37	0.0018	0.0135	0.0585	0.20
632	2.79	0.0018	0.0135	0.0526	0.15
632	1.75	0.0018	0.0135	0.0547	0.10
20	0.00	0.0018	0.1358		
20	1.53	0.0018	0.1358	1.5605	2.38
20	2.20	0.0018	0.1358	0.9766	2.14
20	3.46	0.0018	0.1358	0.4639	1.60
55	0.00	0.0018	0.0691		
55	1.55	0.0018	0.0691	0.9751	1.51
55	2.24	0.0018	0.0691	0.5208	1.17
55	2.70	0.0018	0.0691	0.3645	0.98
55	2.58	0.0018	0.0691	0.2820	0.73
55	1.28	0.0018	0.0691	0.2298	0.29
123	0.00	0.0018	0.0402		
123	1.24	0.0018	0.0402	0.7800	0.96
123	1.77	0.0018	0.0402	0.4878	0.86
123	2.18	0.0018	0.0402	0.3552	0.77
123	3.02	0.0018	0.0402	0.2340	0.71
123	2.65	0.0018	0.0402	0.1995	0.53
123	2.40	0.0018	0.0402	0.1713	0.41
187	0.00	0.0018	0.0304		
187	1.55	0.0018	0.0304	0.5201	0.81
187	2.14	0.0018	0.0304	0.3471	0.74
187	2.88	0.0018	0.0304	0.2336	0.67
187	3.46	0.0018	0.0304	0.1590	0.55
187	3.09	0.0018	0.0304	0.1239	0.38
187	2.45	0.0018	0.0304	0.1086	0.27
297	0.00	0.0018	0.0223		
297	1.72	0.0018	0.0223	0.3717	0.64
297	2.97	0.0018	0.0223	0.1888	0.56
297	3.53	0.0018	0.0223	0.1263	0.45
297	3.36	0.0018	0.0223	0.0940	0.32
297	2.91	0.0018	0.0223	0.0844	0.25
297	2.35	0.0018	0.0223	0.0787	0.18
444	0.00	0.0018	0.0171		
444	2.18	0.0018	0.0171	0.2234	0.49
444	3.11	0.0018	0.0171	0.1356	0.42
444	3.69	0.0018	0.0171	0.0901	0.33

444	3.54	0.0018	0.0171	0.0729	0.26
444	3.21	0.0018	0.0171	0.0683	0.22
444	2.36	0.0018	0.0171	0.0626	0.15
632	0.00	0.0018	0.0135		
632	2.51	0.0018	0.0135	0.1523	0.38
632	3.75	0.0018	0.0135	0.0831	0.31
632	3.51	0.0018	0.0135	0.0621	0.22
632	3.20	0.0018	0.0135	0.0555	0.18
632	2.74	0.0018	0.0135	0.0526	0.14
632	2.39	0.0018	0.0135	0.0496	0.12
20	0.00	0.0018	0.1358		
20	1.68	0.0018	0.1358	1.4189	2.38
20	2.29	0.0018	0.1358	0.4427	1.01
20	1.28	0.0018	0.1358	0.4071	0.52
55	0.00	0.0018	0.0691		
55	1.36	0.0018	0.0691	1.1142	1.51
55	2.25	0.0018	0.0691	0.5578	1.25
55	2.52	0.0018	0.0691	0.4119	1.04
55	2.32	0.0018	0.0691	0.3734	0.87
55	2.25	0.0018	0.0691	0.2611	0.59
123	0.00	0.0018	0.0402		
123	1.99	0.0018	0.0402	0.4592	0.91
123	1.79	0.0018	0.0402	0.4221	0.75
123	2.36	0.0018	0.0402	0.2846	0.67
123	2.45	0.0018	0.0402	0.2414	0.59
123	2.62	0.0018	0.0402	0.1948	0.51
123	2.04	0.0018	0.0402	0.1674	0.34
187	0.00	0.0018	0.0304		
187	1.69	0.0018	0.0304	0.5034	0.85
187	2.44	0.0018	0.0304	0.2743	0.67
187	2.43	0.0018	0.0304	0.2524	0.61
187	2.62	0.0018	0.0304	0.2238	0.59
187	2.85	0.0018	0.0304	0.1609	0.46
187	2.29	0.0018	0.0304	0.1077	0.25
297	0.00	0.0018	0.0223		
297	2.43	0.0018	0.0223	0.2443	0.59
297	3.30	0.0018	0.0223	0.1431	0.47
297	3.46	0.0018	0.0223	0.1216	0.42
297	3.54	0.0018	0.0223	0.1088	0.38
297	2.56	0.0018	0.0223	0.0813	0.21
297	1.61	0.0018	0.0223	0.0833	0.13

444	0.00	0.0018	0.0171		
444	2.12	0.0018	0.0171	0.2405	0.51
444	2.41	0.0018	0.0171	0.2007	0.48
444	3.36	0.0018	0.0171	0.1091	0.37
444	3.38	0.0018	0.0171	0.0771	0.26
444	2.55	0.0018	0.0171	0.0656	0.17
444	1.53	0.0018	0.0171	0.0689	0.11
632	0.00	0.0018	0.0135		
632	2.41	0.0018	0.0135	0.1584	0.38
632	3.75	0.0018	0.0135	0.0731	0.27
632	3.49	0.0018	0.0135	0.0602	0.21
632	2.94	0.0018	0.0135	0.0562	0.16
632	2.02	0.0018	0.0135	0.0522	0.11
632	1.92	0.0018	0.0135	0.0525	0.10

NACA 0020 3 BLADES, 48% SOLIDITY					
PA (W)	**Efficiency (%)**	**del_rho**	**del_V**	**del_η**	**del_η*eff**
21	0.00	0.0018	0.1312		
21	4.31	0.0018	0.1312	0.8224	3.54
21	4.90	0.0018	0.1312	0.4493	2.20
21	4.80	0.0018	0.1312	0.3134	1.50
53	0.00	0.0018	0.0703		
53	3.79	0.0018	0.0703	0.6785	2.57
53	5.77	0.0018	0.0703	0.2752	1.59
53	5.87	0.0018	0.0703	0.1868	1.10
53	5.88	0.0018	0.0703	0.1465	0.86
53	2.20	0.0018	0.0703	0.1617	0.36
127	0.00	0.0018	0.0394		
127	3.26	0.0018	0.0394	0.4877	1.59
127	4.25	0.0018	0.0394	0.3470	1.47
127	5.92	0.0018	0.0394	0.1890	1.12
127	7.44	0.0018	0.0394	0.1176	0.88
127	6.43	0.0018	0.0394	0.1049	0.67
127	3.55	0.0018	0.0394	0.0993	0.35
189	0.00	0.0018	0.0303		
189	4.19	0.0018	0.0303	0.3187	1.33
189	6.66	0.0018	0.0303	0.1865	1.24
189	8.73	0.0018	0.0303	0.1084	0.95
189	8.16	0.0018	0.0303	0.0993	0.81
189	7.17	0.0018	0.0303	0.0802	0.58

189	3.67	0.0018	0.0303	0.0714	0.26
300	0.00	0.0018	0.0222		
300	1.64	0.0018	0.0222	0.6782	1.11
300	4.95	0.0018	0.0222	0.2032	1.01
300	9.01	0.0018	0.0222	0.0856	0.77
300	8.25	0.0018	0.0222	0.0686	0.57
300	6.10	0.0018	0.0222	0.0573	0.35
300	4.97	0.0018	0.0222	0.0529	0.26
447	0.00	0.0018	0.0170		
447	5.61	0.0018	0.0170	0.1278	0.72
447	7.60	0.0018	0.0170	0.0921	0.70
447	8.11	0.0018	0.0170	0.0797	0.65
447	8.36	0.0018	0.0170	0.0613	0.51
447	8.09	0.0018	0.0170	0.0500	0.40
447	8.48	0.0018	0.0170	0.0410	0.35
637	0.00	0.0018	0.0135		
637	4.92	0.0018	0.0135	0.1215	0.60
637	8.80	0.0018	0.0135	0.0585	0.52
637	8.13	0.0018	0.0135	0.0429	0.35
637	7.42	0.0018	0.0135	0.0354	0.26
637	5.94	0.0018	0.0135	0.0338	0.20
637	4.20	0.0018	0.0135	0.0377	0.16
21	0.00	0.0018	0.1312		
21	3.33	0.0018	0.1312	1.0409	3.47
21	4.63	0.0018	0.1312	0.4907	2.27
21	4.54	0.0018	0.1312	0.2837	1.29
53	0.00	0.0018	0.0703		
53	4.14	0.0018	0.0703	0.6243	2.58
53	5.90	0.0018	0.0703	0.2348	1.38
53	5.12	0.0018	0.0703	0.1588	0.81
53	2.77	0.0018	0.0703	0.1554	0.43
53	1.64	0.0018	0.0703	0.1940	0.32
127	0.00	0.0018	0.0394		
127	5.09	0.0018	0.0394	0.2948	1.50
127	5.79	0.0018	0.0394	0.2145	1.24
127	6.71	0.0018	0.0394	0.1409	0.94
127	5.78	0.0018	0.0394	0.1120	0.65
127	3.73	0.0018	0.0394	0.1004	0.37
127	2.74	0.0018	0.0394	0.1008	0.28
189	0.00	0.0018	0.0303		
189	3.81	0.0018	0.0303	0.3548	1.35

189	5.26	0.0018	0.0303	0.2405	1.26
189	8.13	0.0018	0.0303	0.1056	0.86
189	8.56	0.0018	0.0303	0.0893	0.76
189	7.30	0.0018	0.0303	0.0784	0.57
189	3.33	0.0018	0.0303	0.0733	0.24
300	0.00	0.0018	0.0222		
300	2.10	0.0018	0.0222	0.5201	1.09
300	7.72	0.0018	0.0222	0.1167	0.90
300	8.77	0.0018	0.0222	0.0893	0.78
300	8.42	0.0018	0.0222	0.0655	0.55
300	6.27	0.0018	0.0222	0.0571	0.36
300	3.11	0.0018	0.0222	0.0591	0.18
447	0.00	0.0018	0.0170		
447	1.69	0.0018	0.0170	0.4876	0.82
447	3.08	0.0018	0.0170	0.2604	0.80
447	4.75	0.0018	0.0170	0.1568	0.75
447	7.03	0.0018	0.0170	0.0988	0.69
447	8.24	0.0018	0.0170	0.0682	0.56
447	8.04	0.0018	0.0170	0.0474	0.38
637	0.00	0.0018	0.0135		
637	7.52	0.0018	0.0135	0.0759	0.57
637	8.72	0.0018	0.0135	0.0504	0.44
637	8.39	0.0018	0.0135	0.0391	0.33
637	8.17	0.0018	0.0135	0.0347	0.28
637	6.45	0.0018	0.0135	0.0332	0.21
637	5.21	0.0018	0.0135	0.0339	0.18
21	0.00	0.0018	0.1312		
21	3.44	0.0018	0.1312	0.9760	3.35
21	5.48	0.0018	0.1312	0.4904	2.69
21	2.56	0.0018	0.1312	0.2888	0.74
53	0.00	0.0018	0.0703		
53	2.54	0.0018	0.0703	1.1141	2.83
53	6.20	0.0018	0.0703	0.2189	1.36
53	5.70	0.0018	0.0703	0.1849	1.05
53	5.81	0.0018	0.0703	0.1552	0.90
53	2.58	0.0018	0.0703	0.1524	0.39
127	0.00	0.0018	0.0394		
127	2.05	0.0018	0.0394	0.8209	1.68
127	4.96	0.0018	0.0394	0.3124	1.55
127	6.79	0.0018	0.0394	0.1707	1.16
127	5.95	0.0018	0.0394	0.1269	0.76

127	6.05	0.0018	0.0394	0.1064	0.64
127	4.18	0.0018	0.0394	0.0983	0.41
189	0.00	0.0018	0.0303		
189	3.48	0.0018	0.0303	0.4107	1.43
189	8.51	0.0018	0.0303	0.1260	1.07
189	7.72	0.0018	0.0303	0.0928	0.72
189	5.83	0.0018	0.0303	0.0726	0.42
189	3.38	0.0018	0.0303	0.0737	0.25
189	1.79	0.0018	0.0303	0.0986	0.18
300	0.00	0.0018	0.0222		
300	2.09	0.0018	0.0222	0.5201	1.09
300	5.00	0.0018	0.0222	0.2006	1.00
300	6.80	0.0018	0.0222	0.1321	0.90
300	8.44	0.0018	0.0222	0.0713	0.60
300	6.87	0.0018	0.0222	0.0594	0.41
300	4.69	0.0018	0.0222	0.0538	0.25
447	0.00	0.0018	0.0170		
447	6.39	0.0018	0.0170	0.1126	0.72
447	7.55	0.0018	0.0170	0.0906	0.68
447	8.22	0.0018	0.0170	0.0747	0.61
447	7.74	0.0018	0.0170	0.0566	0.44
447	7.29	0.0018	0.0170	0.0449	0.33
447	7.47	0.0018	0.0170	0.0417	0.31
637	0.00	0.0018	0.0135		
637	3.06	0.0018	0.0135	0.2214	0.68
637	6.23	0.0018	0.0135	0.0969	0.60
637	9.15	0.0018	0.0135	0.0563	0.52
637	8.84	0.0018	0.0135	0.0482	0.43
637	8.39	0.0018	0.0135	0.0451	0.38
637	8.13	0.0018	0.0135	0.0370	0.30

NACA 0022 3 BLADES, 48% SOLIDITY					
PA (W)	**Efficiency (%)**	**del_rho**	**del_V**	**del_η**	**del_η*eff**
28	0.00	0.0018	0.1064		
28	2.30	0.0018	0.1064	1.2002	2.76
28	3.76	0.0018	0.1064	0.5793	2.18
28	1.00	0.0018	0.1064	0.3312	0.33
78	0.00	0.0018	0.0539		
78	3.00	0.0018	0.0539	0.4462	1.34
78	3.19	0.0018	0.0539	0.3475	1.11

78	3.05	0.0018	0.0539	0.2752	0.84
78	3.06	0.0018	0.0539	0.2386	0.73
78	0.67	0.0018	0.0539	0.2409	0.16
138	0.00	0.0018	0.0369		
138	3.36	0.0018	0.0369	0.3808	1.28
138	4.21	0.0018	0.0369	0.2696	1.13
138	4.77	0.0018	0.0369	0.1847	0.88
138	3.94	0.0018	0.0369	0.1328	0.52
138	3.32	0.0018	0.0369	0.1209	0.40
138	1.61	0.0018	0.0369	0.1212	0.20
239	0.00	0.0018	0.0256		
239	1.21	0.0018	0.0256	0.8432	1.02
239	2.63	0.0018	0.0256	0.3571	0.94
239	5.94	0.0018	0.0256	0.1048	0.62
239	5.98	0.0018	0.0256	0.0897	0.54
239	5.45	0.0018	0.0256	0.0759	0.41
239	2.18	0.0018	0.0256	0.0802	0.18
379	0.00	0.0018	0.0189		
379	3.86	0.0018	0.0189	0.1862	0.72
379	6.12	0.0018	0.0189	0.0943	0.58
379	6.49	0.0018	0.0189	0.0799	0.52
379	5.67	0.0018	0.0189	0.0644	0.37
379	3.26	0.0018	0.0189	0.0575	0.19
379	1.63	0.0018	0.0189	0.0721	0.12
566	0.00	0.0018	0.0144		
566	5.23	0.0018	0.0144	0.0980	0.51
566	6.50	0.0018	0.0144	0.0732	0.48
566	6.24	0.0018	0.0144	0.0619	0.39
566	5.54	0.0018	0.0144	0.0529	0.29
566	4.24	0.0018	0.0144	0.0459	0.19
566	3.17	0.0018	0.0144	0.0451	0.14
805	0.00	0.0018	0.0114		
805	4.11	0.0018	0.0114	0.1103	0.45
805	5.84	0.0018	0.0114	0.0682	0.40
805	5.70	0.0018	0.0114	0.0570	0.33
805	5.55	0.0018	0.0114	0.0415	0.23
805	5.28	0.0018	0.0114	0.0371	0.20
805	3.56	0.0018	0.0114	0.0363	0.13
28	0.00	0.0018	0.1064		
28	3.07	0.0018	0.1064	0.7439	2.29
28	2.23	0.0018	0.1064	0.4912	1.09

28	1.67	0.0018	0.1064	0.4094	0.68
78	0.00	0.0018	0.0539		
78	2.75	0.0018	0.0539	0.6242	1.72
78	3.38	0.0018	0.0539	0.3070	1.04
78	3.14	0.0018	0.0539	0.2575	0.81
78	1.62	0.0018	0.0539	0.1972	0.32
78	0.60	0.0018	0.0539	0.2549	0.15
138	0.00	0.0018	0.0369		
138	2.67	0.0018	0.0369	0.5201	1.39
138	3.93	0.0018	0.0369	0.2743	1.08
138	4.06	0.0018	0.0369	0.1986	0.81
138	3.94	0.0018	0.0369	0.1534	0.61
138	3.86	0.0018	0.0369	0.1382	0.53
138	2.63	0.0018	0.0369	0.1252	0.33
239	0.00	0.0018	0.0256		
239	2.60	0.0018	0.0256	0.3713	0.97
239	5.13	0.0018	0.0256	0.1460	0.75
239	5.27	0.0018	0.0256	0.1337	0.70
239	6.39	0.0018	0.0256	0.0818	0.52
239	5.29	0.0018	0.0256	0.0670	0.35
239	1.05	0.0018	0.0256	0.1213	0.13
379	0.00	0.0018	0.0189		
379	3.23	0.0018	0.0189	0.2324	0.75
379	4.39	0.0018	0.0189	0.1505	0.66
379	6.16	0.0018	0.0189	0.0892	0.55
379	6.70	0.0018	0.0189	0.0762	0.51
379	4.82	0.0018	0.0189	0.0634	0.31
379	2.28	0.0018	0.0189	0.0616	0.14
566	0.00	0.0018	0.0144		
566	1.95	0.0018	0.0144	0.3095	0.60
566	5.25	0.0018	0.0144	0.1000	0.52
566	6.26	0.0018	0.0144	0.0712	0.45
566	5.56	0.0018	0.0144	0.0589	0.33
566	4.67	0.0018	0.0144	0.0482	0.23
566	3.82	0.0018	0.0144	0.0444	0.17
805	0.00	0.0018	0.0114		
805	5.84	0.0018	0.0114	0.0660	0.39
805	5.74	0.0018	0.0114	0.0529	0.30
805	5.66	0.0018	0.0114	0.0391	0.22
805	4.85	0.0018	0.0114	0.0358	0.17
805	3.69	0.0018	0.0114	0.0355	0.13

805	2.62	0.0018	0.0114	0.0419	0.11
28	0.00	0.0018	0.1064		
28	3.78	0.0018	0.1064	0.5396	2.04
28	2.09	0.0018	0.1064	0.4066	0.85
28	0.92	0.0018	0.1064	0.3763	0.35
78	0.00	0.0018	0.0539		
78	2.87	0.0018	0.0539	0.5780	1.66
78	3.52	0.0018	0.0539	0.4006	1.41
78	3.35	0.0018	0.0539	0.1981	0.66
78	1.80	0.0018	0.0539	0.1804	0.32
78	0.91	0.0018	0.0539	0.2070	0.19
138	0.00	0.0018	0.0369		
138	2.49	0.0018	0.0369	0.5572	1.39
138	3.85	0.0018	0.0369	0.3125	1.20
138	4.04	0.0018	0.0369	0.2176	0.88
138	4.28	0.0018	0.0369	0.1766	0.76
138	4.05	0.0018	0.0369	0.1563	0.63
138	2.44	0.0018	0.0369	0.1094	0.27
239	0.00	0.0018	0.0256		
239	4.61	0.0018	0.0256	0.1792	0.83
239	6.71	0.0018	0.0256	0.0880	0.59
239	6.09	0.0018	0.0256	0.0800	0.49
239	5.72	0.0018	0.0256	0.0762	0.44
239	5.07	0.0018	0.0256	0.0747	0.38
239	1.88	0.0018	0.0256	0.0833	0.16
379	0.00	0.0018	0.0189		
379	2.62	0.0018	0.0189	0.2902	0.76
379	6.23	0.0018	0.0189	0.0908	0.57
379	6.75	0.0018	0.0189	0.0720	0.49
379	5.19	0.0018	0.0189	0.0615	0.32
379	3.72	0.0018	0.0189	0.0575	0.21
379	2.06	0.0018	0.0189	0.0640	0.13
566	0.00	0.0018	0.0144		
566	6.04	0.0018	0.0144	0.0830	0.50
566	6.39	0.0018	0.0144	0.0749	0.48
566	5.95	0.0018	0.0144	0.0642	0.38
566	5.07	0.0018	0.0144	0.0508	0.26
566	4.43	0.0018	0.0144	0.0465	0.21
566	3.50	0.0018	0.0144	0.0439	0.15
805	0.00	0.0018	0.0114		
805	2.94	0.0018	0.0114	0.1607	0.47

805	4.77	0.0018	0.0114	0.0923	0.44
805	5.69	0.0018	0.0114	0.0559	0.32
805	5.44	0.0018	0.0114	0.0419	0.23
805	4.87	0.0018	0.0114	0.0359	0.17
805	2.92	0.0018	0.0114	0.0391	0.11

NACA 0022 6 BLADES, 48% SOLIDITY					
PA (W)	**Efficiency (%)**	**del_rho**	**del_V**	**del_η**	**del_η*eff**
27	0.00	0.0018	0.1094		
27	1.45	0.0018	0.1094	1.0409	1.51
27	1.56	0.0018	0.1094	0.5821	0.91
27	0.67	0.0018	0.1094	0.4455	0.30
72	0.00	0.0018	0.0571		
72	1.53	0.0018	0.0571	0.5784	0.89
72	1.58	0.0018	0.0571	0.5208	0.82
72	1.68	0.0018	0.0571	0.4230	0.71
72	1.67	0.0018	0.0571	0.3823	0.64
72	1.06	0.0018	0.0571	0.2795	0.30
132	0.00	0.0018	0.0381		
132	1.05	0.0018	0.0381	0.7429	0.78
132	1.25	0.0018	0.0381	0.5780	0.72
132	1.97	0.0018	0.0381	0.2381	0.47
132	1.95	0.0018	0.0381	0.2160	0.42
132	1.36	0.0018	0.0381	0.1898	0.26
132	1.19	0.0018	0.0381	0.1765	0.21
228	0.00	0.0018	0.0265		
228	0.99	0.0018	0.0265	0.6001	0.59
228	1.52	0.0018	0.0265	0.3550	0.54
228	2.06	0.0018	0.0265	0.1987	0.41
228	2.12	0.0018	0.0265	0.1565	0.33
228	1.77	0.0018	0.0265	0.1258	0.22
228	1.12	0.0018	0.0265	0.1183	0.13
362	0.00	0.0018	0.0195		
362	1.38	0.0018	0.0195	0.3124	0.43
362	2.28	0.0018	0.0195	0.1498	0.34
362	2.54	0.0018	0.0195	0.1001	0.25
362	2.17	0.0018	0.0195	0.0921	0.20
362	1.27	0.0018	0.0195	0.0826	0.10
362	0.83	0.0018	0.0195	0.1053	0.09
540	0.00	0.0018	0.0149		

540	1.27	0.0018	0.0149	0.2605	0.33
540	1.83	0.0018	0.0149	0.1586	0.29
540	2.29	0.0018	0.0149	0.1130	0.26
540	2.44	0.0018	0.0149	0.0749	0.18
540	2.05	0.0018	0.0149	0.0635	0.13
540	1.40	0.0018	0.0149	0.0658	0.09
768	0.00	0.0018	0.0118		
768	2.25	0.0018	0.0118	0.1048	0.24
768	2.52	0.0018	0.0118	0.0871	0.22
768	2.66	0.0018	0.0118	0.0712	0.19
768	2.39	0.0018	0.0118	0.0555	0.13
768	1.61	0.0018	0.0118	0.0542	0.09
768	1.21	0.0018	0.0118	0.0590	0.07
27	0.00	0.0018	0.1094		
27	1.55	0.0018	0.1094	0.9189	1.42
27	1.75	0.0018	0.1094	0.6807	1.19
27	1.01	0.0018	0.1094	0.4755	0.48
72	0.00	0.0018	0.0571		
72	1.22	0.0018	0.0571	0.8668	1.06
72	1.42	0.0018	0.0571	0.6245	0.89
72	1.57	0.0018	0.0571	0.4738	0.74
72	1.54	0.0018	0.0571	0.3919	0.60
72	0.39	0.0018	0.0571	0.3294	0.13
132	0.00	0.0018	0.0381		
132	1.01	0.0018	0.0381	0.7800	0.79
132	1.16	0.0018	0.0381	0.6501	0.75
132	1.74	0.0018	0.0381	0.3130	0.54
132	1.93	0.0018	0.0381	0.2454	0.47
132	1.87	0.0018	0.0381	0.1982	0.37
132	0.71	0.0018	0.0381	0.1806	0.13
228	0.00	0.0018	0.0265		
228	0.65	0.0018	0.0265	0.9748	0.63
228	2.21	0.0018	0.0265	0.1659	0.37
228	2.05	0.0018	0.0265	0.1470	0.30
228	1.84	0.0018	0.0265	0.1299	0.24
228	1.14	0.0018	0.0265	0.1187	0.13
228	0.85	0.0018	0.0265	0.1268	0.11
362	0.00	0.0018	0.0195		
362	0.66	0.0018	0.0195	0.7428	0.49
362	1.52	0.0018	0.0195	0.2742	0.42
362	2.18	0.0018	0.0195	0.1620	0.35

362	2.54	0.0018	0.0195	0.0984	0.25
362	1.71	0.0018	0.0195	0.0759	0.13
362	0.76	0.0018	0.0195	0.1125	0.09
540	0.00	0.0018	0.0149		
540	0.87	0.0018	0.0149	0.4107	0.36
540	2.18	0.0018	0.0149	0.1252	0.27
540	2.61	0.0018	0.0149	0.0917	0.24
540	2.62	0.0018	0.0149	0.0747	0.20
540	1.86	0.0018	0.0149	0.0631	0.12
540	1.11	0.0018	0.0149	0.0725	0.08
768	0.00	0.0018	0.0118		
768	0.61	0.0018	0.0118	0.5033	0.31
768	1.25	0.0018	0.0118	0.2234	0.28
768	1.91	0.0018	0.0118	0.1333	0.25
768	2.56	0.0018	0.0118	0.0633	0.16
768	2.11	0.0018	0.0118	0.0540	0.11
768	1.37	0.0018	0.0118	0.0563	0.08
27	0.00	0.0018	0.1094		
27	1.49	0.0018	0.1094	0.9761	1.45
27	1.68	0.0018	0.1094	0.7449	1.25
27	1.51	0.0018	0.1094	0.5823	0.88
72	0.00	0.0018	0.0571		
72	1.29	0.0018	0.0571	0.7095	0.92
72	1.40	0.0018	0.0571	0.5785	0.81
72	1.52	0.0018	0.0571	0.4471	0.68
72	1.51	0.0018	0.0571	0.3652	0.55
72	0.84	0.0018	0.0571	0.2776	0.23
132	0.00	0.0018	0.0381		
132	1.17	0.0018	0.0381	0.6784	0.79
132	1.81	0.0018	0.0381	0.3011	0.54
132	1.80	0.0018	0.0381	0.2799	0.50
132	1.89	0.0018	0.0381	0.2106	0.40
132	1.56	0.0018	0.0381	0.1885	0.29
132	1.11	0.0018	0.0381	0.1701	0.19
228	0.00	0.0018	0.0265		
228	0.84	0.0018	0.0265	0.7428	0.62
228	1.80	0.0018	0.0265	0.2843	0.51
228	2.10	0.0018	0.0265	0.1713	0.36
228	2.19	0.0018	0.0265	0.1521	0.33
228	1.91	0.0018	0.0265	0.1204	0.23
228	0.66	0.0018	0.0265	0.1426	0.09

362	0.00	0.0018	0.0195		
362	1.55	0.0018	0.0195	0.2695	0.42
362	1.86	0.0018	0.0195	0.2116	0.39
362	2.44	0.0018	0.0195	0.1246	0.30
362	2.48	0.0018	0.0195	0.0801	0.20
362	1.38	0.0018	0.0195	0.0798	0.11
362	0.62	0.0018	0.0195	0.1327	0.08
540	0.00	0.0018	0.0149		
540	0.48	0.0018	0.0149	0.8209	0.39
540	1.89	0.0018	0.0149	0.1570	0.30
540	2.65	0.0018	0.0149	0.0741	0.20
540	2.18	0.0018	0.0149	0.0650	0.14
540	1.24	0.0018	0.0149	0.0689	0.09
540	0.78	0.0018	0.0149	0.0910	0.07
768	0.00	0.0018	0.0118		
768	2.03	0.0018	0.0118	0.1186	0.24
768	2.53	0.0018	0.0118	0.0845	0.21
768	2.67	0.0018	0.0118	0.0673	0.18
768	2.36	0.0018	0.0118	0.0550	0.13
768	1.57	0.0018	0.0118	0.0541	0.08
768	1.15	0.0018	0.0118	0.0603	0.07

NACA 0022 3 BLADES, 41% SOLIDITY					
PA (W)	**Efficiency (%)**	**del_rho**	**del_V**	**del_η**	**del_η*eff**
25	0.00	0.0018	0.1158		
25	1.84	0.0018	0.1158	1.4184	2.62
25	2.48	0.0018	0.1158	0.3878	0.96
25	1.75	0.0018	0.1158	0.3152	0.55
74	0.00	0.0018	0.0562		
74	1.13	0.0018	0.0562	1.4178	1.60
74	2.34	0.0018	0.0562	0.4880	1.14
74	2.59	0.0018	0.0562	0.3639	0.94
74	2.06	0.0018	0.0562	0.3024	0.62
74	1.86	0.0018	0.0562	0.2351	0.44
129	0.00	0.0018	0.0388		
129	1.37	0.0018	0.0388	0.9175	1.25
129	1.92	0.0018	0.0388	0.6001	1.15
129	2.48	0.0018	0.0388	0.3904	0.97
129	2.94	0.0018	0.0388	0.2095	0.62
129	2.72	0.0018	0.0388	0.1460	0.40

129	1.92	0.0018	0.0388	0.1275	0.24
222	0.00	0.0018	0.0270		
222	1.53	0.0018	0.0270	0.6000	0.92
222	2.99	0.0018	0.0270	0.2301	0.69
222	3.33	0.0018	0.0270	0.2008	0.67
222	3.77	0.0018	0.0270	0.1636	0.62
222	3.57	0.0018	0.0270	0.1297	0.46
222	3.04	0.0018	0.0270	0.0883	0.27
353	0.00	0.0018	0.0198		
353	0.63	0.0018	0.0198	1.1996	0.76
353	3.08	0.0018	0.0198	0.1801	0.55
353	4.37	0.0018	0.0198	0.0791	0.35
353	3.28	0.0018	0.0198	0.0705	0.23
353	2.15	0.0018	0.0198	0.0704	0.15
353	1.32	0.0018	0.0198	0.0818	0.11
527	0.00	0.0018	0.0152		
527	3.32	0.0018	0.0152	0.1378	0.46
527	3.90	0.0018	0.0152	0.1104	0.43
527	3.97	0.0018	0.0152	0.1021	0.41
527	4.62	0.0018	0.0152	0.0683	0.32
527	3.71	0.0018	0.0152	0.0607	0.23
527	3.14	0.0018	0.0152	0.0565	0.18
750	0.00	0.0018	0.0120		
750	2.34	0.0018	0.0120	0.1863	0.44
750	3.99	0.0018	0.0120	0.0922	0.37
750	4.72	0.0018	0.0120	0.0677	0.32
750	4.39	0.0018	0.0120	0.0568	0.25
750	2.95	0.0018	0.0120	0.0476	0.14
750	1.88	0.0018	0.0120	0.0501	0.09
25	0.00	0.0018	0.1158		
25	2.73	0.0018	0.1158	0.8677	2.37
25	2.75	0.0018	0.1158	0.7813	2.15
25	3.20	0.0018	0.1158	0.4760	1.52
74	0.00	0.0018	0.0562		
74	1.77	0.0018	0.0562	0.7093	1.26
74	2.23	0.0018	0.0562	0.4881	1.09
74	2.36	0.0018	0.0562	0.3266	0.77
74	1.99	0.0018	0.0562	0.2970	0.59
74	1.03	0.0018	0.0562	0.2358	0.24
129	0.00	0.0018	0.0388		
129	1.75	0.0018	0.0388	0.6783	1.19

129	2.13	0.0018	0.0388	0.4591	0.98
129	2.94	0.0018	0.0388	0.3126	0.92
129	3.06	0.0018	0.0388	0.2410	0.74
129	2.97	0.0018	0.0388	0.1814	0.54
129	2.18	0.0018	0.0388	0.1365	0.30
222	0.00	0.0018	0.0270		
222	1.27	0.0018	0.0270	0.7090	0.90
222	2.52	0.0018	0.0270	0.2948	0.74
222	3.33	0.0018	0.0270	0.2008	0.67
222	3.30	0.0018	0.0270	0.1725	0.57
222	2.78	0.0018	0.0270	0.0978	0.27
222	1.60	0.0018	0.0270	0.0959	0.15
353	0.00	0.0018	0.0198		
353	2.30	0.0018	0.0198	0.2840	0.65
353	3.63	0.0018	0.0198	0.1429	0.52
353	4.81	0.0018	0.0198	0.0855	0.41
353	4.47	0.0018	0.0198	0.0770	0.34
353	3.86	0.0018	0.0198	0.0707	0.27
353	1.93	0.0018	0.0198	0.0704	0.14
527	0.00	0.0018	0.0152		
527	0.94	0.0018	0.0152	0.6240	0.59
527	3.24	0.0018	0.0152	0.1494	0.48
527	4.32	0.0018	0.0152	0.0741	0.32
527	3.59	0.0018	0.0152	0.0603	0.22
527	2.66	0.0018	0.0152	0.0554	0.15
527	1.75	0.0018	0.0152	0.0599	0.10
750	0.00	0.0018	0.0120		
750	1.07	0.0018	0.0120	0.4458	0.48
750	2.85	0.0018	0.0120	0.1480	0.42
750	3.91	0.0018	0.0120	0.0927	0.36
750	4.42	0.0018	0.0120	0.0558	0.25
750	2.84	0.0018	0.0120	0.0484	0.14
750	1.55	0.0018	0.0120	0.0536	0.08
25	0.00	0.0018	0.1158		
25	2.84	0.0018	0.1158	0.7442	2.12
25	3.47	0.0018	0.1158	0.3681	1.28
25	2.27	0.0018	0.1158	0.3205	0.73
74	0.00	0.0018	0.0562		
74	2.09	0.0018	0.0562	0.5781	1.21
74	2.25	0.0018	0.0562	0.5038	1.13
74	2.24	0.0018	0.0562	0.3202	0.72

74	1.30	0.0018	0.0562	0.2401	0.31
74	0.73	0.0018	0.0562	0.2472	0.18
129	0.00	0.0018	0.0388		
129	1.47	0.0018	0.0388	0.8665	1.27
129	2.90	0.0018	0.0388	0.2896	0.84
129	3.08	0.0018	0.0388	0.1920	0.59
129	2.57	0.0018	0.0388	0.1581	0.41
129	2.23	0.0018	0.0388	0.1431	0.32
129	0.55	0.0018	0.0388	0.2214	0.12
222	0.00	0.0018	0.0270		
222	2.34	0.0018	0.0270	0.3395	0.79
222	2.78	0.0018	0.0270	0.2522	0.70
222	3.32	0.0018	0.0270	0.1845	0.61
222	3.40	0.0018	0.0270	0.1725	0.59
222	3.53	0.0018	0.0270	0.1195	0.42
222	1.53	0.0018	0.0270	0.0981	0.15
353	0.00	0.0018	0.0198		
353	2.96	0.0018	0.0198	0.1801	0.53
353	4.05	0.0018	0.0198	0.1186	0.48
353	4.35	0.0018	0.0198	0.0902	0.39
353	4.00	0.0018	0.0198	0.0796	0.32
353	2.54	0.0018	0.0198	0.0690	0.18
353	1.56	0.0018	0.0198	0.0758	0.12
527	0.00	0.0018	0.0152		
527	3.09	0.0018	0.0152	0.1538	0.48
527	4.06	0.0018	0.0152	0.1053	0.43
527	4.24	0.0018	0.0152	0.0913	0.39
527	3.95	0.0018	0.0152	0.0611	0.24
527	2.57	0.0018	0.0152	0.0564	0.14
527	1.83	0.0018	0.0152	0.0590	0.11
750	0.00	0.0018	0.0120		
750	3.89	0.0018	0.0120	0.0965	0.38
750	4.52	0.0018	0.0120	0.0710	0.32
750	4.34	0.0018	0.0120	0.0573	0.25
750	3.76	0.0018	0.0120	0.0495	0.19
750	2.46	0.0018	0.0120	0.0484	0.12
750	1.62	0.0018	0.0120	0.0523	0.08

NACA 0022 3 BLADES, 55% SOLIDITY					
PA (W)	**Efficiency (%)**	**del_rho**	**del_V**	**del_η**	**del_η*eff**

18	0.00	0.0018	0.1458		
18	7.23	0.0018	0.1458	0.7112	5.14
18	7.20	0.0018	0.1458	0.5233	3.77
18	1.51	0.0018	0.1458	0.3406	0.51
44	0.00	0.0018	0.0787		
44	4.55	0.0018	0.0787	0.8668	3.95
44	6.28	0.0018	0.0787	0.6004	3.77
44	8.91	0.0018	0.0787	0.3132	2.79
44	8.13	0.0018	0.0787	0.2457	2.00
44	5.11	0.0018	0.0787	0.1666	0.85
83	0.00	0.0018	0.0520		
83	3.50	0.0018	0.0520	0.8666	3.03
83	7.63	0.0018	0.0520	0.3471	2.65
83	10.56	0.0018	0.0520	0.1826	1.93
83	11.45	0.0018	0.0520	0.1352	1.55
83	10.94	0.0018	0.0520	0.1069	1.17
83	3.34	0.0018	0.0520	0.1060	0.35
143	0.00	0.0018	0.0361		
143	10.63	0.0018	0.0361	0.1723	1.83
143	13.19	0.0018	0.0361	0.1056	1.39
143	13.74	0.0018	0.0361	0.0768	1.06
143	11.93	0.0018	0.0361	0.0730	0.87
143	8.39	0.0018	0.0361	0.0648	0.54
143	6.55	0.0018	0.0361	0.0647	0.42
227	0.00	0.0018	0.0265		
227	4.21	0.0018	0.0265	0.4035	1.70
227	11.18	0.0018	0.0265	0.1248	1.39
227	13.55	0.0018	0.0265	0.0740	1.00
227	10.88	0.0018	0.0265	0.0650	0.71
227	8.42	0.0018	0.0265	0.0601	0.51
227	5.89	0.0018	0.0265	0.0555	0.33
339	0.00	0.0018	0.0203		
339	5.34	0.0018	0.0203	0.2581	1.38
339	14.27	0.0018	0.0203	0.0721	1.03
339	13.83	0.0018	0.0203	0.0678	0.94
339	12.17	0.0018	0.0203	0.0507	0.62
339	8.76	0.0018	0.0203	0.0426	0.37
339	6.15	0.0018	0.0203	0.0426	0.26
483	0.00	0.0018	0.0161		
483	2.93	0.0018	0.0161	0.3867	1.13
483	8.73	0.0018	0.0161	0.1156	1.01

483	12.97	0.0018	0.0161	0.0672	0.87
483	13.58	0.0018	0.0161	0.0551	0.75
483	13.76	0.0018	0.0161	0.0481	0.66
483	13.65	0.0018	0.0161	0.0427	0.58
18	0.00	0.0018	0.1458		
18	7.04	0.0018	0.1458	0.7112	5.01
18	7.68	0.0018	0.1458	0.4627	3.55
18	4.40	0.0018	0.1458	0.3630	1.60
44	0.00	0.0018	0.0787		
44	7.84	0.0018	0.0787	0.4341	3.40
44	8.28	0.0018	0.0787	0.2457	2.03
44	7.41	0.0018	0.0787	0.2081	1.54
44	4.96	0.0018	0.0787	0.1714	0.85
44	3.39	0.0018	0.0787	0.1565	0.53
83	0.00	0.0018	0.0520		
83	5.33	0.0018	0.0520	0.5034	2.69
83	8.64	0.0018	0.0520	0.2949	2.55
83	11.12	0.0018	0.0520	0.1727	1.92
83	10.91	0.0018	0.0520	0.1375	1.50
83	10.01	0.0018	0.0520	0.1127	1.13
83	5.78	0.0018	0.0520	0.0926	0.53
143	0.00	0.0018	0.0361		
143	6.15	0.0018	0.0361	0.3323	2.04
143	10.52	0.0018	0.0361	0.1761	1.85
143	13.42	0.0018	0.0361	0.0975	1.31
143	11.72	0.0018	0.0361	0.0734	0.86
143	7.77	0.0018	0.0361	0.0657	0.51
143	3.72	0.0018	0.0361	0.0770	0.29
227	0.00	0.0018	0.0265		
227	11.23	0.0018	0.0265	0.1281	1.44
227	12.68	0.0018	0.0265	0.0709	0.90
227	12.30	0.0018	0.0265	0.0652	0.80
227	9.71	0.0018	0.0265	0.0594	0.58
227	7.87	0.0018	0.0265	0.0566	0.45
227	4.38	0.0018	0.0265	0.0581	0.25
339	0.00	0.0018	0.0203		
339	10.32	0.0018	0.0203	0.1170	1.21
339	13.12	0.0018	0.0203	0.0816	1.07
339	13.13	0.0018	0.0203	0.0614	0.81
339	12.75	0.0018	0.0203	0.0506	0.65
339	10.90	0.0018	0.0203	0.0483	0.53

339	8.55	0.0018	0.0203	0.0426	0.36
483	0.00	0.0018	0.0161		
483	12.20	0.0018	0.0161	0.0771	0.94
483	13.71	0.0018	0.0161	0.0569	0.78
483	13.57	0.0018	0.0161	0.0456	0.62
483	12.92	0.0018	0.0161	0.0387	0.50
483	11.60	0.0018	0.0161	0.0353	0.41
483	9.40	0.0018	0.0161	0.0319	0.30
18	0.00	0.0018	0.1458		
18	5.02	0.0018	0.1458	1.2009	6.03
18	4.79	0.0018	0.1458	0.3702	1.78
18	3.98	0.0018	0.1458	0.3362	1.34
44	0.00	0.0018	0.0787		
44	5.82	0.0018	0.0787	0.6786	3.95
44	8.03	0.0018	0.0787	0.3909	3.14
44	8.38	0.0018	0.0787	0.3013	2.52
44	7.86	0.0018	0.0787	0.2384	1.87
44	6.04	0.0018	0.0787	0.1697	1.02
83	0.00	0.0018	0.0520		
83	4.33	0.0018	0.0520	0.6783	2.94
83	9.12	0.0018	0.0520	0.2565	2.34
83	10.89	0.0018	0.0520	0.1590	1.73
83	9.74	0.0018	0.0520	0.1092	1.06
83	7.74	0.0018	0.0520	0.0962	0.74
83	4.93	0.0018	0.0520	0.0947	0.47
143	0.00	0.0018	0.0361		
143	10.71	0.0018	0.0361	0.1704	1.83
143	12.05	0.0018	0.0361	0.1261	1.52
143	13.92	0.0018	0.0361	0.0827	1.15
143	10.01	0.0018	0.0361	0.0688	0.69
143	7.99	0.0018	0.0361	0.0659	0.53
143	5.31	0.0018	0.0361	0.0677	0.36
227	0.00	0.0018	0.0265		
227	6.64	0.0018	0.0265	0.2512	1.67
227	10.25	0.0018	0.0265	0.1458	1.50
227	13.06	0.0018	0.0265	0.0981	1.28
227	14.02	0.0018	0.0265	0.0845	1.19
227	12.68	0.0018	0.0265	0.0686	0.87
227	8.82	0.0018	0.0265	0.0574	0.51
339	0.00	0.0018	0.0203		
339	13.26	0.0018	0.0203	0.0837	1.11

339	13.82	0.0018	0.0203	0.0732	1.01
339	13.56	0.0018	0.0203	0.0551	0.75
339	10.04	0.0018	0.0203	0.0460	0.46
339	9.23	0.0018	0.0203	0.0435	0.40
339	6.19	0.0018	0.0203	0.0423	0.26
483	0.00	0.0018	0.0161		
483	9.72	0.0018	0.0161	0.0999	0.97
483	12.24	0.0018	0.0161	0.0705	0.86
483	13.19	0.0018	0.0161	0.0549	0.72
483	14.03	0.0018	0.0161	0.0430	0.60
483	13.47	0.0018	0.0161	0.0389	0.52
483	12.19	0.0018	0.0161	0.0369	0.45

NACA 0022 2 BLADES, 41% SOLIDITY					
PA (W)	**Efficiency (%)**	**del_rho**	**del_V**	**del_η**	**del_η*eff**
14	0.00	0.0018	0.1712		
14	5.94	0.0018	0.1712	0.7463	4.44
14	8.18	0.0018	0.1712	0.3484	2.85
14	1.83	0.0018	0.1712	0.3751	0.69
39	0.00	0.0018	0.0856		
39	7.20	0.0018	0.0856	0.3076	2.21
39	8.31	0.0018	0.0856	0.1984	1.65
39	7.41	0.0018	0.0856	0.1552	1.15
39	4.93	0.0018	0.0856	0.1459	0.72
39	4.04	0.0018	0.0856	0.1438	0.58
68	0.00	0.0018	0.0596		
68	4.69	0.0018	0.0596	0.4221	1.98
68	8.95	0.0018	0.0596	0.1873	1.68
68	10.16	0.0018	0.0596	0.1287	1.31
68	9.05	0.0018	0.0596	0.1017	0.92
68	7.65	0.0018	0.0596	0.0964	0.74
68	4.62	0.0018	0.0596	0.1016	0.47
117	0.00	0.0018	0.0414		
117	6.75	0.0018	0.0414	0.1984	1.34
117	9.13	0.0018	0.0414	0.1348	1.23
117	10.09	0.0018	0.0414	0.1042	1.05
117	10.17	0.0018	0.0414	0.0798	0.81
117	9.27	0.0018	0.0414	0.0745	0.69
117	8.39	0.0018	0.0414	0.0653	0.55
185	0.00	0.0018	0.0304		

185	8.08	0.0018	0.0304	0.1250	1.01
185	10.35	0.0018	0.0304	0.0864	0.89
185	11.33	0.0018	0.0304	0.0625	0.71
185	9.91	0.0018	0.0304	0.0554	0.55
185	9.52	0.0018	0.0304	0.0501	0.48
185	7.10	0.0018	0.0304	0.0511	0.36
277	0.00	0.0018	0.0233		
277	5.77	0.0018	0.0233	0.1437	0.83
277	9.57	0.0018	0.0233	0.0705	0.67
277	10.34	0.0018	0.0233	0.0557	0.58
277	10.23	0.0018	0.0233	0.0435	0.44
277	9.99	0.0018	0.0233	0.0408	0.41
277	7.62	0.0018	0.0233	0.0410	0.31
394	0.00	0.0018	0.0184		
394	6.57	0.0018	0.0184	0.0971	0.64
394	8.60	0.0018	0.0184	0.0638	0.55
394	9.97	0.0018	0.0184	0.0475	0.47
394	10.26	0.0018	0.0184	0.0361	0.37
394	9.30	0.0018	0.0184	0.0344	0.32
394	8.85	0.0018	0.0184	0.0338	0.30
14	0.00	0.0018	0.1712		
14	4.82	0.0018	0.1712	0.9774	4.71
14	8.02	0.0018	0.1712	0.3416	2.74
14	7.18	0.0018	0.1712	0.2969	2.13
39	0.00	0.0018	0.0856		
39	5.25	0.0018	0.0856	0.4468	2.35
39	8.37	0.0018	0.0856	0.2110	1.77
39	7.10	0.0018	0.0856	0.1463	1.04
39	5.45	0.0018	0.0856	0.1398	0.76
39	3.81	0.0018	0.0856	0.1473	0.56
68	0.00	0.0018	0.0596		
68	3.69	0.0018	0.0596	0.5574	2.06
68	4.43	0.0018	0.0596	0.4462	1.98
68	10.03	0.0018	0.0596	0.1550	1.55
68	10.00	0.0018	0.0596	0.1174	1.17
68	6.68	0.0018	0.0596	0.0960	0.64
68	5.64	0.0018	0.0596	0.0964	0.54
117	0.00	0.0018	0.0414		
117	8.49	0.0018	0.0414	0.1472	1.25
117	9.79	0.0018	0.0414	0.1166	1.14
117	10.14	0.0018	0.0414	0.0954	0.97

117	9.19	0.0018	0.0414	0.0795	0.73
117	8.76	0.0018	0.0414	0.0682	0.60
117	6.38	0.0018	0.0414	0.0660	0.42
185	0.00	0.0018	0.0304		
185	6.28	0.0018	0.0304	0.1696	1.06
185	9.49	0.0018	0.0304	0.1025	0.97
185	11.32	0.0018	0.0304	0.0635	0.72
185	9.50	0.0018	0.0304	0.0521	0.50
185	8.81	0.0018	0.0304	0.0494	0.44
185	5.87	0.0018	0.0304	0.0550	0.32
277	0.00	0.0018	0.0233		
277	7.35	0.0018	0.0233	0.1068	0.78
277	9.59	0.0018	0.0233	0.0715	0.69
277	10.34	0.0018	0.0233	0.0522	0.54
277	9.77	0.0018	0.0233	0.0404	0.39
277	9.29	0.0018	0.0233	0.0391	0.36
277	5.72	0.0018	0.0233	0.0473	0.27
394	0.00	0.0018	0.0184		
394	4.54	0.0018	0.0184	0.1459	0.66
394	9.05	0.0018	0.0184	0.0598	0.54
394	10.42	0.0018	0.0184	0.0421	0.44
394	10.24	0.0018	0.0184	0.0354	0.36
394	10.04	0.0018	0.0184	0.0333	0.33
394	8.08	0.0018	0.0184	0.0346	0.28
14	0.00	0.0018	0.1712		
14	4.52	0.0018	0.1712	1.0422	4.71
14	8.53	0.0018	0.1712	0.3347	2.86
14	4.01	0.0018	0.1712	0.2741	1.10
39	0.00	0.0018	0.0856		
39	3.61	0.0018	0.0856	0.7095	2.56
39	8.24	0.0018	0.0856	0.2499	2.06
39	8.84	0.0018	0.0856	0.1893	1.67
39	6.75	0.0018	0.0856	0.1428	0.96
39	2.51	0.0018	0.0856	0.1785	0.45
68	0.00	0.0018	0.0596		
68	7.02	0.0018	0.0596	0.2610	1.83
68	9.19	0.0018	0.0596	0.1714	1.57
68	9.94	0.0018	0.0596	0.1507	1.50
68	9.29	0.0018	0.0596	0.1061	0.99
68	7.05	0.0018	0.0596	0.0993	0.70
68	4.82	0.0018	0.0596	0.1006	0.48

117	0.00	0.0018	0.0414		
117	4.36	0.0018	0.0414	0.3396	1.48
117	6.31	0.0018	0.0414	0.2269	1.43
117	7.86	0.0018	0.0414	0.1707	1.34
117	10.05	0.0018	0.0414	0.1182	1.19
117	9.84	0.0018	0.0414	0.0879	0.86
117	7.63	0.0018	0.0414	0.0646	0.49
185	0.00	0.0018	0.0304		
185	8.44	0.0018	0.0304	0.1203	1.02
185	10.07	0.0018	0.0304	0.0895	0.90
185	10.91	0.0018	0.0304	0.0678	0.74
185	8.50	0.0018	0.0304	0.0512	0.44
185	5.87	0.0018	0.0304	0.0550	0.32
185	4.51	0.0018	0.0304	0.0643	0.29
277	0.00	0.0018	0.0233		
277	8.11	0.0018	0.0233	0.0991	0.80
277	9.64	0.0018	0.0233	0.0757	0.73
277	11.02	0.0018	0.0233	0.0542	0.60
277	10.69	0.0018	0.0233	0.0471	0.50
277	10.41	0.0018	0.0233	0.0425	0.44
277	9.73	0.0018	0.0233	0.0391	0.38
394	0.00	0.0018	0.0184		
394	3.43	0.0018	0.0184	0.1980	0.68
394	7.35	0.0018	0.0184	0.0831	0.61
394	10.25	0.0018	0.0184	0.0469	0.48
394	10.42	0.0018	0.0184	0.0388	0.40
394	9.83	0.0018	0.0184	0.0332	0.33
394	6.12	0.0018	0.0184	0.0392	0.24

APPENDIX F

DIFFERENT AIRFOILS AT SAME REYNOLDS NUMBER

SANDIA DATA FROM 0 TO 180 DEGREES

Re = 360000 NACA0021				NACA0018				NACA-0025			
α	Cl	Cd	Cl-Cd	α	Cl	Cd	Cl-Cd	α	Cl	Cd	Cl-CD
0	0.000	0.011	-0.011	0	0.000	0.010	-0.010	0	0.000	0.012	-0.012
1	0.110	0.011	0.099	1	0.110	0.010	0.100	1	0.098	0.012	0.086
2	0.220	0.011	0.209	2	0.220	0.010	0.210	2	0.172	0.013	0.160
3	0.302	0.012	0.291	3	0.330	0.011	0.319	3	0.268	0.013	0.255
4	0.404	0.012	0.392	4	0.440	0.011	0.429	4	0.361	0.014	0.347
5	0.500	0.013	0.487	5	0.524	0.012	0.512	5	0.450	0.014	0.435
6	0.589	0.014	0.575	6	0.623	0.013	0.610	6	0.530	0.015	0.515
7	0.673	0.015	0.658	7	0.710	0.015	0.696	7	0.606	0.016	0.590
8	0.743	0.016	0.727	8	0.788	0.016	0.772	8	0.670	0.017	0.653
9	0.803	0.018	0.785	9	0.853	0.018	0.835	9	0.726	0.019	0.707
10	0.850	0.020	0.831	10	0.898	0.019	0.879	10	0.771	0.020	0.751
11	0.878	0.022	0.856	11	0.925	0.021	0.904	11	0.804	0.022	0.782
12	0.894	0.024	0.870	12	0.928	0.024	0.904	12	0.830	0.024	0.806
13	0.897	0.026	0.871	13	0.910	0.026	0.885	13	0.847	0.026	0.821
14	0.894	0.029	0.865	14	0.880	0.094	0.786	14	0.857	0.029	0.828
15	0.884	0.104	0.780	16	0.801	0.196	0.605	15	0.866	0.031	0.834
16	0.872	0.196	0.676	18	0.732	0.238	0.494	16	0.874	0.034	0.840
18	0.849	0.238	0.611	20	0.700	0.282	0.418	17	0.882	0.038	0.845
20	0.840	0.282	0.558	22	0.705	0.329	0.376	18	0.889	0.041	0.848
22	0.845	0.329	0.516	25	0.772	0.405	0.367	19	0.899	0.045	0.854
25	0.887	0.405	0.482	30	0.855	0.570	0.285	20	0.911	0.049	0.863
30	0.855	0.570	0.285	35	0.980	0.745	0.235	21	0.922	0.053	0.868
35	0.980	0.745	0.235	40	1.035	0.920	0.115	22	0.938	0.058	0.880
40	1.035	0.920	0.115	45	1.050	1.075	-0.025	23	0.953	0.063	0.890
45	1.050	1.075	-0.025	50	1.020	1.215	-0.195	24	0.972	0.069	0.903
50	1.020	1.215	-0.195	55	0.955	1.345	-0.390	25	0.991	0.075	0.916
55	0.955	1.345	-0.390	60	0.875	1.470	-0.595	26	1.015	0.081	0.933
60	0.875	1.470	-0.595	65	0.760	1.575	-0.815	27	1.040	0.088	0.952
65	0.760	1.575	-0.815	70	0.630	1.665	-1.035	30	0.855	0.570	0.285
70	0.630	1.665	-1.035	75	0.500	1.735	-1.235	35	0.980	0.745	0.235
75	0.500	1.735	-1.235	80	0.365	1.780	-1.415	40	1.035	0.920	0.115
80	0.365	1.780	-1.415	85	0.230	1.800	-1.570	45	1.050	1.075	-0.025
85	0.230	1.800	-1.570	90	0.090	1.800	-1.710	50	1.020	1.215	-0.195
90	0.090	1.800	-1.710	95	-0.050	1.780		55	0.955	1.345	-0.390
95	-0.050	1.780		100	-0.185	1.750		60	0.875	1.470	-0.595
100	-0.185	1.750		105	-0.320	1.700		65	0.760	1.575	-0.815
105	-0.320	1.700		110	-0.450	1.635		70	0.630	1.665	-1.035
110	-0.450	1.635		115	-0.575	1.555		75	0.500	1.735	-1.235
115	-0.575	1.555		120	-0.670	1.465		80	0.365	1.780	-1.415

120	-0.670	1.465		125	-0.760	1.350		85	0.230	1.800	-1.570
125	-0.760	1.350		130	-0.850	1.225		90	0.090	1.800	-1.710
130	-0.850	1.225		135	-0.930	1.085		95	-0.050	1.780	
135	-0.930	1.085		140	-0.980	0.925		100	-0.185	1.750	
140	-0.980	0.925		145	-0.900	0.755		105	-0.320	1.700	
145	-0.900	0.755		150	-0.770	0.576		110	-0.450	1.635	
150	-0.770	0.575		155	-0.670	0.420		115	-0.575	1.555	
155	-0.670	0.420		160	-0.635	0.320		120	-0.670	1.465	
160	-0.635	0.320		165	-0.680	0.230		125	-0.760	1.350	
165	-0.680	0.230		170	-0.850	0.140		130	-0.850	1.225	
170	-0.850	0.140		175	-0.660	0.055		135	-0.930	1.085	
175	-0.660	0.055		180	0.000	0.025		140	-0.980	0.925	
180	0.000	0.025						145	-0.900	0.755	
								150	-0.770	0.575	
								155	-0.670	0.420	
								160	-0.635	0.320	
								165	-0.680	0.230	
								170	-0.850	0.140	
								175	-0.660	0.055	
								180	0.000	0.025	

NACA-0012				**NACA-0015**			
α	Cl	Cd	Cl-Cd	α	Cl	Cd	Cl-Cd
0	0.000	0.008	-0.008	0	0.000	0.009	-0.009
1	0.110	0.008	0.102	1	0.110	0.009	0.101
2	0.220	0.008	0.212	2	0.220	0.009	0.211
3	0.330	0.009	0.321	3	0.330	0.010	0.320
4	0.440	0.010	0.430	4	0.440	0.011	0.430
5	0.550	0.011	0.539	5	0.550	0.011	0.539
6	0.660	0.013	0.648	6	0.660	0.013	0.647
7	0.770	0.014	0.757	7	0.739	0.014	0.725
8	0.854	0.016	0.839	8	0.824	0.016	0.808
9	0.935	0.017	0.919	9	0.895	0.017	0.877
10	0.981	0.018	0.963	10	0.944	0.013	0.931
11	0.913	0.020	0.893	11	0.957	0.021	0.936
12	0.483	0.022	0.462	12	0.929	0.023	0.905
13	0.276	0.022	0.254	13	0.856	0.026	0.831
14	0.289	0.106	0.183	14	0.748	0.028	0.720
15	0.331	0.190	0.141	15	0.635	0.031	0.604
16	0.379	0.210	0.169	16	0.538	0.124	0.414
17	0.446	0.231	0.215	17	0.485	0.217	0.268
18	0.505	0.252	0.253	18	0.478	0.238	0.240

19	0.559	0.274	0.285	19	0.491	0.260	0.231
20	0.612	0.297	0.315	20	0.525	0.282	0.243
21	0.664	0.320	0.344	21	0.562	0.305	0.257
22	0.718	0.344	0.374	22	0.605	0.329	0.276
23	0.772	0.369	0.403	23	0.653	0.354	0.299
24	0.825	0.394	0.431	24	0.702	0.379	0.323
25	0.878	0.420	0.458	25	0.751	0.405	0.346
26	0.931	0.446	0.485	26	0.806	0.432	0.374
27	0.985	0.473	0.512	27	0.879	0.460	0.419
30	0.915	0.570	0.345	30	0.855	0.570	0.285
35	1.020	0.745	0.275	35	0.980	0.745	0.235
40	1.075	0.920	0.155	40	1.035	0.920	0.115
45	1.085	1.075	0.010	45	1.050	1.075	-0.025
50	1.040	1.215	-0.175	50	1.020	1.215	-0.195
55	0.965	1.345	-0.380	55	0.955	1.345	-0.390
60	0.875	1.470	-0.595	60	0.875	1.470	-0.595
65	0.765	1.575	-0.810	65	0.760	1.575	-0.815
70	0.650	1.665	-1.015	70	0.530	1.665	-1.135
75	0.515	1.735	-1.220	75	0.500	1.735	-1.235
80	0.370	1.780	-1.410	80	0.365	1.780	-1.415
85	0.220	1.800	-1.580	85	0.230	1.800	-1.570
90	0.070	1.800	-1.730	90	0.090	1.800	-1.710
95	-0.070	1.780		95	-0.050	1.780	
100	-0.220	1.750		100	-0.185	1.750	
105	-0.370	1.700		105	-0.320	1.700	
110	-0.510	1.635		110	-0.450	1.635	
115	-0.625	1.555		115	-0.575	1.555	
120	-0.735	1.465		120	-0.670	1.465	
125	-0.840	1.350		125	-0.760	1.350	
130	-0.910	1.225		130	-0.850	1.225	
135	-0.945	1.085		135	-0.930	1.085	
140	-0.945	0.925		140	-0.980	0.925	
145	-0.910	0.755		145	-0.900	0.755	
150	-0.850	0.575		150	-0.770	0.575	
155	-0.740	0.420		155	-0.670	0.420	
160	-0.660	0.320		160	-0.635	0.320	
165	-0.675	0.230		165	-0.680	0.230	
170	-0.850	0.140		170	-0.850	0.140	
175	-0.690	0.055		175	-0.660	0.055	
180	0.000	0.025		180	0.000	0.025	

APPENDIX G

SAME AIRFOILS AT DIFFERENT REYNOLDS NUMBER

SANDIA DATA FROM 0 TO 180

Re = 360000 NACA0021			Re = 80000 NACA0021			Re = 100000000 NACA0021		
alpha	Cl	Cd	alpha	Cl	Cd	alpha	Cl	Cd
0	0	0.0111	0	0	0.0177	0	0	0.0089
1	0.11	0.0111	1	0.0921	0.0178	1	0.11	0.0089
2	0.22	0.0113	2	0.1839	0.0181	2	0.22	0.009
3	0.3024	0.0117	3	0.2731	0.0186	3	0.33	0.0092
4	0.4044	0.0122	4	0.3564	0.0194	4	0.44	0.0096
5	0.4998	0.0129	5	0.4324	0.0204	5	0.5192	0.0101
6	0.5891	0.0138	6	0.4953	0.0217	6	0.6191	0.0108
7	0.6728	0.0149	7	0.5445	0.0233	7	0.7102	0.0117
8	0.7434	0.0163	8	0.5751	0.0252	8	0.7939	0.0128
9	0.8026	0.0178	9	0.5874	0.0273	9	0.8694	0.014
10	0.85	0.0195	10	0.578	0.0297	10	0.9364	0.0154
11	0.8779	0.0215	11	0.5564	0.07	11	0.9862	0.017
12	0.8938	0.0237	12	0.5228	0.123	12	1.0257	0.0187
13	0.8973	0.026	14	0.4296	0.158	13	1.0492	0.0206
14	0.8937	0.0286	16	0.3499	0.196	14	1.0657	0.0226
15	0.884	0.104	18	0.3221	0.238	15	1.0709	0.0248
16	0.8717	0.196	20	0.3475	0.282	16	1.069	0.0273
18	0.8489	0.238	22	0.4091	0.3295	17	1.0641	0.03
20	0.8397	0.282	25	0.5297	0.405	18	1.0588	0.135
22	0.8453	0.329	30	0.855	0.57	20	1.0554	0.282
25	0.8866	0.405	35	0.98	0.745	22	1.0644	0.329
30	0.855	0.57	40	1.035	0.92	25	1.1018	0.405
35	0.98	0.745	45	1.05	1.075	30	0.855	0.57
40	1.035	0.92	50	1.02	1.215	35	0.98	0.745
45	1.05	1.075	55	0.955	1.345	40	1.035	0.92
50	1.02	1.215	60	0.875	1.47	45	1.05	1.075
55	0.955	1.345	65	0.76	1.575	50	1.02	1.215
60	0.875	1.47	70	0.63	1.665	55	0.955	1.345
65	0.76	1.575	75	0.5	1.735	60	0.875	1.47
70	0.63	1.665	80	0.365	1.78	65	0.76	1.575
75	0.5	1.735	85	0.23	1.8	70	0.63	1.665
80	0.365	1.78	90	0.09	1.8	75	0.5	1.735
85	0.23	1.8	95	-0.05	1.78	80	0.365	1.78
90	0.09	1.8	100	-0.185	1.75	85	0.23	1.8
95	-0.05	1.78	105	-0.32	1.7	90	0.09	1.8
100	-0.185	1.75	110	-0.45	1.635	95	-0.05	1.78
105	-0.32	1.7	115	-0.575	1.555	100	-0.185	1.75
110	-0.45	1.635	120	-0.67	1.4651	105	-0.32	1.7

115	-0.575	1.555	125	-0.76	1.35	110	-0.45	1.635
120	-0.67	1.465	130	-0.85	1.225	115	-0.575	1.555
125	-0.76	1.35	135	-0.93	1.085	120	-0.67	1.465
130	-0.85	1.225	140	-0.98	0.925	125	-0.76	1.35
135	-0.93	1.085	145	-0.9	0.755	130	-0.85	1.225
140	-0.98	0.925	150	-0.77	0.575	135	-0.93	1.085
145	-0.9	0.755	155	-0.67	0.42	140	-0.98	0.925
150	-0.77	0.575	160	-0.635	0.32	145	-0.9	0.755
155	-0.67	0.42	165	-0.68	0.23	150	-0.77	0.575
160	-0.635	0.32	170	-0.85	0.14	155	-0.67	0.42
165	-0.68	0.23	175	-0.66	0.055	160	-0.635	0.32
170	-0.85	0.14	180	0	0.025	165	-0.68	0.23
175	-0.66	0.055				170	-0.85	0.14
180	0	0.025				175	-0.66	0.055
						180	0	0.025

APPENDIX H

SAME AIRFOILS AT DIFFERENT REYNOLDS NUMBER COEFFICIENT OF LIFT FOR ALL SOURCE COMPARISON

Theory of Wing Sections NACA0012					
Re = 3e6		Re = 6e6		Re = 9e6	
α	Cl	α	Cl	α	Cl
0	0	0	0	0	0
2	0.22	2	0.22	2	0.22
4	0.45	4	0.45	4	0.45
6	0.65	6	0.65	6	0.67
8	0.89	8	0.88	8	0.88
10	1.1	10	1.12	10	1.12
11	1.2	11	1.21	11	1.21
12	1.27	12	1.31	12	1.32
13	1.37	13	1.38	13	1.41
14	1.42	14	1.42	14	1.48
15	1.49	15	1.55	15	1.58
16	1.51	16	1.6	16	1.57
16.5	1.52	17	1.42	17	1.35
17	1.34	18	1.09	18	1.06
18	0.98				
19	0.91				
20	0.88				

Sandia NACA 0012					
Re = 2e6		Re = 5e6		Re = 10e6	
α	Cl	α	Cl	α	Cl
0	0	0	0	0	0
1	0.11	1	0.11	1	0.11
2	0.22	2	0.22	2	0.22
3	0.33	3	0.33	3	0.33
4	0.44	4	0.44	4	0.44
5	0.55	5	0.55	5	0.55
6	0.66	6	0.66	6	0.66
7	0.77	7	0.77	7	0.77
8	0.88	8	0.88	8	0.88
9	0.99	9	0.99	9	0.99
10	1.0727	10	1.1	10	1.1
11	1.1539	11	1.1842	11	1.21
12	1.2072	12	1.2673	12	1.2906
13	1.2169	13	1.3242	13	1.3687
14	1.1614	14	1.3423	14	1.4171
15	1.0478	15	1.3093	15	1.4214

16	0.9221	16	1.2195	16	1.2941
17	0.7826	17	1.0365	17	1.12
18	0.7163	18	0.9054	18	0.9795
19	0.7091	19	0.8412	19	0.8983
20	0.7269	20	0.8233	20	0.8668

Fluent NACA 0012					
Re = .685e6		**Re = 2.05e6**		**Re = 9.04e6**	
α	**Cl**	**α**	**Cl**	**α**	**Cl**
0	6.53061E-05	0	0.000175964	0	0.00027061
3	0.309202052	3	0.309369982	3	0.312311156
6	0.599107026	6	0.603190335	6	0.606473208
9	0.804110953	9	0.804828224	9	0.806435824
10	0.848203371	10	0.843563442	10	0.840933135
11	0.870011772	11	0.857181219	11	0.856616084
12	0.876788508	12	0.870079119	12	0.847073374
13	0.864295942	13	0.839024092	13	0.826090434
14	0.835214345	14	0.82103836	14	0.815126513

Javafoil NACA 0012	
α	**Cl**
0	0
1	0.12
2	0.239
3	0.358
4	0.475
5	0.59
6	0.701
7	0.803
8	0.88
9	0.809
10	0.87
11	0.922
12	0.962
13	0.991
14	1.007
15	1.012
16	1.007
17	0.992

18	0.969
19	0.94
20	0.906

Flat Plate Theory NACA 0012		
α	**α (rad)**	**Cl**
0	0	0
5	0.087266463	0.173648178
10	0.174532925	0.342020143
15	0.261799388	0.5
20	0.34906585	0.64278761

APPENDIX I

DIFFERENT AIRFOILS AT SAME REYNOLDS NUMBER COEFFICIENT OF LIFT AND DRAG FROM THEORY OF WING SECTIONS

NACA 0006			NACA 0009			NACA 00012			NACA 65_3-018		
Re = 6e6			Re = 6e6			Re = 6e6			Re = 6e6		
α	Cl	Cd	α	Cl	Cd	α	Cl	Cd	α	Cl	Cd
0	0	0.005	0	0	0.0055	0	0	0.0058	0	0	0.0045
2	0.2	0.0052	1	0.11	0.0057	2	0.22	0.006	2	0.24	0.0046
4	0.4	0.0057	3	0.28	0.0058	4	0.45	0.0068	4	0.41	0.0055
6	0.63	0.007	4	0.42	0.0062	6	0.65	0.0078	6	0.6	0.009
8	0.83	0.0096	5	0.55	0.0066	8	0.88	0.0092	8	0.82	0.0105
9	0.85	0.0102	8	0.86	0.0081	10	1.12	0.016	10	1.03	0.013
10	0.83		10	1.1	0.0105	11	1.21	0.013	12	1.19	0.0179
12	0.8		11	1.2	0.012	12	1.31	0.0138	14	1.3	0.3
14	0.74		13	1.32	0.014	13	1.38		16	1.34	
			14	1.29		14	1.42		18	1.33	
			16	1.14		15	1.55		20	1.32	
			17	1.05		16	1.6		22	1.08	
						17	1.42		24	0.98	
						18	1.09				

APPENDIX J

COEFFICIENT OF LIFT FOR A FLAT PLATE

Flat Plate Theory				
α (deg)	**α (rad)**	**Cl**	**Cd**	**Cl/Cd**
0	1.75E-12	3.49E-12	6.09E-24	5.73E+11
5	0.087266	0.173648	0.015192	11.43005
10	0.174533	0.34202	0.060307	5.671282
15	0.261799	0.5	0.133975	3.732051
20	0.349066	0.642788	0.233956	2.747477
25	0.436332	0.766044	0.357212	2.144507
30	0.523599	0.866025	0.5	1.732051
35	0.610865	0.939693	0.65798	1.428148
40	0.698132	0.984808	0.826352	1.191754
45	0.785398	1	1	1
50	0.872665	0.984808	1.173648	0.8391
55	0.959931	0.939693	1.34202	0.700208
60	1.047198	0.866025	1.5	0.57735
65	1.134464	0.766044	1.642788	0.466308
70	1.22173	0.642788	1.766044	0.36397
75	1.308997	0.5	1.866025	0.267949
80	1.396263	0.34202	1.939693	0.176327
85	1.48353	0.173648	1.984808	0.087489
90	1.570796	1.23E-16	2	6.13E-17
95	1.658063	-0.17365	1.984808	-0.087489
100	1.745329	-0.34202	1.939693	-0.176327
105	1.832596	-0.5	1.866025	-0.267949
110	1.919862	-0.64279	1.766044	-0.36397
115	2.007129	-0.76604	1.642788	-0.466308
120	2.094395	-0.86603	1.5	-0.57735
125	2.181662	-0.93969	1.34202	-0.700208
130	2.268928	-0.98481	1.173648	-0.8391
135	2.356194	-1	1	-1
140	2.443461	-0.98481	0.826352	-1.191754
145	2.530727	-0.93969	0.65798	-1.428148
150	2.617994	-0.86603	0.5	-1.732051
155	2.70526	-0.76604	0.357212	-2.144507
160	2.792527	-0.64279	0.233956	-2.747477
165	2.879793	-0.5	0.133975	-3.732051
170	2.96706	-0.34202	0.060307	-5.671282
175	3.054326	-0.17365	0.015192	-11.43005
180	3.141593	-2.5E-16	3E-32	-8.16E+15

APPENDIX K

COEFFICIENTS OF LIFT AND DRAG FROM NACA

NACA 0006		NACA 0009		NACA 0012		NACA 0015		NACA 0018		NACA0021	
3.21E+06		3.21E+06		3.23E+06		3.20E+06		3.15E+06		3.19E+06	
α	Cl	α	Cl	α	Cl	α	Cl	α	Cl	α	Cl
-2.12	-0.15	-2.27	-0.17	-4.44	-0.31	-4.47	-0.33	30.57	0.93	30.77	0.98
-2.12	-0.14	-2.18	-0.16	-4.36	-0.31	-4.38	-0.32	30.57	0.94	30.68	0.99
-2.12	-0.14	-2.18	-0.16	-4.36	-0.31	-4.38	-0.32	30.48	0.94	30.60	0.99
-2.03	-0.14	-2.10	-0.15	-4.27	-0.30	-4.29	-0.31	30.48	0.94	30.52	1.00
-2.03	-0.13	-2.10	-0.15	-4.19	-0.30	-4.20	-0.31	30.40	0.95	30.43	1.00
-1.95	-0.13	-2.01	-0.15	-4.10	-0.29	-4.11	-0.30	30.40	0.95	30.35	1.01
-1.86	-0.12	-2.01	-0.14	-4.02	-0.29	-4.11	-0.30	30.31	0.95	30.26	1.01
-1.78	-0.12	-1.93	-0.14	-3.93	-0.28	-4.02	-0.30	30.31	0.96	30.18	1.01
-1.70	-0.11	-1.93	-0.14	-3.93	-0.28	-4.02	-0.29	30.23	0.96	30.10	1.02
-1.70	-0.11	-1.85	-0.13	-3.85	-0.28	-3.93	-0.29	30.15	0.96	30.01	1.02
-1.61	-0.11	-1.76	-0.13	-3.85	-0.27	-3.84	-0.29	30.15	0.96	30.01	1.03
-1.61	-0.11	-1.68	-0.12	-3.76	-0.27	-3.76	-0.28	30.06	0.96	29.93	1.03
-1.53	-0.10	-1.59	-0.12	-3.68	-0.26	-3.67	-0.28	29.98	0.97	29.93	1.03
-1.44	-0.10	-1.59	-0.12	-3.59	-0.26	-3.67	-0.27	29.89	0.97	29.84	1.04
-1.36	-0.09	-1.51	-0.11	-3.51	-0.25	-3.58	-0.27	29.81	0.98	29.76	1.04
-1.36	-0.09	-1.51	-0.11	-3.43	-0.25	-3.58	-0.26	29.73	0.98	29.68	1.04
-1.27	-0.09	-1.43	-0.10	-3.34	-0.24	-3.58	-0.26	29.73	0.98	29.59	1.05
-1.27	-0.08	-1.34	-0.10	-3.26	-0.24	-3.49	-0.25	29.64	0.98	29.51	1.05
-1.19	-0.08	-1.26	-0.09	-3.17	-0.24	-3.40	-0.25	29.56	0.99	29.51	1.06
-1.10	-0.08	-1.26	-0.09	-3.17	-0.23	-3.31	-0.25	29.47	0.99	29.42	1.06
-1.02	-0.07	-1.17	-0.09	-3.09	-0.23	-3.22	-0.24	29.39	1.00	29.43	1.06
-0.93	-0.07	-1.09	-0.08	-3.00	-0.22	-3.22	-0.24	29.31	1.00	29.34	1.07
-0.85	-0.06	-1.01	-0.08	-2.92	-0.22	-3.13	-0.24	29.22	1.00	29.26	1.07
-0.76	-0.06	-0.92	-0.07	-2.83	-0.21	-3.13	-0.23	29.14	1.01	29.17	1.08
-0.76	-0.05	-0.84	-0.07	-2.75	-0.21	-3.04	-0.23	29.05	1.01	29.09	1.08
-0.68	-0.05	-0.84	-0.06	-2.75	-0.20	-2.95	-0.22	28.97	1.02	29.00	1.08
-0.68	-0.05	-0.76	-0.06	-2.66	-0.20	-2.86	-0.22	28.89	1.02	28.92	1.09
-0.59	-0.04	-0.76	-0.06	-2.66	-0.20	-2.77	-0.21	28.80	1.03	28.84	1.09
-0.51	-0.04	-0.67	-0.05	-2.66	-0.19	-2.68	-0.21	28.72	1.03	28.75	1.10
-0.42	-0.03	-0.59	-0.05	-2.58	-0.19	-2.68	-0.20	28.63	1.03	28.67	1.10
-0.42	-0.03	-0.50	-0.04	-2.58	-0.18	-2.59	-0.20	28.55	1.04	28.58	1.11
-0.34	-0.02	-0.42	-0.04	-2.50	-0.18	-2.59	-0.20	28.47	1.04	28.50	1.11
-0.34	-0.02	-0.42	-0.03	-2.41	-0.17	-2.50	-0.19	28.38	1.05	28.42	1.11
-0.34	-0.02	-0.34	-0.03	-2.33	-0.17	-2.50	-0.19	28.30	1.05	28.33	1.12
-0.25	-0.01	-0.34	-0.03	-2.33	-0.17	-2.41	-0.18	28.21	1.06	28.25	1.12
-0.25	-0.01	-0.25	-0.02	-2.24	-0.17	-2.32	-0.18	28.21	1.06	28.16	1.13

-0.25	0.00	-0.25	-0.02	-2.24	-0.16	-2.23	-0.17	28.13	1.07	28.17	1.13
-0.17	0.00	-0.17	-0.02	-2.16	-0.16	-2.24	-0.17	28.13	1.07	28.08	1.13
-0.08	0.01	-0.17	-0.01	-2.07	-0.15	-2.15	-0.16	28.05	1.07	28.08	1.14
-0.08	0.01	-0.17	-0.01	-1.99	-0.15	-2.15	-0.16	27.96	1.08	28.00	1.14
0.00	0.01	-0.08	0.00	-1.90	-0.14	-2.06	-0.15	27.88	1.08	27.91	1.14
0.00	0.02	-0.08	0.00	-1.82	-0.14	-1.97	-0.15	27.79	1.08	27.83	1.15
0.00	0.02	0.00	0.00	-1.73	-0.13	-1.88	-0.15	27.79	1.09	27.75	1.15
0.08	0.02	0.08	0.01	-1.65	-0.13	-1.79	-0.14	27.71	1.09	27.66	1.16
0.08	0.03	0.17	0.01	-1.57	-0.13	-1.79	-0.14	27.62	1.09	27.58	1.16
0.17	0.03	0.25	0.02	-1.48	-0.12	-1.70	-0.13	27.54	1.10	27.49	1.17
0.25	0.04	0.34	0.02	-1.40	-0.12	-1.70	-0.13	27.46	1.10	27.41	1.17
0.25	0.04	0.42	0.03	-1.40	-0.11	-1.70	-0.12	27.37	1.10	27.41	1.17
0.34	0.05	0.42	0.03	-1.31	-0.11	-1.61	-0.12	27.29	1.11	27.32	1.17
0.34	0.05	0.50	0.03	-1.31	-0.10	-1.52	-0.11	27.20	1.11	27.24	1.17
0.42	0.05	0.50	0.03	-1.31	-0.10	-1.43	-0.11	27.21	1.12	27.16	1.18
0.51	0.06	0.59	0.04	-1.23	-0.09	-1.34	-0.10	27.12	1.12	27.07	1.18
0.59	0.06	0.67	0.04	-1.14	-0.09	-1.25	-0.10	27.04	1.13	26.99	1.19
0.68	0.07	0.67	0.05	-1.14	-0.09	-1.16	-0.10	27.04	1.13	26.90	1.19
0.76	0.07	0.76	0.05	-1.06	-0.09	-1.07	-0.09	26.95	1.13	26.82	1.20
0.85	0.08	0.76	0.06	-1.06	-0.08	-1.07	-0.09	26.95	1.14	26.74	1.20
0.93	0.08	0.84	0.06	-0.97	-0.08	-1.07	-0.08	26.87	1.14	26.65	1.20
1.02	0.08	0.84	0.06	-0.89	-0.07	-1.07	-0.08	26.79	1.14	26.57	1.21
1.10	0.09	0.92	0.07	-0.80	-0.07	-0.98	-0.07	26.70	1.15	26.48	1.21
1.19	0.09	1.01	0.07	-0.72	-0.06	-0.89	-0.07	26.62	1.15	26.40	1.22
1.27	0.10	1.09	0.08	-0.72	-0.06	-0.89	-0.06	26.62	1.15	26.32	1.22
1.36	0.10	1.17	0.08	-0.63	-0.06	-0.80	-0.06	26.53	1.15	26.23	1.23
1.44	0.11	1.17	0.09	-0.63	-0.05	-0.81	-0.05	26.45	1.16	26.15	1.23
1.53	0.11	1.26	0.09	-0.63	-0.05	-0.81	-0.05	26.36	1.16	26.06	1.23
1.53	0.11	1.26	0.09	-0.55	-0.04	-0.72	-0.05	26.28	1.17	25.98	1.24
1.61	0.12	1.34	0.09	-0.55	-0.04	-0.63	-0.04	26.20	1.17	25.90	1.24
1.61	0.12	1.43	0.10	-0.47	-0.03	-0.54	-0.04	26.20	1.17	25.81	1.25
1.61	0.13	1.51	0.10	-0.38	-0.03	-0.54	-0.03	26.11	1.18	25.73	1.25
1.70	0.13	1.59	0.11	-0.30	-0.02	-0.45	-0.03	26.11	1.18	25.64	1.25
1.70	0.14	1.68	0.11	-0.21	-0.02	-0.36	-0.02	26.03	1.19	25.64	1.26
1.78	0.14	1.76	0.12	-0.13	-0.02	-0.36	-0.02	25.94	1.19	25.56	1.26
1.86	0.14	1.85	0.12	-0.13	-0.01	-0.27	-0.02	25.86	1.20	25.47	1.26
1.86	0.15	1.93	0.12	-0.04	-0.01	-0.27	-0.01	25.78	1.20	25.39	1.27
1.95	0.15	2.01	0.13	-0.04	-0.01	-0.18	-0.01	25.69	1.20	25.31	1.27
1.95	0.15	2.01	0.13	-0.04	0.00	-0.09	0.00	25.69	1.21	25.22	1.27
2.03	0.16	2.01	0.14	0.04	0.00	-0.09	0.00	25.61	1.21	25.14	1.27
2.03	0.16	2.10	0.14	0.04	0.01	0.00	0.00	25.61	1.21	25.05	1.27

2.12	0.16	2.10	0.15	0.13	0.01	0.00	0.01	25.53	1.22	24.97	1.28
2.12	0.17	2.10	0.15	0.13	0.02	0.09	0.01	25.44	1.22	24.88	1.28
2.20	0.17	2.10	0.15	0.21	0.02	0.09	0.02	25.36	1.23	24.80	1.28
2.20	0.18	2.18	0.16	0.21	0.02	0.18	0.02	25.27	1.23	24.72	1.28
2.29	0.18	2.18	0.16	0.30	0.02	0.27	0.03	25.19	1.24	24.63	1.28
2.29	0.18	2.27	0.16	0.30	0.03	0.27	0.03	25.10	1.24	24.55	1.29
2.37	0.18	2.27	0.17	0.38	0.03	0.36	0.04	25.11	1.24	24.46	1.29
2.37	0.19	2.35	0.17	0.47	0.04	0.45	0.04	25.02	1.24	24.38	1.29
2.46	0.19	2.35	0.18	0.55	0.04	0.54	0.05	25.02	1.25	24.29	1.30
2.46	0.19	2.43	0.18	0.63	0.05	0.63	0.05	24.94	1.25	24.21	1.30
2.54	0.20	2.43	0.18	0.72	0.05	0.72	0.05	24.94	1.26	24.13	1.30
2.63	0.20	2.43	0.18	0.72	0.06	0.80	0.06	24.85	1.26	24.04	1.30
2.71	0.21	2.52	0.19	0.80	0.06	0.89	0.06	24.85	1.26	23.96	1.30
2.71	0.21	2.52	0.19	0.80	0.06	0.98	0.07	24.77	1.27	23.87	1.30
2.80	0.21	2.60	0.20	0.80	0.06	1.07	0.07	24.77	1.27	23.79	1.31
2.88	0.22	2.69	0.20	0.89	0.07	1.07	0.08	24.69	1.27	23.70	1.31
2.97	0.22	2.77	0.21	0.97	0.07	1.07	0.08	24.69	1.27	23.62	1.31
2.97	0.23	2.85	0.21	1.06	0.08	1.16	0.09	24.60	1.28	23.53	1.31
3.05	0.23	2.94	0.21	1.06	0.08	1.16	0.09	24.52	1.28	23.45	1.31
3.05	0.24	2.94	0.22	1.14	0.09	1.25	0.10	24.43	1.29	23.36	1.31
3.14	0.24	3.02	0.22	1.14	0.09	1.34	0.10	24.43	1.29	23.28	1.31
3.22	0.24	3.10	0.23	1.14	0.09	1.43	0.10	24.35	1.29	23.19	1.31
3.31	0.25	3.19	0.23	1.23	0.10	1.52	0.11	24.35	1.30	23.11	1.32
3.39	0.25	3.19	0.24	1.31	0.10	1.61	0.11	24.27	1.30	23.03	1.32
3.39	0.26	3.27	0.24	1.40	0.11	1.61	0.12	24.18	1.31	22.94	1.32
3.48	0.26	3.27	0.24	1.48	0.11	1.70	0.12	24.18	1.31	22.86	1.33
3.48	0.27	3.36	0.25	1.56	0.12	1.70	0.12	24.10	1.31	22.86	1.33
3.56	0.27	3.44	0.25	1.65	0.12	1.70	0.13	24.01	1.32	22.77	1.33
3.65	0.27	3.52	0.26	1.73	0.13	1.79	0.13	24.01	1.32	22.78	1.34
3.65	0.28	3.61	0.26	1.73	0.13	1.79	0.14	23.93	1.32	22.78	1.34
3.73	0.28	3.61	0.27	1.82	0.13	1.88	0.14	23.93	1.33	22.78	1.35
3.73	0.29	3.69	0.27	1.82	0.14	1.88	0.15	23.93	1.33	22.78	1.35
3.81	0.29	3.69	0.27	1.90	0.14	1.97	0.15	23.85	1.34	22.78	1.36
3.81	0.30	3.78	0.28	1.99	0.15	1.97	0.15	23.76	1.34	22.78	1.36
3.90	0.30	3.86	0.28	2.07	0.15	1.97	0.15	23.68	1.34	22.78	1.36
3.98	0.30	3.86	0.29	2.16	0.16	2.06	0.16	23.68	1.35	22.78	1.37
4.07	0.31	3.94	0.29	2.16	0.16	2.06	0.16	23.59	1.35	22.78	1.37
4.15	0.31	3.94	0.29	2.24	0.17	2.15	0.17	23.59	1.36	22.78	1.38
4.24	0.32	3.94	0.30	2.24	0.17	2.24	0.17	23.51	1.36	22.78	1.38
4.32	0.32	4.03	0.30	2.33	0.17	2.23	0.17	23.43	1.37	22.78	1.39
4.41	0.33	4.03	0.30	2.41	0.18	2.32	0.17	23.43	1.37	22.70	1.39

4.49	0.33	4.03	0.31	2.50	0.18	2.41	0.18	23.43	1.38	22.61	1.39
4.49	0.34	4.11	0.31	2.58	0.19	2.41	0.18	23.34	1.38	22.53	1.39
4.58	0.34	4.20	0.32	2.58	0.19	2.50	0.18	23.34	1.38	22.44	1.39
4.58	0.34	4.28	0.32	2.66	0.20	2.50	0.19	23.34	1.39	22.36	1.39
4.66	0.35	4.28	0.33	2.66	0.20	2.59	0.19	23.26	1.39	22.28	1.39
4.75	0.35	4.36	0.33	2.75	0.20	2.59	0.20	23.26	1.40	22.19	1.39
4.75	0.36	4.36	0.33	2.83	0.21	2.68	0.20	23.17	1.40	22.11	1.39
4.83	0.36	4.45	0.34	2.92	0.21	2.68	0.20	23.09	1.41	22.02	1.39
4.83	0.37	4.53	0.34	3.00	0.22	2.77	0.20	23.09	1.41	21.94	1.39
4.92	0.37	4.62	0.35	3.00	0.22	2.86	0.21	23.01	1.41	21.85	1.39
5.00	0.37	4.70	0.35	3.09	0.22	2.86	0.21	23.01	1.42	21.77	1.39
5.00	0.38	4.70	0.36	3.09	0.23	2.95	0.22	23.01	1.42	21.68	1.39
5.09	0.38	4.78	0.36	3.09	0.23	2.95	0.22	22.92	1.43	21.60	1.38
5.09	0.39	4.78	0.36	3.17	0.24	3.04	0.23	22.92	1.43	21.51	1.38
5.09	0.39	4.87	0.36	3.26	0.24	3.13	0.23	22.92	1.44	21.43	1.38
5.17	0.40	4.95	0.37	3.34	0.24	3.22	0.24	22.84	1.44	21.34	1.38
5.17	0.40	5.04	0.37	3.34	0.25	3.31	0.24	22.84	1.44	21.26	1.38
5.26	0.40	5.04	0.38	3.43	0.25	3.31	0.25	22.84	1.45	21.17	1.38
5.26	0.41	5.12	0.38	3.43	0.26	3.40	0.25	22.84	1.45	21.09	1.38
5.34	0.41	5.12	0.38	3.43	0.26	3.49	0.25	22.84	1.46	21.00	1.38
5.43	0.42	5.20	0.39	3.51	0.27	3.58	0.26	22.84	1.46	20.92	1.38
5.51	0.42	5.20	0.39	3.51	0.27	3.58	0.26	22.84	1.47	20.83	1.38
5.59	0.43	5.29	0.39	3.60	0.28	3.67	0.27	22.84	1.47	20.75	1.38
5.59	0.43	5.29	0.39	3.68	0.28	3.67	0.27	22.84	1.48	20.66	1.37
5.68	0.43	5.29	0.40	3.76	0.28	3.76	0.28	22.84	1.48	20.58	1.37
5.68	0.44	5.37	0.40	3.85	0.29	3.76	0.28	22.84	1.48	20.49	1.36
5.76	0.44	5.45	0.41	3.85	0.29	3.84	0.29	22.84	1.49	20.41	1.36
5.85	0.45	5.54	0.41	3.93	0.30	3.93	0.29	22.84	1.49	20.41	1.36
5.93	0.45	5.62	0.42	3.93	0.30	3.93	0.29	22.76	1.49	20.32	1.36
6.02	0.46	5.71	0.42	4.02	0.31	4.02	0.29	22.67	1.49	20.23	1.35
6.02	0.46	5.71	0.42	4.10	0.31	4.02	0.30	22.59	1.49	20.15	1.35
6.10	0.46	5.79	0.43	4.19	0.31	4.11	0.30	22.51	1.49	20.06	1.35
6.10	0.47	5.79	0.43	4.27	0.32	4.11	0.31	22.42	1.49	19.98	1.35
6.19	0.47	5.87	0.44	4.36	0.32	4.20	0.31	22.34	1.49	19.98	1.34
6.27	0.48	5.96	0.44	4.36	0.33	4.20	0.31	22.25	1.49	19.89	1.34
6.36	0.48	6.04	0.45	4.44	0.33	4.20	0.32	22.17	1.48	19.81	1.34
6.44	0.49	6.13	0.45	4.44	0.33	4.29	0.32	22.17	1.49	19.72	1.34
6.44	0.49	6.21	0.45	4.53	0.34	4.38	0.33	22.17	1.49	19.64	1.34
6.53	0.49	6.21	0.46	4.61	0.34	4.47	0.33	22.17	1.50	19.55	1.33
6.53	0.50	6.21	0.46	4.61	0.35	4.56	0.34	22.17	1.49	19.47	1.33
6.61	0.50	6.29	0.47	4.69	0.35	4.65	0.34	22.25	1.49	19.38	1.32

6.70	0.50	6.29	0.47	4.69	0.35	4.65	0.34	22.25	1.48	19.30	1.32
6.78	0.51	6.38	0.48	4.78	0.36	4.74	0.35	22.17	1.48	19.30	1.32
6.87	0.51	6.38	0.48	4.86	0.36	4.74	0.35	22.08	1.48	19.21	1.31
6.87	0.52	6.46	0.48	4.95	0.37	4.83	0.36	22.00	1.48	19.21	1.31
6.95	0.52	6.46	0.48	4.95	0.37	4.92	0.36	21.91	1.48	19.12	1.30
6.95	0.53	6.46	0.49	5.03	0.38	5.01	0.37	21.83	1.48	19.04	1.30
7.04	0.53	6.55	0.49	5.03	0.38	5.10	0.37	21.75	1.48	18.95	1.29
7.12	0.53	6.55	0.50	5.03	0.39	5.10	0.38	21.66	1.47	18.87	1.29
7.12	0.54	6.63	0.50	5.12	0.39	5.19	0.38	21.58	1.47	18.78	1.28
7.21	0.54	6.63	0.51	5.12	0.39	5.19	0.39	21.49	1.47	18.70	1.28
7.21	0.55	6.71	0.51	5.20	0.40	5.28	0.39	21.41	1.47	18.61	1.28
7.29	0.55	6.71	0.51	5.20	0.40	5.37	0.39	21.32	1.47	18.53	1.27
7.37	0.56	6.80	0.52	5.29	0.41	5.36	0.40	21.24	1.46	18.44	1.27
7.46	0.56	6.88	0.52	5.29	0.41	5.45	0.40	21.16	1.46	18.35	1.26
7.54	0.56	6.97	0.53	5.37	0.41	5.45	0.41	21.07	1.45	18.27	1.26
7.54	0.57	7.05	0.53	5.46	0.42	5.54	0.41	20.99	1.45	18.18	1.25
7.63	0.57	7.05	0.54	5.54	0.42	5.63	0.42	20.90	1.44	18.18	1.25
7.63	0.58	7.13	0.54	5.63	0.42	5.63	0.42	20.82	1.44	18.10	1.25
7.71	0.58	7.13	0.54	5.71	0.42	5.72	0.43	20.73	1.44	18.10	1.25
7.80	0.59	7.22	0.55	5.79	0.43	5.72	0.43	20.65	1.43	18.01	1.24
7.88	0.59	7.30	0.55	5.88	0.43	5.81	0.44	20.57	1.43	18.01	1.24
7.88	0.59	7.39	0.56	5.88	0.44	5.90	0.44	20.48	1.42	17.93	1.23
7.97	0.59	7.47	0.56	5.96	0.44	5.90	0.44	20.40	1.42	17.92	1.23
7.97	0.60	7.55	0.57	5.96	0.45	5.99	0.45	20.31	1.41	17.84	1.22
8.05	0.60	7.64	0.57	6.05	0.45	5.99	0.45	20.23	1.41	17.75	1.22
8.05	0.61	7.72	0.57	6.13	0.46	6.08	0.46	20.14	1.41	17.75	1.22
8.14	0.61	7.72	0.58	6.22	0.46	6.17	0.46	20.06	1.40	17.67	1.22
8.14	0.61	7.80	0.58	6.30	0.46	6.17	0.47	19.97	1.40	17.67	1.21
8.22	0.62	7.80	0.59	6.30	0.47	6.26	0.47	19.89	1.39	17.58	1.21
8.31	0.62	7.89	0.59	6.39	0.47	6.26	0.47	19.81	1.39	17.50	1.21
8.31	0.62	7.97	0.60	6.39	0.48	6.35	0.48	19.72	1.39	17.50	1.20
8.39	0.63	8.06	0.60	6.47	0.48	6.44	0.48	19.64	1.39	17.41	1.20
8.39	0.63	8.14	0.60	6.56	0.49	6.53	0.49	19.55	1.38	17.33	1.20
8.48	0.64	8.22	0.61	6.64	0.49	6.53	0.49	19.47	1.38	17.33	1.19
8.56	0.64	8.22	0.61	6.72	0.50	6.62	0.49	19.38	1.37	17.24	1.19
8.65	0.65	8.31	0.62	6.72	0.50	6.62	0.49	19.38	1.37	17.24	1.19
8.73	0.65	8.31	0.62	6.81	0.50	6.71	0.50	19.30	1.37	17.15	1.18
8.82	0.66	8.39	0.63	6.81	0.51	6.80	0.50	19.30	1.37	17.15	1.18
8.90	0.66	8.48	0.63	6.89	0.51	6.89	0.51	19.22	1.36	17.07	1.18
8.99	0.66	8.48	0.63	6.98	0.52	6.98	0.51	19.13	1.36	17.07	1.18
9.07	0.67	8.56	0.64	7.06	0.52	7.06	0.52	19.05	1.35	16.98	1.17

9.16	0.67	8.56	0.64	7.15	0.53	7.15	0.52	18.96	1.35	16.90	1.17
9.24	0.68	8.64	0.65	7.15	0.53	7.15	0.53	18.88	1.34	16.81	1.16
9.32	0.68	8.73	0.65	7.15	0.53	7.24	0.53	18.88	1.34	16.73	1.16
9.41	0.69	8.81	0.66	7.23	0.54	7.24	0.54	18.79	1.34	16.64	1.15
9.49	0.69	8.90	0.66	7.23	0.54	7.33	0.54	18.71	1.33	16.64	1.15
9.58	0.69	8.98	0.66	7.32	0.55	7.42	0.54	18.62	1.33	16.56	1.15
9.58	0.70	9.06	0.67	7.40	0.55	7.51	0.55	18.54	1.32	16.55	1.15
9.66	0.70	9.15	0.67	7.40	0.56	7.60	0.55	18.46	1.32	16.47	1.14
9.75	0.71	9.15	0.68	7.49	0.56	7.60	0.56	18.37	1.31	16.47	1.14
9.83	0.71	9.23	0.68	7.49	0.57	7.69	0.56	18.29	1.31	16.38	1.14
9.83	0.71	9.23	0.69	7.49	0.57	7.69	0.57	18.20	1.30	16.38	1.13
9.92	0.71	9.23	0.69	7.57	0.57	7.69	0.57	18.12	1.30	16.30	1.13
10.00	0.72	9.32	0.69	7.57	0.58	7.78	0.58	18.03	1.30	16.21	1.12
10.09	0.72	9.32	0.70	7.66	0.58	7.87	0.58	17.95	1.29	16.13	1.12
10.17	0.72	9.40	0.70	7.74	0.59	7.96	0.59	17.86	1.29	16.13	1.12
10.26	0.72	9.40	0.71	7.82	0.59	7.96	0.59	17.78	1.28	16.04	1.11
10.34	0.73	9.48	0.71	7.82	0.60	7.96	0.59	17.78	1.28	16.04	1.11
10.43	0.73	9.57	0.72	7.91	0.60	7.96	0.60	17.70	1.28	15.95	1.11
10.51	0.74	9.65	0.72	7.91	0.61	8.05	0.60	17.70	1.27	15.87	1.10
10.60	0.74	9.73	0.72	7.99	0.61	8.14	0.61	17.61	1.27	15.78	1.10
10.68	0.75	9.73	0.73	8.08	0.61	8.23	0.61	17.53	1.27	15.70	1.10
10.77	0.75	9.82	0.73	8.08	0.61	8.32	0.62	17.44	1.26	15.70	1.09
10.85	0.75	9.82	0.73	8.16	0.61	8.41	0.62	17.36	1.26	15.61	1.09
10.94	0.76	9.90	0.74	8.16	0.62	8.41	0.63	17.36	1.25	15.53	1.09
11.02	0.76	9.99	0.74	8.25	0.62	8.50	0.63	17.27	1.25	15.44	1.08
11.10	0.77	9.99	0.75	8.33	0.63	8.49	0.63	17.27	1.24	15.44	1.08
11.19	0.77	10.07	0.75	8.42	0.63	8.49	0.64	17.19	1.24	15.36	1.08
11.27	0.78	10.07	0.75	8.50	0.64	8.58	0.64	17.10	1.23	15.36	1.07
11.36	0.78	10.15	0.76	8.59	0.64	8.58	0.64	17.02	1.23	15.27	1.07
11.44	0.78	10.24	0.76	8.59	0.64	8.67	0.65	16.94	1.23	15.18	1.06
11.53	0.78	10.24	0.77	8.67	0.65	8.67	0.65	16.94	1.22	15.10	1.06
11.61	0.78	10.32	0.77	8.67	0.65	8.76	0.66	16.85	1.22	15.01	1.05
11.70	0.78	10.32	0.78	8.76	0.66	8.76	0.66	16.85	1.21	14.93	1.05
11.78	0.79	10.41	0.78	8.84	0.66	8.85	0.67	16.85	1.21	14.84	1.05
11.87	0.79	10.49	0.78	8.92	0.67	8.94	0.67	16.77	1.20	14.84	1.04
11.95	0.79	10.57	0.79	9.01	0.67	9.03	0.68	16.68	1.20	14.76	1.04
12.04	0.80	10.66	0.79	9.01	0.68	9.12	0.68	16.60	1.20	14.67	1.03
12.12	0.80	10.66	0.80	9.09	0.68	9.21	0.69	16.51	1.19	14.67	1.03
12.21	0.81	10.74	0.80	9.09	0.68	9.21	0.69	16.43	1.19	14.58	1.03
12.29	0.81	10.74	0.80	9.09	0.69	9.30	0.69	16.34	1.18	14.58	1.02
12.38	0.82	10.83	0.81	9.18	0.69	9.30	0.69	16.26	1.18	14.50	1.02

12.46	0.82	10.83	0.81	9.26	0.70	9.39	0.70	16.18	1.17	14.41	1.01
12.55	0.82	10.91	0.81	9.35	0.70	9.48	0.70	16.09	1.17	14.41	1.01
12.63	0.82	10.91	0.81	9.43	0.71	9.57	0.71	16.09	1.16	14.33	1.01
12.72	0.82	10.91	0.82	9.52	0.71	9.57	0.71	16.01	1.16	14.33	1.01
12.80	0.82	10.99	0.82	9.60	0.72	9.66	0.72	15.92	1.16	14.24	1.00
12.88	0.82	10.99	0.83	9.69	0.72	9.66	0.72	15.84	1.15	14.16	1.00
12.97	0.83	11.08	0.83	9.69	0.72	9.75	0.73	15.75	1.15	14.16	0.99
13.05	0.83	11.08	0.84	9.77	0.73	9.75	0.73	15.67	1.14	14.07	0.99
13.14	0.83	11.16	0.84	9.85	0.73	9.84	0.73	15.58	1.14	14.07	0.98
13.22	0.83	11.25	0.84	9.85	0.74	9.84	0.73	15.50	1.13	13.98	0.98
13.31	0.83	11.33	0.85	9.94	0.74	9.93	0.74	15.50	1.13	13.90	0.98
13.39	0.84	11.41	0.85	9.94	0.74	9.92	0.74	15.42	1.13	13.81	0.97
13.48	0.84	11.50	0.86	9.94	0.75	10.01	0.74	15.42	1.12	13.73	0.97
13.56	0.84	11.58	0.86	10.02	0.75	10.01	0.75	15.33	1.12	13.64	0.96
13.65	0.84	11.67	0.87	10.02	0.75	10.10	0.75	15.25	1.11	13.56	0.96
13.73	0.84	11.75	0.87	10.11	0.76	10.19	0.76	15.25	1.11	13.47	0.95
13.82	0.85	11.75	0.87	10.19	0.76	10.28	0.76	15.16	1.10	13.38	0.95
13.90	0.85	11.83	0.88	10.28	0.77	10.37	0.77	15.16	1.10	13.30	0.94
13.99	0.85	11.92	0.88	10.36	0.77	10.46	0.77	15.08	1.09	13.30	0.94
14.07	0.85	12.00	0.89	10.45	0.78	10.55	0.78	14.99	1.09	13.21	0.94
14.16	0.85	12.08	0.89	10.45	0.78	10.64	0.78	14.91	1.09	13.21	0.93
14.24	0.85	12.08	0.90	10.45	0.79	10.64	0.78	14.82	1.08	13.13	0.93
14.33	0.86	12.17	0.90	10.53	0.79	10.73	0.79	14.74	1.08	13.04	0.92
14.41	0.86	12.17	0.90	10.53	0.79	10.73	0.79	14.66	1.07	13.04	0.92
14.50	0.86	12.17	0.90	10.53	0.80	10.82	0.80	14.57	1.07	12.96	0.91
14.58	0.86	12.25	0.91	10.62	0.80	10.91	0.80	14.49	1.06	12.95	0.91
14.66	0.86	12.34	0.91	10.62	0.81	11.00	0.81	14.49	1.06	12.87	0.91
14.75	0.86	12.42	0.92	10.62	0.81	11.09	0.81	14.40	1.06	12.78	0.90
14.83	0.87	12.50	0.92	10.70	0.82	11.18	0.82	14.40	1.05	12.70	0.90
14.92	0.87	12.59	0.93	10.70	0.82	11.18	0.82	14.40	1.05	12.61	0.89
15.00	0.87	12.59	0.93	10.79	0.83	11.18	0.83	14.32	1.04	12.53	0.89
15.09	0.87	12.67	0.93	10.87	0.83	11.18	0.83	14.23	1.04	12.53	0.88
15.17	0.87	12.67	0.94	10.95	0.83	11.27	0.83	14.15	1.03	12.44	0.88
15.26	0.87	12.76	0.94	11.04	0.83	11.36	0.84	14.06	1.03	12.44	0.88
15.34	0.87	12.76	0.95	11.12	0.83	11.45	0.84	13.98	1.03	12.35	0.87
15.43	0.87	12.84	0.95	11.21	0.84	11.54	0.85	13.90	1.02	12.27	0.87
15.51	0.87	12.84	0.95	11.29	0.84	11.54	0.85	13.81	1.02	12.27	0.86
15.60	0.87	12.92	0.96	11.38	0.85	11.62	0.86	13.73	1.01	12.18	0.86
15.68	0.88	13.01	0.96	11.46	0.85	11.62	0.86	13.64	1.01	12.18	0.85
15.77	0.88	13.09	0.96	11.46	0.86	11.71	0.87	13.64	1.00	12.10	0.85
15.85	0.88	13.18	0.97	11.55	0.86	11.80	0.87	13.56	1.00	12.01	0.84

15.94	0.88	13.26	0.97	11.55	0.86	11.80	0.88	13.56	0.99	11.93	0.84
16.02	0.88	13.26	0.98	11.63	0.87	11.89	0.88	13.47	0.99	11.92	0.84
16.11	0.88	13.34	0.98	11.72	0.87	11.89	0.88	13.39	0.99	11.84	0.83
16.19	0.88	13.34	0.98	11.80	0.88	11.98	0.89	13.30	0.98	11.84	0.83
16.28	0.88	13.34	0.99	11.88	0.88	11.98	0.89	13.30	0.98	11.75	0.82
16.36	0.88	13.43	0.99	11.97	0.89	12.07	0.89	13.22	0.97	11.67	0.82
16.45	0.88	13.43	0.99	12.05	0.89	12.07	0.90	13.22	0.97	11.67	0.82
16.53	0.88	13.51	1.00	12.05	0.90	12.16	0.90	13.22	0.96	11.58	0.82
16.61	0.88	13.59	1.00	12.14	0.90	12.16	0.91	13.14	0.96	11.50	0.81
16.70	0.88	13.68	1.01	12.14	0.90	12.25	0.91	13.05	0.96	11.41	0.81
16.78	0.88	13.68	1.01	12.22	0.91	12.25	0.91	12.97	0.95	11.33	0.81
16.87	0.88	13.76	1.02	12.22	0.91	12.25	0.92	12.88	0.95	11.33	0.80
16.95	0.88	13.76	1.02	12.31	0.91	12.34	0.92	12.80	0.94	11.24	0.80
17.04	0.88	13.85	1.02	12.31	0.92	12.34	0.93	12.80	0.94	11.24	0.80
17.12	0.88	13.93	1.03	12.31	0.92	12.43	0.93	12.71	0.93	11.24	0.79
17.21	0.88	13.93	1.03	12.39	0.93	12.52	0.93	12.71	0.93	11.15	0.79
17.29	0.88	14.01	1.04	12.39	0.93	12.61	0.94	12.63	0.92	11.07	0.78
17.38	0.88	14.01	1.04	12.39	0.94	12.70	0.94	12.54	0.92	11.07	0.78
17.46	0.87	14.10	1.05	12.48	0.94	12.79	0.95	12.54	0.92	10.98	0.78
17.55	0.87	14.10	1.05	12.48	0.94	12.88	0.95	12.46	0.91	10.98	0.78
17.63	0.87	14.18	1.05	12.56	0.95	12.97	0.96	12.46	0.91	10.90	0.77
17.72	0.87	14.27	1.06	12.65	0.95	13.06	0.96	12.37	0.90	10.81	0.77
17.80	0.87	14.35	1.06	12.73	0.96	13.15	0.97	12.37	0.90	10.73	0.76
17.89	0.87	14.43	1.07	12.73	0.96	13.23	0.97	12.29	0.90	10.72	0.76
17.97	0.87	14.52	1.07	12.82	0.97	13.23	0.98	12.29	0.89	10.64	0.76
18.06	0.87	14.60	1.08	12.82	0.97	13.32	0.98	12.21	0.89	10.64	0.75
18.14	0.87	14.69	1.08	12.90	0.97	13.32	0.98	12.12	0.89	10.64	0.75
18.23	0.87	14.77	1.08	12.98	0.98	13.32	0.99	12.04	0.88	10.55	0.74
18.31	0.87	14.77	1.09	13.07	0.98	13.41	0.99	11.95	0.88	10.47	0.74
18.39	0.86	14.85	1.09	13.15	0.99	13.41	1.00	11.87	0.87	10.38	0.74
18.48	0.86	14.94	1.10	13.24	0.99	13.50	1.00	11.78	0.87	10.38	0.73
18.56	0.86	15.02	1.10	13.32	1.00	13.59	1.01	11.78	0.86	10.30	0.73
18.65	0.86	15.11	1.11	13.41	1.00	13.68	1.01	11.70	0.86	10.29	0.72
18.73	0.86	15.11	1.11	13.49	1.01	13.77	1.02	11.70	0.85	10.29	0.72
18.82	0.86	15.19	1.11	13.58	1.01	13.86	1.02	11.61	0.85	10.21	0.71
18.90	0.86	15.19	1.11	13.58	1.01	13.95	1.03	11.53	0.85	10.21	0.71
18.99	0.86	15.27	1.12	13.66	1.02	13.95	1.03	11.53	0.84	10.12	0.71
19.07	0.86	15.36	1.12	13.66	1.02	14.04	1.03	11.45	0.84	10.04	0.70
19.16	0.85	15.44	1.13	13.75	1.03	14.04	1.04	11.45	0.83	10.04	0.70
19.24	0.85	15.52	1.13	13.83	1.03	14.13	1.04	11.36	0.83	9.95	0.70
19.33	0.85	15.52	1.14	13.91	1.04	14.22	1.05	11.36	0.82	9.95	0.69

19.41	0.85	15.61	1.14	14.00	1.04	14.31	1.05	11.28	0.82	9.87	0.69
19.50	0.85	15.61	1.14	14.00	1.05	14.40	1.06	11.28	0.82	9.78	0.68
19.58	0.85	15.69	1.15	14.00	1.05	14.49	1.06	11.19	0.81	9.69	0.68
19.67	0.85	15.78	1.15	14.08	1.05	14.58	1.07	11.11	0.81	9.61	0.68
19.75	0.85	15.86	1.16	14.08	1.06	14.67	1.07	11.02	0.80	9.61	0.67
19.84	0.85	15.94	1.16	14.17	1.06	14.67	1.08	10.94	0.80	9.52	0.67
19.92	0.85	15.94	1.17	14.25	1.07	14.67	1.08	10.94	0.80	9.44	0.66
20.01	0.85	16.03	1.17	14.34	1.07	14.75	1.08	10.85	0.80	9.35	0.66
20.09	0.85	16.03	1.17	14.42	1.08	14.75	1.09	10.77	0.79	9.27	0.65
20.17	0.85	16.11	1.18	14.51	1.08	14.84	1.09	10.77	0.79	9.18	0.65
20.26	0.85	16.20	1.18	14.59	1.08	14.84	1.10	10.69	0.79	9.09	0.64
20.34	0.85	16.28	1.19	14.59	1.09	14.93	1.10	10.69	0.78	9.01	0.64
20.43	0.85	16.36	1.19	14.68	1.09	14.93	1.10	10.69	0.78	9.01	0.64
20.51	0.85	16.45	1.20	14.68	1.09	15.02	1.11	10.60	0.78	8.92	0.63
20.60	0.85	16.53	1.20	14.76	1.10	15.11	1.11	10.52	0.77	8.92	0.63
20.68	0.85	16.62	1.20	14.84	1.10	15.20	1.12	10.43	0.77	8.84	0.62
20.77	0.85	16.62	1.21	14.93	1.11	15.29	1.12	10.35	0.76	8.75	0.62
20.85	0.85	16.70	1.21	15.01	1.11	15.38	1.13	10.26	0.76	8.67	0.61
20.94	0.85	16.70	1.22	15.10	1.12	15.47	1.13	10.18	0.75	8.58	0.61
21.02	0.85	16.78	1.22	15.10	1.12	15.56	1.13	10.18	0.75	8.49	0.61
21.11	0.85	16.87	1.22	15.18	1.12	15.65	1.14	10.09	0.75	8.49	0.60
21.19	0.84	16.87	1.23	15.18	1.12	15.65	1.14	10.09	0.75	8.41	0.60
21.28	0.84	16.95	1.23	15.27	1.13	15.65	1.15	10.01	0.74	8.41	0.60
21.36	0.84	17.03	1.23	15.35	1.13	15.74	1.15	10.01	0.74	8.32	0.59
21.45	0.84	17.12	1.23	15.44	1.14	15.74	1.16	9.93	0.74	8.32	0.59
21.53	0.84	17.20	1.24	15.44	1.14	15.74	1.16	9.93	0.73	8.24	0.59
21.62	0.84	17.29	1.24	15.52	1.14	15.83	1.17	9.84	0.73	8.24	0.58
21.70	0.84	17.37	1.25	15.52	1.15	15.92	1.17	9.76	0.72	8.15	0.58
21.79	0.84	17.45	1.25	15.61	1.15	16.01	1.17	9.76	0.72	8.07	0.57
21.87	0.84	17.45	1.25	15.69	1.16	16.10	1.18	9.67	0.71	7.98	0.57
21.96	0.84	17.54	1.25	15.77	1.16	16.10	1.18	9.67	0.71	7.89	0.57
22.04	0.84	17.62	1.26	15.86	1.16	16.19	1.18	9.59	0.71	7.81	0.56
22.12	0.84	17.70	1.26	15.94	1.17	16.19	1.19	9.50	0.70	7.72	0.56
22.21	0.84	17.71	1.26	15.94	1.17	16.28	1.19	9.50	0.70	7.72	0.55
22.29	0.84	17.79	1.26	16.03	1.18	16.36	1.20	9.42	0.69	7.64	0.55
22.38	0.84	17.87	1.26	16.03	1.18	16.45	1.20	9.42	0.69	7.64	0.54
22.46	0.84	17.96	1.26	16.03	1.19	16.54	1.21	9.42	0.68	7.55	0.54
22.55	0.84	18.04	1.26	16.11	1.19	16.63	1.21	9.33	0.68	7.47	0.54
22.63	0.84	18.04	1.26	16.20	1.19	16.72	1.22	9.33	0.68	7.46	0.53
22.72	0.84	18.04	1.25	16.28	1.20	16.81	1.22	9.25	0.67	7.46	0.53
22.80	0.84	18.04	1.25	16.37	1.20	16.81	1.22	9.16	0.67	7.38	0.52

22.89	0.84	18.04	1.24	16.45	1.21	16.90	1.23	9.16	0.66	7.38	0.52
22.97	0.84	18.12	1.24	16.54	1.21	16.99	1.23	9.08	0.66	7.38	0.51
23.06	0.84	18.12	1.23	16.62	1.22	17.08	1.24	9.08	0.65	7.29	0.51
23.14	0.84	18.12	1.23	16.62	1.22	17.17	1.24	9.00	0.65	7.21	0.51
23.23	0.84	18.12	1.23	16.71	1.23	17.26	1.25	8.91	0.64	7.21	0.50
23.31	0.84	18.12	1.22	16.79	1.23	17.26	1.25	8.83	0.64	7.12	0.50
23.40	0.84	18.12	1.22	16.87	1.23	17.35	1.26	8.74	0.64	7.12	0.50
23.48	0.84	18.21	1.21	16.96	1.24	17.35	1.26	8.66	0.64	7.03	0.49
23.57	0.83	18.20	1.21	17.04	1.24	17.35	1.27	8.57	0.63	6.95	0.49
23.65	0.83	18.20	1.20	17.04	1.25	17.44	1.27	8.57	0.63	6.86	0.48
23.74	0.83	18.12	1.20	17.13	1.25	17.53	1.27	8.49	0.62	6.86	0.48
23.82	0.83	18.12	1.20	17.13	1.26	17.62	1.28	8.49	0.62	6.78	0.47
23.90	0.83	18.12	1.19	17.21	1.26	17.71	1.28	8.40	0.61	6.78	0.47
23.99	0.83	18.12	1.19	17.30	1.27	17.80	1.29	8.32	0.61	6.69	0.47
24.07	0.83	18.12	1.18	17.38	1.27	17.89	1.29	8.32	0.61	6.61	0.46
24.16	0.83	18.12	1.18	17.47	1.27	17.98	1.30	8.24	0.61	6.52	0.46
24.24	0.83	18.12	1.17	17.55	1.28	18.07	1.30	8.24	0.60	6.43	0.45
24.33	0.83	18.12	1.17	17.64	1.28	18.16	1.31	8.15	0.60	6.35	0.45
24.41	0.83	18.12	1.17	17.72	1.29	18.24	1.31	8.07	0.59	6.26	0.44
24.50	0.83	18.12	1.16	17.72	1.29	18.33	1.32	8.07	0.59	6.26	0.44
24.58	0.83	18.12	1.16	17.80	1.29	18.42	1.32	7.98	0.58	6.18	0.44
24.67	0.83	18.12	1.15	17.80	1.30	18.51	1.32	7.98	0.58	6.18	0.44
24.75	0.83	18.20	1.15	17.89	1.30	18.51	1.33	7.90	0.57	6.09	0.43
24.84	0.83	18.20	1.14	17.97	1.30	18.60	1.33	7.81	0.57	6.01	0.43
24.92	0.83	18.29	1.14	18.06	1.31	18.60	1.34	7.73	0.57	6.01	0.42
25.01	0.83	18.29	1.14	18.14	1.31	18.69	1.34	7.64	0.56	5.92	0.42
25.09	0.83	18.37	1.14	18.14	1.32	18.78	1.35	7.56	0.56	5.92	0.42
25.18	0.83	18.37	1.13	18.23	1.32	18.87	1.35	7.48	0.55	5.83	0.41
25.26	0.83	18.45	1.13	18.23	1.33	18.96	1.36	7.39	0.55	5.75	0.41
25.35	0.83	18.45	1.12	18.31	1.33	19.05	1.36	7.31	0.54	5.66	0.41
25.43	0.83	18.54	1.12	18.40	1.34	19.14	1.37	7.22	0.54	5.58	0.40
25.52	0.83	18.54	1.12	18.48	1.34	19.23	1.37	7.22	0.54	5.58	0.40
25.60	0.83	18.62	1.11	18.57	1.34	19.32	1.37	7.14	0.53	5.49	0.39
25.68	0.83	18.70	1.11	18.65	1.35	19.41	1.38	7.14	0.53	5.49	0.39
25.77	0.83	18.79	1.11	18.73	1.35	19.50	1.38	7.14	0.52	5.41	0.38
25.85	0.83	18.87	1.10	18.82	1.36	19.50	1.39	7.05	0.52	5.32	0.38
25.94	0.83	18.95	1.10	18.90	1.36	19.59	1.39	7.05	0.51	5.23	0.37
26.02	0.83	19.04	1.10	18.99	1.37	19.59	1.40	6.97	0.51	5.15	0.37
26.11	0.83	19.04	1.09	19.07	1.37	19.68	1.40	6.88	0.50	5.06	0.37
26.19	0.83	19.12	1.09	19.07	1.38	19.77	1.41	6.80	0.50	4.98	0.36
26.28	0.83	19.20	1.09	19.16	1.38	19.86	1.41	6.72	0.50	4.89	0.36

26.36	0.83	19.29	1.09	19.16	1.38	19.95	1.42	6.63	0.49	4.89	0.35
26.45	0.83	19.37	1.08	19.24	1.39	20.04	1.42	6.55	0.49	4.81	0.35
26.53	0.83	19.45	1.08	19.24	1.39	20.12	1.42	6.46	0.48	4.81	0.34
26.62	0.83	19.54	1.07	19.33	1.39	20.12	1.43	6.38	0.48	4.72	0.34
26.70	0.83	19.62	1.07	19.33	1.40	20.21	1.43	6.38	0.47	4.63	0.34
26.79	0.83	19.70	1.07	19.41	1.40	20.21	1.43	6.29	0.47	4.63	0.33
26.87	0.83	19.70	1.06	19.50	1.41	20.30	1.44	6.29	0.47	4.63	0.33
26.96	0.82	19.79	1.06	19.58	1.41	20.39	1.44	6.29	0.46	4.55	0.32
27.04	0.82	19.87	1.06	19.66	1.41	20.48	1.45	6.21	0.46	4.55	0.32
27.13	0.82	19.96	1.06	19.75	1.42	20.48	1.45	6.12	0.45	4.46	0.31
27.21	0.82	20.04	1.05	19.83	1.42	20.57	1.45	6.04	0.45	4.38	0.31
27.30	0.82	20.12	1.05	19.92	1.43	20.57	1.46	5.96	0.44	4.37	0.30
27.38	0.82	20.21	1.04	20.00	1.43	20.66	1.46	5.87	0.44	4.29	0.30
27.46	0.82	20.29	1.04	20.09	1.44	20.75	1.47	5.79	0.43	4.29	0.30
27.55	0.82	20.37	1.03	20.17	1.44	20.84	1.47	5.70	0.43	4.20	0.29
27.63	0.82	20.46	1.03	20.17	1.45	20.93	1.47	5.70	0.43	4.12	0.29
27.72	0.82	20.46	1.03	20.26	1.45	21.02	1.48	5.62	0.42	4.03	0.28
27.80	0.82	20.54	1.03	20.34	1.45	21.11	1.48	5.62	0.42	3.95	0.28
27.89	0.82	20.62	1.03	20.43	1.46	21.20	1.49	5.62	0.41	3.86	0.27
27.97	0.82	20.71	1.03	20.51	1.46	21.29	1.49	5.62	0.41	3.86	0.27
28.06	0.82	20.71	1.02	20.59	1.47	21.38	1.50	5.53	0.40	3.78	0.27
28.14	0.82	20.79	1.02	20.68	1.47	21.47	1.50	5.45	0.40	3.77	0.27
28.23	0.82	20.87	1.02	20.76	1.47	21.56	1.51	5.36	0.40	3.77	0.26
28.31	0.82	20.96	1.01	20.85	1.48	21.65	1.51	5.28	0.39	3.69	0.26
28.40	0.82	21.04	1.01	20.93	1.48	21.74	1.52	5.20	0.39	3.69	0.25
28.48	0.82	21.12	1.00	21.02	1.49	21.83	1.52	5.11	0.38	3.60	0.25
28.57	0.82	21.21	1.00	21.10	1.49	21.92	1.52	5.11	0.38	3.52	0.24
28.65	0.82	21.29	1.00	21.19	1.49	21.92	1.52	5.03	0.37	3.43	0.24
28.74	0.82	21.38	1.00	21.27	1.50	22.01	1.52	5.03	0.37	3.35	0.24
28.82	0.82	21.46	1.00	21.35	1.50	22.10	1.52	5.03	0.37	3.26	0.23
28.91	0.82	21.54	0.99	21.44	1.51	22.19	1.53	4.94	0.36	3.17	0.23
28.99	0.82	21.63	0.99	21.52	1.51	22.28	1.53	4.94	0.36	3.09	0.22
29.08	0.82	21.71	0.99	21.61	1.52	22.37	1.52	4.94	0.35	3.09	0.22
29.16	0.82	21.71	0.98	21.69	1.52	22.46	1.52	4.86	0.35	3.00	0.22
29.25	0.82	21.79	0.98	21.78	1.52	22.46	1.52	4.86	0.34	3.00	0.21
29.33	0.82	21.88	0.98	21.86	1.53	22.37	1.53	4.77	0.34	2.92	0.21
29.41	0.82	21.96	0.98	21.95	1.53	22.37	1.53	4.69	0.33	2.92	0.20
29.50	0.82	22.04	0.98	22.03	1.53	22.46	1.54	4.60	0.33	2.83	0.20
29.58	0.82	22.13	0.97	22.11	1.54	22.46	1.53	4.52	0.33	2.83	0.20
29.67	0.82	22.21	0.97	22.20	1.54	22.37	1.53	4.43	0.32	2.75	0.20
29.75	0.82	22.29	0.97	22.28	1.54	22.37	1.52	4.35	0.32	2.75	0.19

29.84	0.82	22.38	0.97	22.37	1.53	22.37	1.52	4.27	0.31	2.66	0.19
29.92	0.82	22.38	0.96	22.45	1.53	22.46	1.52	4.27	0.31	2.66	0.19
30.01	0.82	22.46	0.96	22.54	1.53	22.46	1.51	4.18	0.30	2.57	0.18
30.09	0.82	22.54	0.96	22.45	1.53	22.46	1.51	4.10	0.30	2.57	0.18
30.18	0.82	22.63	0.96	22.37	1.54	22.55	1.50	4.01	0.30	2.49	0.18
30.26	0.82	22.63	0.95	22.37	1.53	22.55	1.50	3.93	0.29	2.49	0.17
30.35	0.82	22.71	0.95	22.45	1.53	22.64	1.49	3.93	0.29	2.40	0.17
30.43	0.82	22.80	0.95	22.45	1.52	22.64	1.49	3.84	0.29	2.32	0.17
30.52	0.82	22.88	0.95	22.45	1.52	22.64	1.48	3.84	0.28	2.23	0.16
30.60	0.82	22.88	0.94	22.54	1.52	22.64	1.48	3.84	0.28	2.23	0.16
30.69	0.82	22.96	0.94	22.54	1.51	22.64	1.48	3.76	0.27	2.15	0.16
30.77	0.82	23.05	0.94	22.54	1.51	22.64	1.47	3.76	0.27	2.15	0.15
30.86	0.82	23.13	0.94	22.54	1.50	22.64	1.47	3.67	0.26	2.06	0.15
		23.13	0.94	22.53	1.50	22.64	1.46	3.59	0.26	1.97	0.14
		23.21	0.94	22.53	1.49	22.64	1.46	3.51	0.26	1.89	0.14
		23.30	0.93	22.45	1.49	22.55	1.45	3.42	0.25	1.80	0.14
		23.38	0.93	22.45	1.49	22.55	1.45	3.34	0.25	1.72	0.13
		23.38	0.93	22.45	1.48	22.55	1.44	3.25	0.24	1.72	0.13
		23.46	0.93	22.45	1.48	22.55	1.44	3.17	0.24	1.63	0.12
		23.55	0.93	22.45	1.47	22.55	1.43	3.08	0.23	1.63	0.12
		23.63	0.92	22.45	1.47	22.55	1.43	3.08	0.23	1.55	0.11
		23.71	0.92	22.45	1.46	22.56	1.43	3.00	0.23	1.46	0.11
		23.80	0.92	22.45	1.46	22.56	1.42	3.00	0.22	1.37	0.10
		23.88	0.92	22.45	1.45	22.56	1.42	2.91	0.22	1.29	0.10
		23.97	0.92	22.45	1.45	22.56	1.41	2.83	0.21	1.20	0.10
		24.05	0.91	22.45	1.45	22.56	1.41	2.75	0.21	1.20	0.09
		24.13	0.91	22.45	1.44	22.65	1.40	2.66	0.20	1.12	0.09
		24.22	0.91	22.36	1.44	22.65	1.40	2.58	0.20	1.12	0.09
		24.30	0.91	22.36	1.43	22.65	1.39	2.49	0.19	1.12	0.08
		24.38	0.91	22.36	1.43	22.65	1.39	2.41	0.19	1.03	0.08
		24.47	0.90	22.36	1.42	22.65	1.39	2.41	0.19	1.03	0.07
		24.55	0.90	22.36	1.42	22.65	1.38	2.32	0.18	0.94	0.07
		24.63	0.90	22.36	1.41	22.65	1.38	2.32	0.18	0.86	0.07
		24.72	0.89	22.36	1.41	22.65	1.37	2.32	0.17	0.77	0.06
		24.80	0.89	22.36	1.41	22.65	1.37	2.32	0.17	0.69	0.06
		24.88	0.89	22.36	1.40	22.65	1.36	2.24	0.16	0.60	0.05
		24.97	0.89	22.36	1.40	22.65	1.36	2.24	0.16	0.52	0.05
		25.05	0.89	22.36	1.39	22.65	1.35	2.15	0.16	0.52	0.04
		25.14	0.89	22.36	1.39	22.74	1.35	2.07	0.15	0.43	0.04
		25.14	0.89	22.36	1.38	22.74	1.34	1.99	0.15	0.43	0.03
		25.22	0.89	22.36	1.38	22.74	1.34	1.90	0.14	0.34	0.03

		25.30	0.89	22.36	1.38	22.74	1.34	1.82	0.14	0.26	0.03
		25.39	0.88	22.36	1.37	22.74	1.33	1.82	0.13	0.26	0.02
		25.47	0.88	22.36	1.37	22.83	1.33	1.73	0.13	0.26	0.02
		25.55	0.88	22.36	1.36	22.92	1.33	1.73	0.13	0.17	0.01
		25.64	0.88	22.36	1.36	22.92	1.32	1.65	0.12	0.17	0.01
		25.72	0.88	22.36	1.35	23.01	1.32	1.56	0.12	0.09	0.00
		25.80	0.87	22.36	1.35	23.02	1.32	1.48	0.12	0.00	0.00
		25.89	0.87	22.36	1.34	23.11	1.31	1.39	0.11	-0.09	0.00
		25.97	0.87	22.36	1.34	23.11	1.31	1.39	0.11	-0.17	0.00
		26.05	0.87	22.36	1.34	23.20	1.30	1.31	0.11	-0.17	-0.01
		26.14	0.87	22.36	1.33	23.29	1.30	1.31	0.10	-0.26	-0.01
		26.22	0.86	22.36	1.33	23.29	1.29	1.23	0.10	-0.26	-0.01
		26.31	0.86	22.36	1.32	23.38	1.29	1.14	0.09	-0.34	-0.02
		26.31	0.86	22.36	1.32	23.38	1.29	1.06	0.09	-0.34	-0.02
		26.39	0.86	22.36	1.31	23.47	1.28	0.97	0.09	-0.43	-0.03
		26.47	0.86	22.36	1.31	23.47	1.28	0.97	0.08	-0.43	-0.03
		26.56	0.86	22.36	1.30	23.47	1.27	0.89	0.08	-0.51	-0.03
		26.64	0.86	22.36	1.30	23.47	1.27	0.89	0.07	-0.52	-0.04
		26.72	0.86	22.36	1.30	23.47	1.26	0.89	0.07	-0.60	-0.04
		26.81	0.85	22.36	1.29	23.47	1.26	0.80	0.06	-0.60	-0.04
		26.89	0.85	22.36	1.29	23.56	1.25	0.80	0.06	-0.69	-0.05
		26.97	0.85	22.36	1.28	23.56	1.25	0.72	0.05	-0.77	-0.05
		27.06	0.85	22.36	1.28	23.56	1.25	0.63	0.05	-0.86	-0.06
		27.14	0.85	22.36	1.27	23.65	1.24	0.55	0.05	-0.94	-0.06
		27.23	0.85	22.36	1.27	23.65	1.24	0.46	0.04	-1.03	-0.07
		27.31	0.84	22.36	1.27	23.74	1.23	0.38	0.04	-1.11	-0.07
		27.39	0.84	22.36	1.26	23.83	1.23	0.38	0.03	-1.11	-0.07
		27.48	0.84	22.36	1.26	23.83	1.22	0.30	0.03	-1.20	-0.08
		27.56	0.84	22.36	1.25	23.92	1.22	0.30	0.02	-1.20	-0.08
		27.64	0.84	22.36	1.25	23.92	1.22	0.21	0.02	-1.20	-0.09
		27.73	0.84	22.36	1.24	23.92	1.21	0.13	0.02	-1.29	-0.09
		27.81	0.83	22.36	1.24	24.01	1.21	0.04	0.01	-1.29	-0.10
		27.89	0.83	22.36	1.23	24.02	1.20	-0.04	0.01	-1.37	-0.10
		27.98	0.83	22.35	1.23	24.11	1.20	-0.13	0.00	-1.46	-0.10
		28.06	0.83	22.35	1.23	24.20	1.20	-0.13	0.00	-1.54	-0.11
		28.14	0.83	22.35	1.22	24.29	1.19	-0.13	-0.01	-1.63	-0.11
		28.23	0.83	22.35	1.22	24.38	1.19	-0.21	-0.01	-1.63	-0.12
		28.31	0.83	22.35	1.21	24.47	1.18	-0.21	-0.02	-1.72	-0.12
		28.40	0.83	22.35	1.21	24.56	1.18	-0.30	-0.02	-1.80	-0.12
		28.48	0.83	22.35	1.20	24.65	1.17	-0.38	-0.02	-1.80	-0.13
		28.56	0.82	22.35	1.20	24.74	1.17	-0.46	-0.03	-1.89	-0.13

		28.65	0.82	22.35	1.19	24.83	1.16	-0.55	-0.03	-1.97	-0.13
		28.73	0.82	22.35	1.19	24.92	1.16	-0.63	-0.04	-1.97	-0.14
		28.81	0.82	22.35	1.19	25.01	1.16	-0.63	-0.04	-2.06	-0.14
		28.90	0.82	22.35	1.18	25.10	1.15	-0.72	-0.05	-2.14	-0.14
		28.98	0.82	22.35	1.18	25.19	1.15	-0.72	-0.05		
		29.06	0.82	22.35	1.17	25.28	1.14	-0.80	-0.05		
		29.15	0.82	22.35	1.17	25.37	1.14	-0.89	-0.06		
		29.23	0.81	22.35	1.16	25.37	1.13	-0.97	-0.06		
		29.32	0.81	22.35	1.16	25.46	1.13	-1.06	-0.07		
		29.40	0.81	22.35	1.15	25.46	1.13	-1.14	-0.07		
		29.48	0.81	22.35	1.15	25.55	1.12	-1.22	-0.08		
		29.57	0.81	22.35	1.15	25.64	1.12	-1.31	-0.08		
		29.65	0.81	22.35	1.14	25.73	1.12	-1.31	-0.09		
		29.73	0.81	22.35	1.14	25.73	1.11	-1.39	-0.09		
		29.82	0.81	22.35	1.13	25.82	1.11	-1.39	-0.09		
		29.90	0.81	22.35	1.13	25.82	1.11	-1.48	-0.10		
		29.98	0.81	22.43	1.13	25.91	1.10	-1.56	-0.10		
		30.07	0.81	22.52	1.12	26.01	1.10	-1.65	-0.11		
		30.15	0.81	22.60	1.12	26.10	1.09	-1.73	-0.11		
		30.23	0.81	22.60	1.12	26.19	1.09	-1.73	-0.12		
		30.32	0.81	22.69	1.12	26.28	1.08	-1.82	-0.12		
		30.40	0.81	22.69	1.11	26.37	1.08	-1.82	-0.12		
		30.49	0.80	22.77	1.11	26.46	1.07	-1.90	-0.13		
		30.57	0.80	22.86	1.10	26.55	1.07	-1.98	-0.13		
		30.65	0.80	22.94	1.10	26.64	1.07	-2.07	-0.14		
		30.74	0.80	23.02	1.09	26.73	1.06	-2.15	-0.14		
		30.82	0.80	23.11	1.09	26.82	1.06	-2.24	-0.15		
				23.19	1.08	26.91	1.05	-2.32	-0.15		
				23.28	1.08	27.00	1.05	-2.32	-0.16		
				23.36	1.08	27.09	1.04	-2.41	-0.16		
				23.44	1.07	27.18	1.04				
				23.53	1.07	27.27	1.04				
				23.61	1.06	27.36	1.04				
				23.70	1.06	27.45	1.03				
				23.78	1.05	27.54	1.03				
				23.87	1.05	27.63	1.03				
				23.87	1.05	27.72	1.02				
				23.95	1.04	27.81	1.02				
				24.03	1.04	27.90	1.01				
				24.12	1.04	27.99	1.01				
				24.20	1.04	28.08	1.00				

				24.29	1.04	28.08	1.00				
				24.37	1.03	28.17	0.99				
				24.45	1.03	28.18	0.99				
				24.54	1.03	28.27	0.99				
				24.62	1.03	28.36	0.99				
				24.62	1.02	28.36	0.98				
				24.71	1.02	28.45	0.98				
				24.79	1.02	28.54	0.98				
				24.88	1.01	28.63	0.97				
				24.96	1.01	28.72	0.97				
				25.04	1.01	28.72	0.96				
				25.13	1.01	28.81	0.96				
				25.21	1.01	28.81	0.96				
				25.30	1.00	28.90	0.95				
				25.38	1.00	28.99	0.95				
				25.47	1.00	28.99	0.95				
				25.55	1.00	29.08	0.95				
				25.63	1.00	29.17	0.94				
				25.72	0.99	29.26	0.94				
				25.80	0.99	29.35	0.94				
				25.89	0.99	29.44	0.93				
				25.97	0.99	29.53	0.93				
				26.05	0.98	29.62	0.92				
				26.14	0.98	29.71	0.92				
				26.14	0.98	29.71	0.91				
				26.22	0.98	29.80	0.91				
				26.31	0.97	29.80	0.91				
				26.39	0.97	29.89	0.90				
				26.39	0.97	29.98	0.90				
				26.48	0.97	30.07	0.90				
				26.56	0.97	30.16	0.89				
				26.64	0.97	30.25	0.89				
				26.73	0.97	30.35	0.88				
				26.81	0.96	30.44	0.88				
				26.90	0.96	30.53	0.88				
				26.98	0.95	30.53	0.87				
				27.07	0.95	30.62	0.87				
				27.07	0.95	30.71	0.87				
				27.15	0.95	30.80	0.87				
				27.23	0.95	30.80	0.86				
				27.32	0.94	30.89	0.86				

				27.40	0.94						
				27.49	0.94						
				27.57	0.94						
				27.57	0.93						
				27.65	0.93						
				27.74	0.93						
				27.82	0.93						
				27.91	0.93						
				27.99	0.93						
				27.99	0.92						
				28.08	0.92						
				28.16	0.92						
				28.24	0.92						
				28.33	0.92						
				28.41	0.92						
				28.50	0.92						
				28.58	0.92						
				28.67	0.92						
				28.75	0.92						
				28.83	0.92						
				28.92	0.92						
				29.00	0.91						
				29.09	0.91						
				29.17	0.91						
				29.26	0.90						
				29.34	0.90						
				29.42	0.90						
				29.51	0.90						
				29.59	0.90						
				29.68	0.90						
				29.76	0.90						
				29.85	0.89						
				29.93	0.89						
				30.01	0.89						
				30.10	0.89						
				30.18	0.89						
				30.27	0.88						
				30.35	0.88						
				30.44	0.88						
				30.52	0.88						
				30.60	0.88						

				30.69	0.88						
				30.77	0.87						
				30.86	0.87						

NACA 0006		NACA 0009		NACA 0012		NACA 0015		NACA 0018		NACA0021	
3.21E+06		3.21E+06		3.23E+06		3.20E+06		3.15E+06		3.19E+06	
α	Cd	α	Cd	α	Cd	α	Cd	α	Cd	α	Cd
-2.38	0.04	-2.67	0.05	-4.80	0.08	-4.72	0.09	-2.73	0.07	-2.40	0.06
-2.30	0.04	-2.59	0.05	-4.71	0.08	-4.63	0.09	-2.64	0.07	-2.31	0.06
-2.21	0.04	-2.50	0.05	-4.63	0.07	-4.54	0.08	-2.56	0.07	-2.23	0.06
-2.13	0.04	-2.42	0.05	-4.54	0.07	-4.45	0.08	-2.48	0.07	-2.15	0.06
-2.04	0.04	-2.34	0.05	-4.46	0.07	-4.36	0.08	-2.39	0.07	-2.06	0.06
-1.96	0.04	-2.25	0.05	-4.38	0.07	-4.27	0.08	-2.31	0.07	-1.98	0.06
-1.87	0.04	-2.17	0.05	-4.29	0.07	-4.18	0.08	-2.22	0.07	-1.89	0.06
-1.79	0.04	-2.09	0.05	-4.21	0.06	-4.09	0.08	-2.14	0.07	-1.81	0.06
-1.70	0.04	-2.00	0.04	-4.12	0.06	-4.00	0.07	-2.05	0.07	-1.72	0.05
-1.62	0.04	-1.92	0.04	-4.04	0.06	-3.91	0.07	-1.97	0.07	-1.64	0.05
-1.53	0.04	-1.84	0.04	-3.96	0.07	-3.91	0.07	-1.89	0.07	-1.56	0.05
-1.45	0.04	-1.75	0.04	-3.87	0.07	-3.82	0.07	-1.80	0.07	-1.47	0.05
-1.36	0.04	-1.67	0.04	-3.79	0.06	-3.73	0.07	-1.72	0.07	-1.39	0.05
-1.28	0.04	-1.58	0.04	-3.70	0.06	-3.64	0.06	-1.63	0.07	-1.30	0.05
-1.19	0.04	-1.50	0.04	-3.62	0.06	-3.55	0.06	-1.55	0.06	-1.22	0.05
-1.11	0.04	-1.42	0.04	-3.53	0.06	-3.46	0.06	-1.47	0.06	-1.13	0.05
-1.02	0.04	-1.33	0.04	-3.45	0.06	-3.37	0.06	-1.38	0.06	-1.05	0.05
-0.94	0.04	-1.25	0.04	-3.37	0.06	-3.28	0.06	-1.30	0.06	-0.96	0.05
-0.85	0.04	-1.17	0.04	-3.28	0.06	-3.19	0.06	-1.21	0.06	-0.88	0.05
-0.77	0.04	-1.08	0.04	-3.20	0.06	-3.10	0.06	-1.13	0.06	-0.79	0.05
-0.68	0.04	-1.00	0.04	-3.11	0.06	-3.01	0.06	-1.04	0.06	-0.71	0.05
-0.60	0.04	-0.92	0.04	-3.03	0.06	-2.92	0.06	-0.96	0.06	-0.62	0.05
-0.51	0.04	-0.83	0.04	-2.94	0.06	-2.83	0.06	-0.88	0.06	-0.54	0.05
-0.43	0.04	-0.75	0.04	-2.86	0.06	-2.74	0.06	-0.79	0.06	-0.46	0.05
-0.34	0.04	-0.66	0.04	-2.78	0.06	-2.65	0.06	-0.71	0.06	-0.37	0.05
-0.26	0.04	-0.58	0.04	-2.69	0.05	-2.56	0.06	-0.62	0.06	-0.29	0.05
-0.17	0.04	-0.50	0.04	-2.61	0.05	-2.47	0.06	-0.54	0.06	-0.20	0.05
-0.09	0.04	-0.41	0.04	-2.52	0.05	-2.38	0.06	-0.45	0.06	-0.12	0.05
0.00	0.04	-0.33	0.04	-2.44	0.05	-2.29	0.05	-0.37	0.06	-0.03	0.05
0.09	0.04	-0.25	0.04	-2.36	0.05	-2.20	0.05	-0.29	0.06	0.05	0.05
0.17	0.04	-0.16	0.04	-2.27	0.05	-2.11	0.05	-0.20	0.06	0.14	0.05
0.26	0.04	-0.08	0.04	-2.19	0.05	-2.02	0.05	-0.12	0.06	0.22	0.05
0.34	0.04	0.00	0.04	-2.10	0.05	-1.93	0.05	-0.03	0.06	0.30	0.05

0.43	0.04	0.09	0.04	-2.02	0.05	-1.84	0.05	0.05	0.06	0.39	0.05
0.51	0.04	0.17	0.04	-1.93	0.05	-1.75	0.05	0.14	0.06	0.47	0.05
0.60	0.04	0.26	0.04	-1.85	0.05	-1.66	0.05	0.22	0.06	0.56	0.05
0.68	0.04	0.34	0.04	-1.77	0.05	-1.57	0.05	0.30	0.06	0.64	0.05
0.77	0.04	0.42	0.04	-1.68	0.05	-1.48	0.05	0.39	0.06	0.73	0.05
0.85	0.04	0.51	0.04	-1.60	0.05	-1.39	0.05	0.47	0.06	0.73	0.06
0.94	0.04	0.59	0.04	-1.51	0.05	-1.30	0.05	0.56	0.06	0.81	0.06
1.02	0.04	0.67	0.04	-1.43	0.05	-1.21	0.05	0.64	0.06	0.90	0.06
1.11	0.04	0.76	0.04	-1.35	0.05	-1.12	0.05	0.73	0.06	0.98	0.06
1.19	0.04	0.84	0.04	-1.26	0.05	-1.03	0.05	0.81	0.06	1.07	0.06
1.28	0.04	0.93	0.04	-1.18	0.05	-0.94	0.05	0.89	0.06	1.15	0.06
1.36	0.04	1.01	0.04	-1.09	0.05	-0.85	0.05	0.98	0.06	1.24	0.05
1.45	0.04	1.09	0.04	-1.01	0.04	-0.76	0.05	1.06	0.06	1.32	0.05
1.53	0.04	1.18	0.04	-0.92	0.04	-0.67	0.05	1.15	0.06	1.40	0.05
1.62	0.04	1.26	0.04	-0.84	0.04	-0.58	0.05	1.23	0.06	1.49	0.05
1.70	0.04	1.34	0.04	-0.76	0.04	-0.49	0.05	1.32	0.06	1.57	0.05
1.79	0.04	1.43	0.04	-0.67	0.04	-0.40	0.05	1.40	0.06	1.66	0.05
1.87	0.04	1.51	0.04	-0.59	0.04	-0.31	0.05	1.49	0.06	1.74	0.05
1.96	0.04	1.59	0.04	-0.50	0.04	-0.22	0.05	1.57	0.06	1.83	0.05
2.04	0.04	1.68	0.04	-0.42	0.04	-0.13	0.05	1.65	0.06	1.91	0.05
2.13	0.05	1.76	0.04	-0.34	0.04	-0.04	0.05	1.74	0.06	2.00	0.05
2.21	0.05	1.85	0.04	-0.25	0.05	0.04	0.05	1.82	0.06	2.08	0.05
2.30	0.05	1.93	0.04	-0.17	0.05	0.13	0.05	1.91	0.07	2.17	0.05
2.38	0.05	2.01	0.04	-0.08	0.05	0.22	0.05	1.99	0.07	2.25	0.06
2.47	0.05	2.10	0.04	0.00	0.05	0.31	0.05	2.08	0.07	2.33	0.06
2.55	0.05	2.18	0.04	0.09	0.05	0.40	0.05	2.16	0.07	2.42	0.06
2.64	0.05	2.26	0.04	0.17	0.05	0.49	0.05	2.25	0.07	2.50	0.06
2.72	0.05	2.35	0.04	0.25	0.05	0.58	0.05	2.33	0.07	2.59	0.06
2.81	0.05	2.43	0.04	0.34	0.05	0.67	0.05	2.41	0.07	2.67	0.06
2.89	0.05	2.52	0.04	0.42	0.05	0.76	0.05	2.50	0.07	2.76	0.06
2.98	0.05	2.60	0.05	0.51	0.05	0.85	0.05	2.58	0.07	2.84	0.06
3.06	0.05	2.68	0.05	0.59	0.05	0.94	0.05	2.67	0.07	2.93	0.06
3.15	0.06	2.77	0.05	0.68	0.05	1.03	0.05	2.75	0.07	3.01	0.07
3.23	0.06	2.85	0.05	0.76	0.05	1.12	0.05	2.84	0.07	3.10	0.07
3.32	0.06	2.93	0.05	0.84	0.05	1.21	0.05	2.92	0.07	3.18	0.07
3.40	0.06	3.02	0.05	0.93	0.05	1.30	0.05	3.00	0.07	3.27	0.07
3.49	0.06	3.10	0.05	1.01	0.05	1.39	0.05	3.09	0.07	3.35	0.07
3.57	0.06	3.19	0.05	1.10	0.05	1.48	0.05	3.17	0.07	3.44	0.07
3.66	0.07	3.27	0.05	1.18	0.05	1.57	0.05	3.26	0.07	3.52	0.07
3.74	0.07	3.35	0.05	1.27	0.05	1.66	0.05	3.34	0.07	3.61	0.07
3.83	0.07	3.44	0.05	1.35	0.05	1.75	0.05	3.43	0.07	3.69	0.07

3.91	0.07	3.52	0.05	1.43	0.05	1.84	0.05	3.51	0.07	3.77	0.07
4.00	0.07	3.60	0.05	1.52	0.05	1.93	0.05	3.60	0.07	3.86	0.07
4.09	0.07	3.69	0.05	1.60	0.05	2.02	0.05	3.68	0.07	3.94	0.07
4.17	0.07	3.77	0.06	1.69	0.05	2.11	0.05	3.76	0.07	4.03	0.07
4.26	0.07	3.86	0.06	1.77	0.05	2.20	0.06	3.85	0.07	4.11	0.07
4.34	0.07	3.94	0.06	1.85	0.05	2.29	0.06	3.93	0.07	4.20	0.07
4.43	0.07	4.02	0.06	1.94	0.05	2.38	0.06	4.02	0.07	4.28	0.07
4.51	0.07	4.11	0.06	2.02	0.05	2.47	0.06	4.10	0.08	4.37	0.08
4.60	0.07	4.19	0.06	2.11	0.05	2.56	0.06	4.19	0.08	4.45	0.08
4.68	0.07	4.27	0.06	2.19	0.05	2.65	0.06	4.27	0.08	4.54	0.08
4.77	0.08	4.36	0.06	2.28	0.05	2.74	0.06	4.36	0.08	4.62	0.08
4.85	0.08	4.44	0.07	2.36	0.05	2.83	0.06	4.44	0.08	4.71	0.08
4.94	0.08	4.53	0.07	2.44	0.05	2.92	0.06	4.44	0.09	4.79	0.09
5.02	0.08	4.61	0.07	2.53	0.05	3.01	0.06	4.53	0.09	4.88	0.09
5.02	0.09	4.69	0.07	2.61	0.05	3.10	0.06	4.61	0.09	4.96	0.09
5.11	0.09	4.78	0.07	2.70	0.05	3.19	0.06	4.70	0.09	5.05	0.09
5.19	0.09	4.86	0.07	2.78	0.05	3.28	0.06	4.78	0.09	5.13	0.09
5.28	0.09	4.95	0.08	2.87	0.05	3.37	0.06	4.86	0.09	5.21	0.09
5.36	0.09	5.03	0.08	2.95	0.05	3.46	0.06	4.95	0.09	5.30	0.09
5.45	0.10	5.11	0.08	3.03	0.05	3.55	0.06	5.03	0.09	5.38	0.09
5.53	0.10	5.20	0.08	3.12	0.05	3.64	0.06	5.12	0.09	5.47	0.09
5.62	0.10	5.28	0.08	3.20	0.05	3.73	0.06	5.20	0.10	5.55	0.10
5.70	0.10	5.37	0.09	3.29	0.05	3.82	0.06	5.29	0.10	5.64	0.10
5.79	0.10	5.45	0.09	3.37	0.05	3.91	0.06	5.37	0.10	5.72	0.10
5.87	0.11	5.53	0.09	3.45	0.05	4.00	0.07	5.46	0.10	5.81	0.10
5.96	0.11	5.62	0.10	3.54	0.05	4.09	0.07	5.54	0.10	5.89	0.10
6.04	0.11	5.70	0.10	3.62	0.06	4.18	0.07	5.62	0.10	5.98	0.10
6.13	0.12	5.79	0.10	3.71	0.06	4.27	0.07	5.71	0.11	6.06	0.10
6.21	0.12	5.87	0.10	3.79	0.07	4.36	0.07	5.79	0.11	6.15	0.10
6.30	0.12	5.95	0.11	3.88	0.07	4.45	0.07	5.88	0.11	6.23	0.11
6.38	0.12	6.04	0.11	3.96	0.07	4.54	0.07	5.96	0.11	6.32	0.11
6.47	0.13	6.12	0.11	4.05	0.07	4.63	0.07	6.05	0.11	6.40	0.11
6.55	0.13	6.21	0.11	4.13	0.07	4.72	0.08	6.13	0.11	6.49	0.12
6.64	0.13	6.29	0.11	4.21	0.07	4.81	0.08	6.13	0.11	6.57	0.12
6.72	0.14	6.37	0.11	4.30	0.07	4.90	0.08	6.22	0.11	6.66	0.12
6.81	0.14	6.46	0.12	4.38	0.07	4.99	0.08	6.30	0.12	6.74	0.12
6.81	0.14	6.54	0.12	4.47	0.07	5.08	0.08	6.39	0.12	6.83	0.13
6.89	0.14	6.62	0.12	4.55	0.07	5.17	0.08	6.47	0.12	6.91	0.13
6.98	0.14	6.71	0.12	4.63	0.08	5.26	0.09	6.56	0.12	7.00	0.13
7.06	0.15	6.79	0.12	4.72	0.08	5.35	0.09	6.64	0.13	7.08	0.13
7.15	0.15	6.88	0.12	4.80	0.08	5.44	0.09	6.73	0.13	7.17	0.14

7.23	0.15	6.96	0.13	4.89	0.08	5.53	0.10	6.81	0.13	7.25	0.14
7.32	0.15	7.04	0.13	4.97	0.08	5.62	0.10	6.89	0.13	7.34	0.14
7.40	0.16	7.13	0.13	5.06	0.08	5.71	0.10	6.98	0.13	7.42	0.14
7.49	0.16	7.21	0.13	5.14	0.08	5.80	0.10	7.06	0.13	7.51	0.14
7.57	0.16	7.29	0.13	5.22	0.08	5.89	0.11	7.15	0.14	7.59	0.14
7.66	0.16	7.38	0.13	5.31	0.09	5.98	0.11	7.23	0.14	7.68	0.15
7.74	0.17	7.46	0.13	5.39	0.09	6.07	0.11	7.32	0.14	7.76	0.15
7.83	0.17	7.55	0.14	5.48	0.09	6.16	0.11	7.40	0.14	7.85	0.15
7.83	0.17	7.63	0.14	5.56	0.09	6.25	0.11	7.49	0.14	7.93	0.15
7.91	0.17	7.71	0.14	5.65	0.09	6.34	0.11	7.57	0.15	8.01	0.15
7.91	0.18	7.80	0.14	5.73	0.10	6.43	0.12	7.66	0.15	8.10	0.15
8.00	0.18	7.88	0.14	5.81	0.10	6.52	0.12	7.74	0.15	8.18	0.15
8.09	0.19	7.97	0.15	5.90	0.10	6.61	0.12	7.83	0.15	8.27	0.15
8.17	0.19	8.05	0.15	5.98	0.10	6.70	0.12	7.91	0.15	8.35	0.15
8.26	0.20	8.13	0.15	6.07	0.11	6.79	0.12	7.99	0.15	8.44	0.16
8.34	0.20	8.22	0.15	6.15	0.11	6.88	0.12	8.08	0.16	8.52	0.16
8.34	0.20	8.30	0.15	6.24	0.11	6.97	0.12	8.16	0.16	8.61	0.16
8.43	0.21	8.39	0.15	6.32	0.11	7.06	0.12	8.25	0.16	8.69	0.17
8.51	0.21	8.47	0.16	6.40	0.11	7.15	0.13	8.33	0.16	8.78	0.17
8.60	0.22	8.55	0.16	6.49	0.11	7.24	0.13	8.42	0.16	8.86	0.17
8.68	0.22	8.64	0.16	6.57	0.12	7.33	0.13	8.50	0.17	8.95	0.17
8.77	0.23	8.64	0.16	6.66	0.12	7.42	0.13	8.59	0.17	9.03	0.17
8.77	0.23	8.72	0.16	6.74	0.12	7.51	0.14	8.67	0.18	9.12	0.17
8.77	0.23	8.72	0.17	6.83	0.13	7.60	0.14	8.67	0.18	9.20	0.17
8.85	0.24	8.81	0.17	6.91	0.13	7.69	0.14	8.76	0.18	9.29	0.17
8.85	0.24	8.89	0.17	6.99	0.13	7.69	0.15	8.76	0.18	9.37	0.18
8.94	0.25	8.97	0.17	7.08	0.13	7.78	0.15	8.84	0.18	9.46	0.18
9.02	0.25	9.06	0.17	7.16	0.13	7.87	0.15	8.93	0.19	9.54	0.19
9.11	0.26	9.14	0.18	7.25	0.14	7.96	0.16	9.01	0.19	9.63	0.19
9.11	0.26	9.22	0.18	7.33	0.14	8.04	0.16	9.10	0.19	9.71	0.19
9.19	0.26	9.31	0.18	7.42	0.14	8.13	0.16	9.18	0.20	9.80	0.19
9.19	0.27	9.39	0.19	7.50	0.15	8.22	0.16	9.27	0.20	9.88	0.20
9.19	0.27	9.48	0.19	7.59	0.15	8.31	0.16	9.35	0.20	9.97	0.20
9.28	0.28	9.56	0.19	7.67	0.15	8.40	0.16	9.44	0.21	10.05	0.20
9.28	0.28	9.65	0.20	7.75	0.15	8.40	0.17	9.52	0.21	10.14	0.21
9.36	0.29	9.73	0.20	7.84	0.15	8.49	0.17	9.61	0.21	10.22	0.21
9.36	0.29	9.81	0.21	7.92	0.16	8.58	0.17	9.69	0.21	10.31	0.21
9.45	0.30	9.90	0.21	8.01	0.16	8.67	0.17	9.78	0.21	10.31	0.22
9.45	0.30	9.98	0.22	8.09	0.16	8.76	0.17	9.86	0.22	10.39	0.22
9.45	0.30	10.07	0.22	8.18	0.16	8.85	0.17	9.95	0.22	10.48	0.22
9.53	0.31	10.15	0.22	8.26	0.16	8.85	0.18	10.03	0.22	10.56	0.22

9.53	0.31	10.23	0.23	8.34	0.17	8.94	0.18	10.03	0.23	10.65	0.23
9.62	0.32	10.32	0.23	8.43	0.17	9.03	0.18	10.11	0.23	10.73	0.23
9.62	0.32	10.40	0.23	8.51	0.17	9.12	0.18	10.20	0.23	10.82	0.23
9.70	0.33	10.49	0.23	8.60	0.17	9.12	0.19	10.28	0.23	10.90	0.24
9.70	0.33	10.57	0.23	8.68	0.17	9.21	0.19	10.29	0.24	10.99	0.24
9.70	0.33	10.65	0.24	8.77	0.18	9.30	0.19	10.37	0.24	11.07	0.24
9.79	0.34	10.74	0.24	8.85	0.18	9.39	0.19	10.45	0.24	11.16	0.24
9.79	0.34	10.82	0.24	8.93	0.18	9.48	0.19	10.54	0.25	11.24	0.25
9.87	0.35	10.91	0.25	9.02	0.19	9.57	0.20	10.62	0.25	11.33	0.25
9.87	0.35	10.99	0.25	9.10	0.19	9.66	0.20	10.71	0.25	11.41	0.25
9.87	0.36	10.99	0.26	9.19	0.19	9.66	0.20	10.79	0.25	11.50	0.25
9.96	0.36	11.08	0.26	9.27	0.19	9.75	0.20	10.88	0.25	11.58	0.25
9.96	0.36	11.08	0.26	9.36	0.20	9.84	0.20	10.96	0.26	11.67	0.26
9.96	0.37	11.16	0.26	9.44	0.20	9.93	0.21	11.05	0.26	11.75	0.26
10.04	0.37	11.24	0.26	9.52	0.20	10.02	0.21	11.13	0.26	11.84	0.26
10.04	0.38	11.24	0.27	9.61	0.21	10.11	0.21	11.22	0.26	11.92	0.27
10.04	0.38	11.33	0.27	9.69	0.21	10.11	0.22	11.30	0.27	12.01	0.27
10.13	0.39	11.41	0.27	9.78	0.21	10.20	0.22	11.39	0.27	12.09	0.28
10.13	0.39	11.50	0.27	9.86	0.21	10.20	0.22	11.47	0.27	12.18	0.28
10.13	0.39	11.50	0.28	9.86	0.22	10.29	0.22	11.47	0.28	12.26	0.28
10.21	0.40	11.58	0.28	9.95	0.22	10.38	0.22	11.56	0.28	12.35	0.29
10.21	0.40	11.66	0.28	10.03	0.22	10.38	0.23	11.64	0.28	12.44	0.29
10.21	0.41	11.75	0.29	10.11	0.23	10.47	0.23	11.73	0.28	12.52	0.30
10.30	0.41	11.83	0.29	10.20	0.23	10.56	0.23	11.81	0.29	12.61	0.30
10.30	0.42	11.92	0.29	10.28	0.23	10.65	0.23	11.90	0.29	12.69	0.31
10.30	0.42	12.00	0.30	10.37	0.23	10.65	0.24	11.98	0.29	12.78	0.31
10.38	0.42	12.09	0.30	10.45	0.23	10.74	0.24	12.07	0.30	12.86	0.31
10.38	0.43	12.17	0.31	10.54	0.23	10.83	0.24	12.15	0.30	12.86	0.31
10.38	0.43	12.25	0.31	10.62	0.23	10.92	0.25	12.24	0.31	12.95	0.31
10.38	0.44	12.34	0.31	10.62	0.24	11.01	0.25	12.32	0.31	13.03	0.32
10.47	0.44	12.42	0.31	10.70	0.24	11.10	0.26	12.41	0.32	13.12	0.32
10.47	0.45	12.50	0.32	10.79	0.24	11.19	0.26	12.49	0.32	13.12	0.32
10.55	0.45	12.59	0.32	10.87	0.25	11.19	0.26	12.58	0.32	13.20	0.32
10.55	0.45	12.67	0.32	10.96	0.25	11.28	0.26	12.66	0.32	13.29	0.33
10.55	0.45	12.76	0.33	11.04	0.26	11.37	0.27	12.75	0.32	13.37	0.33
10.64	0.46	12.84	0.33	11.13	0.26	11.46	0.27	12.83	0.33	13.46	0.34
10.64	0.46	12.93	0.34	11.21	0.27	11.55	0.28	12.92	0.33	13.54	0.34
10.64	0.47	13.01	0.34	11.30	0.27	11.64	0.28	13.00	0.33	13.63	0.34
10.64	0.47	13.09	0.35	11.30	0.27	11.73	0.28	13.08	0.34	13.71	0.35
10.64	0.48	13.18	0.35	11.38	0.27	11.82	0.28	13.17	0.34	13.80	0.35
10.72	0.48	13.18	0.35	11.46	0.27	11.91	0.29	13.25	0.35	13.88	0.35

10.72	0.48	13.26	0.35	11.55	0.27	12.00	0.29	13.34	0.35	13.88	0.35
10.72	0.49	13.35	0.35	11.63	0.27	12.09	0.30	13.42	0.35	13.97	0.35
10.81	0.49	13.43	0.36	11.72	0.27	12.18	0.30	13.51	0.36	14.05	0.36
10.81	0.50	13.51	0.36	11.80	0.28	12.27	0.31	13.59	0.36	14.14	0.36
10.81	0.50	13.60	0.37	11.89	0.28	12.36	0.31	13.68	0.37	14.22	0.37
10.81	0.51	13.68	0.37	11.97	0.29	12.45	0.32	13.77	0.37	14.31	0.37
10.81	0.51	13.77	0.38	12.05	0.29	12.54	0.32	13.85	0.38	14.39	0.38
10.89	0.51	13.85	0.38	12.14	0.30	12.63	0.33	13.93	0.38	14.48	0.38
10.89	0.52	13.94	0.38	12.22	0.30	12.72	0.33	13.94	0.38	14.56	0.38
10.89	0.52	14.02	0.39	12.31	0.31	12.81	0.33	14.02	0.38	14.65	0.39
10.89	0.53	14.10	0.39	12.39	0.31	12.90	0.33	14.10	0.39	14.73	0.39
10.89	0.53	14.19	0.40	12.48	0.31	12.99	0.34	14.19	0.39	14.82	0.39
10.98	0.54	14.27	0.40	12.56	0.31	13.08	0.34	14.19	0.39	14.82	0.40
10.98	0.54	14.36	0.40	12.64	0.31	13.08	0.34	14.27	0.39	14.90	0.40
10.98	0.54	14.44	0.41	12.73	0.32	13.17	0.34	14.36	0.39	14.99	0.40
11.06	0.55	14.52	0.41	12.81	0.32	13.26	0.35	14.44	0.40	15.08	0.41
11.06	0.55	14.61	0.41	12.81	0.32	13.35	0.35	14.53	0.40	15.16	0.41
11.06	0.56	14.69	0.42	12.90	0.32	13.44	0.36	14.61	0.40	15.25	0.41
11.15	0.56	14.78	0.42	12.98	0.33	13.53	0.36	14.61	0.41	15.25	0.42
11.15	0.57	14.86	0.43	13.07	0.33	13.62	0.37	14.70	0.41	15.33	0.42
11.15	0.57	14.95	0.43	13.07	0.33	13.71	0.37	14.78	0.41	15.42	0.42
11.15	0.58	15.03	0.44	13.15	0.33	13.80	0.37	14.87	0.42	15.50	0.42
11.15	0.58	15.11	0.44	13.24	0.34	13.80	0.38	14.95	0.42	15.59	0.43
11.15	0.58	15.20	0.44	13.32	0.34	13.89	0.38	15.04	0.42	15.67	0.43
11.23	0.59	15.28	0.45	13.32	0.34	13.98	0.38	15.12	0.43	15.76	0.44
11.23	0.59	15.37	0.45	13.40	0.34	14.07	0.38	15.21	0.43	15.84	0.44
11.32	0.60	15.45	0.46	13.40	0.35	14.16	0.38	15.29	0.44	15.93	0.45
11.32	0.60	15.54	0.46	13.49	0.35	14.25	0.39	15.38	0.44	16.01	0.45
11.32	0.61	15.62	0.47	13.57	0.36	14.34	0.39	15.46	0.45	16.10	0.45
11.32	0.61	15.70	0.47	13.66	0.36	14.43	0.40	15.55	0.45	16.18	0.46
11.40	0.61	15.79	0.47	13.74	0.37	14.52	0.40	15.63	0.46	16.27	0.46
11.40	0.62	15.87	0.48	13.83	0.37	14.52	0.41	15.72	0.46	16.35	0.47
11.49	0.62	15.96	0.48	13.91	0.37	14.61	0.41	15.80	0.46	16.44	0.47
11.49	0.62	16.04	0.49	13.99	0.38	14.61	0.41	15.89	0.47	16.52	0.48
11.49	0.63	16.12	0.49	14.08	0.38	14.70	0.42	15.97	0.47	16.61	0.48
11.57	0.63	16.21	0.50	14.08	0.38	14.79	0.42	16.06	0.48	16.69	0.48
11.57	0.64	16.29	0.50	14.16	0.38	14.88	0.43	16.14	0.48	16.78	0.49
11.57	0.64	16.38	0.50	14.25	0.38	14.97	0.43	16.23	0.49	16.86	0.49
11.57	0.64	16.46	0.51	14.33	0.39	14.97	0.43	16.31	0.49	16.87	0.49
11.57	0.65	16.55	0.51	14.42	0.39	15.06	0.43	16.40	0.49	16.95	0.49
11.66	0.65	16.63	0.52	14.50	0.40	15.15	0.43	16.48	0.50	17.04	0.50

11.66	0.66	16.71	0.52	14.59	0.40	15.24	0.44	16.57	0.50	17.12	0.50
11.66	0.66	16.80	0.53	14.67	0.41	15.33	0.44	16.65	0.51	17.21	0.51
11.74	0.67	16.80	0.53	14.75	0.41	15.42	0.45	16.74	0.51	17.29	0.51
11.74	0.67	16.88	0.53	14.84	0.41	15.51	0.45	16.82	0.52	17.38	0.52
11.74	0.67	16.88	0.53	14.84	0.42	15.60	0.46	16.91	0.52	17.38	0.52
11.74	0.68	16.88	0.54	14.92	0.42	15.69	0.46	17.00	0.53	17.46	0.52
11.83	0.68	16.97	0.54	15.01	0.42	15.69	0.47	17.08	0.53	17.46	0.53
11.83	0.69	16.97	0.55	15.01	0.42	15.78	0.47	17.08	0.53	17.55	0.53
11.91	0.69	17.05	0.55	15.09	0.42	15.78	0.48	17.16	0.53	17.63	0.54
11.91	0.69	17.14	0.56	15.09	0.43	15.87	0.48	17.25	0.53	17.72	0.54
11.91	0.70	17.14	0.56	15.18	0.43	15.96	0.48	17.33	0.54	17.80	0.55
12.00	0.70	17.14	0.56	15.26	0.44	16.04	0.49	17.42	0.54	17.89	0.55
12.00	0.70	17.22	0.57	15.34	0.44	16.13	0.49	17.42	0.55	17.97	0.55
12.00	0.71	17.22	0.57	15.43	0.45	16.22	0.50	17.50	0.55	18.06	0.55
12.09	0.71	17.22	0.58	15.51	0.45	16.31	0.50	17.51	0.55	18.14	0.56
12.09	0.72	17.31	0.58	15.60	0.45	16.31	0.50	17.59	0.55	18.23	0.56
12.09	0.72	17.31	0.59	15.68	0.46	16.40	0.50	17.67	0.56	18.32	0.57
12.17	0.73	17.31	0.59	15.77	0.46	16.49	0.50	17.76	0.56	18.40	0.57
12.17	0.73	17.39	0.59	15.85	0.47	16.58	0.51	17.84	0.56	18.49	0.58
12.17	0.73	17.39	0.60	15.85	0.47	16.67	0.51	17.93	0.57	18.57	0.58
12.26	0.74	17.39	0.60	15.94	0.47	16.76	0.52	18.02	0.57	18.57	0.59
12.26	0.74	17.48	0.61	15.94	0.48	16.85	0.52	18.10	0.58	18.66	0.59
12.26	0.75	17.48	0.61	16.02	0.48	16.94	0.53	18.19	0.58	18.66	0.59
12.34	0.75	17.48	0.62	16.10	0.48	17.03	0.53	18.27	0.59	18.74	0.59
12.34	0.76	17.56	0.62	16.10	0.49	17.12	0.53	18.36	0.59	18.83	0.60
12.34	0.76	17.56	0.62	16.19	0.49	17.21	0.54	18.44	0.60	18.91	0.60
12.34	0.76	17.56	0.63	16.27	0.49	17.30	0.54	18.53	0.60	19.00	0.61
12.34	0.77	17.65	0.63	16.36	0.49	17.39	0.55	18.61	0.60	19.08	0.61
12.34	0.77	17.65	0.64	16.44	0.50	17.48	0.55	18.70	0.61	19.08	0.62
12.43	0.78	17.65	0.64	16.53	0.50	17.57	0.56	18.78	0.61	19.17	0.62
12.43	0.78	17.65	0.65	16.61	0.51	17.66	0.56	18.78	0.62	19.25	0.62
12.43	0.79	17.65	0.65	16.70	0.51	17.75	0.57	18.87	0.62	19.34	0.63
12.51	0.79	17.73	0.65	16.70	0.51	17.84	0.57	18.87	0.62	19.43	0.63
12.51	0.79	17.73	0.66	16.78	0.51	17.93	0.58	18.87	0.63	19.43	0.64
12.51	0.80	17.74	0.66	16.86	0.52	17.93	0.58	18.95	0.63	19.51	0.64
12.51	0.80	17.74	0.67	16.95	0.52	18.02	0.58	19.04	0.63	19.51	0.64
12.51	0.81	17.74	0.67	17.03	0.53	18.02	0.58	19.12	0.64	19.60	0.65
12.60	0.81	17.74	0.68	17.03	0.53	18.11	0.59	19.21	0.64	19.68	0.65
12.68	0.82	17.74	0.68	17.12	0.53	18.20	0.59	19.29	0.65	19.68	0.66
12.68	0.82	17.74	0.68	17.12	0.53	18.20	0.60	19.29	0.65	19.77	0.66
12.77	0.82	17.74	0.69	17.20	0.54	18.29	0.60	19.38	0.65	19.77	0.66

12.77	0.83	17.82	0.69	17.20	0.54	18.29	0.60	19.38	0.66	19.85	0.67
12.77	0.83	17.82	0.70	17.29	0.54	18.38	0.61	19.46	0.66	19.94	0.67
12.85	0.84	17.82	0.70	17.29	0.55	18.47	0.61	19.55	0.67	19.94	0.67
12.85	0.84	17.82	0.71	17.37	0.55	18.56	0.62	19.63	0.67	20.02	0.67
12.85	0.85	17.83	0.71	17.45	0.55	18.65	0.62	19.72	0.67	20.11	0.68
12.85	0.85	17.83	0.71	17.54	0.56	18.65	0.63	19.80	0.68	20.19	0.68
12.85	0.86	17.91	0.72	17.62	0.56	18.74	0.63	19.89	0.68	20.28	0.69
12.94	0.86	17.91	0.72	17.71	0.56	18.83	0.63	19.97	0.69	20.28	0.69
12.94	0.86	17.91	0.73	17.79	0.57	18.92	0.64	20.06	0.69	20.37	0.69
12.94	0.87	17.91	0.73	17.88	0.57	19.01	0.64	20.14	0.70	20.37	0.70
13.02	0.87	17.91	0.74	17.88	0.58	19.10	0.65	20.23	0.70	20.37	0.70
13.02	0.88	17.91	0.74	17.96	0.58	19.19	0.65	20.23	0.70	20.37	0.71
13.02	0.88	17.91	0.74	17.96	0.58	19.28	0.66	20.31	0.71	20.45	0.71
13.11	0.89	17.91	0.75	18.05	0.59	19.37	0.66	20.32	0.71	20.54	0.72
13.11	0.89	17.91	0.75	18.13	0.59	19.37	0.67	20.32	0.72	20.62	0.72
13.19	0.89	18.00	0.76	18.21	0.60	19.46	0.67	20.40	0.72	20.71	0.72
13.19	0.90	18.00	0.76	18.30	0.60	19.46	0.67	20.49	0.73	20.71	0.73
13.28	0.90	18.00	0.77	18.38	0.60	19.55	0.68	20.57	0.73	20.79	0.73
13.28	0.91	18.00	0.77	18.47	0.61	19.55	0.68	20.66	0.73	20.88	0.73
13.28	0.91	18.00	0.77	18.47	0.61	19.64	0.68	20.74	0.74	20.96	0.73
13.28	0.92	18.00	0.78	18.55	0.62	19.64	0.69	20.83	0.74	20.96	0.74
13.28	0.92	18.00	0.78	18.64	0.62	19.73	0.69	20.91	0.75	20.97	0.74
13.28	0.92	18.00	0.79	18.64	0.63	19.82	0.69	21.00	0.75	21.05	0.75
13.28	0.93	18.00	0.79	18.72	0.63	19.82	0.70	21.08	0.76	21.05	0.75
13.36	0.93	18.00	0.80	18.72	0.63	19.91	0.70	21.17	0.76	21.14	0.76
13.45	0.94	18.00	0.80	18.81	0.64	19.91	0.71	21.17	0.77	21.14	0.76
13.45	0.94	18.00	0.80	18.89	0.64	20.00	0.71	21.25	0.77	21.22	0.76
13.45	0.95	18.00	0.81	18.97	0.64	20.00	0.71	21.25	0.77	21.22	0.77
13.45	0.95	18.01	0.81	19.06	0.65	20.09	0.72	21.34	0.77	21.31	0.77
13.45	0.95	18.01	0.82	19.14	0.65	20.18	0.72	21.42	0.78	21.31	0.78
13.53	0.96	18.01	0.82	19.23	0.66	20.27	0.73	21.51	0.78	21.40	0.78
13.53	0.96	18.01	0.83	19.23	0.66	20.36	0.73	21.59	0.79	21.48	0.79
13.53	0.97	18.01	0.83	19.31	0.66	20.36	0.73	21.68	0.79	21.57	0.79
13.53	0.97	18.01	0.83	19.31	0.67	20.45	0.74	21.68	0.80	21.65	0.80
13.53	0.98	18.01	0.84	19.40	0.67	20.45	0.74	21.76	0.80	21.74	0.80
13.62	0.98	18.01	0.84	19.48	0.67	20.54	0.75	21.76	0.80	21.82	0.80
13.62	0.98	18.01	0.85	19.57	0.68	20.63	0.75	21.76	0.80	21.82	0.81
13.70	0.99	18.01	0.85	19.65	0.68	20.72	0.76	21.85	0.81	21.82	0.81
13.79	0.99	18.01	0.86	19.73	0.69	20.72	0.76	21.85	0.81	21.82	0.82
13.79	1.00	18.01	0.86	19.82	0.69	20.81	0.76	21.85	0.82	21.82	0.82
13.79	1.00	18.01	0.86	19.90	0.70	20.81	0.77	21.94	0.82	21.91	0.83

13.79	1.01	18.01	0.87	19.99	0.70	20.90	0.77	22.02	0.83	21.91	0.83
13.87	1.01	18.10	0.87	19.99	0.71	20.90	0.77	22.11	0.83	21.91	0.83
13.87	1.01	18.10	0.88	20.07	0.71	20.99	0.77	22.19	0.84	22.00	0.84
13.96	1.01	18.10	0.88	20.07	0.71	20.99	0.78	22.28	0.84	22.00	0.84
13.96	1.02	18.10	0.89	20.16	0.72	20.99	0.78	22.28	0.84	22.08	0.85
13.96	1.02	18.10	0.89	20.16	0.72	21.08	0.79	22.36	0.85	22.17	0.85
14.04	1.03	18.10	0.89	20.24	0.72	21.08	0.79	22.36	0.85	22.17	0.86
14.04	1.03	18.10	0.90	20.24	0.73	21.17	0.80	22.45	0.86	22.17	0.86
14.04	1.04	18.10	0.90	20.33	0.73	21.26	0.80	22.53	0.86	22.25	0.86
14.04	1.04	18.10	0.91	20.41	0.74	21.35	0.81	22.53	0.87	22.26	0.87
14.04	1.04	18.10	0.91	20.49	0.74	21.44	0.81	22.62	0.87	22.34	0.87
14.13	1.05	18.10	0.92	20.58	0.75	21.53	0.82	22.62	0.87	22.34	0.87
14.13	1.05	18.10	0.92	20.66	0.75	21.62	0.82	22.70	0.87	22.34	0.88
14.21	1.05	18.10	0.92	20.75	0.75	21.62	0.82	22.70	0.88	22.34	0.88
14.21	1.06	18.10	0.93	20.83	0.76	21.62	0.83	22.79	0.88	22.34	0.89
14.21	1.06	18.10	0.93	20.83	0.76	21.62	0.83	22.79	0.88	22.34	0.89
14.30	1.07	18.19	0.94	20.92	0.76	21.62	0.84	22.79	0.89	22.43	0.90
14.30	1.07	18.19	0.94	20.92	0.77	21.71	0.84	22.88	0.89	22.43	0.90
14.38	1.07	18.19	0.94	21.00	0.77	21.71	0.85	22.88	0.90	22.43	0.90
14.38	1.08	18.19	0.95	21.09	0.77	21.71	0.85	22.88	0.90	22.43	0.91
14.38	1.08	18.19	0.95	21.09	0.78	21.80	0.86	22.88	0.91	22.52	0.91
14.47	1.09	18.19	0.96	21.17	0.78	21.80	0.86	22.88	0.91	22.52	0.92
14.47	1.09	18.19	0.96	21.25	0.78	21.89	0.86	22.96	0.91	22.52	0.92
14.47	1.10	18.19	0.97	21.34	0.78	21.98	0.87	22.96	0.92	22.52	0.93
14.55	1.10	18.19	0.97	21.42	0.79	21.98	0.87	22.96	0.92	22.52	0.93
14.55	1.11	18.19	0.97	21.42	0.79	22.07	0.87	22.97	0.93	22.52	0.93
14.55	1.11	18.28	0.98	21.51	0.80	22.07	0.88	22.97	0.93	22.61	0.94
14.64	1.11	18.28	0.98	21.51	0.80	22.07	0.88	22.97	0.94	22.61	0.94
14.64	1.12	18.28	0.99	21.59	0.81	22.16	0.89	22.97	0.94	22.61	0.95
14.72	1.12	18.28	0.99	21.59	0.81	22.16	0.89	22.97	0.94	22.61	0.95
14.72	1.13	18.28	1.00	21.68	0.82	22.25	0.90	22.97	0.95	22.61	0.96
14.81	1.13	18.28	1.00	21.76	0.82	22.34	0.90	22.97	0.95	22.61	0.96
14.81	1.13	18.28	1.00	21.85	0.82	22.34	0.91	22.97	0.96	22.69	0.96
14.81	1.14	18.28	1.01	21.93	0.83	22.43	0.91	22.97	0.96	22.69	0.97
14.89	1.14	18.28	1.01	22.01	0.83	22.43	0.92	22.97	0.97	22.70	0.97
14.89	1.14	18.28	1.02	22.10	0.84	22.43	0.92	22.97	0.97	22.70	0.98
14.89	1.15	18.28	1.02	22.18	0.84	22.43	0.92	23.06	0.97	22.70	0.98
14.89	1.15	18.28	1.03	22.18	0.85	22.43	0.93	23.06	0.98	22.70	0.99
14.89	1.16	18.28	1.03	22.18	0.85	22.43	0.93	23.06	0.98	22.70	0.99
14.98	1.16	18.28	1.03	22.18	0.86	22.43	0.94	23.06	0.99	22.70	1.00
14.98	1.17	18.37	1.04	22.18	0.86	22.52	0.94	23.06	0.99	22.70	1.00

15.06	1.17	18.45	1.04	22.27	0.86	22.52	0.95	23.15	1.00	22.70	1.00
15.06	1.17	18.45	1.05	22.27	0.87	22.52	0.95	23.15	1.00	22.70	1.01
15.15	1.18	18.45	1.05	22.35	0.87	22.52	0.96	23.15	1.01	22.70	1.01
15.15	1.18	18.45	1.06	22.35	0.88	22.52	0.96	23.15	1.01	22.70	1.02
15.15	1.19	18.45	1.06	22.35	0.88	22.52	0.97	23.15	1.01	22.70	1.02
15.23	1.19	18.54	1.06	22.35	0.89	22.52	0.97	23.15	1.02	22.70	1.03
15.23	1.20	18.54	1.07	22.35	0.89	22.52	0.97	23.15	1.02	22.79	1.03
15.23	1.20	18.54	1.07	22.44	0.89	22.52	0.98	23.15	1.03	22.79	1.03
15.23	1.20	18.54	1.08	22.44	0.90	22.52	0.98	23.15	1.03	22.79	1.04
15.32	1.21	18.54	1.08	22.44	0.90	22.52	0.99	23.24	1.04	22.79	1.04
15.32	1.21	18.54	1.09	22.44	0.91	22.52	0.99	23.24	1.04	22.79	1.05
15.40	1.21	18.63	1.09	22.44	0.91	22.52	1.00	23.24	1.04	22.79	1.05
15.40	1.22	18.63	1.09	22.44	0.92	22.52	1.00	23.32	1.05	22.79	1.06
15.49	1.22	18.63	1.10	22.44	0.92	22.52	1.01	23.32	1.05	22.79	1.06
15.49	1.23	18.63	1.10	22.44	0.93	22.52	1.01	23.32	1.06	22.80	1.06
15.57	1.23	18.63	1.11	22.44	0.93	22.52	1.01	23.33	1.06	22.80	1.07
15.57	1.23	18.63	1.11	22.44	0.93	22.52	1.02	23.33	1.07	22.80	1.07
15.57	1.23	18.63	1.12	22.44	0.94	22.52	1.02	23.33	1.07	22.88	1.08
15.66	1.24	18.63	1.12	22.44	0.94	22.52	1.03	23.41	1.08	22.88	1.08
15.66	1.24	18.63	1.12	22.44	0.95	22.52	1.03	23.41	1.08	22.97	1.08
15.66	1.25	18.71	1.13	22.44	0.95	22.61	1.04	23.41	1.08	22.97	1.09
15.74	1.25	18.71	1.13	22.44	0.96	22.61	1.04	23.41	1.09	22.97	1.09
15.74	1.26	18.72	1.14	22.44	0.96	22.61	1.05	23.50	1.09	23.05	1.10
15.83	1.26	18.80	1.14	22.44	0.97	22.61	1.05	23.50	1.10	23.06	1.10
15.91	1.26	18.80	1.15	22.44	0.97	22.61	1.06	23.50	1.10	23.06	1.10
15.91	1.27	18.80	1.15	22.44	0.97	22.61	1.06	23.50	1.11	23.06	1.11
16.00	1.27	18.88	1.15	22.44	0.98	22.61	1.06	23.59	1.11	23.06	1.11
16.00	1.28	18.89	1.16	22.44	0.98	22.61	1.07	23.59	1.11	23.14	1.12
16.00	1.28	18.89	1.16	22.44	0.99	22.61	1.07	23.59	1.12	23.23	1.12
16.09	1.29	18.97	1.17	22.44	0.99	22.70	1.08	23.59	1.12	23.23	1.13
16.09	1.29	18.97	1.17	22.44	1.00	22.70	1.08	23.67	1.13	23.31	1.13
16.17	1.29	18.97	1.18	22.44	1.00	22.70	1.09	23.67	1.13	23.31	1.13
16.17	1.30	18.97	1.18	22.44	1.01	22.79	1.09	23.68	1.14	23.40	1.14
16.17	1.30	18.97	1.18	22.44	1.01	22.79	1.10	23.68	1.14	23.40	1.14
16.26	1.31	18.97	1.19	22.44	1.01	22.79	1.10	23.68	1.14	23.49	1.15
16.26	1.31	18.97	1.19	22.44	1.02	22.79	1.11	23.68	1.15	23.49	1.15
16.26	1.32	18.97	1.20	22.44	1.02	22.79	1.11	23.76	1.15	23.57	1.16
16.34	1.32	18.97	1.20	22.44	1.03	22.79	1.11	23.76	1.16	23.57	1.16
16.34	1.32	19.06	1.21	22.44	1.03	22.79	1.12	23.76	1.16	23.57	1.17
16.43	1.33	19.06	1.21	22.44	1.04	22.79	1.12	23.76	1.17	23.66	1.17
16.43	1.33	19.14	1.21	22.44	1.04	22.88	1.13	23.77	1.17	23.66	1.17

16.51	1.34	19.14	1.22	22.44	1.04	22.88	1.13	23.85	1.18	23.74	1.18
		19.23	1.22	22.44	1.05	22.88	1.14	23.94	1.18	23.83	1.18
		19.23	1.23	22.44	1.05	22.88	1.14	23.94	1.18	23.83	1.19
		19.23	1.23	22.44	1.06	22.88	1.15	23.94	1.19	23.92	1.19
		19.31	1.24	22.44	1.06	22.88	1.15	23.94	1.19	23.92	1.20
		19.31	1.24	22.44	1.07	22.88	1.15	23.94	1.20	23.92	1.20
		19.31	1.24	22.45	1.07	22.88	1.16	24.02	1.20	24.00	1.20
		19.40	1.25	22.45	1.08	22.97	1.16	24.02	1.21	24.00	1.21
		19.40	1.25	22.45	1.08	22.97	1.17	24.11	1.21	24.09	1.21
		19.40	1.26	22.45	1.08	22.97	1.17	24.11	1.21	24.09	1.22
		19.40	1.26	22.45	1.09	22.97	1.18	24.20	1.22	24.17	1.22
		19.40	1.27	22.45	1.09	22.97	1.18	24.20	1.22	24.18	1.23
		19.40	1.27	22.45	1.10	22.97	1.19	24.20	1.23	24.26	1.23
		19.40	1.27	22.45	1.10	22.97	1.19	24.20	1.23	24.26	1.23
		19.40	1.28	22.45	1.11	22.97	1.20	24.20	1.24	24.35	1.23
		19.40	1.28	22.36	1.11	22.97	1.20	24.20	1.24	24.35	1.24
		19.40	1.29	22.36	1.12	22.97	1.20	24.28	1.25	24.35	1.24
		19.49	1.29	22.36	1.12	22.97	1.21	24.28	1.25	24.35	1.25
		19.57	1.29	22.36	1.12	22.97	1.21	24.29	1.25	24.35	1.25
		19.57	1.30	22.36	1.13	22.97	1.22	24.37	1.26	24.35	1.26
		19.66	1.30	22.36	1.13	23.06	1.22	24.37	1.26	24.44	1.26
		19.66	1.30	22.36	1.14	23.15	1.22	24.46	1.27	24.52	1.27
		19.66	1.30	22.36	1.14	23.15	1.23	24.54	1.27	24.61	1.27
		19.66	1.31	22.36	1.15	23.24	1.23	24.54	1.28	24.61	1.27
		19.74	1.31	22.36	1.15	23.24	1.24	24.63	1.28	24.69	1.28
		19.74	1.32	22.36	1.15	23.24	1.24	24.63	1.28	24.69	1.28
		19.74	1.32	22.36	1.16	23.33	1.25	24.63	1.29	24.78	1.29
		19.83	1.33	22.36	1.16	23.33	1.25	24.71	1.29	24.78	1.29
		19.83	1.33	22.37	1.17	23.33	1.25	24.71	1.30	24.86	1.30
		19.91	1.33	22.37	1.17	23.42	1.26	24.71	1.30	24.86	1.30
		20.00	1.34	22.37	1.18	23.42	1.26	24.72	1.31	24.87	1.30
		20.00	1.34	22.37	1.18	23.42	1.27	24.72	1.31	24.87	1.31
		20.00	1.35	22.37	1.19	23.51	1.27	24.72	1.31	24.95	1.31
		20.00	1.35	22.28	1.19	23.51	1.28	24.72	1.32	24.95	1.32
		20.00	1.36	22.28	1.19	23.51	1.28	24.80	1.32	24.95	1.32
		20.08	1.36	22.28	1.20	23.51	1.29	24.80	1.33	25.04	1.33
		20.08	1.36	22.28	1.20	23.60	1.29	24.80	1.33	25.04	1.33
		20.08	1.37	22.28	1.21	23.60	1.30	24.89	1.34	25.12	1.34
		20.08	1.37	22.28	1.21	23.60	1.30	24.89	1.34	25.21	1.34
		20.08	1.38	22.28	1.22	23.60	1.30	24.89	1.35	25.21	1.34
		20.08	1.38	22.28	1.22	23.60	1.31	24.98	1.35	25.30	1.35

		20.09	1.39	22.28	1.23	23.69	1.31	24.98	1.35	25.30	1.35
		20.09	1.39	22.28	1.23	23.69	1.32	24.98	1.36	25.30	1.36
		20.09	1.39	22.28	1.23	23.69	1.32	25.06	1.36	25.38	1.36
		20.17	1.40	22.28	1.24	23.69	1.33	25.06	1.37	25.38	1.37
		20.17	1.40	22.28	1.24	23.69	1.33	25.06	1.37	25.38	1.37
		20.26	1.41	22.28	1.25	23.69	1.34	25.06	1.38	25.47	1.37
		20.26	1.41	22.28	1.25	23.78	1.34	25.15	1.38	25.47	1.38
		20.34	1.42	22.37	1.26	23.78	1.34	25.23	1.38	25.47	1.38
		20.34	1.42	22.37	1.26	23.87	1.35	25.24	1.39	25.56	1.39
		20.34	1.42	22.37	1.27	23.87	1.35	25.24	1.39	25.56	1.39
		20.34	1.43	22.37	1.27	23.96	1.36	25.24	1.40	25.64	1.40
		20.34	1.43	22.37	1.27	23.96	1.36	25.24	1.40	25.73	1.40
				22.37	1.28	23.96	1.37	25.24	1.41	25.73	1.40
				22.37	1.28	24.04	1.37	25.24	1.41	25.81	1.40
				22.37	1.29	24.04	1.38	25.32	1.42	25.81	1.40
				22.37	1.29	24.04	1.38	25.41	1.42	25.90	1.41
				22.37	1.30	24.04	1.39	25.49	1.42	25.90	1.41
				22.37	1.30	24.04	1.39	25.50	1.43	25.90	1.42
				22.37	1.30	24.13	1.39	25.58	1.43	25.98	1.42
				22.37	1.31	24.13	1.40	25.58	1.43	25.98	1.43
				22.37	1.31	24.22	1.40	25.58	1.44	25.99	1.43
				22.37	1.32	24.22	1.40	25.67	1.44	26.07	1.44
				22.37	1.32	24.31	1.41	25.67	1.45	26.07	1.44
				22.37	1.33	24.31	1.41	25.67	1.45	26.07	1.44
				22.37	1.33	24.40	1.42	25.75	1.45	26.16	1.45
				22.37	1.34	24.40	1.42	25.75	1.46	26.16	1.45
				22.37	1.34	24.40	1.43	25.75	1.46	26.16	1.46
				22.37	1.34	24.49	1.43	25.84	1.47	26.16	1.46
				22.37	1.35	24.49	1.44	25.84	1.47	26.16	1.47
				22.37	1.35	24.58	1.44	25.84	1.48	26.25	1.47
				22.37	1.36	24.58	1.44	25.84	1.48	26.25	1.47
				22.37	1.36	24.67	1.44	25.84	1.48	26.33	1.47
				22.37	1.37	24.67	1.45	25.84	1.49	26.33	1.48
				22.37	1.37	24.67	1.45	25.93	1.49	26.42	1.48
				22.37	1.38	24.67	1.46	25.93	1.50	26.42	1.49
				22.46	1.38	24.76	1.46	26.01	1.50	26.50	1.49
				22.46	1.38	24.76	1.47	26.10	1.51	26.50	1.49
				22.46	1.39	24.76	1.47	26.10	1.51	26.59	1.50
				22.46	1.39	24.85	1.48	26.18	1.52	26.59	1.50
				22.46	1.40	24.85	1.48	26.19	1.52	26.67	1.51
				22.46	1.40	24.94	1.49	26.19	1.52		

				22.46	1.41	24.94	1.49	26.27	1.53		
				22.46	1.41	24.94	1.49	26.27	1.53		
				22.54	1.41	25.03	1.50	26.36	1.54		
				22.54	1.42	25.03	1.50	26.44	1.54		
				22.63	1.42	25.03	1.51	26.44	1.55		
				22.63	1.42	25.03	1.51	26.53	1.55		
				22.63	1.43	25.12	1.52	26.53	1.55		
				22.71	1.43	25.12	1.52	26.53	1.56		
				22.71	1.44	25.12	1.53	26.61	1.56		
				22.80	1.44	25.12	1.53	26.61	1.57		
				22.88	1.45	25.21	1.53	26.62	1.57		
				22.88	1.45	25.21	1.54	26.70	1.58		
				22.88	1.45	25.21	1.54	26.70	1.58		
				22.97	1.46	25.30	1.55	26.70	1.59		
				22.97	1.46	25.30	1.55	26.79	1.59		
				22.97	1.47	25.39	1.56	26.79	1.59		
				23.05	1.47	25.39	1.56	26.79	1.60		
				23.05	1.48	25.39	1.57	26.87	1.60		
				23.05	1.48	25.48	1.57				
				23.14	1.49	25.48	1.58				
				23.14	1.49	25.48	1.58				
				23.14	1.49	25.48	1.58				
				23.22	1.50	25.57	1.59				
				23.22	1.50	25.57	1.59				
				23.22	1.51						
				23.22	1.51						
				23.31	1.52						
				23.31	1.52						
				23.31	1.52						
				23.39	1.53						
				23.39	1.53						
				23.48	1.54						
				23.56	1.54						
				23.56	1.55						
				23.64	1.55						
				23.64	1.56						
				23.73	1.56						
				23.81	1.56						
				23.81	1.57						
				23.90	1.57						
				23.90	1.58						

				23.90	1.58						
				23.98	1.59						
				23.98	1.59						
				23.98	1.60						
				24.07	1.60						
				24.07	1.60						
				24.07	1.61						
				24.07	1.61						
				24.15	1.62						
				24.15	1.62						
				24.24	1.63						
				24.24	1.63						
				24.32	1.63						
				24.41	1.63						
				24.41	1.64						
				24.49	1.64						
				24.57	1.65						

APPENDIX L

COEFFICIENTS OF LIFT AND DRAG USED FOR COMPUTATIONAL MODEL

NACA0009				NACA0015				NACA0020			
α	Cl	Cd	Cl/Cd	α	Cl	Cd	Cl/Cd	α	Cl	Cd	Cl/Cd
0	0.00	0.01	0.00	0	0.00	0.01	0.00	0	0.00	0.01	0.00
1	0.11	0.01	9.07	1	0.11	0.01	9.07	1	0.11	0.01	9.07
2	0.22	0.01	17.79	2	0.22	0.01	17.79	2	0.22	0.01	17.79
3	0.33	0.01	25.88	3	0.33	0.01	25.88	3	0.33	0.01	25.88
4	0.44	0.01	33.11	4	0.44	0.01	33.11	4	0.44	0.01	33.11
5	0.56	0.01	39.31	5	0.56	0.01	39.31	5	0.56	0.01	39.31
6	0.67	0.02	44.39	6	0.67	0.02	44.39	6	0.67	0.02	44.39
7	0.78	0.02	48.32	7	0.78	0.02	48.32	7	0.78	0.02	48.32
8	0.89	0.02	51.16	8	0.89	0.02	51.16	8	0.89	0.02	51.16
9	1.00	0.02	53.00	9	1.00	0.02	53.00	9	1.00	0.02	53.00
10	1.10	0.02	53.43	10	1.11	0.02	53.97	10	1.11	0.02	53.97
11	1.20	0.02	53.23	11	1.22	0.02	54.21	11	1.22	0.02	54.21
12	1.30	0.02	52.52	12	1.33	0.02	53.87	12	1.33	0.02	53.87
13	1.32	0.03	48.49	13	1.44	0.03	53.06	13	1.40	0.03	51.43
14	1.29	0.15	8.60	14	1.50	0.03	50.06	14	1.44	0.03	48.06
15	1.14	0.17	6.71	15	1.55	0.03	46.98	15	1.46	0.03	44.25
16	1.05	0.19	5.53	16	1.60	0.04	44.05	16	1.47	0.04	40.47
17	0.87	0.21	4.14	17	1.42	0.04	37.37	17	1.48	0.04	36.91
18	0.72	0.23	3.14	18	1.09	0.04	27.25	18	1.48	0.04	33.70
19	0.74	0.25	2.97	19	0.60	0.28	2.14	19	1.40	0.06	23.33
20	0.75	0.28	2.69	20	0.60	0.29	2.07	20	0.60	0.28	2.14
21	0.78	0.31	2.52	21	0.62	0.30	2.07	21	0.58	0.30	1.93
25	0.86	0.43	2.00	25	0.70	0.39	1.80	25	0.67	0.39	1.72
30	0.99	0.58	1.71	30	0.87	0.59	1.47	30	0.83	0.57	1.46
35	1.08	0.74	1.45	35	0.99	0.72	1.38	35	0.96	0.71	1.35
40	1.10	0.96	1.15	40	1.04	0.94	1.11	40	1.03	0.92	1.12
45	1.10	1.10	1.00	45	1.05	1.05	1.00	45	1.04	1.04	1.00
50	1.07	1.27	0.84	50	1.01	1.22	0.83	50	1.00	1.20	0.83
55	0.99	1.41	0.70	55	0.95	1.40	0.68	55	0.95	1.38	0.68
60	0.89	1.52	0.59	60	0.86	1.53	0.56	60	0.85	1.52	0.56
65	0.76	1.59	0.48	65	0.75	1.60	0.47	65	0.75	1.60	0.47
70	0.61	1.65	0.37	70	0.62	1.62	0.38	70	0.63	1.65	0.38
75	0.47	1.74	0.27	75	0.47	1.71	0.28	75	0.49	1.71	0.29
80	0.32	1.80	0.18	80	0.35	1.81	0.19	80	0.37	1.79	0.21
85	0.18	1.81	0.10	85	0.22	1.82	0.12	85	0.25	1.80	0.14
90	0.03	1.82	0.02	90	0.09	1.81	0.05	90	0.13	1.79	0.07
95	-0.11	1.81	-0.06	95	-0.04	1.79	-0.02	95	-0.01	1.77	0.00

100	-0.26	1.80	-0.15	100	-0.16	1.76	-0.09	100	-0.14	1.74	-0.08
105	-0.40	1.76	-0.23	105	-0.29	1.72	-0.17	105	-0.27	1.70	-0.16
110	-0.54	1.70	-0.32	110	-0.41	1.61	-0.26	110	-0.39	1.62	-0.24
115	-0.67	1.53	-0.44	115	-0.56	1.56	-0.36	115	-0.53	1.53	-0.35
120	-0.76	1.48	-0.51	120	-0.67	1.45	-0.46	120	-0.66	1.45	-0.45
125	-0.85	1.32	-0.64	125	-0.78	1.32	-0.59	125	-0.75	1.37	-0.55
130	-0.91	1.23	-0.74	130	-0.86	1.29	-0.66	130	-0.83	1.28	-0.65
135	-0.96	1.06	-0.91	135	-0.94	1.12	-0.84	135	-0.93	1.16	-0.80
140	-0.98	0.94	-1.05	140	-0.98	0.96	-1.02	140	-0.98	1.00	-0.98
145	-0.95	0.75	-1.26	145	-0.93	0.77	-1.20	145	-0.91	0.80	-1.14
150	-0.87	0.57	-1.52	150	-0.79	0.60	-1.32	150	-0.76	0.62	-1.23
155	-0.75	0.40	-1.87	155	-0.67	0.41	-1.64	155	-0.66	0.44	-1.51
160	-0.67	0.28	-2.38	160	-0.63	0.31	-2.04	160	-0.63	0.32	-1.97
161	-0.67	0.26	-2.57	161	-0.63	0.29	-2.18	161	-0.63	0.31	-2.03
162	-0.67	0.24	-2.79	162	-0.64	0.27	-2.37	162	-0.64	0.30	-2.14
163	-0.67	0.22	-3.05	163	-0.65	0.25	-2.60	163	-0.66	0.28	-2.36
164	-0.68	0.20	-3.40	164	-0.66	0.23	-2.87	164	-0.67	0.26	-2.58
165	-0.69	0.19	-3.63	165	-0.68	0.22	-3.09	165	-0.70	0.24	-2.92
166	-0.70	0.17	-4.12	166	-0.73	0.20	-3.65	166	-0.74	0.22	-3.36
167	-0.72	0.15	-4.80	167	-0.82	0.18	-4.56	167	-0.83	0.20	-4.15
168	-0.82	0.13	-6.31	168	-0.91	0.16	-5.69	168	-0.92	0.18	-5.11
169	-0.93	0.12	-7.75	169	-1.02	0.14	-7.29	169	-1.03	0.16	-6.44
170	-0.95	0.11	-8.64	170	-1.05	0.12	-8.75	170	-1.07	0.14	-7.64
171	-0.90	0.09	-10.00	171	-1.00	0.10	-10.00	171	-1.03	0.12	-8.58
172	-0.80	0.07	-11.43	172	-0.93	0.08	-11.63	172	-0.95	0.09	-10.56
173	-0.70	0.05	-14.00	173	-0.80	0.06	-13.33	173	-0.82	0.07	-11.71
174	-0.60	0.04	-15.00	174	-0.68	0.04	-17.00	174	-0.69	0.05	-14.38
175	-0.50	0.03	-16.67	175	-0.55	0.03	-18.33	175	-0.55	0.04	-14.47
176	-0.40	0.03	-14.55	176	-0.42	0.02	-21.00	176	-0.42	0.03	-14.00
177	-0.30	0.03	-12.00	177	-0.30	0.01	-30.00	177	-0.31	0.02	-15.50
178	-0.20	0.02	-10.00	178	-0.20	0.01	-25.00	178	-0.22	0.01	-22.00
179	-0.10	0.02	-6.67	179	-0.10	0.01	-16.67	179	-0.11	0.01	-13.75
180	0.00	0.01	0.00	180	0.00	0.01	0.00	180	0.00	0.01	0.00

NACA0022				**NACA65$_3$-018**			
α	**Cl**	**Cd**	**Cl/Cd**	**α**	**Cl**	**Cd**	**Cl/Cd**
0	0.00	0.01	0.00	0	0.00	0.01	0.00
1	0.11	0.01	9.07	1	0.12	0.01	9.80
2	0.22	0.01	17.79	2	0.24	0.01	19.21
3	0.33	0.01	25.88	3	0.32	0.01	24.84

4	0.44	0.01	33.11	4	0.41	0.01	30.54
5	0.56	0.01	39.31	5	0.50	0.01	35.38
6	0.67	0.02	44.39	6	0.60	0.02	39.95
7	0.78	0.02	48.32	7	0.71	0.02	44.11
8	0.89	0.02	51.16	8	0.82	0.02	47.19
9	1.00	0.02	53.00	9	0.92	0.02	48.76
10	1.11	0.02	53.97	10	1.03	0.02	50.03
11	1.22	0.02	54.21	11	1.10	0.02	48.79
12	1.28	0.02	51.71	12	1.19	0.02	48.08
13	1.31	0.03	48.12	13	1.25	0.03	45.92
14	1.34	0.03	44.72	14	1.30	0.03	43.39
15	1.36	0.03	41.22	15	1.33	0.03	40.31
16	1.37	0.04	37.72	16	1.34	0.04	36.89
17	1.38	0.04	34.41	17	1.31	0.04	32.79
18	1.38	0.04	31.42	18	1.33	0.05	26.60
19	1.39	0.05	28.83	19	1.33	0.06	22.17
20	1.30	0.05	24.60	20	1.32	0.08	16.50
21	0.58	0.30	1.93	22	1.08	0.11	9.82
25	0.66	0.38	1.74	24	0.98	0.22	4.45
30	0.82	0.56	1.46	30	0.92	0.45	2.04
35	0.95	0.70	1.36	35	0.99	0.70	1.41
40	1.02	0.91	1.12	40	1.04	0.91	1.14
45	1.03	1.03	1.00	45	1.05	1.03	1.02
50	0.99	1.18	0.84	50	1.00	1.19	0.84
55	0.94	1.35	0.70	55	0.94	1.27	0.74
60	0.85	1.49	0.57	60	0.85	1.40	0.61
65	0.75	1.57	0.48	65	0.74	1.47	0.50
70	0.63	1.62	0.39	70	0.61	1.52	0.40
75	0.50	1.68	0.30	75	0.46	1.58	0.29
80	0.38	1.75	0.22	80	0.34	1.65	0.21
85	0.26	1.76	0.15	85	0.21	1.68	0.13
90	0.13	1.75	0.07	90	0.08	1.71	0.05
95	0.01	1.73	0.01	95	-0.02	1.70	-0.01
100	-0.13	1.71	-0.08	100	-0.15	1.67	-0.09
105	-0.26	1.67	-0.16	105	-0.28	1.63	-0.17
110	-0.39	1.59	-0.25	110	-0.40	1.56	-0.26
115	-0.52	1.50	-0.35	115	-0.54	1.47	-0.37
120	-0.65	1.42	-0.46	120	-0.66	1.39	-0.47
125	-0.75	1.34	-0.56	125	-0.76	1.32	-0.58
130	-0.83	1.25	-0.66	130	-0.85	1.23	-0.69
135	-0.92	1.14	-0.81	135	-0.93	1.11	-0.83

140	-0.97	1.01	-0.96	140	-0.97	1.02	-0.95
145	-0.91	0.81	-1.13	145	-0.91	0.82	-1.12
150	-0.75	0.63	-1.20	150	-0.82	0.63	-1.30
155	-0.66	0.44	-1.49	155	-0.76	0.45	-1.69
160	-0.63	0.32	-1.95	160	-0.74	0.33	-2.27
161	-0.64	0.31	-2.03	161	-0.74	0.32	-2.34
162	-0.65	0.30	-2.13	162	-0.76	0.31	-2.48
163	-0.67	0.28	-2.37	163	-0.77	0.29	-2.70
164	-0.68	0.26	-2.59	164	-0.78	0.27	-2.94
165	-0.71	0.24	-2.93	165	-0.79	0.24	-3.23
166	-0.75	0.22	-3.38	166	-0.83	0.22	-3.70
167	-0.84	0.20	-4.16	167	-0.86	0.20	-4.22
168	-0.93	0.18	-5.12	168	-0.91	0.18	-4.96
169	-1.04	0.16	-6.44	169	-0.94	0.16	-5.76
170	-1.08	0.14	-7.64	170	-0.95	0.14	-6.65
171	-1.04	0.12	-8.58	171	-0.94	0.12	-7.68
172	-0.96	0.09	-10.56	172	-0.93	0.09	-10.13
173	-0.83	0.07	-11.74	173	-0.80	0.07	-11.20
174	-0.70	0.05	-14.34	174	-0.68	0.05	-13.89
175	-0.55	0.04	-14.33	175	-0.55	0.04	-14.19
176	-0.42	0.03	-13.86	176	-0.42	0.03	-13.72
177	-0.30	0.02	-14.85	177	-0.30	0.02	-14.70
178	-0.20	0.01	-19.80	178	-0.20	0.01	-19.61
179	-0.10	0.01	-12.38	179	-0.10	0.01	-12.25
180	0.00	0.01	0.00	180	0.00	0.01	0.00

APPENDIX M

FINAL ANALYSIS CODE

```
% The Utah Helical Turbine Analysis Code
% This code is designed to calculate the torque and drag forces
produced by
% operation of a Helical turbine in a fluid flow.
% note: in this code it is assumed that the fluid flow is to the left
and
% that the turbine spins in a clock-wise rotation
% for plotting purposed assume 0 deg is at top of the of the turbine
and
% the point (0,0) is at the center of the turbine

clear
clc
load c22_3_47_45.txt
RPM = c22_3_47_45(:,2);
T_S = c22_3_47_45(:,3);

load coef_22.txt
a_dat = coef_22(:,1);
cl_dat = abs(coef_22(:,2));
cd_dat = coef_22(:,3);


%% Input variables
blades = 3; % number of blades in the turbine (NACA0020)
% twist = 60; % degrees of twist of blades
height = 10; % height of turbine blades in inches (34)
dia = 10; % diameter in inches (24)
rho = .00235; % fluid density in slug/ft^3 water(1.94) air (.00235)
Vfs = 60; % free stream velocity in mph (5 ft/sec)
%20: 20-26, 25-35, 30-40, 45-60
%22: 20-30, 25-36, 30-43, 45-65
%65: 20-27, 25-35, 30-40, 45-60

c = 2.88; % cord length in inches (7)
phi = 0; % degree removal of the trailing edge of the cord from the
circ
sections = 360;
Vfs=Vfs*1.3;
a =
get_a(blades,height,dia,rho,Vfs,c,RPM(1),phi,sections,a_dat,cl_dat,cd_d
at,T_S(1));

%% Conversions
hm = height*.0254; % conversion of height to meters
diam = dia * .0254; % conversion of diameter to meters
rm = diam/2; % radius in meters
rhom = rho*515.379; % conversion of density to kg/m^3
Vfsm = Vfs*0.44704; % conversion of free stream velocity to m/s
cm = c*.0254; % conversion of cord length to meters
A = hm*cm*blades/sections*2*pi;% m^2
Transitional_rpm = Vfsm*60/(2*pi*rm);
```

```
for gi = 1:length(RPM)
rpm = RPM(gi); % initial rpm guess (100)
%Vfsm = vfsm-log10((rpm+50)/2+1);

%% stream velocity
% This section calculates the portion of the fluid flow on the airfiol
% blade as produced by the free stream velocity

for ai = 1:sections
    sv(:,:,ai) = [-Vfsm 0]; % free stream velocity in vector form
    ci(ai) = (ai-1)*360/sections;
% this loop applies a penalty to the free stream velocity magnitude at
% the back end of the turbine to account for the effects of the front
% end of the turbine

if ci(ai) > 210
if ci(ai) <330
           sv(:,:,ai) = [-(Vfsm*(a)) 0];
end
end
    col(:,:,ai) = coords(rm,ci(ai));
    le_prime(:,:,ai) = [.25*cm*cosd(phi), .25*cm*sind(phi)];
    le(:,:,ai)= [le_prime(1,1,ai)*cosd(ci(ai))-
le_prime(1,2,ai)*sind(ci(ai))+col(1,1,ai), -
le_prime(1,1,ai)*sind(ci(ai))-
le_prime(1,2,ai)*cosd(ci(ai))+col(1,2,ai)];
    bi(ai) =
ci(ai)+acosd((rm+.25*cm*sind(phi))/sqrt(le(1,1,ai)^2+le(1,2,ai)^2));
    svi(:,:,ai) = col(:,:,ai)+sv(:,:,ai);
end

%% induced velocity from rotation
% This section calculated the induced velocity, as seen by each blade
tip,
% that results from the rotation of the turbine

 is = (rpm/60*2*pi*rm); % induced velocity scaler m/s

% plot of induced velocity vectors
for ai = 1:sections
    iv(:,:,ai) = coords(is,ci(ai)-90); % induced velocity in vector
form
    ivv(:,:,ai) = col(:,:,ai)+iv(:,:,ai);
end

%% resultant velocity vectors
% This section of code finds the resultant velocity vectors for each
blade
% location. These are a vactor sum of the free stream and induced
% velocities.

% plot of resultant velocity vectors
for ai = 1:sections
    rv(:,:,ai) = iv(:,:,ai)+sv(:,:,ai)+col(:,:,ai);
end
```

```
te_new(1,1) = .75*cm*cosd(180-phi);
te_new(1,2) = .75*cm*sind(180-phi);

for ai = 1:sections
    te_rot(1,1,ai) = (te_new(1,1)*cosd(-ci(ai))-te_new(1,2)*sind(-
ci(ai))); % Rotates the x coord by 90 deg
    te_rot(1,2,ai) = (te_new(1,1)*sind(-ci(ai))+te_new(1,2)*cosd(-
ci(ai))); % Rotates the y coord by 90 deg
    te(:,:,ai) = te_rot(:,:,ai)+col(:,:,ai);
end

%% retriving airfoil coefficients for each angle of attack
% This section of code calculated the angle of attack between the blade
% cord length and resultant velocity for each blade location. Using
this
% angle the coefficients of lift and drag are found from a supplied
text
% file.

for ai = 1:sections
    rvp(:,:,ai) = rv(:,:,ai)-col(:,:,ai);
    rvps(:,:,ai) = rvp(:,:,ai)/sqrt(rvp(1,1,ai)^2+rvp(1,2,ai)^2);
    tep(:,:,ai) = te(:,:,ai)-col(:,:,ai);
    teps(:,:,ai) = tep(:,:,ai)/sqrt(tep(1,1,ai)^2+tep(1,2,ai)^2);
    Matrix1 = (rvps(:,:,ai)'*teps(:,:,ai));
    temp1 = Matrix1(1,1)+Matrix1(2,2);
    temp2 = temp1*100000;
    temp3 = round(temp2)/100000;
    alph = acosd(temp3);
    alpha(ai) = alph;
end

for ai = 1:sections
    cl(ai) = interp1(a_dat,cl_dat,alpha(ai));
    cd(ai) = interp1(a_dat,cd_dat,alpha(ai));
end

% figure(1)
% clf
% hold on
% plot(bi,alpha)
% title('Angle of Attack as a Function of Blade Location')
% xlabel('Degrees Clockwise from Positive Y Axis')
% ylabel('Magnitude of Angle of Attack')
% hold off


%% calculation of lift and drag force vextors
% This section of code uses the Coefficients and resultant velocity to
% calculate the lift and drag vectors for each blade section.

for ai = 1:sections
    VR(ai) = sqrt(rvp(1,1,ai)^2+rvp(1,2,ai)^2); % magnitude of the
resultant velocity
    L_mag(ai) = .5*rhom*VR(ai)^2*A*cl(ai); % Calculate lift magnitude
    D_mag(ai) = .5*rhom*VR(ai)^2*A*cd(ai); % Calculate drag magnitude
```

```
    D(:,:,ai) = rvps(:,:,ai)*D_mag(ai)+col(:,:,ai);  % Calculate drag
vectors
% The following sub section is used to determine which direction the
% lift vector should face.
    dir_test(:,:,ai) = -rvps(:,:,ai)*cm*.25+col(:,:,ai); % Finds the
rv-c point
    test(ai) = sqrt(dir_test(1,1,ai)^2+dir_test(1,2,ai)^2); % Subtracts
the radius from the rv-c point
    cont(ai) = sqrt(le(1,1,ai)^2+le(1,2,ai)^2);
if abs(test(ai)) > abs(cont(ai))
        dir(ai) = -1;
elseif abs(test(ai)) < abs(cont(ai))
        dir(ai) = -1;
if ci(ai) > 90
            dir(ai) = 1;
end
else
        dir(ai) = 0;
end
if ci(ai) == 180
        dir(ai) = dir(ai)*(-1);
end
if ci(ai) == 0
if phi < 0
            dir(ai) = dir(ai)*(-1);
end
end

    l_dir(1,1,ai) = (rvps(1,1,ai)*cosd(-90)-rvps(1,2,ai)*sind(-90)); %
Rotates the x coord by 90 deg
    l_dir(1,2,ai) = (rvps(1,1,ai)*sind(-90)+rvps(1,2,ai)*cosd(-90)); %
Rotates the y coord by 90 deg

    L(:,:,ai) = l_dir(:,:,ai)*L_mag(ai)*dir(ai)+col(:,:,ai); %
Calculate the lift vector

end

%% Solving for normal and tangential vectors
% This section resolves the lift and drag vectors into their normal and
% tangential components.
% Positive tangent is in the clockwise direction. Positive normal
points
% out from the center.

for ai = 1:sections
%     alpha(ai) = alpha(ai)+phi;
    Dt(ai) = D_mag(ai)*cosd(alpha(ai));
    Dn(ai) = D_mag(ai)*sind(alpha(ai))*dir(ai);
    lt_dir(ai) = 1;
if alpha(ai) < 90
        lt_dir(ai) = -1;
end
    Lt(ai) = L_mag(ai)*sind(alpha(ai))*lt_dir(ai);
    Ln(ai) = L_mag(ai)*cosd(alpha(ai))*dir(ai);

% Finds the unit length vector in the tangent direction
```

```
    uvec(:,:,ai) = coords(1,ci(ai)-90);
    uvecn(:,:,ai) = coords(1,ci(ai));
% Finds the vector in the tangent direction
    Tv(:,:,ai) = (Dt(ai)+Lt(ai))*uvec(:,:,ai)+col(:,:,ai);
% Finds the vector in the normal direction
    Nv(:,:,ai) = (Dn(ai)+Ln(ai))*uvecn(:,:,ai)+col(:,:,ai);

end

%% Solving for Resultant forces
% This section uses the normal and tangential vector to solve for the
% resulting forces and torques.

Ft = -(sum(Dt)+sum(Lt));
Torque(gi) = Ft*rm; %(1-hi/10);
T_Shaft(gi) = -2*rhom*rm^3*Vfsm*rpm*2*pi/60*(1-a)+Torque(gi);
end

for ai = 1:16
TSi(ai)=T_S(ai)/T_Shaft(ai);
end
TS = mean(TSi)
Fudge=(-.0019*Vfs^2+.2012*Vfs-2.4418)
figure(1)
plot(RPM,T_S,RPM,T_Shaft)
legend('experimental data','Computational data')
xlabel('RPM')
ylabel('T shaft')

figure(2)
plot(RPM,T_Shaft)
xlabel('RPM')
ylabel('T s')

figure(3)
plot(RPM,Torque)
xlabel('RPM')
ylabel('F_t x r')



% This function uses the experimental no load speed to find the needed
a value for convergence at the computational no load speed.
function a =
get_a(blades,height,dia,rho,Vfs,c,rpm,phi,sections,a_dat,cl_dat,cd_dat,
T_shaft)
atemp=0;
count = 0;
while count<3
%% Conversions
hm = height*.0254; % conversion of height to meters
diam = dia * .0254; % conversion of diameter to meters
rm = diam/2; % radius in meters
rhom = rho*515.379; % conversion of density to kg/m^3
Vfsm = Vfs*0.44704; % conversion of free stream velocity to m/s
cm = c*.0254; % conversion of cord length to meters
A = hm*cm*blades/sections*2*pi;% m^2
```

```
Transitional_rpm = Vfsm*60/(2*pi*rm);


%Vfsm = vfsm-log10((rpm+50)/2+1);

%% stream velocity
% This section calculates the portion of the fluid flow on the airfiol
% blade as produced by the free stream velocity

for ai = 1:sections
    sv(:,:,ai) = [-Vfsm 0]; % free stream velocity in vector form
    ci(ai) = (ai-1)*360/sections;
% this loop applies a penalty to the free stream velocity magnitude at
% the back end of the turbine to account for the effects of the front
% end of the turbine

if ci(ai) > 210
if ci(ai) <330
           sv(:,:,ai) = [-(Vfsm*atemp) 0];
end
end
    col(:,:,ai) = coords(rm,ci(ai));
    le_prime(:,:,ai) = [.25*cm*cosd(phi), .25*cm*sind(phi)];
    le(:,:,ai)= [le_prime(1,1,ai)*cosd(ci(ai))-
le_prime(1,2,ai)*sind(ci(ai))+col(1,1,ai), -
le_prime(1,1,ai)*sind(ci(ai))-
le_prime(1,2,ai)*cosd(ci(ai))+col(1,2,ai)];
    bi(ai) =
ci(ai)+acosd((rm+.25*cm*sind(phi))/sqrt(le(1,1,ai)^2+le(1,2,ai)^2));
    svi(:,:,ai) = col(:,:,ai)+sv(:,:,ai);
end

%% induced velocity from rotation
% This section calculated the induced velocity, as seen by each blade
tip,
% that results from the rotation of the turbine

 is = (rpm/60*2*pi*rm); % induced velocity scaler m/s

% plot of induced velocity vectors
for ai = 1:sections
    iv(:,:,ai) = coords(is,ci(ai)-90); % induced velocity in vector
form
    ivv(:,:,ai) = col(:,:,ai)+iv(:,:,ai);
end

%% resultant velocity vectors
% This section of code finds the resultant velocity vectors for each
blade
% location. These are a vactor sum of the free stream and induced
% velocities.

% plot of resultant velocity vectors
for ai = 1:sections
    rv(:,:,ai) = iv(:,:,ai)+sv(:,:,ai)+col(:,:,ai);
end
```

```
te_new(1,1) = .75*cm*cosd(180-phi);
te_new(1,2) = .75*cm*sind(180-phi);

for ai = 1:sections
    te_rot(1,1,ai) = (te_new(1,1)*cosd(-ci(ai))-te_new(1,2)*sind(-
ci(ai))); % Rotates the x coord by 90 deg
    te_rot(1,2,ai) = (te_new(1,1)*sind(-ci(ai))+te_new(1,2)*cosd(-
ci(ai))); % Rotates the y coord by 90 deg
    te(:,:,ai) = te_rot(:,:,ai)+col(:,:,ai);
end

%% retriving airfoil coefficients for each angle of attack
% This section of code calculated the angle of attack between the blade
% cord length and resultant velocity for each blade location. Using
this
% angle the coefficients of lift and drag are found from a supplied
text
% file.

for ai = 1:sections
    rvp(:,:,ai) = rv(:,:,ai)-col(:,:,ai);
    rvps(:,:,ai) = rvp(:,:,ai)/sqrt(rvp(1,1,ai)^2+rvp(1,2,ai)^2);
    tep(:,:,ai) = te(:,:,ai)-col(:,:,ai);
    teps(:,:,ai) = tep(:,:,ai)/sqrt(tep(1,1,ai)^2+tep(1,2,ai)^2);
    Matrix1 = (rvps(:,:,ai)'*teps(:,:,ai));
    temp1 = Matrix1(1,1)+Matrix1(2,2);
    temp2 = temp1*100000;
    temp3 = round(temp2)/100000;
    alph = acosd(temp3);
    alpha(ai) = alph;
end

for ai = 1:sections
    cl(ai) = interp1(a_dat,cl_dat,alpha(ai));
    cd(ai) = interp1(a_dat,cd_dat,alpha(ai));
end

% figure(1)
% clf
% hold on
% plot(bi,alpha)
% title('Angle of Attack as a Function of Blade Location')
% xlabel('Degrees Clockwise from Positive Y Axis')
% ylabel('Magnitude of Angle of Attack')
% hold off


%% calculation of lift and drag force vextors
% This section of code uses the Coefficients and resultant velocity to
% calculate the lift and drag vectors for each blade section.

for ai = 1:sections
    VR(ai) = sqrt(rvp(1,1,ai)^2+rvp(1,2,ai)^2); % magnitude of the
resultant velocity
    L_mag(ai) = .5*rhom*VR(ai)^2*A*cl(ai); % Calculate lift magnitude
    D_mag(ai) = .5*rhom*VR(ai)^2*A*cd(ai); % Calculate drag magnitude
```

```
    D(:,:,ai) = rvps(:,:,ai)*D_mag(ai)+col(:,:,ai);  % Calculate drag
vectors
% The following sub section is used to determine which direction the
% lift vector should face.
    dir_test(:,:,ai) = -rvps(:,:,ai)*cm*.25+col(:,:,ai); % Finds the
rv-c point
    test(ai) = sqrt(dir_test(1,1,ai)^2+dir_test(1,2,ai)^2); % Subtracts
the radius from the rv-c point
    cont(ai) = sqrt(le(1,1,ai)^2+le(1,2,ai)^2);
if abs(test(ai)) > abs(cont(ai))
        dir(ai) = -1;
elseif abs(test(ai)) < abs(cont(ai))
        dir(ai) = -1;
if ci(ai) > 90
            dir(ai) = 1;
end
else
        dir(ai) = 0;
end
if ci(ai) == 180
        dir(ai) = dir(ai)*(-1);
end
if ci(ai) == 0
if phi < 0
            dir(ai) = dir(ai)*(-1);
end
end

    l_dir(1,1,ai) = (rvps(1,1,ai)*cosd(-90)-rvps(1,2,ai)*sind(-90)); %
Rotates the x coord by 90 deg
    l_dir(1,2,ai) = (rvps(1,1,ai)*sind(-90)+rvps(1,2,ai)*cosd(-90)); %
Rotates the y coord by 90 deg

    L(:,:,ai) = l_dir(:,:,ai)*L_mag(ai)*dir(ai)+col(:,:,ai); %
Calculate the lift vector

end

%% Solving for normal and tangential vectors
% This section resolves the lift and drag vectors into their normal and
% tangential components.
% Positive tangent is in the clockwise direction. Positive normal
points
% out from the center.

for ai = 1:sections
%     alpha(ai) = alpha(ai)+phi;
    Dt(ai) = D_mag(ai)*cosd(alpha(ai));
    Dn(ai) = D_mag(ai)*sind(alpha(ai))*dir(ai);
    lt_dir(ai) = 1;
if alpha(ai) < 90
        lt_dir(ai) = -1;
end
    Lt(ai) = L_mag(ai)*sind(alpha(ai))*lt_dir(ai);
    Ln(ai) = L_mag(ai)*cosd(alpha(ai))*dir(ai);

% Finds the unit length vector in the tangent direction
```

```
    uvec(:,:,ai) = coords(1,ci(ai)-90);
    uvecn(:,:,ai) = coords(1,ci(ai));
% Finds the vector in the tangent direction
    Tv(:,:,ai) = (Dt(ai)+Lt(ai))*uvec(:,:,ai)+col(:,:,ai);
% Finds the vector in the normal direction
    Nv(:,:,ai) = (Dn(ai)+Ln(ai))*uvecn(:,:,ai)+col(:,:,ai);

end

%% Solving for Resultant forces
% This section uses the normal and tangential vector to solve for the
% resulting forces and torques.

Ft = -(sum(Dt)+sum(Lt));
Torque = Ft*rm; %(1-hi/10);
atemp = 1-(Torque-T_shaft)/(2*rhom*rm^3*Vfsm*rpm*2*pi/60);
count = count+1;
end
a = atemp
```

APPENDIX N

PARAMETER ANALYSIS CODE

```
% The Utah Helical Turbine Analysis Code
% This code is designed to calculate the torque and drag forces
produced by
% opperation of a Helical turbine in a fluid flow.
% note: in this code it is assumed that the fluid flow is to the left
and
% that the turbine spins in a clock-wise rotation
% for plotting purposed assume 0 deg is at top of the of the turbine
and
% the point (0,0) is at the center of the turbine

clear
clc

%% Input variables
blades = 3; % number of blades in the turbine (NACA0020)
twist = 120; % degrees of twist of blades
height = 10; % height of turbine blades in inches (34)
dia = 10; % diameter in inches (24)
rho = .00235; % fluid density in slug/ft^3
Vfs = 40; % free stream velocity in mph (5 ft/sec)
c = 2.88; % cord length in inches (7)
rpm = 200; % initial rpm guess (100)
phi = 0; % degree removal of the trailing edge of the cord from the
circ
load coef_22.txt
a_dat = coef_22(:,1);
cl_dat = coef_22(:,2);
cd_dat = coef_22(:,3);

%% Conversions
hm = height*.0254; % conversion of height to meters
diam = dia * .0254; % conversion of diameter to meters
rm = diam/2; % radius in meters
rhom = rho*515.379; % conversion of density to kg/m^3
Vfsm = Vfs*0.44704; % conversion of free stream velocity to m/s
cm = c*.0254; % conversion of cord length to meters
A = hm*cm;% m^2
O = zeros(1,2,12);
%% stream velocity
% This section calculates the portion of the fluid flow on the airfiol
% blade as produced by the free stream velocity

clf
% subplot(2,2,1)
figure(1)
hold on
% plot of turbine circumference
 t=(0:360)*2*pi/360;
 plot( rm*cos(t), rm*sin(t), 'k');
axis([-rm*1.5, rm*1.5, -rm*1.5, rm*1.5])
% plot of free stream velocity vectors
for ai = 1:12
    sv(:,:,ai) = [-Vfsm 0]; % free stream velocity in vector form
```

```
    bi(ai) = (ai-1)*30;
    le(:,:,ai) = coords(rm,bi(ai));
% this loop applies a penalty to the free stream velocity magnitude at
% the back end of the turbine to account for the effects of the front
% end of the turbine
%     if le(1,1,ai)<0
%         sv(1,1,ai) = -Vfsm-Vfs*le(1,1,ai);
%     end
    p = profile_original(bi(ai),cm,rm,phi);
    plot(p(:,1),p(:,2))
    svi(:,:,ai) = le(:,:,ai)+sv(:,:,ai);
    vectarrow(le(:,:,ai),svi(:,:,ai))
end
title('Free Stream Velocity')
hold off

%% induced velocity from rotation
% This section calculated the induced velocity, as seen by each blade
tip,
% that results from the rotation of the turbine

 is = (rpm/60*2*pi*rm); % induced velocity scaler m/s
%is = Vfsm;

% subplot(2,2,2)
figure(2)
clf
hold on
% plot of turbine circumference
 t=(0:360)*2*pi/360;
 plot( rm*cos(t), rm*sin(t), 'k');
axis([-rm*1.5, rm*1.5, -rm*1.5, rm*1.5])
% plot of induced velocity vectors
for ai = 1:12
    iv(:,:,ai) = coords(is,bi(ai)-90); % induced velocity in vector
form
    p = profile_original(bi(ai),cm,rm,phi);
    plot(p(:,1),p(:,2))
    ivv(:,:,ai) = le(:,:,ai)+iv(:,:,ai);
    vectarrow(le(:,:,ai),ivv(:,:,ai))
end
title('Induced Velocity from Rotation')
hold off

%% resultant velocity vectors
% This section of code finds the resultant velocity vectors for each
blade
% location. These are a vactor sum of the free stream and induced
% velocities.

% (2,2,3)
figure(3)
clf
hold on
% plot of turbine circumference
 t=(0:360)*2*pi/360;
 plot( rm*cos(t), rm*sin(t), 'k');
```

```
axis([-rm*1.5, rm*1.5, -rm*1.5, rm*1.5])
% plot of resultant velocity vectors
for ai = 1:12
    rv(:,:,ai) = iv(:,:,ai)+sv(:,:,ai)+le(:,:,ai);
    vectarrow(le(:,:,ai),rv(:,:,ai))
    p = profile_original(bi(ai),cm,rm,phi);
    plot(p(:,1),p(:,2))
%     theta = asind(cm/(2*rm))*2;
%     te(:,:,ai) = coords(rm,bi(ai)-theta);
%     vectarrow(le(:,:,ai),te(:,:,ai))
end
title('Resultant Velocity')
hold off

% (2,2,3)
figure(4)
clf
hold on
% plot of turbine circumference
 t=(0:360)*2*pi/360;
 plot( rm*cos(t), rm*sin(t), 'k');
% axis([-rm*1.5, rm*1.5, -rm*1.5, rm*1.5])
% plot of resultant velocity vectors
    te_new(1,1) = cm*cosd(180-phi);
    te_new(1,2) = cm*sind(180-phi);
    rn = cm*sind(phi)+rm;
for ai = 1:12
%     rv(:,:,ai) = ivv(:,:,ai)+sv/10;
    vectarrow(le(:,:,ai),rv(:,:,ai))
%     p = profile(bi(ai),cm,rm);
%     plot(p(:,1),p(:,2))
%     theta = asind(cm/(2*rm))*2;
%     te_circ(:,:,ai) = coords(rm,bi(ai)-theta);
    te_rot(1,1,ai) = (te_new(1,1)*cosd(-bi(ai))-te_new(1,2)*sind(-
bi(ai))); % Rotates the x coord by 90 deg
    te_rot(1,2,ai) = (te_new(1,1)*sind(-bi(ai))+te_new(1,2)*cosd(-
bi(ai))); % Rotates the y coord by 90 deg
    te(:,:,ai) = te_rot(:,:,ai)+le(:,:,ai);
    vectarrow_b(te(:,:,ai),le(:,:,ai))
end
title('Angle of Attack')
hold off


%% retriving airfoil coefficients for each angle of attack
% This section of code calculated the angle of attack between the blade
% cord length and resultant velocity for each blade location. Using
this
% angle the coefficients of lift and drag are found from a supplied
text
% file.

% subplot(2,2,4)
figure(5)
clf
hold on
% plot of...
```

```
for ai = 1:12
    rvp(:,:,ai) = rv(:,:,ai)-le(:,:,ai);
    rvps(:,:,ai) = rvp(:,:,ai)/sqrt(rvp(1,1,ai)^2+rvp(1,2,ai)^2);
    tep(:,:,ai) = te(:,:,ai)-le(:,:,ai);
    teps(:,:,ai) = tep(:,:,ai)/sqrt(tep(1,1,ai)^2+tep(1,2,ai)^2);
    Matrix1 = (rvps(:,:,ai)'*teps(:,:,ai));
    temp1(ai) = Matrix1(1,1)+Matrix1(2,2);
    alpha(ai) = acosd(temp1(ai));

end

for ai = 1:12
    cl(ai) = interp1(a_dat,cl_dat,alpha(ai));
    cd(ai) = interp1(a_dat,cd_dat,alpha(ai));
end

% for ai = 1:12
%     [Cl   Cd  Cm  Cp  M]= coeff(alpha(ai));
%     cl(ai) = Cl;
%     cd(ai) = Cd;
% end

plot(bi,alpha)
title('Angle of Attack as a Function of Blade Location')
xlabel('Degrees Clockwise from Positive Y Axis')
ylabel('Magnitude of Angle of Attack')
hold off

%% calculation of lift and drag force vextors
% This section of code uses the Coefficients and resultant velocity to
% calculate the lift and drag vectors for each blade section.

figure(6)
clf
hold on

for ai = 1:12
    VR(ai) = sqrt(rvp(1,1,ai)^2+rvp(1,2,ai)^2); % magnitude of the
resultant velocity
    L_mag(ai) = .5*rhom*VR(ai)^2*A*cl(ai); % Calculate lift magnitude
    D_mag(ai) = .5*rhom*VR(ai)^2*A*cd(ai); % Calculate drag magnitude
%ce(:,:,ai) = le(:,:,ai)-(le(:,:,ai)-te(:,:,ai))/2; % Find point for
center of airfoil
    D(:,:,ai) = rvps(:,:,ai)*D_mag(ai)+le(:,:,ai);  % Calculate drag
vectors
% The following sub section is used to determine which direction the
% lift vector should face.
%    dir_test(:,:,ai) = abs(rv(:,:,ai)-(te(:,:,ai)-le(:,:,ai)); % Finds
the rv-c point
%     dir_test(:,:,ai) = abs(rvps(:,:,ai)*cm-te(:,:,ai)); % Finds the
rv-c point
    dir_test(:,:,ai) = abs(rvps(:,:,ai)*cm+le(:,:,ai)+(le(:,:,ai)-
te(:,:,ai))); % Finds the rv-c point
    test(ai) = sqrt(dir_test(1,1,ai)^2+dir_test(1,2,ai)^2)-(rm-
cm*sind(phi)); % Subtracts the radius from the rv-c point
if test(ai) > 0
        dir(ai) = 1;
```

```
elseif test(ai) < 0
        dir(ai) = -1;
else
        dir(ai) = 0;
end
%     c_dir(:,:,ai) = (le(:,:,ai)-ce(:,:,ai))/ sqrt((le(1,1,1)-
ce(1,1,1))^2+(le(1,1,1)-ce(1,2,1))^2); % Finds the unit vector in the
direction of the cord length
    l_dir(1,1,ai) = (rvps(1,1,ai)*cosd(-90)-rvps(1,2,ai)*sind(-90)); %
Rotates the x coord by 90 deg
    l_dir(1,2,ai) = (rvps(1,1,ai)*sind(-90)+rvps(1,2,ai)*cosd(-90)); %
Rotates the y coord by 90 deg

    L(:,:,ai) = l_dir(:,:,ai)*L_mag(ai)*dir(ai)+le(:,:,ai); % Calculate
the lift vector

    p = profile_original(bi(ai),cm,rm,phi);
    plot(p(:,1),p(:,2))
    vectarrow_g(le(:,:,ai),L(:,:,ai))
    vectarrow_k(le(:,:,ai),D(:,:,ai))
    axis([-rm*1.5, rm*1.5, -rm*1.5, rm*1.5])
end
hold off

%% Solving for normal and tangential vectors
% This section resolves the lift and drag vectors into their normal and
% tangential components.
% Positive tangent is in the clockwise direction. Positive normal
points
% out from the center.
figure(7)
clf
hold on
for ai = 1:12
%     alpha(ai) = alpha(ai)+phi;
    Dt(ai) = D_mag(ai)*cosd(alpha(ai));
    Dn(ai) = D_mag(ai)*sind(alpha(ai))*dir(ai);
    lt_dir(ai) = 1;
if alpha(ai) < 90
        lt_dir(ai) = -1;
end
    Lt(ai) = L_mag(ai)*sind(alpha(ai))*lt_dir(ai);
    Ln(ai) = L_mag(ai)*cosd(alpha(ai))*dir(ai);

% Finds the unit length vector in the tangent direction
%    uvec(:,:,ai) = (le(:,:,ai)-te_circ(:,:,ai))/
%    sqrt((le(1,1,1)-te_circ(1,1,1))^2+(le(1,1,1)-te_circ(1,2,1))^2);
    uvec(:,:,ai) = coords(1,bi(ai)-90);
    uvecn(:,:,ai) = coords(1,bi(ai));
%     uvecn(1,1,ai) = (uvec(1,1,ai)*cosd(-90)-uvec(1,2,ai)*sind(-90));
% Rotates the x coord by 90 deg
%     uvecn(1,2,ai) = (uvec(1,1,ai)*sind(-90)+uvec(1,2,ai)*cosd(-90));
% Rotates the y coord by 90 deg
% Finds the vector in the tangent direction
    Tv(:,:,ai) = (Dt(ai)+Lt(ai))*uvec(:,:,ai)+le(:,:,ai);
% Finds the vector in the normal direction
    Nv(:,:,ai) = (Dn(ai)+Ln(ai))*uvecn(:,:,ai)+le(:,:,ai);
```

```
    vectarrow_g(le(:,:,ai),Nv(:,:,ai))
    vectarrow_k(le(:,:,ai),Tv(:,:,ai))
    t=(0:360)*2*pi/360;
    plot( rm*cos(t), rm*sin(t), 'k');

end
hold off

figure(8)
clf
for ai = 1:12
    hold on
    vectarrow(le(:,:,ai),Nv(:,:,ai))
    vectarrow_m(le(:,:,ai),Tv(:,:,ai))
    vectarrow_b(te(:,:,ai),le(:,:,ai))
    vectarrow_g(le(:,:,ai),L(:,:,ai))
    vectarrow_k(le(:,:,ai),D(:,:,ai))
    axis([-4, 4, -4, 4])
%     r = input('press enter')
%     clf
end
hold off
%% Solving for Resultant forces
% This section uses the normal and tangential vector to solve for the
% resulting forces and torques.

Ft = -(sum(Dt)+sum(Lt));
Torque = Ft*rm
% ce_length = sqrt(ce(1,1,1)^2+ce(1,2,1)^2);
% for ai = 1:12
%     Fn(ai) = Dn(ai) + Ln(ai);
%     ce_unit(:,:,ai) = ce(:,:,ai)/ce_length;
%     Fn_vector(:,:,ai) = Fn(ai)*ce_unit(:,:,ai);
% end
% Fnx = sum(Fn_vector(1,1,:));
% Fny = sum(Fn_vector(1,2,:));
%


 figure(9)
 clf
 hold on
%  for ai = 1:12
 plot(bi,Dt,bi,-Lt)
%  end
 hold off
```

APPENDIX O

PITCH ANGLE ANALYSIS CODE

```
% Adjusting phi

clear
clc

%% Input variables
blades = 3; % number of blades in the turbine (NACA0020)
twist = 120; % degrees of twist of blades
height = 10; % height of turbine blades in inches (34)
dia = 10; % diameter in inches (24)
rho = .00235; % fluid density in slug/ft^3
Vfs = 50; % free stream velocity in mph (5 ft/sec)
c = 2.5; % cord length in inches (7)
rpm = 0; % initial rpm guess (100)
phi = 0; % degree removal of the trailing edge of the cord from the
line tangent to the circ at the col
load coef_22.txt
a_dat = coef_22(:,1);
cl_dat = coef_22(:,2);
cd_dat = coef_22(:,3);

%% Conversions
hm = height*.0254; % conversion of height to meters
diam = dia * .0254; % conversion of diameter to meters
rm = diam/2; % radius in meters
rhom = rho*515.379; % conversion of density to kg/m^3
Vfsm = Vfs*0.44704; % conversion of free stream velocity to m/s
cm = c*.0254; % conversion of cord length to meters
A = hm*cm/(twist);% m^2
O = zeros(1,2,12);
%% stream velocity
% This section calculates the portion of the fluid flow on the airfiol
% blade as produced by the free stream velocity


% subplot(2,2,1)
figure(1)
clf
hold on
% plot of turbine circumference
 t=(0:360)*2*pi/360;
 plot( rm*cos(t), rm*sin(t), 'k');
axis([-rm*1.5, rm*1.5, -rm*1.5, rm*1.5])
% plot of free stream velocity vectors
for ai = 1:12
    sv(:,:,ai) = [-Vfsm 0]; % free stream velocity in vector form
    ci(ai) = (ai-1)*30;
    col(:,:,ai) = coords(rm,ci(ai));
    le_prime(:,:,ai) = [.25*cm*cosd(phi), .25*cm*sind(phi)];
    le(:,:,ai)= [le_prime(1,1,ai)*cosd(ci(ai))-
le_prime(1,2,ai)*sind(ci(ai))+col(1,1,ai), -
```

```
le_prime(1,1,ai)*sind(ci(ai))-
le_prime(1,2,ai)*cosd(ci(ai))+col(1,2,ai)];
    bi(ai) =
ci(ai)+acosd((rm+.25*cm*sind(phi))/sqrt(le(1,1,ai)^2+le(1,2,ai)^2));
% this loop applies a penalty to the free stream velocity magnitude at
% the back end of the turbine to account for the effects of the front
% end of the turbine
%     if le(1,1,ai)<0
%         sv(1,1,ai) = -Vfsm-Vfs*le(1,1,ai)*1.5;
%     end
    p = profile(ci(ai),cm,rm,phi,le(:,:,ai));
    plot(p(:,1),p(:,2))
    svi(:,:,ai) = col(:,:,ai)+sv(:,:,ai);
    vectarrow(col(:,:,ai),svi(:,:,ai))
end
title('Free Stream Velocity')
hold off

%% induced velocity from rotation
% This section calculated the induced velocity, as seen by each blade
tip,
% that results from the rotation of the turbine

 is = (rpm/60*2*pi*rm); % induced velocity scaler m/s
%is = Vfsm;

% subplot(2,2,2)
figure(2)
clf
hold on
% plot of turbine circumference
 t=(0:360)*2*pi/360;
 plot( rm*cos(t), rm*sin(t), 'k');
axis([-rm*1.5, rm*1.5, -rm*1.5, rm*1.5])
% plot of induced velocity vectors
for ai = 1:12
    iv(:,:,ai) = coords(is,ci(ai)-90); % induced velocity in vector
form
    p = profile(ci(ai),cm,rm,phi,le(:,:,ai));
    plot(p(:,1),p(:,2))
    ivv(:,:,ai) = col(:,:,ai)+iv(:,:,ai);
    vectarrow(col(:,:,ai),ivv(:,:,ai))
end
title('Induced Velocity from Rotation')
hold off

%% resultant velocity vectors
% This section of code finds the resultant velocity vectors for each
blade
% location. These are a vector sum of the free stream and induced
% velocities.

% (2,2,3)
figure(3)
clf
hold on
% plot of turbine circumference
```

```
 t=(0:360)*2*pi/360;
 plot( rm*cos(t), rm*sin(t), 'k');
% axis([-rm*1.5, rm*1.5, -rm*1.5, rm*1.5])
% plot of resultant velocity vectors
for ai = 1:12
    rv(:,:,ai) = iv(:,:,ai)+sv(:,:,ai)+col(:,:,ai);
    vectarrow(col(:,:,ai),rv(:,:,ai))
    p = profile(ci(ai),cm,rm,phi,le(:,:,ai));
    plot(p(:,1),p(:,2))
%     theta = asind(cm/(2*rm))*2;
%     te(:,:,ai) = coords(rm,bi(ai)-theta);
%     vectarrow(le(:,:,ai),te(:,:,ai))
end
title('Resultant Velocity')
hold off

% (2,2,3)
figure(4)
clf
hold on
% plot of turbine circumference
 t=(0:360)*2*pi/360;
 plot( rm*cos(t), rm*sin(t), 'k');
% axis([-rm*1.5, rm*1.5, -rm*1.5, rm*1.5])

    te_new(1,1) = .75*cm*cosd(180-phi);
    te_new(1,2) = .75*cm*sind(180-phi);

for ai = 1:12

    vectarrow(col(:,:,ai),rv(:,:,ai))

    te_rot(1,1,ai) = (te_new(1,1)*cosd(-ci(ai))-te_new(1,2)*sind(-
ci(ai))); % Rotates the x coord by 90 deg
    te_rot(1,2,ai) = (te_new(1,1)*sind(-ci(ai))+te_new(1,2)*cosd(-
ci(ai))); % Rotates the y coord by 90 deg
    te(:,:,ai) = te_rot(:,:,ai)+col(:,:,ai);
    vectarrow_b(te(:,:,ai),le(:,:,ai))

end
title('Angle of Attack')
hold off


%% retrieving airfoil coefficients for each angle of attack
% This section of code calculated the angle of attack between the blade
% cord length and resultant velocity for each blade location. Using
this
% angle the coefficients of lift and drag are found from a supplied
text
% file.

% subplot(2,2,4)
figure(5)
clf
hold on
% plot of...
```

```
for ai = 1:12
    rvp(:,:,ai) = rv(:,:,ai)-col(:,:,ai);
    rvps(:,:,ai) = rvp(:,:,ai)/sqrt(rvp(1,1,ai)^2+rvp(1,2,ai)^2);
    tep(:,:,ai) = te(:,:,ai)-col(:,:,ai);
    teps(:,:,ai) = tep(:,:,ai)/sqrt(tep(1,1,ai)^2+tep(1,2,ai)^2);
    Matrix1 = (rvps(:,:,ai)'*teps(:,:,ai));
    temp1(ai) = Matrix1(1,1)+Matrix1(2,2);
    alpha(ai) = acosd(temp1(ai));

end

for ai = 1:12
    cl(ai) = interp1(a_dat,cl_dat,alpha(ai));
    cd(ai) = interp1(a_dat,cd_dat,alpha(ai));
end


plot(ci,alpha)
title('Angle of Attack as a Function of Blade Location')
xlabel('Degrees Clockwise from Positive Y Axis')
ylabel('Magnitude of Angle of Attack')
hold off

%% calculation of lift and drag force vextors
% This section of code uses the Coefficients and resultant velocity to
% calculate the lift and drag vectors for each blade section.

figure(6)
clf
hold on

for ai = 1:12
    VR(ai) = sqrt(rvp(1,1,ai)^2+rvp(1,2,ai)^2); % magnitude of the
resultant velocity
    L_mag(ai) = .5*rhom*VR(ai)^2*A*cl(ai); % Calculate lift magnitude
    D_mag(ai) = .5*rhom*VR(ai)^2*A*cd(ai); % Calculate drag magnitude
%ce(:,:,ai) = le(:,:,ai)-(le(:,:,ai)-te(:,:,ai))/2; % Find point for
center of airfoil
    D(:,:,ai) = rvps(:,:,ai)*D_mag(ai)+col(:,:,ai);  % Calculate drag
vectors
% The following sub section is used to determine which direction the
% lift vector should face.
%    dir_test(:,:,ai) = abs(rv(:,:,ai)-(te(:,:,ai)-le(:,:,ai)); % Finds
the rv-c point
%     dir_test(:,:,ai) = abs(rvps(:,:,ai)*cm-te(:,:,ai)); % Finds the
rv-c point
%     dir_test(:,:,ai) = abs(rvps(:,:,ai)*cm+col(:,:,ai)-
.75*(le(:,:,ai)-te(:,:,ai))); % Finds the rv-c point
%     test(ai) = sqrt(dir_test(1,1,ai)^2+dir_test(1,2,ai)^2)-(rm-
cm*sind(phi)); % Subtracts the radius from the rv-c point
    dir_test(:,:,ai) = -rvps(:,:,ai)*cm*.25+col(:,:,ai); % Finds the
rv-c point
    test(ai) = sqrt(dir_test(1,1,ai)^2+dir_test(1,2,ai)^2); % Subtracts
the radius from the rv-c point
    cont(ai) = sqrt(le(1,1,ai)^2+le(1,2,ai)^2);
if abs(test(ai)) > abs(cont(ai))
        dir(ai) = -1;
```

```
%         if ci(ai) > 90
%             dir(ai) = -1;
%         end
elseif abs(test(ai)) < abs(cont(ai))
        dir(ai) = -1;
if ci(ai) > 90
            dir(ai) = 1;
end
else
        dir(ai) = 0;
end
if ci(ai) == 180
        dir(ai) = dir(ai)*(-1);
end
if ci(ai) == 0
if phi < 0
            dir(ai) = dir(ai)*(-1);
end
end

%     c_dir(:,:,ai) = (le(:,:,ai)-ce(:,:,ai))/ sqrt((le(1,1,1)-
ce(1,1,1))^2+(le(1,1,1)-ce(1,2,1))^2); % Finds the unit vector in the
direction of the cord length
    l_dir(1,1,ai) = (rvps(1,1,ai)*cosd(-90)-rvps(1,2,ai)*sind(-90)); %
Rotates the x coord by 90 deg
    l_dir(1,2,ai) = (rvps(1,1,ai)*sind(-90)+rvps(1,2,ai)*cosd(-90)); %
Rotates the y coord by 90 deg

    L(:,:,ai) = l_dir(:,:,ai)*L_mag(ai)*dir(ai)+col(:,:,ai); %
Calculate the lift vector

    p = profile(ci(ai),cm,rm,phi,le(:,:,ai));
    plot(p(:,1),p(:,2))
    vectarrow_g(col(:,:,ai),L(:,:,ai))
    vectarrow_k(col(:,:,ai),D(:,:,ai))
    axis([-rm*1.5, rm*1.5, -rm*1.5, rm*1.5])
end
title('Lift and Drag Force Vectors')
hold off

%% Solving for normal and tangential vectors
% This section resolves the lift and drag vectors into their normal and
% tangential components.
% Positive tangent is in the clockwise direction. Positive normal
points
% out from the center.
figure(7)
clf
hold on
for ai = 1:12
%     alpha(ai) = alpha(ai)+phi;
    Dt(ai) = D_mag(ai)*cosd(alpha(ai));
    Dn(ai) = D_mag(ai)*sind(alpha(ai))*dir(ai);
    lt_dir(ai) = 1;
if alpha(ai) < 90
        lt_dir(ai) = -1;
end
```

```
    Lt(ai) = L_mag(ai)*sind(alpha(ai))*lt_dir(ai);
    Ln(ai) = L_mag(ai)*cosd(alpha(ai))*dir(ai);

% Finds the unit length vector in the tangent direction
%    uvec(:,:,ai) = (le(:,:,ai)-te_circ(:,:,ai))/
%    sqrt((le(1,1,1)-te_circ(1,1,1))^2+(le(1,1,1)-te_circ(1,2,1))^2);
    uvec(:,:,ai) = coords(1,ci(ai)-90);
    uvecn(:,:,ai) = coords(1,ci(ai));
%     uvecn(1,1,ai) = (uvec(1,1,ai)*cosd(-90)-uvec(1,2,ai)*sind(-90));
% Rotates the x coord by 90 deg
%     uvecn(1,2,ai) = (uvec(1,1,ai)*sind(-90)+uvec(1,2,ai)*cosd(-90));
% Rotates the y coord by 90 deg
% Finds the vector in the tangent direction
    Tv(:,:,ai) = (Dt(ai)+Lt(ai))*2*uvec(:,:,ai)+col(:,:,ai);
% Finds the vector in the normal direction
    Nv(:,:,ai) = (Dn(ai)+Ln(ai))*uvecn(:,:,ai)+col(:,:,ai);
    vectarrow_g(col(:,:,ai),Nv(:,:,ai))
    vectarrow_k(col(:,:,ai),Tv(:,:,ai))
    t=(0:360)*2*pi/360;
    plot( rm*cos(t), rm*sin(t), 'k');

end
title('Normal and Tangential Force Vectors')
hold off

figure(8)
clf
for ai = 1:12
    hold on
    vectarrow(col(:,:,ai),Nv(:,:,ai))
    vectarrow_m(col(:,:,ai),Tv(:,:,ai))
    vectarrow_b(te(:,:,ai),le(:,:,ai))
    vectarrow_g(col(:,:,ai),L(:,:,ai))
    vectarrow_k(col(:,:,ai),D(:,:,ai))
    axis([-4, 4, -4, 4])
%     r = input('press enter')
%     clf
end
hold off
%% Solving for Resultant forces
% This section uses the normal and tangential vector to solve for the
% resulting forces and torques.

Ft = -(sum(Dt)+sum(Lt));
Torque = Ft*rm;
% ce_length = sqrt(ce(1,1,1)^2+ce(1,2,1)^2);
% for ai = 1:12
%     Fn(ai) = Dn(ai) + Ln(ai);
%     ce_unit(:,:,ai) = ce(:,:,ai)/ce_length;
%     Fn_vector(:,:,ai) = Fn(ai)*ce_unit(:,:,ai);
% end
% Fnx = sum(Fn_vector(1,1,:));
% Fny = sum(Fn_vector(1,2,:));
%


 figure(9)
```

```
 clf
 hold on
%  for ai = 1:12
 plot(ci,Dt,ci,-Lt)
%  end
 hold off
```

APPENDIX P

SUPPORTING CODE

```
% this function looks up tabulated coefficients for the supplied angle
of attack
function  [Cl   Cd  Cm  Cp  M]= coeff(alpha)
% alpha in deg.
% coef for naca0009
% coef_12 for naca0012
% coef_65_018 for naca65-018

load coef_65_018.txt
a = ceil(alpha*10);
if a == 0
    a = 3600;
end
if a < 0
    a = 3600+a;
end
Cl = coef_65_018(a,2);
Cd = coef_65_018(a,3);
Cm = coef_65_018(a,4);
Cp = coef_65_018(a,5);
M = coef_65_018(a,6);

% this function supplies the points for plotting the airfoil around the
circumference
function  p = profile(ci,cm,rm,phi,le)
% where bi is the clockwise angle in degrees from the positive y axis
to
% the leading edge of the airfoil, cm is the cord length, and rm in the
% radius
% load n0009_03_100.txt
load c_65_018.txt

p1 = c_65_018; % (0,0) is the leading edge, (1,0) is the trailing edge

p2 = [(p1(:,1)*(-1)),p1(:,2)]; % (0,0) is the leading edge, (-1,0) is
the trailing edge

p3 = p2*cm; % modified to the correct cord length

p4 = [p3(:,1)*cosd(-phi)-p3(:,2)*sind(-phi),p3(:,1)*sind(-
phi)+p3(:,2)*cosd(-phi)];

a = -ci;

p5 = [p4(:,1)*cosd(a)-p4(:,2)*sind(a),p4(:,1)*sind(a)+p4(:,2)*cosd(a)];

p = [p5(:,1)+le(1),p5(:,2)+le(2)];

% this function is the old profile function that puts the leading edge
on the circumference.
function  p = profile(bi,cm,rm,phi)
% where bi is the clockwise angle in degrees from the positive y axis
to
% the leading edge of the airfoil, cm is the cord length, and rm in the
```

```
% radius
load n0009_03_100.txt

p1 = n0009_03_100; % (0,0) is the leading edge, (1,0) is the trailing
edge

p2 = [(p1(:,1)*(-1)),p1(:,2)]; % (0,0) is the leading edge, (-1,0) is
the trailing edge

p3 = p2*cm; % modified to the correct cord length

p4 = [p3(:,1)*cosd(-phi)-p3(:,2)*sind(-phi),p3(:,1)*sind(-
phi)+p3(:,2)*cosd(-phi)];

le = coords(rm,bi);

theta = asind(cm/(2*rm));

% a = -bi+theta;
a = -bi;

p5 = [p4(:,1)*cosd(a)-p4(:,2)*sind(a),p4(:,1)*sind(a)+p4(:,2)*cosd(a)];

p = [p5(:,1)+le(1),p5(:,2)+le(2)];



% this function supplies the coordinates for the tip of a vector
centered at the origin given a scalar length and a angle from the
positive y axis
function c=coords(rm,theta)
% returns the coordinates for a point in the circumference of a circle
about the origin of
% radius rm at a degree theta from the top of the circle
if theta < 0
    theta = 360+theta;
end
c = [rm*sind(theta) rm*cosd(theta)];

% this function finds the angle between two vectors
function alpha = findangle(v1,v2)

x1 = v1(1);
y1 = v1(2);
x2 = v2(1);
y2 = v2(2);

alpha = atan2(x1*y2-y1*x2,x1*x2+y1*y2)*180/pi;


% this function plots the needed vectors. Other variations of this code
plot vectors of different colors.
function vectarrow(p0,p1)
%Arrowline 3-D vector plot.
%   vectarrow(p0,p1) plots a line vector with arrow pointing from point
p0
%   to point p1. The function can plot both 2D and 3D vector with arrow
```

```
%   depending on the dimension of the input
%
%       2D vector
%       p0 = [1 2];     % Coordinate of the first point p0
%       p1 = [4 5];     % Coordinate of the second point p1
%       vectarrow(p0,p1)
%
%   See also Vectline

%   Rentian Xiong 4-18-05
%   $Revision: 1.0

if max(size(p0))==2
if max(size(p1))==2
          x0 = p0(1);
          y0 = p0(2);
          x1 = p1(1);
          y1 = p1(2);
          plot([x0;x1],[y0;y1],'r');   % Draw a line between p0 and p1

          p = p1-p0;
          alpha = 0.25;  % Size of arrow head relative to the length of
the vector
          beta = 0.25;  % Width of the base of the arrow head relative
to the length

          hu = [x1-alpha*(p(1)+beta*(p(2)+eps)); x1; x1-alpha*(p(1)-
beta*(p(2)+eps))];
          hv = [y1-alpha*(p(2)-beta*(p(1)+eps)); y1; y1-
alpha*(p(2)+beta*(p(1)+eps))];

%           hold on
          plot(hu(:),hv(:),'r')  % Plot arrow head
%           xlabel('x')
%           ylabel('y')
%           hold off
else
          error('p0 and p1 must have the same dimension')
end
else
      error('this function only accepts 2D vectors')
end
```

REFERENCES

1 Gorlov, A. *Development of the Helical Reaction Hydraulic Turbine*; DE-FGO1-96EE 15669; DOE: Boston, MA, 1998.

2 Gorban, A.; Gorlov, A.; Silantyav, V. Limits of Turbine Efficiency for Free Fluid Flow. *Journal of Energy Resources Technology*.**2001**, (123), 311-317.

3 Gorlov, A. Hydraulic Cross-Flow Turbines. October 26-28, 2005. http:// hydropower.inel.gov/hydrokinetic_wave/pdfs/day1/05_crossflow_turbine.pdf (accessed Mar 17, 2010).

4 Gorlov, A. The Helical Turbine: A New Idea for Low-Head Hydro. *Hydro Review*.**1995**, 14 (5), 44-51.

5 Gamble, J. Design of a Hydrokinetic Charging System for Electric River Boats. M.S. Thesis, Arizona State University, Phoenix, AZ, 2010.

6 Paish, O. Small Hydro Power: Technology and Current Status. *Renewable and Sustainable Energy Reviews*. **2002**, 6 (2002), 537-556.

7 Powertech Labs. In-Stream Hydrokinetic Turbines. http://www.hydrovolts.com/ MainPages/Hydrokinetic%20Turbines.htm (accessed Jun 23, 2010).

8 Jung, J.; Lee, J.; Rhee, S.; Song, M.; Hyun, B. Unsteady Flow Around a Two Dimensional Section of a Vertical Axis Turbine for Tidal Stream Energy. *JNAOE*. **2009**, 1 (2),64-69.

9 Melin, T. A Vortex Lattice MATLAB Implementation for Linear Aerodynamic Wing Applications. M.S. Thesis, Royal Institute of Technology, Stockholm, Sweeden, 2000.

10 Ponta, F.; Dutt, G. An Improved Vertical-Axis Water-Current Turbine Incorporating a Channeling Device. *Renewable Energy*.**1999**, 20 (2000), 223-241.

11 Chesna, A.; DiBella, T.; Hutchins, T.; Kropf, S.; Lesica, J.; Mahoney, J.; *Hydroelectric Power Generator;* College of Engineering, Northeastern University: Boston, 2002.

12 Wauquiez, C. Shape Optimization of Low-speed Airfoils using MATLAB and Automatic Differentiation. M.S. Thesis, Royal Institute of Technology, Stockholm, Sweden, 2000.

13 Hwang, S.; Lee, Y.; Kim, S. Optimization of Cycloidal Water Turbine and the Performance Improvement by Individual Blade Control. *Applied Energy*.***2009***, 86 (2009), 1532-1540.*

14 Brunetti, S.; et al. *A Demonstration Floating Platform for a Helical Turbine*; MIME Department, Northeastern University: Boston, 2000.

15 Lowe, S. Omission of Critical Reynolds Number for Open Channel Flows in Many Textbooks. *Journal of Professional Issues in Engineering Education and Practice.***2003**, 1 (58), 68-69.

16 Beri, H.; Yao, Y. Effect of Camber Airfoil on Self Starting of Vertical Axis Wind Turbine *Journal of Environmental Science and Technology* **2011**, 4 (3), 302-312.

17 *A Lift for Low-Rise Hydropower*; Reed Business Information: UK, 1995.

18 Nadis, S.; Hirshberg, C. *Full Speed Ahead and Damn the Dams* ***2001***, 259 (6), 626.

19 Abbott, I.; Doenhoff, A. *Theory of Wing Sections;* Dover Publications, INC: New York, *1949*.

20 Coleman, H.; Steele, W. *Experimentation and Uncertainty Analysis for Engineers*. John Wiley & Sons, Inc. 1989; p 188-193.

21 Hoerner, S. *Fluid-Dynamic Drag;* Hoerner Fluid Dynamics: California, 1992.

22 Ostowari, C.; Naik, D. *Post-Stall Wind Tunnel Data for NACA 44XX Series Airfoil Selections;* DE-AC02-83CH10093; Solar Energy Research Institute: Golden, CO, 1985.

23 Blevins, R. *Applied Fluid Dynamics Handbook;* Krieger Publishing Company: Florida 1984.

24 Aris, R. *Vectors, Tensors, and the Basic Equations of Fluid Mechanics;* Dover Publications, INC: New York, 1962.

25 Mine-Thomson, L. *Theoretical Hydrodynamics;* Dover Publications, INC: New York, 1968**.**

26 Sheldahl, R.; Klimas, P. *Aerodynamic Characteristics of Seven Symmetrical Airfoil Sections Through 180-Degree Angle of Attack for Use in Aerodynamic Analysis of Vertical Axis Wind Turbines;* Sandia National Laboratories: Albuquerque, SAND80-2114, 1981.

27 Tangler, J.; Kocurek, J. *Wind Turbine Post-Stall Airfoil Performance Characteristics Guidelines for Blade-Element Momentum Methods:* American Institute of Aeronautics and Astronautics; (1-10).

28 Lindenburg, C. *Stall Coefficients: Aerodynamic airfoil coefficients at large angles of attack;* ECN-RX-01-004; NREL: Co, 2001.

29 Fox, R.; McDonal, A.; Pritchard, P. *Introduction to Fluid Mechanics.* John Wiley & Sons, Inc. 2003.

30 Jacobs, E; Ward, K; Pinkerton, R. *The Characteristics of 78 Airfoil Selections from Tests in the Variable Density Wind Tunne;* Report No. 460; NACA: Washington D.C.1933**.**

31 Elert, G; *Flow Regimes;* http://physics.info/turbulence/ **1998-2010**.

32 Buckingham, E., *On Physically Similar Systems: Illustration of the Use of Dimensional Equations.* Physical Review, 4, 4, 1914, p 345-376.

33 Hepperle, M.; *Javafoil* http://www.mh-aerotools.de/airfoils/javafoil.htm (accessed Oct 1, 2010).

34 *Hitachi Inverter J300 Series Instruction Manual*. CTi Automation. Tokyo, Japan.

35 Winther, J. *Dynamometer Handbook of Basic Theory and Applications*. Cleveland, Ohio: Eaton Corporation, **1975**.

36 Spalart, P.; Allmaras, S. A one-equation turbulence model for aerodynamic flows. *La Recherche Aerospatiale*. 1, 5-21, 1994.